A Decision Support System for Warning and Evacuation against Multi Sediment Hazards

By

Chen-Yu Chen

2014

Abstract

Faced with threats of sediment disasters in mountainous areas, the establishment of early-warning systems and evacuation strategies is recognized as one of the most important approaches for disaster risk management. Owing to environmental conditions, Japan and Taiwan typically suffer from threats of sediment disasters during typhoons or heavy rainfalls every year; therefore, nationwide rainfall-based sediment warning systems have been established. However, although the existing rainfall-based warning systems in Japan and Taiwan provided a simple and easy-to-apply criterion method to issue alerts, they cannot predict which slope might collapse specifically. Even if the local government received the alerts, it was still difficult to make an appropriate evacuation decision because of lacking definite warning information. According to the statistics, the proportion of Japanese local governments that actually carried out evacuation orders after the sediment disaster alert issued was only 2.2% in 2008, and only 2.8% of inhabitants decided to evacuate when they received a sediment disaster alert. This indicates that the existing warning models are not taken seriously.

In addition, the rainfall-induced disasters and their causes were usually related to flooding and sediment transportation in mountainous areas. For example, rainfall might induce landslides, debris flow, and flood, and the landslide sediment then might become the source material of debris flow as well as the landside sediment and debris flow might form natural dam or block the river. Once the natural dam burst, then it might derive debris flow or flood to cause the secondary disaster. Thus, the rainfall-induced hazards in mountainous areas usually occur as a multi-modal type, i.e., a hazard could affect or trigger another one because of their complex spatial and temporal relationships. However, limited by the complexity of multi-modal disasters and the responsibility of disaster prevention for different government divisions, the existing warning systems only focus on a single type of hazard and lack the capability of overall consideration, especially on the evacuation decision-making. In the past years, some catastrophes showed that if the disaster prevention plan in mountainous areas only considered single hazard individually, it cannot tackle the risk under the extreme climate situation.

The purposes of this study are exploring the insufficiencies of the existing warning systems and investigating the evacuation decision-making factors for local

governments and inhabitants. Based on the results, this study identifies the needs of the new warning system. Moreover, this study proposes a novel method of predicting the occurring time, location, and scale of landslides, and develops a simulation model of multi sediment hazards on a basin scale as well as proposes a specific issuing-alerts system to establish a warning and evacuation decision support system.

This process of this study would be divided mainly into several parts. Firstly, this study evaluated the warning systems for debris flows and slope failures in Taiwan and Japan. It suggests evaluation indexes of warning effectiveness according to several years of statistical data, and discusses the insufficiencies of current rainfall-based warning systems during actual disaster cases. The study results indicate that the existing rainfall-based warning systems cannot accurately predict the occurring time, location, type, and scale of potential disaster. In addition, they also cannot cope with the multi sediment hazards. To improve on the problems, this study recommends developing a new basin-scale warning system, which considers the geological, geomorphologic, and hydrological characteristics of slopes and channels. The new warning system should offer accurate long-time predictions (e.g., over the next 12 hours) and the scenario simulation capacity.

Moreover, this study establishes the evacuation decision-making models based on the pair-wise comparison and the analytical hierarchy process (AHP) for local governments and inhabitants. The results not only show the importance of each evacuation decision factor, but also identify the deficiencies in current disaster prevention actions. The findings show that the evacuation decisions made by different levels of local governments are quite diverse, and the decisions are also various depending on the spatial position. The study also found that local governments and inhabitants all believe that raising the warning hit rate of the existing warning system is more important than reducing the false alert rate. In addition, the research results indicate that *raising the warning hit rate*, *narrowing the unit of warning area*, and *providing more detailed warning information* are the most important improvement direction for existing warning system. Based on the abovementioned recommendations, this study proposes that the new warning system should offer the detailed warning information (e.g., the occurring time, location, type, and scale of disaster), and uses slope units as the target to predict landslides as well as employs unit channels as the target to predict the water level and riverbed deformation.

In addition, the methods of predicting landslides generally can be divided into two types - statistical model (e.g., the existing rainfall-based warning system in Japan and Taiwan) and physically-based model (e.g., the Integrated Rainfall-Infiltration Slope stability (IRIS) mode, which was used in this study). Compared with the statistical model, the physically-based model can provide more detail and precise result, but it is difficult to employ on a basin-scale because of time-consuming calculation. This study proposed a new approach (critical water content method, W_{cr}), which was based on physically-based model and the multiple regressions as well as used the slope units as analysis targets, to predict the occurring time, location, and scale of landslides. This W_{cr} method cannot only offer the similar accuracy to the physically-based model, but also has the high performance on calculation. That is, it can be employed on a basin scale. Compared with the prediction results using the physically-based model (IRIS model), the prediction results of the occurring time and location of landslides using W_{cr} method were almost same as the IRIS model, only the prediction result of the scale of landslides sometime appeared differences. Overall, using W_{cr} method instead of the IRIS mode to predict landslides on a basin scale is feasible. Using the heavy rainfall event in the Shizugawa basin, Uji City, Kyoto Prefecture on August 13-14 in 2012 as verification, the warning hit rate (WHR) is 73.7%, and the failure alert rate (FAR) is 78.6%. These results seem to be better than the existing warning systems. Moreover, because the occurrence of rainfall-induced landslides was attributed to the water content, the W_{cr} method is appropriate to express the risk of landslide on a basin scale.

After that, this study suggests a basin model by combining slope units and unit channels, and integrates the rainfall-infiltration, landslide prediction, sediment supply, sediment runoff, riverbed deformation, and water discharge models to establish the simulation model of multi sediment hazards on a basin scale. The simulation model of multi sediment hazards can provide the simulation result, such as the landslide prediction with slope unit as targets, the overflow prediction with unit channels as targets, the sediment runoff prediction, and the riverbed deformation with unit channels as targets. Through the verification of the investigation results after disaster, the model performed good prediction. To verify the scenario simulation capacity of the simulation model of multi sediment hazards, this study adopted four different typical rainfall patterns to conduct the simulation. The results indicated the occurrence

time, location, and scale of disaster were significantly affected by the rainfall patterns. Therefore, the disaster prevention strategies and plans should consider the different rainfall types to adopt appropriate emergency response and evacuation decision. In addition, because of the high-performance calculation of the regression formulas, the W_{cr} method can simulate the change of the water content for hundreds of slope units on a basin scale, and the model can predict not only the landslides but also the runoff on the slope units. That is, the W_{cr} method can replace the IRIS model and kinematic wave method for landslide prediction and runoff estimation on the slope unit.

Finally, this study proposes the two-levels (yellow/red) alert for three kinds of disasters (landslide, road closure, and flood) to establish the alert-issuing system. Each alert is displayed as easy-to-understand content and has the definite issuing-condition as well as clear instructions on appropriate protection action. Integrating the simulation model of multi sediment hazards on a basin scale and the issuing-alert system, this study develops the Rainfall-Induced Multi Sediment Hazard (RIMSH) warning system. The RIMSH warning system can offer not only the early-warning for inhabitants but also the evacuation, road-closure, and bridge-closure decision-making for local governments. In the abovementioned heavy rainfall event as the verification, the RIMSH warning system provides at least 2.5 hours for evacuation preparation, and at least 1 hour to evacuate inhabitants to the shelters. It really reaches the goal of early warning, and offers enough evacuation time. Moreover, the RIMSH warning system proposes an objective evaluation method to adjust the alert level, and it is useful to assist the decision-maker in making appropriate decisions. In addition, to verify the contribution of the RIMSH warning system to raise the evacuation willing for the local government officials and inhabitants, this study also made a series of questionnaires to explore the effect of more complete warning information. The survey results indicated that if the local government officials obtain the higher forecast rainfall or extra detailed warning information, they will raise the willingness of executing precautionary evacuation. However, although the detailed warning information really could raise the proportion of precautionary evacuation for local governments and inhabitants, the survey results also show that some inhabitants would postpone the evacuation decision.

Keywords: multi-hazard, sediment disaster, warning system, evacuation decision, landslide prediction, flood prediction, road closure

Acknowledgements

I would like to express my sincere gratitude and appreciation to many people that contributed in direct or indirect ways to this dissertation. Furthermore, I would like to thank a number of people for their assistance during my study in Kyoto University, Japan.

Firstly, I would like to acknowledge my supervisor, Prof. Masaharu Fujita, who has given me much valuable advice and guidance in the process of my study. In addition, his abundant knowledge and academic experience have been invaluable to me. Without his patient guidance and illuminating instruction, this dissertation would have never been finished. In addition, I am very grateful to the support of the Executive Yuan, Taiwan, and in particular Minister WuXiong Chen and Director General MingYao Huang for giving me the opportunity to study in Kyoto University.

I am extremely grateful to Prof. Hajime Nakagawa and Dr. Hiroshi Takebayashi, Disaster Prevention Research Institute of Kyoto University, who have given their valuable comments and suggestions for refining this dissertation. Many thanks are also for their encouragement, kindness, idea and patience during my study.

I would also like to express my sincere appreciation to Dr. Daizo Tsutsumi. His work in rainfall-infiltration and slope stability analysis served as a model and inspiration for this dissertation. My gratitude is also for his kindness and patient guidance. In addition, my deepest gratitude goes to Dr. Shusuke Miyata, who has given me much valuable advice and guidance in the process of the paper writing. Many thanks are also for his kind support, help and fruitful discussion. In addition, I am indebted to Japan Weather Association and Asia Air Survey Co., LTD for offering the X-band rainfall data and aerial photo during my research. Besides, I thank all professors and friends in the Research Center for Fluvial and Coastal Disasters, Disaster Prevention Research Institute of Kyoto University, who have made my academic experience rich and memorable. The help of the staff of Kyoto University and also Mrs. Kayo Tanaka has been most helpful. I also want to thank all my friends in Japan, and they have enlarged my knowledge and horizon during my study.

Finally, my deepest gratitude goes to those whose influence may not be so evident but who nevertheless provided the educational and emotional foundation without which this dissertation would have never been possible: my wife, my children, and my family.

Table content

Chapter 1

Introduction

1.1 Background

Generation and transportation of sediment are natural phenomena, and they result in the change of topography and fluvial facies. However, if the process of generation and transportation of sediment causes loss of life and property, as well as damages to roads, bridges, and other infrastructure, the natural phenomena will form sediment disaster. In fact, the disasters in mountainous areas during typhoon or heavy rainfall are usually the result of flooding and the moving of sediment. For example, some rainfall cannot infiltrate into the soil and directly converts to runoff, and a lot of runoff then causes some communities to be inundated as well as forming a flood to wash away roads and bridges [*Chen et al.*, 2011; *Kondo et al.*, 2012; *Miyata and Fujita*, 2013]. On the other hand, some rainfall infiltrates into the slope and results in the rise of pore water pressure, leading to the reduction of effective stress as well as causing landslides [*Iverson*, 2000; *Casadei et al.*, 2003; *Vieira and Fernandes*, 2004; *Tsutsumi et al.*, 2007]. Moreover, the landslide sediment might form debris flow and destroy buildings or enter river channels to cause riverbed rising, reducing the drainage capacity and resulted in inundation, further forming a landslide dam to derive a secondary disaster. Thus, the rainfall-induced disasters in mountainous areas usually occur as a multi-modal type, that is, the result of several hazards caused by the same trigger, one hazard triggering the next or completely coincidental occurrence of various hazards at the same time or timely close with additional spatial overlapping [2008; *Kappes et al*., 2012a; *Kappes et al*., 2012b].

Highland and Bobrowsky [2008] stated that natural hazards such as floods, earthquakes, volcanic eruptions, and landslides can occur simultaneously, or one (or more) of these hazards can trigger one (or more) of the others. For example, earthquake-induced landslide blocks a river, and causes water to back up behind the mass as well as then flood the upstream area. If the dam fails, the impounded water will be suddenly unleashed to cause flooding downstream. This flooding can then add to riverbank and coastal erosion and destabilization through rapid saturation of slopes

and undercutting of cliffs and banks. A multi-hazard event was observed in Tanaguarena, Venezuela in 1999. The heavy rainfall triggered flooding, landslides, flash-flood, and debris-flow in the same area (**Figure 1.1**).

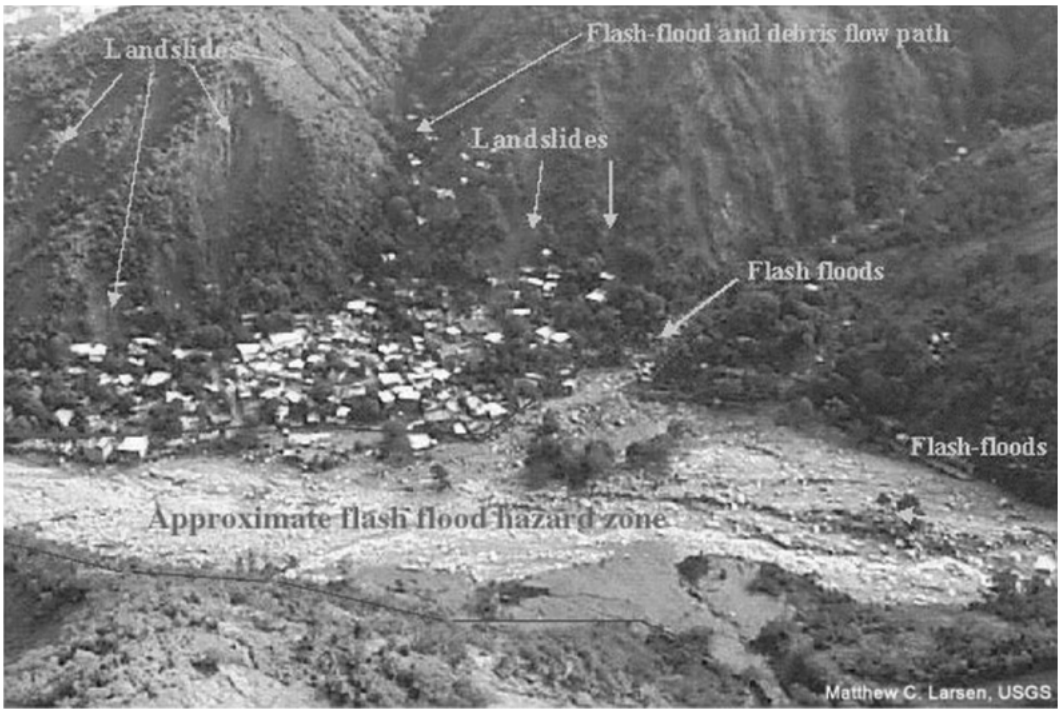

Figure 1.1 The multi-hazard event in Tanaguarena, in coastal Venezuela, South America in 1999. [Highland and Bobrowsky, 2008]

In Taiwan, the similar process happened in 2009. During the fatal landslide which wiped out more than 400 residents in Shaolin Village, Kaohsiung, several sediment hazards were induced during Typhoon Morakot (**Figure 1.2**). From the witness account and aftermath field investigation, the process could be described in **Table 1.1** [*Lee and Dong*, 2009; *Chen et al.*, 2011; *Tsou et al.*, 2011].

From **Table 1.1**, it could be observed that heavy rainfall, debris flow, flood, landslides, landslide-dam were induced one by one within 19 hours, a multi-hazard event was observed on the same location.

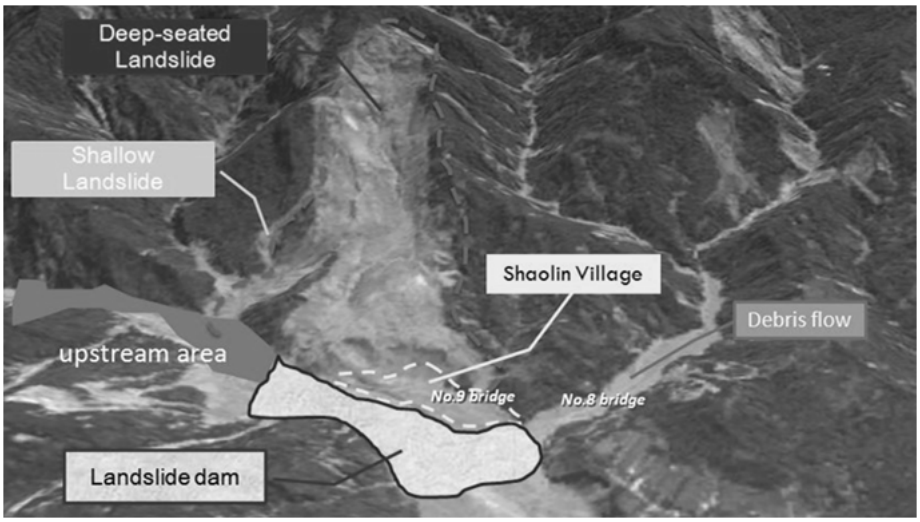

Figure 1.2 A multi-hazard event in Shaolin Village during Typhoon Morakot

Table 1.1 Hazard process of Shaolin Village during Typhoon Morakot

Hazard Type	Time	Description
Flood Shallow landslide Debris flow	14:00 Aug. 8	Shallow landslide
	19:00 Aug. 8	No.8 bridge was crushed by debris flow (the only escape route); No.10 bridge was submerged by the flood
	21:00 Aug. 8	Center of village start flooded
	23:00 Aug. 8	No.9 bridge was submerged by the flood and debris flow
	01:00 Aug. 9	Chi-Shan River flooded
	03:30 Aug. 9	Most of village were flooded to chest
Deep-seated landslide	06:00 Aug. 9	Landslide bury most part of the village
Landslide Dam	07:00 Aug. 9	Landslide dam burst, flood washed the remnant of the village away
Flood Debris Flow	08:40 Aug. 9	Downstream of Chi-Shan river was hit by dam-burst debris with several bridges destroyed

Although hazard analysis methods are already well-established for many natural processes, their joint investigation poses a variety of challenges. Especially, the widely differing characteristics of the single process not only as intensity, return period or parameters of influence on exposures, but also the varying procedures to estimate and quantify them complicate multi-hazard analyses.

The natural hazards are usually still considered as independent from each other, which cannot be supported by observations in the field. However, due to the triggering factors or spatial relationships, some interactions of sediment hazards could be identified. **Table 1.2** shows the influences of one process on the disposition of another one [*Kappes et al.*, 2010a]. For example, landslides supply materials to form debris flow, which would change the riverbed morphology, and further floods might occur

more frequently in the future.

Table 1.2 Matrix for the identification of influences of one process on the disposition of another one. The process in the line is the causing one, the column indicates the affected one. [Kappes et al., 2010a]

Avalanche	Influence on vegetation cover (Removal of forest)	Influence on vegetation cover (Removal of forest)	Influence on vegetation cover	-
-	Debris flows	-	-	Change of river bed morphology (acc. & erosion)
Increased slope roughness	Supply of material	Rock falls	Increase of load	Material accumulation in river bed
Alteration of surface roughness	Supply of material	-	Landslides	Change of river course
-	Remobilisation of material	-	Erosion/ saturation of landslide deposits	Floods

And for triggering effects, it would be vital to identify the procedure of links between hazards. For example, heavy rainfall might trigger landslides or debris flows, but not likely to trigger an earthquake. **Table 1.3** shows the triggering relationships between different types of hazards.

Table 1.3 Matrix opposing all considered hazards towards the range of identified triggers and hazards taken into account to identify triggering relations [Kappes et al., 2010a].

	AV	DF	RF	LS	FL
Avalanches (AV)					x
Debris flows (DF)					x
Rock falls (RF)					x
Landslides (LS)					x
Floods (FL)				x	
Heavy rainfall	x	x		x	x
Earthquake	x		x	x	

For better describing the relationships between multi-hazards, Kappes et al. (2010b) illustrated that spatial, temporal and spatial-temporal should be considered carefully for multi-hazard analysis. **Figure 1.3** explains the most vital elements for multi-hazard research.

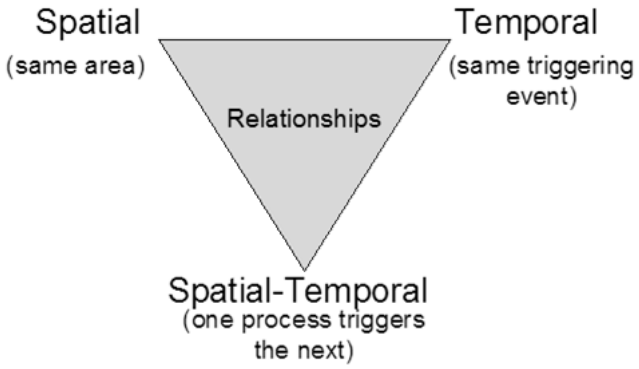

Figure 1.3 Relationships between multi-hazards [Kappes et al., 2010b]

Due to complicated mechanism and process of multi sediment hazards, a basin-scale simulation model, which has the capability of overall consideration, is an essential tool to explore and predict the natural phenomena. Because grid-based analysis units could be easily obtained and managed, as well as the algorithm was simpler, many studies used grid as the unit for slope stability analysis on a basin scale [*Casadei et al.*, 2003; *Chang and Chiang*, 2009]. However, grid cell can't represent geological, geomorphologic, or other environmental boundaries, so the results by the grid-based method were relatively unacceptable in physical terms [*Xie et al.*, 2004]. Hence, some researchers used slope units to conduct the landslide hazard evaluation [*Carrara et al.*, 1991; *Crosta et al.*, 2006] and landslide prediction [*Xie et al.*, 2004; *Wang et al.*, 2006; *Chen and Fujita*, 2014]. **Figure 1.4** showed the difference between grid-based mapping unit and slope unit-based mapping unit.

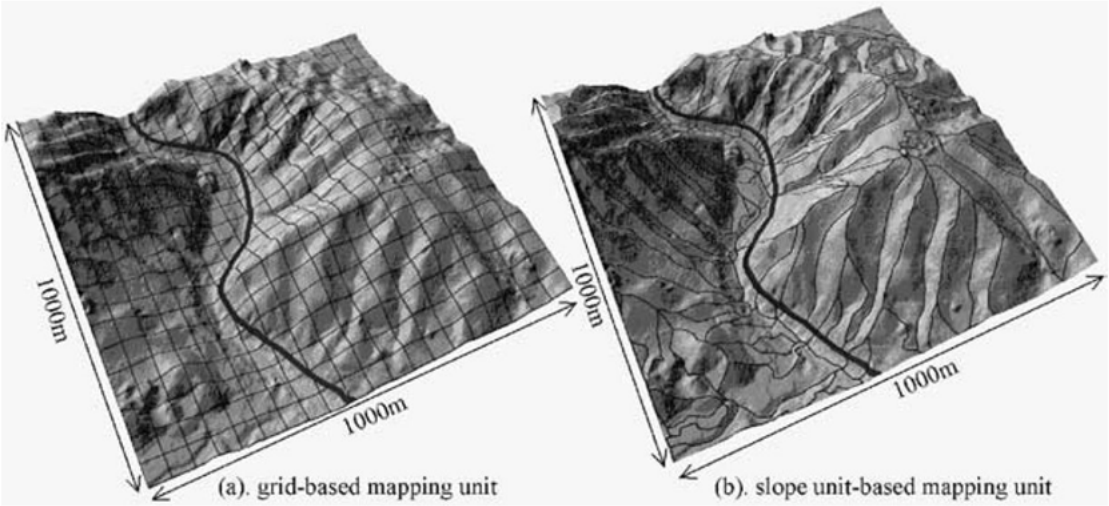

Figure 1.4 Difference between the grid-based mapping unit and the slope unit-based mapping unit. (a) Is the grid-based mapping unit; each even-dividing mapping unit has no relation to topographical characteristics. (b) Shows the slope unit-based mapping unit; each slope unit corresponds to the left/right part of each slope. [*Xie et al.*, 2004]

In addition, the prediction of the rainfall-runoff on a basin scale and the simulation of the sediment transportation in the river channel are important information to disaster management, water resource management, and sediment management in a basin. In prediction of the rainfall-runoff on a basin scale, using the distributed model (e.g., composition of unit channels and unit slopes, see **Figure 1.5**) to conduct a basin model has been extensively used [*Takasao and Shiiba*, 1988; *Tachikawa et al.*, 2004; *Lee et al.*, 2011]. Moreover, the integrated model of rainfall-runoff and sediment-runoff also has been studied by some researches [*Ichikawa et al*., 1999; *Egahsira and Matsuki*, 2000; *Takahashi et al*., 2000]. However, the research which integrated the rainfall-infiltration-runoff model, sediment-generation (e.g., landslides) prediction model, sediment runoff, and riverbed deformation model to simulate the multi sediment hazards on a basin scale is relatively unexplored.

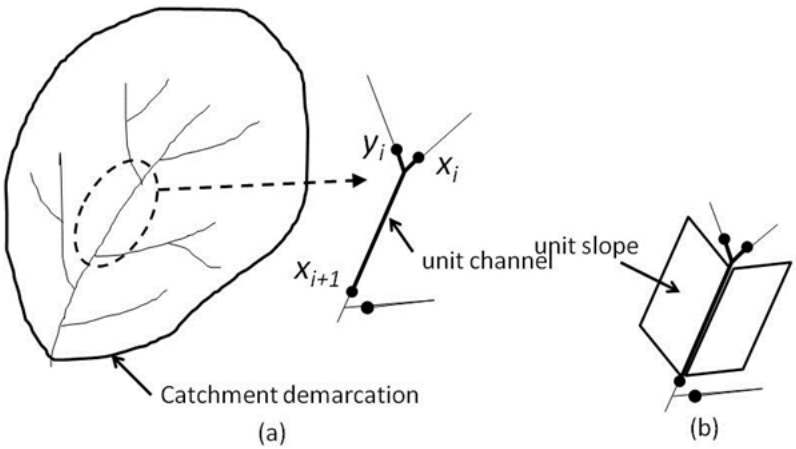

Figure 1.5 Basin model (a)a unit channel has two inflow points and one outflow point (b)each unit channel has two unit slopes

Generally, The countermeasures of sediment disaster prevention can be divided two parts - structural and non-structural methods. The structural methods of sediment disaster prevention primarily use engineering to strength the slope stability, control the erosion of bank and reduce the affected area. For example, a sabo dam is the most common to be taken against debris flow. It can provide several types of functions, such as arrest and storage sediment function, erosion-control function, soil conservation function, and grading function of grains [*NILIM*, 2004]. Moreover, we also employ engineering to control and restrain the slope failure. For instance, we can implement drainage works, vegetation works, cutting of an unstable soil mass and

enhance the slope protection works to mitigate the effect of rainfall. On the other hand, we also can reinforce the surface soil layer in slope by cutting of slope to improve the form, retaining wall works, anchor works, pile works and loading embankment works.

The non-structural methods of sediment disaster prevention can be devoted through three ways:

(1) Developing warning and evacuation system

Facing the climate change in the future, nobody can deny the capacity of engineering is limited. So, even if engineering had been established, it still is the most important thing to identify the risk area and plan the warning and evacuation system for the inhabitants living in the disaster potential area. In addition, comparing with engineering, the warning and evacuation system usually is significant cheaper. **Figure 1.6** illustrates an example of operation of warning and evacuation system [*NILIM*, 2004].

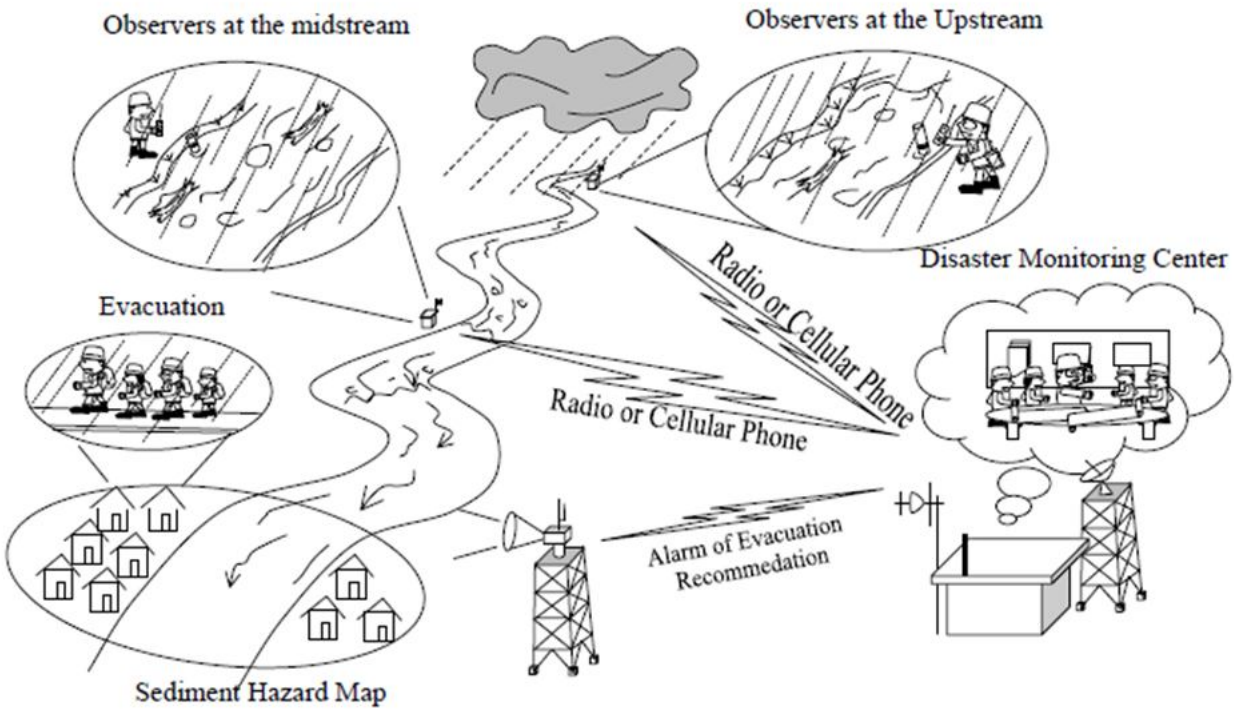

Figure 1.6 Examples of operation of warning and evacuation system [*NILIM*, 2004]

(2) Reinforcing disaster prevention education

According to the relevant researches, when the inhabitants decide to evacuate or not, the personal risk perception plays the indispensable and irreplaceable role [*Lindell et al*., 2005; *Whitehead et al*., 2000; *Dow and Cutter*, 1998; *Gladwin and*

Peacock, 1997; *Baker*, 1991]. The relevant researches also indicate reinforcing disaster prevention education is the foundation of strengthening personal risk perception. The stages and methods of reinforcing disaster education are a variety, but a complete hazard map is essential. **Figure 1.7** is a sample of the landslide-hazard map in Taiwan [*NCDR*, 2013].

(3) Enhancement the slope management

Owing to the fact that human activity in the slope will accelerate erosion and add the unstable factors further causing the slope failure, so how to adequately use and manage slope is a very important issue. Most of the experts suggest that establishing the regulation and enhancement the slope management is necessary.

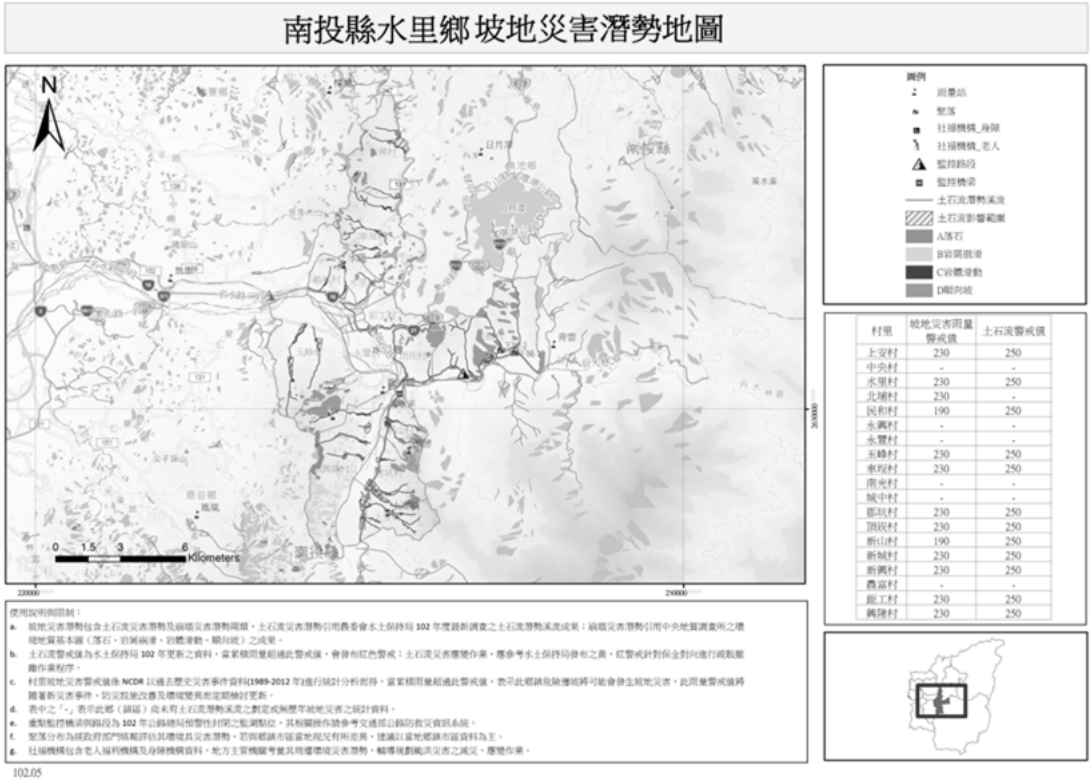

Figure 1.7 Landslide-hazard map in Taiwan [*NCDR*, 2013]

Consequently, faced with the threat of sediment disasters, in addition to government's engineering efforts, establishment of early-warning systems and evacuation of inhabitants are recognized as the most important approaches for disaster risk reduction. In the past decades, there has been a great deal of literature trying to use different methods to create a specific and feasible sediment disaster warning system. Generally, methods of sediment disaster warning can be classified into the direct methods (such as using trip wires, video cameras, ultrasonic and radar gauges,

or monitoring ground vibration), as well as the indirect methods (such as using rainfall, runoff, or monitoring the groundwater level) [*Arattanoand Marchi*, 2008; *Caine*, 1980; *Onda et al.*, 2003; *Osanai et al*., 2010]. Although the direct method has the advantage of high accuracy, considering the operability and evacuation time, most countries adopt the indirect methods to construct their warning systems for sediment disasters. Moreover, partly because rainfall is an important indicator for sediment disasters, and partly because rainfall data are more readily obtained monitoring information, the rainfall-based warning system is most commonly used in various types of sediment disaster warning systems. For example, *Wieczorek and Glade* [2005] conducted a literature review of rainfall-based debris-flow warning models around the world.

In the studies of evacuation decision-making, *Perry* [1979] proposed the evacuation decision-making process of natural disasters can be divided into four oriented discussions: (1) the source of information pertaining to the nature of the threat; (2) the official decision to issue a warning; (3) the channels through which the warning is communicated to the public; (4) the response of the public. *Wolshon et al.* [2001] suggested the hurricane evacuation studies typically consisted of a storm hazard and vulnerability analysis, an evacuee behavioral analysis, a sheltering analysis, and a transportation analysis. *Tierney* [2005] said the early warning and evacuation decision-making process can be divided into seven steps, and contrasting with the practical operational process in Taiwan, the above seven steps can be generalized into three stages (see **Table 1.4**): (1) issuing early warning; (2) official evacuation order issuance and implementation; (3) the inhabitants' evacuation decision-making and action. Any failure in these three stages may cause casualties, so there are many studies exploring in the three stages in the past decades.

Table 1.4 The process of warning issuance and evacuation decision (Modified from Tierney, 2005)

Stages	Steps
(1) Issuing early warning	A. collecting and analyzing the information
(2)Official evacuation order issuance and implementation	B. making evacuation decision
	C. the content and timing of evacuation orders
	D. disseminating the evacuation order and communicating to public
(3)Inhabitants' evacuation decision-making and actions	E. inhabitants' perception of evacuation order
	F. inhabitants' confirmation of evacuation order
	G. inhabitants' evacuation actions

Regarding the studies of evacuation decisions by local governments, *Lindell and Prate* [2007] assisted the Texas government in establishing the hurricane evacuation management decision support system (EMDSS) for the coastal areas. *Regnier* [2008] recommended using the historical hurricane paths with the stochastic model methods to enhance the quality of evacuation decision-making for local government. *Amano and Takayama* [2006] investigated the process of evacuation decision-making by township governments after receiving a sediment disaster alert, as well as considerations and difficulties after the 14th typhoon in 2005 in Japan. The Department of Erosion and Sediment Control (*DESC*) [2007] also collected the problems which the local governments faced while making evacuation decisions in Japan, and published *the Guidelines of Warning System and Evacuation* for local governments. *Chen and Mars* [2008] used depth interviews and questionnaires to survey the evacuation decision of the central government, local governments, and village heads in debris-flow potential areas in Taiwan, and pointed out that the lower-level governments (i.e. close to the disaster potential areas) made evacuation decisions based on current circumstances much more.

In the researches of evacuation decisions by inhabitants, *Dash and Gladwin* [2007] reviewed the studies of hurricane evacuation decisions by inhabitants in the coastal areas in U.S. from past decades, and classified them into warning, risk perception, and evacuation research. They also suggested future research should include inhabitants' evacuation rate (both voluntary and mandatory evacuation), how to use and interpret the hurricane alert, how to add the evacuation behavior patterns and time factor in the evacuation decision support system, the information included in hurricane forecasts, and the timing of those forecasts. In Japan, *Ushiyama, et al.* surveyed the influence of the inhabitants' evacuation decision as affected by disaster alert [*Ushiyama*, 2012; *Ushiyama* et al. 2003]. *Irasawa and Kamaishi* [2010] explored the motivations of the evacuated people and non-evacuated people in torrential rain disaster area in July 2002 in Japan. *Chen, et al.* [2007] focused on the inhabitants in the debris-flow potential areas in Taiwan, and searched the source of evacuation information, evacuation decision-making, and consideration factors for shelters. *Wu* [2009] compared two different debris-flow potential areas on the evacuation decision-making by and behaviors of inhabitants. *Pai* [2008] investigated the evacuation decision-making of disadvantaged groups in debris-flow potential areas, and used binary logistic regression

to establish three evacuation behavior patterns: whether evacuate or not, needing assistance, and evacuation time. *Lin* [2007] researched the evacuation decision-making of commercial population in debris-flow potential areas, and compared them against the cases in other countries.

1.2 Problem statement

Due to geographical and environmental factors, Japanese and Taiwanese people suffer from the threat of typhoons and heavy rainfalls during the flood season every year, and the sediment disasters induced by rainfalls are often the type of disasters most likely to cause casualties. Thus, Japan and Taiwan already established the nationwide rainfall-based sediment disaster warning system and have had much practical operational experience over ten years [*Chen and Fujita*, 2013].

However, according to the statistics by the National Institute for Land and Infrastructure Management [*NILIM*, 2010], the proportion of the local governments actually executing the evacuation order after the sediment disaster alert was issued was only 2.2% in 2008 in Japan, and only 2.8% of the inhabitants decided to evacuate when they received the sediment disaster alert. While the proportion of Taiwan's local governments carrying out the evacuation order is higher than Japan because of the mandate that central government orders local governments to evacuate the endangered inhabitants, the average evacuation rate was only 51.6% in the last five years (2007 – 2011) [*Chen and Fujita*, 2013]. Such low statistical numbers seem to show that the existing warning model is not fully trusted.

In addition, although natural disasters in mountainous areas usually occurred as multi-modal types, most of the existing warning system only considered a single hazard. In past years, some events, e.g. a deep-seated landslide in Shiaolin village in Taiwan during Typhoon Morakot in 2009, showed that a single disaster prevention plan cannot tackle the risk under multi-hazards. In this case, the deep-seated landslide generated sediment more than 2.7×10^7 m^3 in Shiaolin village [*Wu et al.*, 2011]. Within 19 hours, Shiaolin village suffered multi-modal sediment disaster that included a series of flooding, debris flow, deep-seated landslide, natural dam, and dam burst. Based on the disaster event series in Shiaolin village, the period from debris flow red alert issued to bridge 8 being broken (i.e. all the traffic disrupted) was up to 20 hours.

It seems to show that there was enough time to disseminate the alert and evacuate, so the existing rainfall-based warning system in Taiwan indeed had reached the goal of early warning. But this disaster ultimately resulted in 462 deaths; it seemed to indicate that there were still some deficiencies worth discussing in the existing rainfall-based warning system.

Unfortunately, with global warming effect and extreme weather phenomenon, some high precipitations were observed in Japan and Taiwan, related sediment hazards were occurred frequently. That is, the risk of the catastrophe due to the large-scale sediment disaster is becoming much higher. For instance, In Japan, many large-scale landslides were induced by Typhoon Talas in 2011, and some of them created the nature dams and derived the secondary disasters [*Yamakoshi et al.*, 2012; *Chigira et al.*, 2013]. Accordingly, such as high intensity and long duration rainfall phenomenon held a great challenge to sediment hazard mitigation and emergency response, the traditional guidelines and standards only suitable for single sediment hazard, thus were not applicable to the new situation. An advanced concept had to be introduced to deal with the new challenge.

1.3 Research purpose

According to the aforementioned problem statement, even if everyone agrees that the warning and evacuation system is indispensable and irreplaceable for disaster prevention strategy; however, the key factor of evacuation decision-making for the local governments and inhabitants during typhoons and heavy rainfalls seems not to be the alert which issued from the existing rainfall-based warning systems. Besides, faced with the increasingly complex disaster's types, the existing rainfall-based warning systems cannot meet the needs of practical operation. Hence, this study will propose a new advanced warning and evacuation decision support system to offer the appropriate warning information to raise the willing of evacuation, as well as to cope with multi sediment hazards and their complex relationship of spatial and temporal.

The objectives of this study can be described as follows:

(1) Based on analysis of the existing warning systems in Japan and Taiwan, this study tries to identify insufficiencies and limitations of them. Moreover, this study will propose recommendations on future prevention disaster strategy and research.

(2) By investigating the evacuation decision-making factors for local governments and inhabitants, this study tries to indicate actual needs for evacuation decision-making, and proposes the essential element of developing the new advanced warning and evacuation decision support system.
(3) Through developing a simulation model of multi sediment hazards, this study tries to identify and establish the mechanism, process of the sediment-related multi-hazards. The results not only offer the verification of the disaster prevention plan but also provide the foundation of developing the warning system for multi sediment hazards.
(4) Based on the above research results and proposing the new issuing-alert system, this study can establish a decision support system for warning and evacuation against multi sediment hazards.

1.4 Thesis outline

The thesis is divided into seven chapters. The framework of this research and its correspondence of each chapter is shown in **Figure 1.8**. The synopsis of each chapter is described as follows:

Chapter 1 provides some background information about causes of sediment disaster in mountainous areas, countermeasures of sediment disaster prevention, and some studies results of warning model and evacuation decision-making. It also briefly outlines some problems and challenges about the existing warning systems, and then proposes the objectives of this study.

In Chapter 2, this study evaluated the warning systems for debris flows and slope failures in Taiwan and Japan. It discusses the characteristics of the warning models and warning issuing systems in Japan and Taiwan, and also suggests evaluation indexes of warning effectiveness according to several years of statistical data: the warning hit rate, false alert rate, warning cover rate, and remaining time for evacuation. In addition, this study focuses on the insufficiencies of current rainfall-based warning models during actual disaster cases. Finally, this research recommends future disaster prevention strategies and solutions.

In Chapter 3, this study describes the predicament of evacuation decision-making for local governments and inhabitants during typhoons or heavy rainfall. Based on

pair-wise comparison and the analytic hierarchy process (AHP), this study shows the significant difference between evacuation decisions for local governments at different levels and locations, and establishes preliminarily evacuation decision-making models. The same method was also employed to establish the evacuation decision-making models of inhabitants. The findings also indicate that merely using a single disaster warning system is not enough to assist local governments in making evacuation decisions, and proposes the priorities of developing the warning and evacuation support system.

In Chapter 4, firstly, this study describes the advantages and limitation of statistical model and physically-based model for landslide prediction. Then, the study proposes a novel method, which is based on physically-based model and multiple regressions as well as using the slope unit as the slope-stability analysis target, to predict the landslides on a basin scale. This method uses a new warning indicator, critical water content (W_{cr}), which is derived from physically-based model and had a clear physical meaning. The new method also has great performance on calculation to predict the occurring time, location, and scale of landslides. The results showed that the new method can not only predict the landslides but also estimate the runoff of the slopes on a basin scale.

In Chapter 5, this study integrated rainfall-infiltration, slope stability, water discharge, sediment runoff, and riverbed deformation model to simulate multi sediment hazards on a basin scale. In addition, the critical water content method is also employed to simulate the runoff of slopes to replace the kinematic wave method. Using the satellite images and field survey results as verification data, the simulation results, including landslide prediction, water level, water discharge, and the variation of riverbed elevation, are consistent with the verification data. In addition, to verify the scenario simulation capacity of the simulation model for multi sediment hazards, this study adopted four different typical rainfall patterns to conduct the simulation. The results indicated the occurring time, location, and scale of disaster were significant affected by the rainfall patterns.

In Chapter 6, based on the recommends about the warning system and evacuation decision factors in Chapter 2 and 3, this study establishes the new advanced warning system through integrating the research results in Chapter 4 and 5. Using the heavy rainfall disaster event, which occurred in the Shizugawa basin in

2012, located in Uji, Kyoto, as a study case, this study employs the new advanced warning system to predict the circumstances every minute, and used the prediction results to assist the evacuation decision-making. In addition, the questionnaire results also seem to indicate that the complete warning information is useful to raise the evacuation willing.

In Chapter 7, the conclusions, recommends, and the future perspectives of research are outlined.

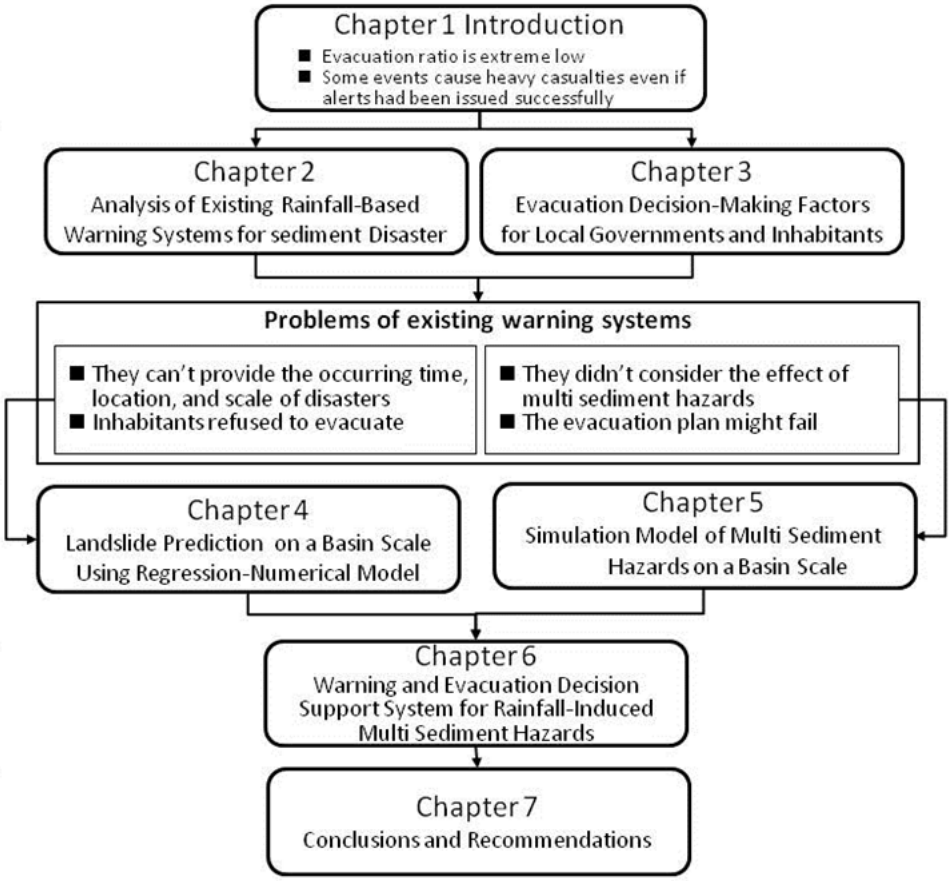

Figure 1.8 The framework of this research and its correspondence of each chapter

References

Amano, A. and Takayama, T. (2006): On the situation of early warning information for sediment-related disasters – Teachings of evacuation from the T0514 disaster, Journal of the Japan Landslide Society, Vol. 43, No. 6, pp. 370–375 (in Japanese).

Arattano, M. and Marchi, L. (2008): Systems and sensors for debris-flow monitoring and warning, Sensors, Vol. 8, pp. 2436–2452.

Baker, E. J. (1991): Hurricane evacuation behavior, International Journal of Mass Emergencies and Disasters, Vol. 9, No. 2, pp. 287.

Caine, N. (1980): The rainfall intensity-duration control of shallow landslides and debris flows, Geografiska Annaler, 62A, pp. 23–27.

Carrara, A., Cardinali, M., Detti, R., Guzzetti, F., Pasqui, V., and Reichenbach, P. (1991): GIS techniques and statistical models in evaluating landslide hazard, Earth Surface Processes and Landforms, Vol. 16, No. 5, pp. 427-445.

Casadei, M., Dietrich, W. E., and Miller, N. L. (2003): Testing a model for predicting the timing and location of shallow landslide initiation in soil-mantled landscapes, Earth Surface Processes and Landforms, Vol. 28, No. 9, pp. 925-950.

Chang, K.T., and Chiang, S.H. (2009): An integrated model for predicting rainfall-induced landslides, Geomorphology, Vol. 105, No. 3–4, pp. 366-373.

Chen, C.Y., and Fujita, M. (2013): An analysis of rainfall-based warning systems for sediment disasters in Japan and Taiwan, International Journal of Erosion Control Engineering, Vol. 6, No. 2, pp. 47-57.

Chen, C.Y., and Fujita, M. (2014): A method for predicting landslides on a basin scale using water content indicator, Journal of Japan Society of Civil Engineers, Ser. B1 (Hydraulic Engineering), Vol. 70, No.4, pp.I_13-I_18.

Chen, L.C., Wu, J.Y., Liu, Y.C., and Lee, I.H. (2007): A study of residential evacuation behavior and decision-making in a vulnerable debris flow area: The case of typhoon Talim, Journal of Chinese Soil and Water Conservation, Vol. 38, No. 4, pp. 325–340 (in Chinese).

Chen, L.C. and Mars, S.Y. (2008): A study of evacuation decisions of governments under large-scale disasters, National Science Council, Taiwan (in Chinese).

Chigira, M., Tsou, C.Y., Matsushi, Y., Hiraishi, N., Matsuzawa, M.(2013): Topographic precursors and geological structures of deep-seated catastrophic landslides caused by Typhoon Talas, Geomorphology, Vol. 201, pp. 479-493.

Chen, Y.S., Kuo, Y.S., Lai, W.C., Tsai, Y.J., Lee, S.P., Chen, K.T., and Shieh, C.L. (2011): Reflection of typhoon Morakot – The challenge of compound disaster simulation, Journal of Mountain Science, Vol. 8, No. 4, pp. 571–581.

Dash, N., and Gladwin, H. (2007): Evacuation decision making and behavioral responses: Individual and household, Natural Hazards Review, Vol.8, No. 3, pp. 69-77.

Department of Erosion and Sediment Control (DESC) (2007): Guidelines for warning systems and evacuations, Japan (in Japanese).

Dow, K. and Cutter, S. L. (1998): Crying wolf: Repeat responses to hurricane evacuation orders, Coastal Management, Vol. 26, No. 4, pp. 237–252.

Egahsira, S., and Matsuki, K. (2000): A method for predicting sediment runoff cased by erosion of stream channel bed, Annual Journal of Hydralic Engineering, JSCE, Vol. 44, pp. 735-740 (in Japanese with English abstract).

Gladwin, H. and Peacock, W. G. (1997): Warning and evacuation: A night of hard choices. In: W. G. Peacock, B. H. Morrow, and H. Gladwin (eds) Hurricane Andrew: Gender, Ethnicity and the Sociology of Disasters Routledge, London, pp. 52–73.

Highland, L. M., and Bobrowsky, P. (2008): The landslide handbook—A guide to understanding landslides, U.S. Geological Survey Circular 1325, Reston, Virginia.

Ichikawa, Y., Satoh, Y., Shiiba, M., Tachikawa, Y., and Tkaara, K. (1999): Development of a water and sediment flow model for a mountainous area, Annuals. Disaster Prevention Res. Inst., Kyoto Univ., Vol. 42, No. B-2, pp. 211-224 (in Japanese with English abstract).

Irasawa, M., and Endo Y. (2010): An opinion poll administered to Kamaishi City residents about at sediment disaster generated by rainfall in July 2002, Journal of Iwate University, Vol. 41, pp. 259-272. (in Japanese)

Iverson, R. M. (2000): Landslide triggering by rain infiltration, Water Resources

Research, Vol. 36, No. 7, pp. 1897-1910.
Kappes, M.S., Keiler, M., and Glade, T. (2010a): From Single- to Multi-Hazard Risk Analyses: a concept addressing emerging challenges, Proceedings of the 'Mountain Risks' International Conference, Firenze, Italy, 24-26 Nov. 2010.
Kappes, M.S., Keiler, M., and Glade, T. (2010b): Consideration of Hazard Interactions in Medium-Scale Multi-Hazard Risk Analyses", Geophysical Research Abstracts Vol. 12, EGU2010-3331, EGU General Assembly 2010, Vienna, Austria.
Kappes, M. S., Keiler, M., von Elverfeldt, K., and Glade, T. (2012a): Challenges of analyzing multi-hazard risk: a review, Natural Hazards, Vol. 64, pp. 1925-1958.
Kappes, M. S., Papathoma-Köhle, M., and Keiler, M. (2012b): Assessing physical vulnerability for multi-hazards using an indicator-based methodology, Applied Geography, Vol. 32, No. 2, pp. 577-590.
Kondo, S., Kataie, Y., Ota, K. (2012): Disaster Response of Municipal Government at Southern area of Wakayama Prefecture after Flood and Sediment Disaste by Typhoon Talas, SEISAN KENKYU, Vol. 64, No. 4, pp. 527-531. (in Japanese)
Lee, C.T., Dong, J.J.(2009): Geological Investigation on the Catastrophic Landslide in Siaolin Village, Southern Taiwan, Sino-Geotechnics, No.122, pp.87-94. (in Chinese)
Lee, G., Kim, S., Jung, K., and Tachikawa, Y. (2011): Development of a large basin rainfall-runoff modeling system using the object-oriented hydrologic modeling system (OHyMoS), KSCE J Civ Eng, Vol. 15, No. 3, pp. 595-606.
Lin, C.Y. (2007): A study of evacuation of commercial populations under large-scale disasters, National Science Council, Taiwan (in Chinese).
Lindell, M. K., Lu, J.-C., and Prater, C. S. (2005): Household decision making and evacuation in response to hurricane Lili, Natural Hazards Review, Vol. 6, No. 4, pp. 171–179.
Lindell, M. and Prater, C. (2007): A hurricane evacuation management decision support system (EMDSS), Natural Hazards, Vol. 40, No. 3, pp. 627–634.
Miyata, S., Fujita, M. (2013): Application of X-band Radar and Runoff Model to Debris Flow Frequently Occurred Creeks in Sakurajima Island, Annuals. Disaster Prevention Res. Inst., Kyoto Univ., Vol. 56, No. B, pp. 457-464 (in Japanese with English abstract).
National Institute for Land and Infrastructure Management (NILIM) (2004): Guidelines for Development of Warning and Evacuation System Against Sediment Disasters in Developing Countries: Planning, Japan.
National Institute for Land and Infrastructure Management (NILIM) (2010): Studies of warning system and evacuation for sediment disaster, 23th Sabo research report (in Japanese).
National Science and Technology Center for Disaster Reduction (NCDR) (2013): Hazard Map Website, http://satis.ncdr.nat.gov.tw/Dmap/102Catalog.aspx (in Chinese).
Osanai, N.,Shimizu, T.,Kuramoto, K.,Kojima, S., andNoro, T. (2010): Japanese early-warning for debris flows and slope failures using rainfall indices with Radial Basis Function Network, Landslides,Vol. 7, pp. 325–338.
Onda, Y., Mizuyama, T., andKato, Y. (2003): Judging the timing of peak rainfall and the initiation of debris flow by monitoring runoff. In Rickenmann, D. and Chen, C.L (eds), Debris-Flow Hazards Mitigation: Mechanics, Prediction, and Assessment, Millpress, Rotterdam, pp. 147–153.
Pai, J.T. (2008): A study of the evacuation of disadvantaged groups under large-scale

disasters, National Science Council (in Chinese).
Perry, R. W. (1979): Evacuation decision-making in natural disasters, Mass Emergencies, Vol.4, pp. 25-38.
Regnier, E. (2008): Public Evacuation Decisions and Hurricane Track Uncertainty, Management Science, Vol.54, No.1, pp. 16-28.
Tachikawa, Y., Nagatani, G., and Takara, K. (2004): Development of stage-discharge relationship equation incorporating saturated-unsaturated flow mechanism, Annual Journal of Hydraulic Engineering, JSCE, Vol. 48, No., pp. 7-12 (in Japanese with English abstract).
Takahashi, T., Inoue, M., Nakagawa, H., and Satofuka, Y. (2000): Prediction of sediment runoff from a mountain watershed, Annual Journal of Hydralic Engineering, JSCE, Vol. 44, pp. 717-722 (in Japanese with English abstract).
Takasao, T., and Shiiba, M. (1988): Incorporation of the effect of concentration of flow into the kinematic wave equations and its applications to runoff system lumping, Journal of Hydrology, Vol. 102, No. 1–4, pp. 301-322.
Tierney, K. (2005): Effective Strategies for Hazard Assessment and Loss Reduction: The Importance of Multidisciplinary and Interdisciplinary Approaches, presented at 2004 National Workshop of Disaster Reduction Related ProjectsTaipei, Taiwan.
Tsou, C.Y., Feng, Z.Y. andChigira, M. (2011): Catastrophic landslide induced by Typhoon Morakot, Shiaolin, Taiwan, Geomorphology, Vol. 127, No. 3-4,pp. 166-178.
Tsutsumi, D., Fujita, M., Hayashi, Y. (2007): Numerical simulation on a landslide due to typhoon 0514 in taketa city, oita prefecture,Annual Journal of Hydralic Engineering, JSCE, Vol. 51, pp. 931-936 (in Japanese with English abstract).
Ushiyama, M. (2012): The possibility of reducing sediment disaster victims based on information, Conference of Japan Society of Erosion Control Engineering 2012, pp. 138–139 (in Japanese).
Ushiyama, M., Imamura, F., and Takara, K. (2003): Investigation of people's behavior in the highly flood disaster information ago – A case study on the typhoon No.0206 July, 2002., Annuals of Disaster Prevention Research Institute Kyoto University, 46(B), 249-262. (in Japanese)
Vieira, B. C., and Fernandes, N. F. (2004): Landslides in Rio de Janeiro: The role played by variations in soil hydraulic conductivity, Hydrological Processes, Vol. 18, No. 4, pp. 791-805.
Wang, C., Esaki, T., Xie, M., and Qiu, C. (2006): Landslide and debris-flow hazard analysis and prediction using GIS in Minamata–Hougawachi area, Japan, Environ Geol, Vol. 51, No. 1, pp. 91-102.
Whitehead, J. C., Edwards, B., Van Willigen, M., Maiolo, J. R., Wilson, K., and Smith, K. T. (2000): Heading for higher ground: Factors affecting real and hypothetical hurricane evacuation behavior, Global Environmental Change Part B: Environmental Hazards, Vol. 2, No. 4, pp. 133–142.
Wieczorek, G.F. and Glade, T. (2005): Climatic factors influencing occurrence of debris flows. In: Jakob, M. and Hunger, O. (eds), Debris-flow Hazards and Related Phenomena, Praxis, Springer Berlin, pp. 325–362.
Wu, J.Y. (2009): A comparative study of residential evacuation decisions and behavior for vulnerable debris flow areas, Journal of Slopeland Hazard Prevention, Vol. 8, No. 1, pp. 1–14 (in Chinese).
Xie, M., Esaki, T., and Zhou, G. (2004): GIS-Based Probabilistic Mapping of Landslide Hazard Using a Three-Dimensional Deterministic Model, Natural Hazards, Vol. 33, No. 2, pp. 265-282.

Chapter 2

Analysis of Existing Rainfall-Based Warning Systems for Sediment Disaster

2.1 Introduction

Faced with threats of sediment disasters, the establishment of early-warning systems and evacuation strategies is recognized as one of the most important approaches for disaster risk management. Over the past few decades, there has been a considerable body of literature reporting on the use of different indices to characterize sediment disaster warning systems, including rainfall, runoff, ultrasonic and radar gauges, ground vibration sensors, video cameras, and trip wires[*Caine*, 1980; *Onda et al.*, 2003; *Arattanoand Marchi*, 2008]. Partly because rainfall is an important indicator of sediment disasters, and partly because rainfall data are more readily obtained, rainfall-based warning systems are the most commonly used sediment disaster warning systems. Owing to environmental conditions, Japan and Taiwan typically suffer from threats of sediment disasters during typhoons or periods of heavy rainfall every year; therefore, nationwide rainfall-based sediment warning systems have been established. Furthermore, these countries have considerable operational experience with sediment disaster management [*DESC*, 2007; *COA*, 2010]. For these reasons, we use the Japanese and Taiwanese sediment disaster warning systems as case studies.

The causes of sediment disasters include earthquakes as well as heavy rainfall; however, the Japanese and Taiwanese sediment disaster warning systems only issue alerts during typhoons or heavy rainfall. The Japanese warning system only applies to debris flows and slope failures, but not to landslides[*Osanai et al.*,2010], and the Taiwanese warning system applies only to debris flows [*Chen*, 2008].

Over the past few decades, there have been a number of studies attempting to establish a rainfall-based sediment disaster-warning model. For example, *Wieczorek and Glade* [2005] conducted a literature review of rainfall-based debris-flow warning models around the world. A complete sediment disaster warning system should be comprised of two parts: a warning model and an issuing system. But because most

studies have only focused on the establishment of a warning model and have not considered complex situations that may be encountered during practical operations, these models usually have had limited success when applied during typhoons or heavy rainfall. Furthermore, the effectiveness of most warning models is based solely on whether an alert was issued before the disaster [*NILIM*, 2007], and do not consider the needs of local governments making evacuation decisions. According to the statistics collected by *NILIM* [2010], the proportion of Japanese local governments that actually carried out evacuation orders after a sediment disaster alert was issued was only 2.2% in 2008, and furthermore, only 2.8% of inhabitants decided to evacuate when they received a sediment disaster alert. This indicates that the existing warning models are not taken seriously.

Taking the Japanese and Taiwanese sediment disaster warning systems as examples, this study explores both warning models and alert-issuing systems, and identifies shortcomings using the available statistical and case study data. This study then recommends disaster prevention strategies.

2.2 Methodology

2.2.1 Rainfall-based warning system in Japan

(1) Warning model

Japan has had a rainfall-based sediment disaster warning system in place since 1984. It uses the short-term rainfall index (e.g., 60 minute cumulative rainfall) and long-term rainfall index (e.g., antecedent rainfall or soil water index) to demarcate the threshold for sediment disasters (critical line, CL)[*Osanai et al*.,2010]. During typhoons or heavy rainfall, rainfall data will be converted to short-term and long-term rainfall indices, and plotted on a graph to form a continuous 'snake line' curve. A sediment disaster alert will be issued when the CL is predicted to be exceeded by the expected rainfall in the following1–3 hours (see **Figure 2.1**) [*Osanai et al*.,2010; *NILIM*, 2001; *DESC et al*., 2005]. The development and evolution of rainfall index are shown in **Table 2.1** [*Osanai et al*, 2010]. Because the previous method of determining the CL required a vast amount of sediment disaster occurrence rainfall data, which did not exist in many regions, the radial basis function network (RBFN) has been used to demarcate the CL since 2005 [*DESC et al.*, 2005]. The RBFN has been implemented

nationwide since 2008 because it is a more objective measure of the CL and does not require as much sediment disaster rainfall data [*Osanai et al.*, 2010]. Furthermore, to solve the problem of insufficient rain-gauge density, the Japan Meteorological Agency (JMA) has produced 1-km grid mesh rainfall data known as the radar automated meteorological data acquisition system (radar AMeDAS) analytical rainfall, and short-duration rainfall forecasts (1–6 hours).

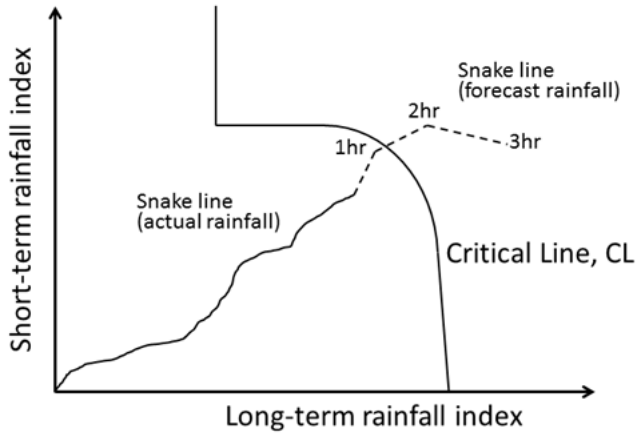

Figure 2.1 Basic concept used for sediment disaster warning models in Japan.

Table 2.1 Summary of rainfall indices and methods setting the critical line used by MLIT in Japan (Osanai et al., 2010)

Year	Short-term rainfall index	Long-term rainfall index	Method of boundary fitting
1984	60-min cumulative rainfall	AP (half time: 24 h)	By eye
1984	Effective rainfall	AP (half time: 24 h)	By eye
1993	AP (half time: 1.5 h)	AP (half time: 72 h)	By eye
2005	60-min cumulative rainfall	Soil-water index	Radial Basis Function Network

(2) Alert-issuing system

A sediment disaster alert in Japan is issued jointly by the Sabo Department of the prefecture and the local meteorological observatory using mass media, telephone, FAX, and the Internet. The warnings are issued in real time; the format and content are as shown in **Figure 2.2 (a)** [*DESC and JMA*, 2005]. The smallest unit of the alert zone is a township. The content of the alert describes which townships are at high risk of a sediment disaster, and addresses possible regions of maximum rainfall and the rainfall intensity in the next 1–3 hours. In addition, the Sabo Department of the prefecture also offers detailed information on their website that displays various levels of sediment disaster risks using a 5-km grid (see **Figure 2.2 (b)**).

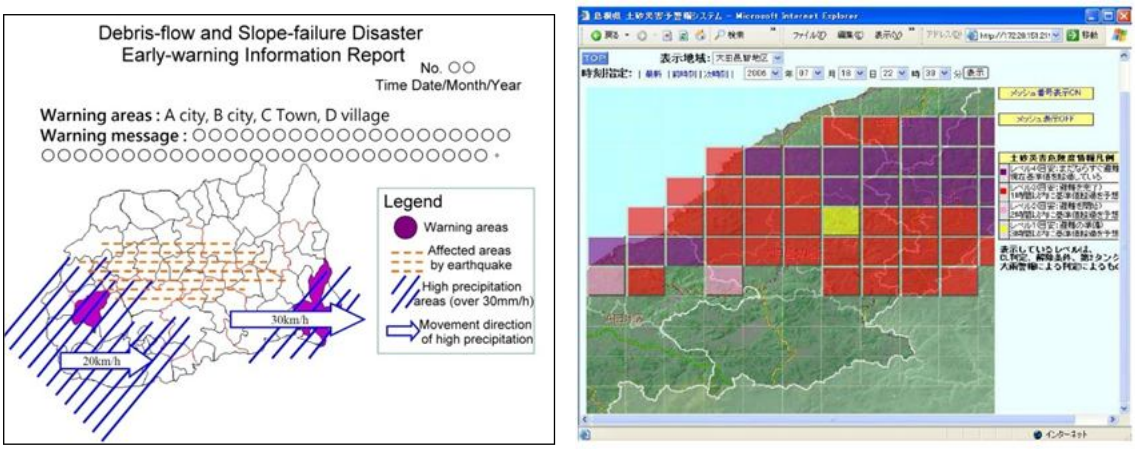

(a) (b)

Figure 2.2 (a)Format and content of a sediment disaster alert [DESC and JMA, 2005] (b) Using 5 km grid meshes to display the various levels of risk online [Osanai et al., 2010]

2.2.2 Rainfall-based warning system in Taiwan

(1)Warning model

The research of sediment disaster warning system had been conducted since Typhoon Ofelia in 1990, but the nationwide rainfall-based sediment disaster warning system was established in 2002 [*Chen*, 2008]. Because Taiwan's Disaster Prevention and Response Act only stipulates debris flows disaster but not slope failures and landslides, Taiwan's sediment disaster warning system was designed only for debris flow disasters. Initially, Taiwan's warning system also used short-term and long-term rainfall indices to define the CL for each township, and the alert would be issued if the snake line exceeded the CL (see **Figure 2.3**) [*Chen*, 2008].

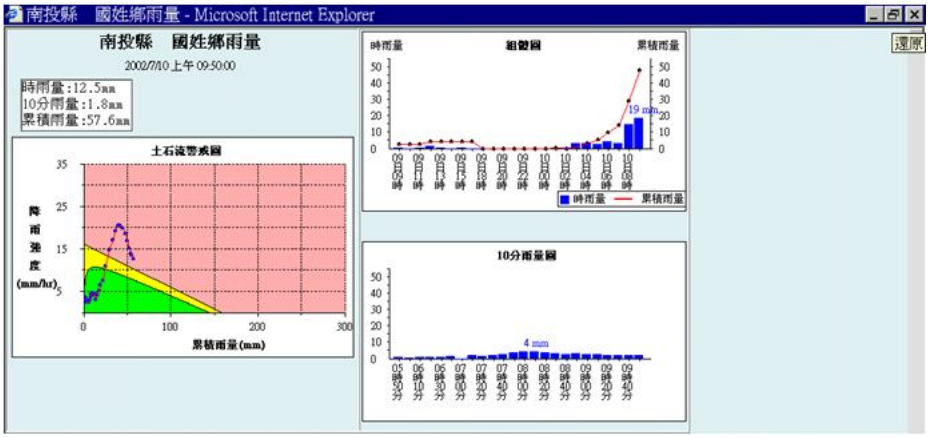

Figure 2.3 The debris-flow warning system used during 2002-2004 in Taiwan (Sample)

However, to meet the demand for alerts at the village-scale and to provide an easy-to-understand index for self-evacuation during typhoons or heavy rainfall, Taiwan developed a new rainfall-based warning model known as the rainfall-triggering index, *RTI*, which is calculated as follows:

$$RTI = I \times R_t \tag{2.1a}$$

where

$$R_t = \sum_{i=0}^{7} \alpha^i R_i \tag{2.2b}$$

where I is the intensity of the rainfall over a 60-minute period, R_t is the effective accumulated rainfall, which is the amount of rainfall for the antecedent i days (i.e., R_i), and α is a weighting factor = 0.8. To determinate representative values of the *RTI* for each township, historical rainfall data for each township were added to a graph, and RTI_{10} (a debris flow occurrence probability of 10%) and RTI_{90} (a debris flow occurrence probability of 90%) were demarcated using a manual method (see **Figure 2.4**) [*Jan and Li*, 2004]. To set a rainfall threshold for easier public understanding and local application, a critical accumulated rainfall, R_c, is calculated by taking the rainfall intensity at 10 mm/hour, i.e., using the value of RTI_{70} divided by 10 and modified to the closest 50-mm interval. According to the list from the Soil and Water Conservation Bureau (*SWCB*), the critical accumulated rainfall in 2014 was in the range of 250–600 mm. The evolution of rainfall thresholds for debris flow in Taiwan is shown in **Table 2.2** [*SWCB,* 2014].

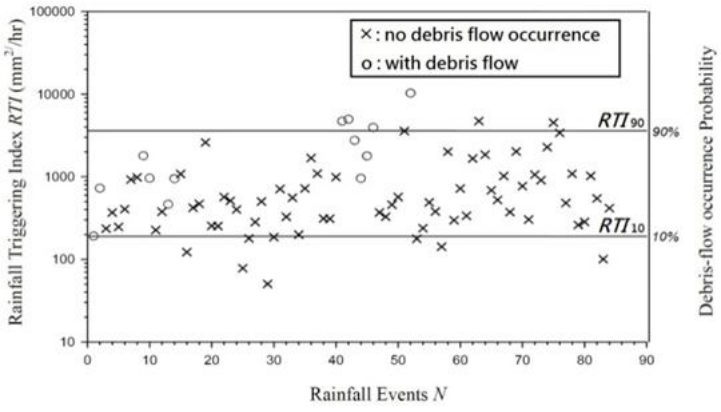

Figure 2.4 Classification of debris-flow occurrence probability based on the rainfall-triggering index [*Jan and Li*., 2004].

Table 2.2 The evolution of rainfall thresholds for debris flow in Taiwan [*SWCB*, 2014]

Year	2005	2006	2007-2008	2009	2010-2011	2012-2014
Rainfall threshold (mm)	200-350	200-450	250-550	250-600	200-600	250-600

The warning model uses rainfall data produced from the 524 rain gauges of the Central Weather Bureau (*CWB*), and the rainfall data are updated every 10 minutes [*Chang,* 2011]. Based on the locations of the rain gauges and potential debris flow torrents, *SWCB* divides each township into several regions, which are designated to refer to the specific rain gauges (see **Table 2.3**).

Table 2.3 List of rainfall thresholds and selected rain gauges in Taiwan (sample) [*SWCB*, 2014].

County	Township	Warning Areas		Critical accumulated rainfall (mm)	Selected rain gauge	
		Villages (Number of potential debris flow torrents per village)	Total number of potential debris flow torrents		1	2
Yilan	Su-ao	Yonchun (2)	2	500	Su-ao	Don-au
		Yonlo (7)	7		Don-au	Su-ao
		Chaoyang(4)	4		Nan-ao	Wushibi
		Nanchen (1), Chan-an (1), Subei(1), Shanwho (4)	7		Su-ao	Donshan
	Dongshan	Zhongshan(5), De-an(2)	7	550	Shinliao	Hanshi
		Dajin(2), Tai-ho(1)	3		Hanshi	Shinliao
		Anping(2), Dongcheng(1)	3		Donshan	Shinliao

(2)Alert-issuing system

Sediment disaster alerts in Taiwan are issued by the central government (*SWCB*) using mass media, telephone, FAX, the Internet, and volunteers. Alerts are issued according to a fixed schedule (i.e., daily at 5:00, 11:00, 17:00, 20:00, and 23:00), and extra alerts will be issued if necessary. Alerts are divided into two levels: yellow and red. A yellow alert means that the sum of the forecast rainfall over the next 24hours and the effective accumulated rainfall, R_p+R_t, is greater than R_c, and the local government and inhabitants should prepare for evacuation. A red alert is issued when R_t is greater than R_c, and the local government could execute mandatory evacuations in the warning areas. The process for issuing debris flow disaster alerts is shown in **Figure 2.5**, and the format of the debris flow disaster alerts is shown in **Figure 2.6**. In

addition, detailed warning information is also presented using Google Maps and Google Earth on the *SWCB* website [*SWCB*, 2014].

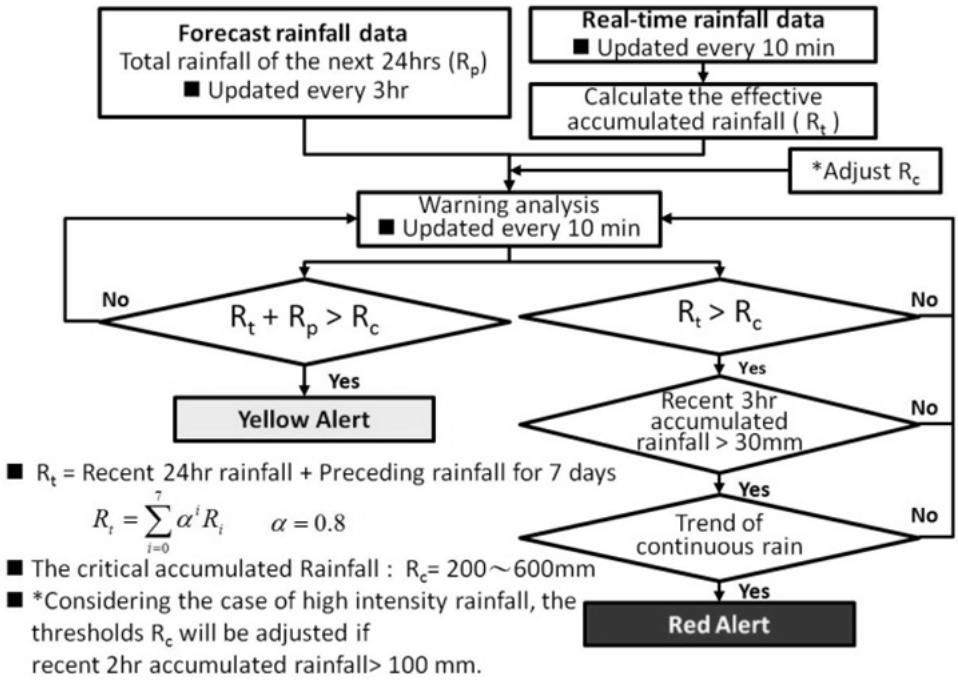

Figure 2.5 Process for issuing debris flow disaster alerts in Taiwan.

Debris-flow Disaster Early-Warning Information Report

Time Date/Month/Year No. OO

Subject: Issuing debris flow disaster Red/Yellow Alert, and the warning areas are showed as the Tables.

Suggestions:OOOOOOOOOOOOOOOOOOOOOOOOOOOOOOOOOOOO

County	Township	Critical Accumulated Rainfall (mm)	Warning Areas		
			The number of potential debris flow torrents	Warning Level	Villages (The number of potential debris flow torrents)
Pingtung	Shizi	500	17	Yellow	Danlo(4), Nanshi(3), Neishi(2), Shizi(2), Zukon(3), Neiwen(2) Chaopu(1)
	Wutai	400	2	Red	Wutai(1)、Ali(1)
	Sandimen	400	1	Red	Dalai(1)
		400	6	Yellow	Chinye(1), Chinsan(1), Anpo(1), Koasoa(3)
OOO	XXX	550	12	Yellow	…
	XXX	450	5	Red	…
	XXX	600	1	Yellow	…
		350	7	Yellow	…

Figure 2.6 Format of debris flow disaster alerts from the SWCB.

2.2.3 Evaluating the effectiveness of the warning models

The effectiveness of the warnings is a significant factor in the evacuation decisions taken by local governments. A good warning system not only needs to promptly issue alerts before a disaster occurs, but must also avoid false alerts since local governments and inhabitants will ignore the warnings if there are too many false alerts.

This study uses four indices to evaluate the effectiveness of a warning model: the hit rate, false alert rate, warning coverage rate, and time available for evacuation. The warning hit rate describes the frequency with which an alert is issued before a sediment disaster occurs. The false alert rate describes whether alerts are being issued where no disaster will occur. The warning coverage rate assesses to what extent the spatial locations of a sediment disaster are issued a warning.

The warning hit rate (WHR) can be expressed as

$$WHR = DEAA / DE \tag{2.2}$$

and the false alert rate (FAR) can be expressed as

$$FAR = WTND / WT \tag{2.3}$$

where DE is the number of sediment disaster events, DEAA is the number of sediment disaster events that were located within the warning areas and occurred after a warning was issued, WT is the number of townships which had been issued a sediment disaster warning, and WTND is the number of townships which had been issued a sediment disaster warning but where no disaster occurred [*NILIM*, 2007]. To characterize the proportion of sediment disasters that were not located within the warning area, as well as the hit rate in the warning area, we define the warning coverage rate (WCR) as

$$WCR = DEA / DE \tag{2.4}$$

and the warning hit rate in the warning area (WHRWA) as

$$WHRWA = DEAA / DEA \tag{2.5}$$

where DEA is the number of sediment disaster events that occurred in the warning areas. **Figure 2.7** illustrates an example of these warning model effectiveness indices.

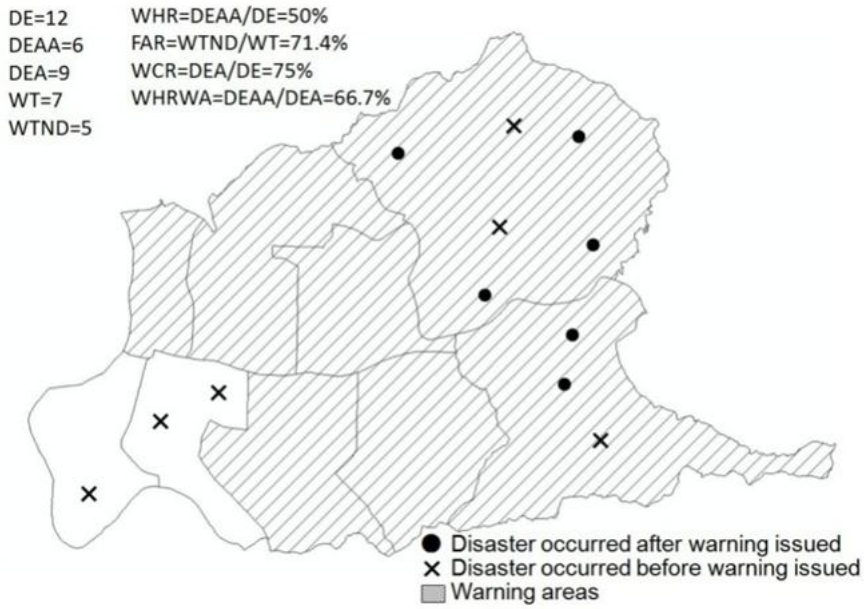

Figure 2.7 Example of the warning model effectiveness indices.

To explore whether the time for evacuation is sufficient, we define the "remaining time for evacuation (RTE)" as the time from the alert being issued to the time the disaster occurs. According to the warning hit rate definition, an alert is regarded as successful if RTE ≥0. However, some time is required for the alert dissemination and the evacuation; we define this time as the "shortest remaining time for evacuation (SRTE)". A valid alert has to be issued at a time at least equal to the SRTE before the disaster occurs. Owing to traffic conditions and the population structure, different regions may have different SRTE values.

Lindell *et al.* [2005] investigated the evacuation behavior of people living in coastal regions during a hurricane, and found that the average evacuation time was 3 hours and 16 minutes. There have been a number of studies of the evacuation time for people living near potential debris flow torrents in mountainous areas of Taiwan. *Pai* [2008] found that the average evacuation time for these groups was 2 hours and 40 minutes; 90 percent could be evacuated in 3 hours, and the evacuation could be completed in 7 hours. *Lin* [2007] suggested that it would take more than 8 hours for the evacuation rate to be greater than 95%. A survey has shown that the average evacuation time is 2.62 hours in Shueili Township of Nantou County, and 3.83 hours in Jiashih Township of Hsin Chu County [*Wu*, 2009]. Accordingly, here, we assume that the SRTE is 3 hours.

2.2.4 Evaluation methods for the evacuation rate

Because township governments are responsible for the making the decision to evacuate, as well as for executing the evacuation in Japan and Taiwan, this study used the township as the assessment unit. The evacuation rate (ER) after an alert is issued is defined as

$$ER = EWT / WT \quad (2.6)$$

where EWT is the number of townships that are located in the warning area and have carried out an evacuation.

2.3 Results and discussion

2.3.1 Comparison of the Japanese and Taiwanese warning systems

Table 2.4 compares the Japanese and Taiwanese warning systems, including the warning models and alert-issuing systems. We will examine the significant differences based on the following factors.

(1)Warning model

The RBFN used in Japan is more objective than the RTI used in Taiwan for defining the CL, and in addition, makes artificially demarcating the CL unnecessary. It can be used in areas lacking historical disaster data and employs only considerable historical rainfall data, which are easier to acquire. Using1-km grid mesh rainfall data as a resource for the warning indices may be an effective means of solving the problem of insufficient rain gauges in the Japanese system.

(2) Alert-issuing system

Sediment disaster alerts are issued by the prefectures in Japan. The unit of a warning area is the township. These prefectures also offer a detailed range for warnings using 5-km grid meshes, which display the risk level using different colors (some prefectures, for example, Nara, offer 1-km grid meshes), so the townships can judge which areas may be at a higher risk of sediment disasters. Because of the lack of technology and budgets to build warning systems at the local government level, sediment disaster alerts are issued by the central government (SWCB) in Taiwan. Alerts that show which village is at a higher risk of debris flow disasters are disseminated to counties and townships simultaneously. To be easily understood by everyone, the high-risk areas for potential debris flow torrents are marked on Google

Earth and Google Maps, and anyone can view this data via the Internet. Moreover, Taiwan's warnings are issued on a fixed schedule (although additional alerts may be issued if necessary). This not only avoids confusing information, but also ensures that all disaster prevention units, the media, and inhabitants can obtain the latest warning information easily by themselves.

Table 2.4 Comparison of the Japanese and Taiwanese warning systems.

Topics		Japan	Taiwan	Comparison
Warning model	Method of defining CL	RBFN	RTI	RBFN is more objective than RTI for defining CL, and it can be used in areas lacking historical disaster data
	Warning indices	60-minute cumulative rainfall and soil-water index	Effective accumulated rainfall and recent 3-hour rainfall	Taiwan's warning system uses the effective accumulated rainfall as the main index
	Types of rainfall data	1-km grid mesh rainfall data and 1–3 hour rainfall forecast	Real-time rain gauge data (10 min updates) and 24-hour rainfall forecast	Using grid mesh rainfall data can solve the problem of having insufficient rain-gauge data
	Who modifies CL?	Prefectures	Central government(SWCB)	-
Alert-issuing system	Who issues alerts?	Prefectures	Central government(SWCB)	-
	Who receives the alerts?	Township	County and Township	-
	Criteria for issuing alerts	Predict if the snake curve will cross CL in 1–3 hours	Effective accumulated rainfall is higher than Rc, as well as recent 3-hour accumulated rainfall is higher than 30 mm, and rainfall will last	The Taiwanese warning system requires more manual operations and experienced operators
	Interval between issuing alerts	Non-fixed	Daily at 5:00, 11:00, 17:00, 20:00, and 23:00; extra alerts will be issued if necessary	All disaster prevention units, media, and inhabitants can obtain the latest warning information easily by themselves if issued on a fixed-time basis
	Levels of alerts	One level (sediment disaster alert)	Two levels (yellow alert and red alert)	Understanding risks using colors may be suitable
	Unit of warning area	Township	Village	-
	Alert dissemination tools	Telephone, FAX, messages, Internet	Telephone, FAX, messages, Internet, volunteers	-
	Format of alerts	Text-based, supplemented by graphics	Table-based, supplemented by text	-
	Presentation of detailed information of the warning areas	5-km grid to present risk levels	Display warning areas using Google Maps and Google Earth	-
	Types of disaster	Debris flows and slope failures	Only debris flows	-

2.3.2 Effectiveness assessment of the existing warning systems in Japan and Taiwan

(1)Japan

According to statistics from *NILIM* [2010], a total of 669 sediment disasters took place in 2008 in Japan. One hundred and ninety-two (28.7%) occurred outside of the warning areas, almost all of which were slope failures. A total of 1,129 townships were designated warning areas during typhoons or heavy rainfalls in Japan in 2008, but only 138 townships suffered sediment disasters. The number of sediment disasters that occurred in the warning areas was 477, and 356 of them occurred after the sediment disaster alerts were issued. The effectiveness of the warning system in 2008 is summarized in **Table 2.5**.

(2) Taiwan

Although the sediment disaster warning system in Taiwan only includes debris flow disasters, for the benefit of comparison, the following statistics include debris flow and slope failure disasters. According to the debris flow annual from *SWCB* [2007–2011], the number of significant disasters investigated by *SWCB* in 2009 in Taiwan was 127. Excluding simple flood disasters, there were 117 sediment disasters, and 113 occurred during Typhoon Morakot in 2009. Twenty-six of them (22.2%) occurred outside of the warning areas, and almost all of these happened in villages that were never designated as potential debris flow torrent areas (i.e., these villages were not within the range of the warning systems). Seventy-two townships were designated as warning areas during typhoons or heavy rainfall in 2009 in Taiwan, but only 30 townships suffered sediment disasters. The number of sediment disasters that occurred in warning areas was 91, and 85 occurred after the sediment disaster alerts were issued. The warning effectiveness in 2009 in Taiwan is summarized in **Table 2.5.**

Based on the statistics of the sediment disaster data in the debris flow annual from *SWCB* for the period 2007–2011, the average warning hit rate was WHR = 45.4%, the average false alert rate was FAR = 75.2%, the average warning cover rate was 62.6%, and the average warning hit rate in the warning areas was 72.6%. These are also listed in **Table 2.5**.

Table 2.5 Effectiveness of the sediment disaster warning systems in Japan and Taiwan (including debris flows and slope failures).

	WT	WTND	FAR =WTND/WT	DE	DEA	DEAA	WHR =DEAA/DE	WCR =DEA/DE	WHRWA =DEAA/DEA	EWT	ER= EWT/WT
Japan (2008)	1129	991	87.8%	669	477	356	53.2%	71.3%	74.6%	25	2.2%
Taiwan (2009)	72	42	58.3%	117	91	85	72.6%	77.8%	93.4%	46	63.9%
Japan (Average in 2008-2010)*	2965	2475	83.4%	2482	-	1460	58.8%	-	-	291	9.8%
Taiwan (Average in 2007-2011)	310	233	75.2%	262	164	119	45.4%	62.6%	72.6%	160	51.6%

*The averages were obtained from *Okamoto et al.* [2012]

(3)False alert rate and impact on evacuation

Based on these sediment disaster-warning statistics for Japan and Taiwan, the warning hit rate was 45–59%, but the false alert rate was greater than 75%. For example, in Japan in 2008, the false alert rate was 87.8%. That is, only 12.2% of the townships that suffered sediment disasters were in the warning areas. Such a large false alert rate is harmful for disaster prevention [*DESC,* 2007; *Amano and Takayama*, 2006]. According to a survey of the evacuation rate in warning areas in Japan in 2008, only 2.2% of the township governments released evacuation orders, and more than 80% of the evacuation orders were released after disasters occurred; moreover, only 2.8% of inhabitants in the alert-issued areas decided to evacuate [*MILIM,* 2010].

Compared with Japan, the evacuation rate in Taiwan was higher (see **Table 2.5**). The main reason was that the Central Emergency Operation Center (*CEOC*) always forced the local governments to evacuate inhabitants living in the warning areas during typhoons.

2.3.3 Affected factors of warning effectiveness

To investigate the practical operational factors that may affect the effectiveness of a sediment disaster warning system, we analyzed statistical data covering the period 2007–2011 in Taiwan. The following trends were observed:

(1) The scale of the disaster (i.e., the number of disasters) was related to warning hit rate, false alert rate, and warning coverage rate (see **Figure 2.8**). The existing rainfall-based warning model was more effective for large-scale disasters. For example, in 2009, the warning hit was 72.6%, the warning coverage rate was

77.8%, and the false alert rate was 58.3%. Similar results have been shown in Japan [*Okamoto et al.*, 2012].

(2) Due to the impact of typhoon Morakot in 2009, there was an increase in the evacuation rate by local governments (see **Figure 2.8**).

(3) Because of the central government mandate to urge local governments to evacuate the inhabitants of warning areas, the SWCB, which is responsible for issuing warnings, came under pressure to reduce the false alert rate. From **Figure 2.8**, the false alert rate has fallen in recent years; however, the warning hit rate also fell. For example, in 2010 and 2011, the warning coverage rates were greater than 60%; however, the alert-issuing operator appears to have become more cautious and has issued alerts too late, possibly due to pressure to reduce the false alert rate. This appears to have resulted in an increase in the warning coverage rate but a decrease in the hit rate.

(4) Because the Taiwanese warning system only considers debris flow disasters, the monitored areas were limited to villages that are in potential debris flow areas. Therefore, the warning coverage rate would be lower if the statistics included slope failure. However, SWCB has continued to investigate new potential debris flow areas since 2008, so the warning coverage rate has started to increase.

(5) Comparison of the two different types of disaster events (typhoons and heavy rainfalls) found that the false alert rates in typhoons and heavy rainfalls was close, but the warning hit rate was different by 400%, and the warning cover rate was different by 220%, as show in **Table 2.6**. In fact, Taiwan's sediment disaster warning model was the same during typhoons or heavy rainfall. The data has a big gap mainly because during typhoons, the Central Weather Bureau (CWB) would regularly provide the total forecast rainfall and forecast rainfall information for the next 24 hours, but not during heavy rainfall events. This forecast rainfall information played an important role in assessing whether the rainfall would last when SWCB needed to decide whether to issue alert or not. That is, the integrity of the forecast rainfall information would also affect the warning effectiveness of sediment disaster warning.

(6) **Table 2.6** also shows that the proportion of local government carrying out evacuation ratio has a difference of 240% in warning areas between typhoons and heavy rainfall. The main reason was that the CEOC usually would not be

established during heavy rainfall. That is, the central government did not strongly ask local governments to carry out evacuation, so the evacuation ratio would be significantly reduced.

These trends indicate that the effectiveness of the Taiwanese warning system is dependent on the scale of the disaster, the decision-making tendencies of the alert-issuing operator, the integrity of the disaster potential data, and the completeness of forecast rainfall data. The central government plays an important role in the evacuation ratio.

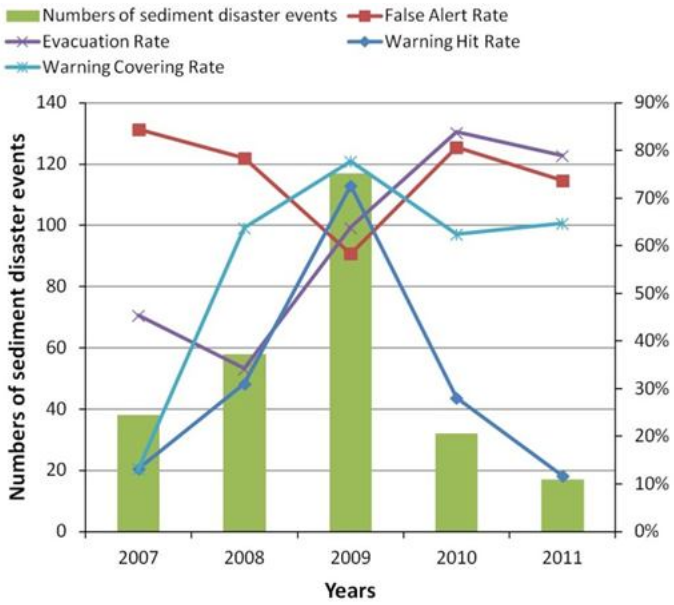

Figure 2.8 Yearly number of sediment disaster events and warning effectiveness in Taiwan.

Table 2.6 The Sediment Disaster Warning Effectiveness during Typhoons and Heavy Rainfall in Taiwan during 2007-2011

	WT	WTND	FAR =WTND/WT	DE	DEA	DEAA	WHR =DEAA/DE	WCR =DEA/DE	WHRWA =DEAA/DEA	EWT	ER= EWT/WT
Typhoon	272	205	75.4%	223	152	114	51.1%	68.2%	75.0%	222	81.6%
Heavy Rainfall	38	28	73.7%	39	12	5	12.8%	30.8%	41.7%	13	34.2%

2.3.4 Appropriate timing for issuing alerts

(1)Sediment disasters occurring timing

The timing of a disaster directly affects the difficulty of evacuation. Based on the environment of mountainous areas and the daily routines of the inhabitants, here we define the period from 21:00 to 07:00 as the difficult period for evacuation (DPE).

During this period, it is difficult not only to disseminate the alert to inhabitants, but also to carry out the evacuation. According to statistics from the SWCB in the period 2007–2011, the proportion of significant sediment disasters occurring in the DPE was 45.9% (see **Figure 2.9**). This proportion became larger than 50.0% during typhoons. Moreover, the proportion of casualties during the DPE was 52.2%.

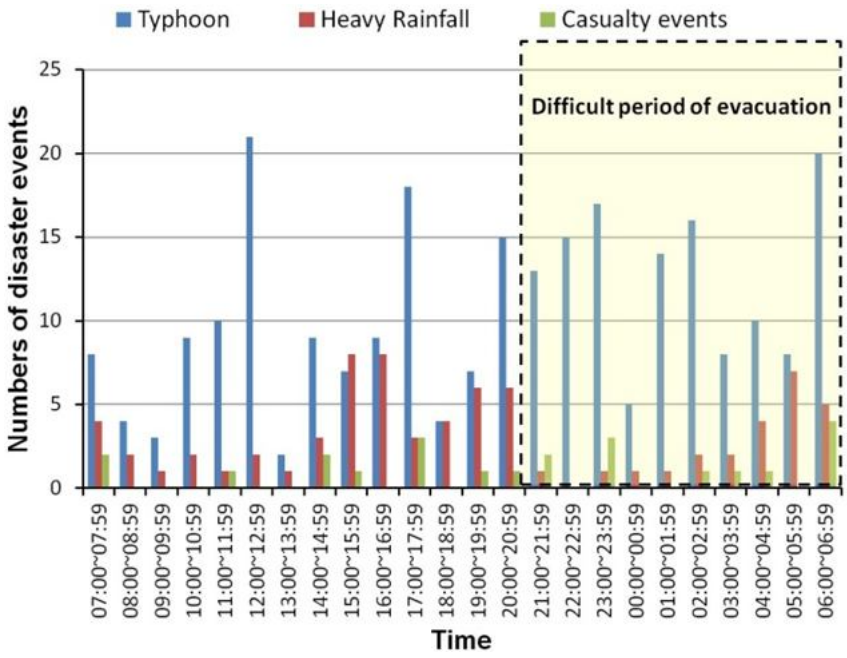

Figure 2.9 Timing of sediment disaster events in Taiwan [*SWCB*, 2007-2011].

(2) Frequency of issuing alerts

In 2002, the SWCB established a nationwide sediment disaster warning system in Taiwan, and following the Japanese warning system, started releasing alerts in real time (i.e., not on a non-fixed schedule; the alerts were issued immediately when the rainfall exceeded the CL). The real-time alerts caused problems; for example, disseminating alerts and evacuations were difficult when the alerts were issued at night, and the local governments and news agencies could not confirm whether an alert that they had was the latest. Furthermore, the alerts were updated faster than what was broadcast on television and what could be distributed by the alert dissemination system. *Amano and Takayama* [2006] also discussed similar problems in Japan. To solve these issues, the *SWCB* started to announce alerts based on a time schedule associated with the *CWB* daily rainfall forecast in 2009, at 04:00, 10:00, 16:00, and 22:00. The *SWCB* currently issues daily alerts at 05:00, 11:00, 17:00, 20:00, and 23:00, with additional alerts if necessary. Furthermore, at 17:00 and 20:00, the

SWCB issues early warnings to areas where the forecast rainfall during the next 12hours may exceed the CL to reduce the possibility of issuing alerts at night.

(3) Remaining time for evacuation

According to statistics for the period 2007–2011 in Taiwan[*SWCB*, 2007–2011], the remaining time for evacuation (RTE) was, on average, 21.6 hours, whereas in Japan in 2008 it was 4.4 hours [*NILIM*, 2010]. Both the Japanese and Taiwanese systems issued warnings with more than the recommended shortest remaining time for evacuation (SRTE) of approximately 3 hours. The main difference was that the Japanese system issued alerts in real time, whereas the Taiwanese system used a fixed-time alert-issuing system. In addition, to avoid issuing alerts at night, Taiwan's warning system issued early alerts for areas where the rainfall was forecasted to exceed the CL during the DPE.

Figure 2.10 shows that over 50% of the RTE values in Taiwan were greater than 12 hours, but over 50% of the RTE values in Japan were less than 2 hours. Considering the practical implications of mountainous areas, such as difficulties with communication and transportation, and a more elderly population, further study into whether an RTE of 2 hours is sufficient is warranted. Moreover, it does not seem reasonable that the current warning hit rate calculation in Japan does not consider the time required to disseminate alerts and evacuate. This time should be modified to include at least the SRTE when labeling a warning as valid.

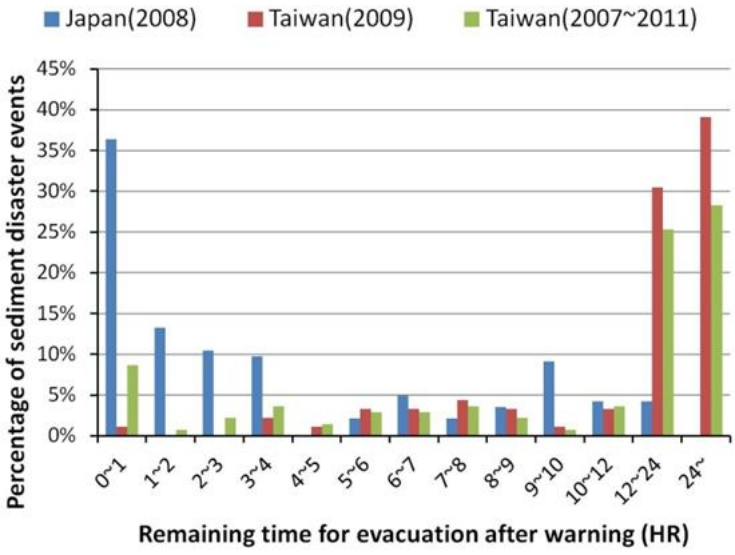

Figure 2.10 Remaining time for evacuation after a warning was issued in Japan and Taiwan [NILIM, 2010; SWCB, 2007-2011].

2.4 Case study: warnings issued during Typhoon Morakot

2.4.1 The Typhoon Morakot disaster in Taiwan

Typhoon Morakot in 2009 is the largest natural disaster in recent years in Taiwan. Its rainfall has the following characteristics:

(1) Long rainfall duration: the duration is longer than 100 hours from August 6 to 11.
(2) High rainfall intensity: the maximum rainfall intensity exceeds 130mm/hr.
(3) Huge accumulated rainfall: the accumulated rainfall in Alishan rain gauge is close to 3,000mm.
(4) Vast rainfall range: the area that the rainfall is more than 1,000mm covers 1/5 of Taiwan.

Such a large-scale, high intensity, and a huge amount of rainfall resulted in serious flooding and sediment disaster in the central and southern Taiwan. The death toll was as high as 699. In addition, the collapsed area in mountain was as large as 59,490 ha, and the collapse rate was as much as 5.52% in catchment, such as collapse magnitude was larger than the Chi-Chi Earthquake in 1999 in Taiwan [*MPDRC*, 2010].

2.4.2 Shiaolin Village

Shiaolin village located in the south of Taiwan was one of most seriously damaged areas during Typhoon Morakot. Within 19 hours, Shiaolin village suffered a multi-hazard event that included a series of flooding, debris flows, deep-seated landslides, natural dams, and dam burst [*Lee and Dong*, 2009; *Chen et al.*, 2011; *Tsou et al.*, 2011]. Prior to Typhoon Morakot, the critical accumulated rainfall, R_c, of Shiaolin village was 450 mm. On August 7, the *SWCB* issued a debris flow yellow alert at 17:00 and a red alert at 23:00. The village was inundated at 15:00 on August 8. Bridge 8, which was located to the south of the village and was the only escape route, was destroyed by a debris flow at 19:00 on August 8, leaving no evacuation routes from the village. At 06:00 on August 9, a deep-seated landslide almost completely buried Shiaolin village and killed 462 people [*MPDRC*, 2010]; the shelter (the Shiaolin elementary school) was also destroyed. The deep-seated landslide blocked the Chi-Shan River and formed a natural dam; this natural dam burst approximately one hour later. The destruction timeline is shown in **Figure 2.11**.

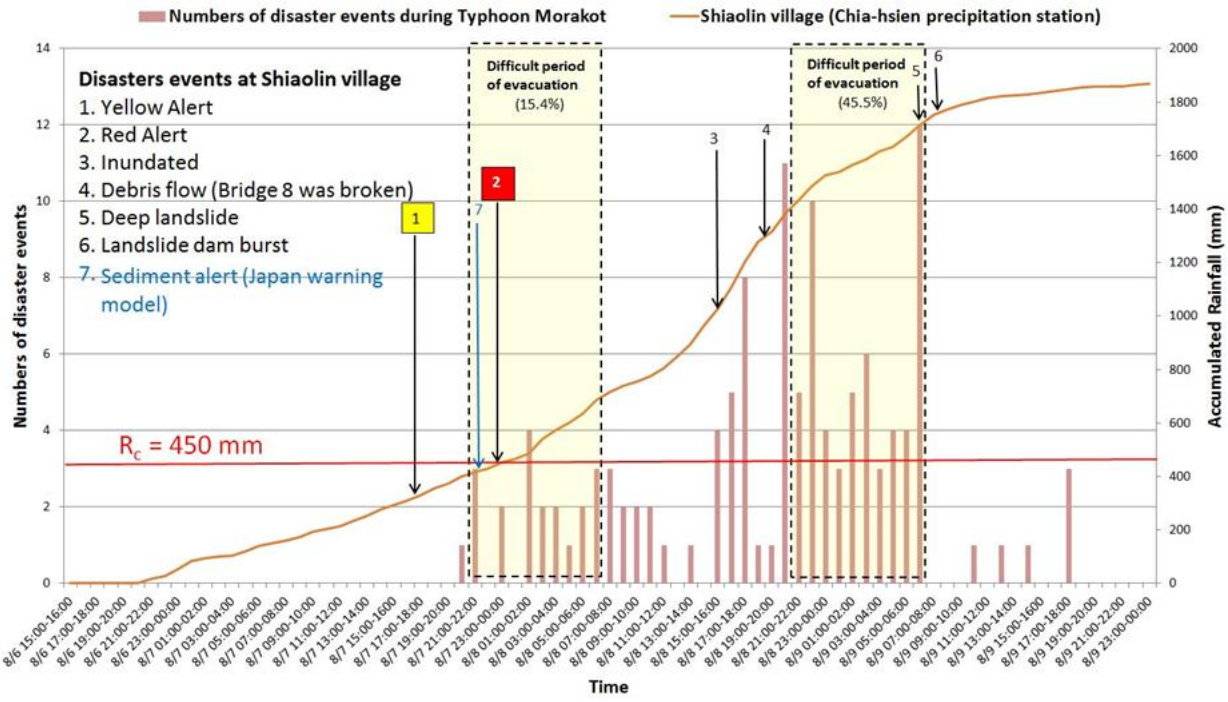

Figure 2.11 Accumulated rainfall and timeline of disaster events in Shiaolin village during typhoon Morakot [*Chen et al.*, 2011].

2.4.3 Existing warning system in Shiaolin Village

Based on the disaster events in Shiaolin village, the period from when the debris flow red alert was issued until Bridge 8 was destroyed was 20 hours. Thus, there was sufficient time to disseminate the alerts and evacuate, so the existing rainfall-based warning system in Taiwan achieved its goal of providing an early warning. However, this disaster ultimately resulted in 462 deaths (including the shelter- the Shiaolin elementary school), which indicates that there remained a number of deficiencies in the existing rainfall-based warning system. These are as follows.

(1) The existing Taiwanese and Japanese warning systems can only show which areas are at higher risk of sediment disasters during typhoons and heavy rainfall. They cannot clearly point out whether a disaster will occur or in which slope or torrent, and they cannot indicate which types of sediment disasters will occur. Even if a local government receives an alert, it is still difficult to carry out an evacuation.

(2) Both the existing Taiwanese and Japanese warning systems are based on models that depend on whether the rainfall exceeds the CL. However, the model cannot describe with certainty the relationship between the rainfall and the scale of the disaster. Therefore, even if the rainfall is predicted to be 1,000 or 2,000 mm, the existing warning model cannot determine the severity of the potential disaster.

(3) Although natural disaster in mountainous areas usually related to flooding and the moving of sediment (i.e., the rainfall-related disasters in mountainous areas usually occur as a multi-modal type, and some disaster events might affect or trigger others with the complex relationship of spatial and temporal.), the existing warning system lacked the scenario simulation capacity and the capability of overall consideration. This study case showed that a single disaster warning system or prevention plan cannot tackle the multi-modal sediment disasters.

(4) According to statistics from Typhoon Morakot, 60.9% of the sediment disasters occurred during the DPE (see **Figure 2.11**). The appropriate time for issuing these alerts is before sunset, and sufficient time should be allowed for an evacuation.

(5) The sediment-disaster warning model can only report the possibility of a disaster. The decision on whether to evacuate must consider other issues, such as the location of the village as well as the location and capacity of shelters, the traffic and communications infrastructure, and the demographics. An effective warning system that can offer accurate long-time predictions (for example, over the next 12 hours) and the scenario simulation capacity will enhance the decision-making ability of governments.

(6) To both consider how to cope with multi sediment hazards and the actual needs of evacuation decision-making, the new warning system in the future must have the capability of overall consideration on a basin scale. That is, a basin scale simulation and warning system is indispensable.

2.5 Summary

Using warning system for debris flows and slope failures in Taiwan and Japan as an example, the research discusses the characteristics of the warning model and alert issuing system of Japan and Taiwan, as well as suggests the evaluation indexes of warning effectiveness, and focuses on the lack of the current rainfall-based warning model through the actual disaster case and several years of statistical data. The results and recommends for future warning system are summarized as the follows.

(1) Existing rainfall-based sediment disaster warning systems in Japan and Taiwan provide significant disaster prevention measures by using a simple and easy-to-apply criterion. However, because the existing rainfall-based warning systems only consider rainfall as a warning index, the hit rate, false alert rate, and

warning coverage rate suffer.

(2) In this study, the sediment disaster warning models and alert issuing systems in Japan and Taiwan were compared. In the warning models, Japan's using RBFN to delineate CL is more objective and less dependent on disaster records which are usually difficult to collect. In the rainfall data, using grid mesh rainfall data in Japan can improve the spatial resolution of rainfall data and reduce the problem of insufficient rain gauge density. Regarding the types of alert, employing yellow and red colors to show the levels of alert seems easier to understand for the general public. Regarding alert-issuing timing, fixed-schedule regular issuing system seems to be better at solving the problem of frequent updating which results in the confusion of old and new information.

(3) This research also assessed specifically the existing warning model in Japan and Taiwan for warning hit rate, false alert rate, and warning cover rate. The results reveal that the scale of the disaster, the operator's decision-making tendencies, the integrity of disaster potential data, and rainfall data were all important variables in warning effectiveness through the analysis of past five years of statistics in Taiwan. In general, faced with larger scale of disaster events, the warning hit rate and warning cover rate will increase, and the false alert rate will drop. The integrity of the sediment disaster potential data will also affect the warning cover rate. Besides, the research also indicates that the attempt to reduce the false alert rate could cause alerts to be issued late to result in reduced warning hit rate. In addition, compared with the statistics of typhoons and heavy rainfall, the forecast rainfall data may affect the decision-making for issuing alerts tremendously.

(4) Taiwan's recent experience shows that the strong order from the central government may be more effective in improving the evacuation rate of sediment disaster warning areas. On the other hand, the remaining time for evacuation (RTE) is another key factor to the success of evacuation. According to the statistics of Japan 2008, among about 50% disaster events the RTE was less than 2 hours. Considering the location, age of the population and the transportation conditions, it is worth to further study the adequate RTE for different areas.

(5) Because the existing warning systems simply used the rainfall data and don't consider the difference in the geological, geomorphologic, and hydrological conditions of space distribution as well as the complex relationship of multi

sediment hazards, they cannot accurately predict the occurring time, location, type, and scale of potential disaster. In addition, they also cannot cope with the multi-modal sediment disaster. To improve on the problems, this study recommends developing a basin scale simulation model and warning system, which considers the geological, geomorphologic, and hydrological characteristics of slopes and channels. The new warning system should offer accurate long-time predictions (e.g., over the next 12 hours) and the scenario simulation capacity.

References

Amano, A. and Takayama, T. (2006): On the situation of early warning information for sediment-related disasters – Lessons from the evacuation of the T0514 disaster, Journal of the Japan Landslide Society, Vol. 43, No. 6, pp.370–375 (in Japanese).

Arattano, M. and Marchi, L. (2008): Systems and sensors for debris-flow monitoring and warning, Sensors, Vol. 8, pp. 2436–2452.

Caine, N. (1980): The rainfall intensity-duration control of shallow landslides and debris flows, Geografiska Annaler, 62A, pp. 23–27.

Chang, P.L. (2011): Introduction of QPESUMS, Central Weather Bureau (CWB) (in Chinese).

Chen, C.Y. (2008): The evolution of debris flow warning system in Taiwan, Soil and Water Conservation Quarterly, Vol. 63, pp. 1–7 (in Chinese).

Chen, Y.S., Kuo, Y.S., Lai, W.C., Tsai, Y.J., Lee, S.P., Chen, K.T., and Shieh, C.L. (2011): Reflection of typhoon Morakot – The challenge of compound disaster simulation, Journal of Mountain Science, Vol. 8, No. 4, pp. 571–581.

Council of Agriculture (COA) (2010): Directions governing evacuations for debris flow disasters (in Chinese).

Department of Erosion and Sediment Control (DESC), Ministry of Land, Infrastructure, Transport and Tourism (MLIT), Japan Meteorological Agency (JMA), and National Institute for Land and Infrastructure Management (NILIM)(2005): Manual for the setting mass-movement disaster warning criterion based on rainfall indices (Draft) (in Japanese).

Department of Erosion and Sediment Control (DESC), Ministry of Land, Infrastructure, Transport and Tourism (MLIT), and Japan Meteorological Agency (JMA), (2005): Guidelines for issuing sediment disaster warning information to joint prefectures and meteorological agencies (in Japanese).

Department of Erosion and Sediment Control (DESC) (2007): Guidelines for warning systems and evacuations (in Japanese).

Jan, C.D. and Li, M.H. (2004): A debris-flow rainfall-based warning model, Journal of Chinese Soil and Water Conservation, Vol. 35, No. 3, pp. 275–285(in Chinese).

Lee, C.T., Dong, J.J.(2009): Geological Investigation on the Catastrophic Landslide in Siaolin Village, Southern Taiwan, Sino-Geotechnics, No.122, pp.87-94. (in Chinese)

Lin, C.Y. (2007): A study of the evacuation of commercial population during a large-scale disaster, National Science Council (in Chinese).

Lindell, M. K., Lu, J.C., and Prater, C. S. (2005): Household decision making and evacuation in response to Hurricane Lili, Natural Hazards Review, Vol. 6, No. 4, pp.

171–179.
Morakot Post-Disaster Reconstruction Council (MPDRC) (2010): Report of post-disaster reconstruction six months after Typhoon Morakot (in Chinese).
National Institute for Land and Infrastructure Management (NILIM)(2001): Manual for setting sediment disaster warning criterion based on rainfall indices (in Japanese).
National Institute for Land and Infrastructure Management (NILIM) (2007): Manual for verifying sediment disaster warnings (Draft) (in Japanese).
National Institute for Land and Infrastructure Management (NILIM)(2010): Studies of warning systems and evacuations for sediment disasters, 23th Sabo Research Report (in Japanese).
Okamoto, A., Tomita, Y., Mizuno, M., Hayashi, S., Nishimoto, H., Ishii, Y., and Chiba, S. (2012): Data analysis of warning and evacuation information for sediment-related disasters, National Institute for Land and Infrastructure Management (NILIM), Japan (in Japanese).
Onda, Y., Mizuyama, T., and Kato, Y. (2003): Judging the timing of peak rainfall and the initiation of debris flow by monitoring runoff. In Rickenmann, D. and Chen, C.L (eds), Debris-Flow Hazards Mitigation: Mechanics, Prediction, and Assessment, Millpress, Rotterdam, pp. 147–153.
Osanai, N., Shimizu, T., Kuramoto, K., Kojima, S., and Noro, T. (2010): Japanese early-warning for debris flows and slope failures using rainfall indices with Radial Basis Function Network, Landslides, Vol. 7, pp. 325–338.
Pai, J.T. (2008): A study of the evacuation of disadvantage groups during a large-scale disaster, National Science Council (in Chinese).
Soil and Water Conservation Bureau (SWCB) (2007-2011): Debris flow annual report (in Chinese).
Soil and Water Conservation Bureau (SWCB) (2011): Manual for issuing debris-flow disaster alerts (in Chinese).
Soil and Water Conservation Bureau (SWCB) (2014): Debris Flow Disaster Information Website, http://246.swcb.gov.tw (in Chinese)
Tsou, C.Y., Feng, Z.Y. andChigira, M. (2011): Catastrophic landslide induced by Typhoon Morakot, Shiaolin, Taiwan, Geomorphology, Vol. 127, No. 3-4,pp. 166-178.
Wieczorek, G.F. and Glade, T. (2005): Climatic factors influencing occurrence of debris flows. In: Jakob, M. and Hunger, O. (eds), Debris-flow Hazards and Related Phenomena, Praxis, Springer Berlin, pp. 325–362.
Wu, J.Y. (2009): A comparative study of residential evacuation decisions and behavior for vulnerable debris flow areas, Journal of Slopeland Hazard Prevention, Vol. 8, No. 1, pp. 1–14(in Chinese).

Chapter 3

Evacuation Decision-Making Factors for Local Governments and Inhabitants

3.1 Introduction

Despite the fact that evacuations have been recognized as an effective approach to reducing casualties in sediment disasters, evacuation decision-making is still a complex problem for local governments and inhabitants. The difficulty lies in how to make appropriate decisions under the pressure of time constraints and other uncertainties, while considering both the safety of the public and evacuation costs (including losses due to disrupted economic activities). According to the findings of *Okamoto et al.* [2012], the proportion of local governments actually executing an evacuation order after a sediment disaster alert is issued was only 12% in 2010 in Japan. While the proportion of Taiwan's local governments carrying out evacuation orders was higher due to a mandate that allows the central government to order local governments to evacuate endangered inhabitants, the average evacuation rate was still only 51.6% over the last five years (2007–2011) [*Chen and Fujita*, 2013].

In Taiwan, the responsibility regarding the decision to evacuate and the implementation of this decision belongs to the county government and township office (hereinafter, referred to as the local government); however, in practice, the village head usually plays an important role.

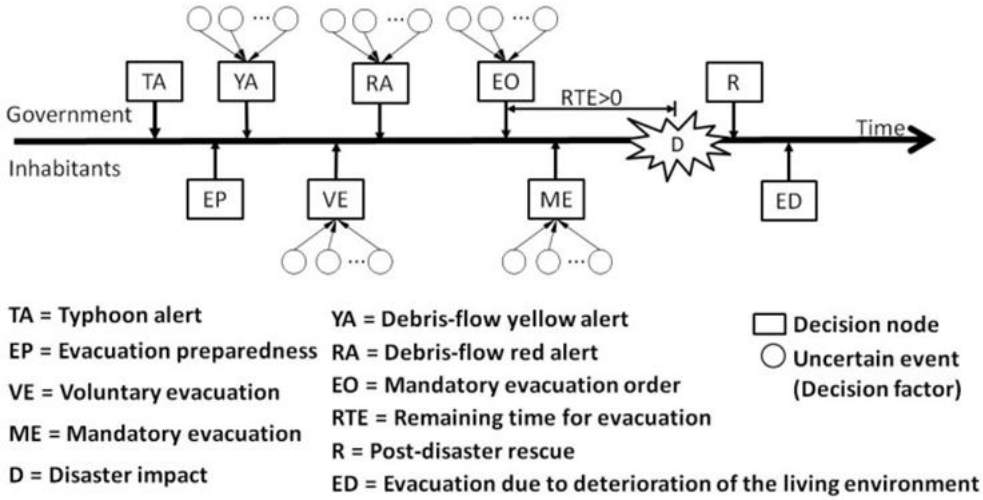

Figure 3.1 Evacuation decision-making process during a typhoon in Taiwan.

Figure 3.1 shows the existing debris flow evacuation mechanisms and processes in Taiwan. Ideally, before the arrival of a hazard, the government issues one of the following alerts in a timely fashion based on changes in environmental conditions: typhoon alerts, debris-flow yellow alerts, debris-flow red alerts, and mandatory evacuation orders. Meanwhile, inhabitants take evacuation actions based on environmental conditions or the aforementioned government-issued warning information, including evacuation preparedness, voluntary evacuation, and mandatory evacuation. However, if the alerts are issued after the hazards occur (or when the inhabitants can no longer evacuate safely), then the hazards can lead to disasters.

Nevertheless, part of the process of issuing alerts is to consider and predict future situations so that comprehensive judgments can be made under ever-changing conditions. Relevant theories and tools have been developed to improve the quality of the decision making. For example, a rainfall-based warning system has been used to assist local governments in issuing sediment disaster alerts in Taiwan and Japan. However, faced with more complex evacuation decisions, local governments still rely on experiential judgment. Currently, no specific evacuation decision support system (EDSS) exists to assist local governments in the decision-making process.

In this study, we only focused on the mandatory evacuation order decisions made by local governments according to the *Disaster Prevention and Protection Act* in Taiwan, and excluded post-disaster rescue or evacuation due to the deterioration of living environments. The evacuation decision-making of inhabitants in this study refers to the decision to evacuate when inhabitants receive typhoon or disaster alerts, or perceive environmental risks.

Previous studies have investigated the evacuation decisions made by local governments and inhabitants (see Chapter 1); however, most of them have not explored the relative weights of each evacuation decision factor. Thus, the studies have been limited in their ability to provide a hierarchical structure for the evacuation decision-making process.

This study referred to relevant literature to establish an analytical hierarchy process (AHP) questionnaire. Experienced experts, including local government officials responsible for making evacuation decisions, as well as inhabitants, were invited to fill out the questionnaire. An evacuation decision-making model was created based on pair-wise comparisons between local governments (including county,

township, and village governments) and their inhabitants. The research process is shown in **Figure 3.2**. Through the hierarchical structure of the decision-making model, this study was able to clearly show the weights of all decision-making factors. This result not only offers a strategy for improving disaster prevention, but also provides the foundation for bettering existing disaster warning systems and developing an evacuation decision support system.

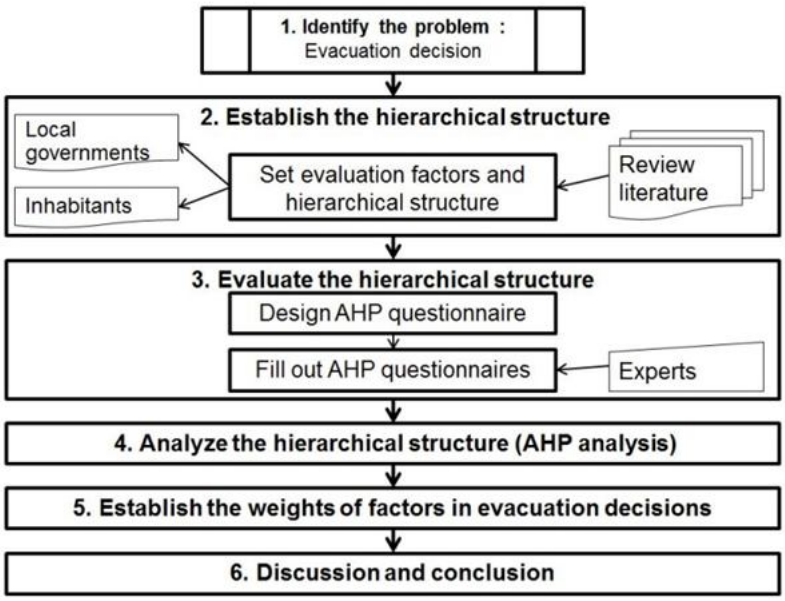

Figure 3.2 Flow chart of establishing the relative weights of each evacuation decision factor.

3.2 Methodology

3.2.1 Questionnaire content

The important factors relevant to evacuation decision-making were obtained from the literature (see **Table 3.1**), as well as from consultations with five experienced local government officials. According to the principles of the analytic hierarchy process (AHP) method, two questionnaires were designed: one for local government officials and the other for inhabitants. The hierarchy and content of the evacuation decision-making factors for local governments and inhabitants are described in **Tables 3.2** and **Table 3.3**.

Table 3.1 Summary of literature pertaining to evacuation decision-making.

Decision maker	Evacuation Decision-making Factors	References
Local government	size and distribution of the resident population in risk area, number of persons per residential household, number of evacuating vehicles per residential household, number of hotel rooms, size and distribution of the transit-dependent resident population, percentage of early evacuating residential households, percentage of residents' protective action recommendation (PAR) compliance/spontaneous evacuation, residential households' trip generation time distribution, evacuees' utilization of the primary evacuation route system, evacuation destinations, residential households' evacuation costs, commercial evacuation costs, governmental evacuation costs, the path and magnitude of hurricane, historical disaster records, alert-issuing time	[Lindell and Prater, 2007] [Regnier, 2008] [Wolshon et al., 2005] (in English)
	sediment disaster warning areas, warning hit rate, false alert rate, hazard areas, the actual on-site rainfall and water levels, disaster occurrence, site situation report, issuing alert before sunset, distribution of disadvantaged groups, the distance to shelters, safety of evacuation routes and shelters, vehicles, capacity of disaster-prevention communities, past experiences, historical disaster records, signs of disaster, communication conditions, partially interrupted traffic	[NILIM, 2010] [DESC, 2007] [Amano and Takayama, 2006] (in Japanese)
	typhoon alert, rainfall forecast, debris-flow alert, actual on-site rainfall and water levels, current circumstances, hazards, historical disaster records, the positions and conditions of shelters, preventive evacuation at highly hazardous areas, the structure of population, disadvantaged members, capacity of disaster-prevention communities, alert issuing time, day or night, superior's order to evacuate, subordinates' suggestion to evacuate, remaining time for evacuation, past experiences, past evacuation experiences without disaster occurring, traffic interrupted, costs of evacuation and shelters, extent of impact on inhabitants' incomes or properties, communication broken	[COA, 2010] [Chen and Mars, 2008] (in Chinese)
Inhabitants	environmental cues, personal experiences, social cues, evacuation impediments, neighbors beginning to evacuate, inhabitants' characteristics(gender, age, education, income, race, marriage), past experiences (including disaster experience and "crying wolf" experience), risk perception, houses' locations and types, local governmental action, channels through which the warning is communicated to the public, family members (elders or children), disaster alert reception, the interpretation for the content of alerts	[Lindell et al., 2005] [Zeigler and Johnson, 1984] [Dow and Cutter, 1998; Whitehead et al., 2000] [Baker, 1991] [Gladwin and Peacock, 1997] (in English)
	receiving sediment disaster alert, whether the content of alerts and evacuation orders are definite or not, day or night, the distance and safety of shelters and evacuation routes, communication vulnerability, disadvantaged members, risk perception, past experiences, intense rainfall beginning, disaster occurring, traffic condition, rainfall forecast, signs of disaster	[Ushiyama, 2012] [Amano and Takayama, 2006] [Irasawa and Kamaishi, 2010] (in Japanese)
	intense rainfall beginning, typhoon alert, receiving evacuation orders, environmental hazard, neighbors beginning evacuation, the possibility of interrupted traffic, disaster experiences, worry for property loss, evacuation experiences without disaster, costs for evacuation, loss of income, safety of shelters and evacuation routes, distance to shelters, accommodation condition of shelters, risk perception, inhabitants' characteristics(education, age, gender), house characteristics, influence from relatives and friends	[Chen et al., 2007] [Lin, 2007] [Pai, 2008] [Wu, 2009] (in Chinese)

Table 3.2 Hierarchy and content of evacuation decision-making factors for local governments.

Level 1 (elements/ clusters)	Level 2 (elements/factors)	Description of the factors
Warning information	Typhoon alert	Consider whether the region is located in a typhoon warning area.
	Forecast rainfall	Based on reports from the Central Weather Bureau (CWB) on rainfall and total rainfall forecast for the next 24 hours to assess the risk of the region.
	Actual rainfall	Based on rainfall data from the closest automatic rainfall station, which can be checked on the CWB website, or referring to a simple rain gauge in the community.
	Debris-flow alert	Based on a debris-flow alert issued by the Soil and Water Conservation Bureau (SWCB).
	Flood alert	Based on a flood alert issued by the Water Resource Agency (WRA).
	Traffic alert	Based on a traffic alert (including information about closed roads or bridges) issued by the Directorate General of Highways (DGH).
	On-site situation report	Based on a site situation report from township governments or village heads, including rainfall, water levels, whether disasters are occurring or not, and recommendations for evacuation.
Current circumstances	Start of intense rainfall	Based on whether rainfall becomes heavier.
	Disaster occurring	Based on whether some disasters have occurred in the region or in the surrounding areas.
	Partial traffic interruption	If certain traffic arteries are interrupted, the evacuation action could be affected.
	Communications disrupted	Consider whether communications in the region are vulnerable to interruption, in which case evacuation action could be affected.
	Disaster occurring at night	Consider the possibility of a disaster occurring at night, and the difficulties presented regarding evacuation of mountainous areas.
Past experience	False alert rate	Past experience when alerts were issued, but no disasters occurred.
	Warning hit rate	Past experience when alerts were issued, and then disasters actually occurred.
	Historical disaster events	Consider whether the frequency of disasters in the region is higher.
Hazard	Being located in a hazard area	Consider whether the region is in the debris-flow potential areas, flooding potential areas, or geologically sensitive areas.
	Vulnerable to interrupted traffic	Consider whether traffic is vulnerable to interruption, isolating a village or community.
Community conditions	Population structure	Consider the distribution and number of disadvantaged members (e.g. elders or children) in a village or community.
	Capability for disaster prevention	Consider whether a village or community has disaster-prevention organizations and adequate supplies to deal with short-term disasters by itself.
	Location of shelters	Consider whether shelters are located in the region or outside of the region, which affects the time and resources required for evacuation.
Administrative considerations	Superior's orders	Consider whether the central government or county government ordered the region to evacuate.
	Costs of evacuation and shelters	Consider the costs (including manpower and budget) of the evacuation and management of shelters.
	Inhabitants' cooperation	Consider whether inhabitants are willing to cooperate with an evacuation.

Table 3.3 Hierarchy and content of evacuation decision-making factors for inhabitants in debris-flow hazard areas.

Level 1 (elements/clusters)	Level 2 (elements/factors)	Description of the factors
Receive alerts	Typhoon alerts	Consider whether the region is located in a typhoon warning area.
	Debris flow alerts	Based on a debris-flow alert issued by the Soil and Water Conservation Bureau (SWCB).
	Flood alerts	Based on a flood alert issued by the Water Resource Agency (WRA).
	Evacuation orders	Based on evacuation orders from the local government, village head, relatives, or friends.
	Community hazards	Consider whether the region is in a debris-flow potential area, flooding potential area, or geologically sensitive area.
Past experience	Disaster experience	Based the disaster experience of an individual or people in the neighborhood.
	False alert experience	Evacuation orders have been followed many times, but no disasters have occurred.
	Potential for isolation	The region has become isolated during previous typhoons or heavy rainfalls (inhabitants could not access school, work, medical care, or food).
	Evacuation drill experience	Evacuation drill or disaster prevention education has provided a better understanding of disaster risks in the region.
	Comparison against historical typhoons	Comparison against historical typhoons and disaster situations has led to a better understanding of the disaster risk.
Circumstances	Start of intense rainfall	Risk perception increases due to obvious increases in rainfall.
	Disaster occurring	Risk perception increases after hearing that a disaster is occurring in the region.
	Neighbors evacuated	Risk perception increases when neighbors start to evacuate.
	Daytime or at night	Consider the difficulty of evacuation at night; evacuation before sunset or the next day is preferred.
Shelter conditions	Distance	Consider the distance to shelters, which will affect the timing and methods used to evacuate.
	Accommodation conditions	Consider the condition of shelters, e.g. accommodation, food; or stay with acquaintances.
	Security	Consider the safety of shelters and the evacuation routes.
Family and income	Disadvantaged members	Consider disadvantaged members (e.g., elders or children) in the family.
	Income affected	Consider that evacuation will decrease income.
	Stolen or unattended livestock	Consider that property could be stolen or no one will be able to care for livestock and farms.

3.2.2 Survey subjects

(1) Local governments

This study focused on the debris-flow potential areas published by the Soil and Water Conservation Bureau, Taiwan (SWCB). According to the 2012 data, there are 1660 potential debris-flow torrent locations in Taiwan distributed over 17 counties, and there have been 327 significant sediment disasters in recent years (2007–2011), as shown in **Table 3.4** [*SWCB*, 2012]. The subjects of this survey included officials from local governments (including counties, townships, and villages) that have suffered significant sediment disasters over the past five years. The statistics of valid questionnaires are shown in **Table 3.4**; questionnaires that were filled out incompletely or those that could not pass the AHP consistency check were removed from consideration.

Due to the high turnover rate of township officials, more than half of the respondents returning questionnaires were novices, despite the fact that the survey targeted townships that had suffered significant sediment disasters in recent years. To ensure that the questionnaire results accurately reflected practical operation scenarios in local governments, we only used questionnaires from respondents who had engaged in disaster prevention for more than two years and had experience in evacuation decision-making.

(2) Inhabitants

The survey focused on inhabitants in debris-flow potential areas to investigate their evacuation decision-making factors. To allow compare against influence from evacuation experience, some of the respondents had evacuation experience while others did not.

Table 3.4 Statistics of debris-flow potential torrents, significant sediment disasters, and effective questionnaires.

	Number of debris-flow potential torrents (2012)	Number of sediment disaster events (2006-2011)	Returned questionn-aires	County (Evacuation decision-making experience)		Town (Evacuation decision-making experience)		Village (Evacuation decision-making experience)		Inhabitant (Evacuation experience)	
				Y	N	Y	N	Y	N	Y	N
Yilan County**	142	49	3				1	1			1
Keelung City*	34	2	2	1							1
Taipei City	50	2	2	1		1					
New Taipei City*	220	6	9	1		1	5				2
Taoyuan County**	51	4	2		1						1
Hsinchu County**	76	3	1					1			
Miaoli County**	78	13	5	1			1			1	2
Taichung City*	106	10	4				1			1	2
Changhua County*	7	1	1								1
Nantou County***	247	54	17	2	2	2	4			2	5
Yunlin County**	12	13	0								
Chiayi County***	80	37	7	2		2				1	2
Tainan City**	48	16	3	1						1	1
Kaohsiung City***	109	67	3	1							2
Pingtung County***	70	34	2	1				1			
Taitung County**	165	8	2	2							
Hualien County**	165	8	15	1	1	4		2	1	3	3
Total	1,660	327	78	14	4	10	12	5	1	9	23

Note : According to traffic conditions, the survey area was divided into **surrounding slopes of cities*, ***shallow mountainous areas*, and ****mountainous areas.*

3.2.3 AHP theory

AHP theory, developed by *Saaty*, is a multiple-attribute decision analysis (MADA) technique that breaks down complex problems into multiple smaller sub-problems using a hierarchical structure. The hierarchical structure is established by assigning a relative weight to each element at each level of the structure through pair-wise comparisons of the relative importance of any two elements. Thus, AHP makes complex issues simpler so that a decision can be reached.

For the pair-wise comparison of the relative importance of any two elements, *Saaty* recommends using a 1 to 9 comparison scale, where 1 indicates two elements of

equal importance, and 9 indicates that one of the two elements being compared is of much greater importance relative to the other. Assuming n elements to be compared and a_{ij} is the relative importance of element i to element j, then the pair-wise comparisons for any element at each level can be written in the form of matrix $\boldsymbol{A}$ in Eq. (3.1), referred to as the pair-wise comparison matrix. Moreover, because the element a_{ij} of matrix $\boldsymbol{A}$ represents the relative importance of elements i and j, the elements in the lower left off-diagonal triangle (i.e., a_{ji}) should be the reciprocals of the elements in the upper right off-diagonal triangle.

$$\boldsymbol{A} = \begin{bmatrix} 1 & a_{12} & \cdots & a_{1n} \\ 1/a_{12} & 1 & \cdots & a_{2n} \\ \vdots & \vdots & \ddots & \vdots \\ 1/a_{1n} & 1/a_{2n} & \cdots & 1 \end{bmatrix} \tag{3.1}$$

If the weights of the n elements are known, then $a_{ij} = w_i/w_j$, where w_i and w_j are the weights of elements i and j, respectively. That is

$$a_{ij}w_j = w_i \quad \text{for i, j = 1,2,……,n} \tag{3.2}$$

$$\sum_{j=1}^{n} a_{ij}w_j = nw_i\,, \quad i = 1,2,\ldots\ldots,n \tag{3.3}$$

or

$$\boldsymbol{Aw} = n\boldsymbol{w} \tag{3.4}$$

where the priority weight vector, $\boldsymbol{w}$ = (w_1, w_2, ..., w_n), is an eigenvector of matrix $\boldsymbol{A}$. In this case, $\boldsymbol{A}$ is said to be consistent if and only if $a_{ik}a_{kj} = a_{ij}$. The problem of solving for a non-zero solution to Eq. (3.4) is known as an eigenvalue problem. In this case, the rank of matrix $\boldsymbol{A}$ is one, because each row of $\boldsymbol{A}$ is a constant multiple of the first row. Thus, all eigenvalues of $\boldsymbol{A}$ are zero, except one. The non-zero eigenvalue λ_{max} is equal to n.

However, in reality, $\boldsymbol{w}$ is not known. Any entry of $\boldsymbol{A}$ is only an estimate of a_{ij}, and matrix $\boldsymbol{A}$ is inconsistent. Thus, the eigenvalue problem for the inconsistent case is

$$\boldsymbol{Aw} = \lambda_{max}\boldsymbol{w} \tag{3.5}$$

where λ_{max}, the largest eigenvalue of matrix $\boldsymbol{A}$, will be close to n, and the other eigenvalues will be close to zero; the closer λ_{max} is to n, the greater the consistency among judgments. Thus, Saaty [1980] defined the consistency index $\text{CI} = \frac{\lambda_{max}-n}{n-1}$. He showed that if CI is < 0.1, then the consistency among judgments is satisfied.

3.2.4 Method of integrating questionnaires

To ensure the consistency of each questionnaire, an effective questionnaire was defined by the conditions where all pair-wise comparison matrices for each cluster satisfied the consistency (i.e., CI < 0.1). Additionally, to remind the respondents to provide consistent answers, they were asked to prioritize all factors in the same cluster before starting the pair-wise comparisons. Such prioritizing of factors can be used to collate the results of the pair-wise comparisons if CI > 0.1, and adjust the pair-wise comparisons by suggestions made by the "Super Decision" software (developed by Saaty, http://www.superdecisions.com). Finally, the "Super Decision" software was used to calculate the weights of all evacuation decision-making factors.

Due to the fact that each AHP questionnaire represents the decision-making model of the respondent, the weights of the factors calculated from each questionnaire were different. Most studies have used an arithmetic or geometric mean method to integrate the results of the questionnaires [*Chen et al*., 2008]. But because extreme values have less influence on the geometric mean relative to the arithmetic mean, this study used the geometric mean method to integrate the weights of the evacuation decision-making factors analyzed from the AHP questionnaires, and normalize the integrated weights to make the sum of the weights equal to 1 in the same cluster. The analysis process is shown in **Figure 3.3**.

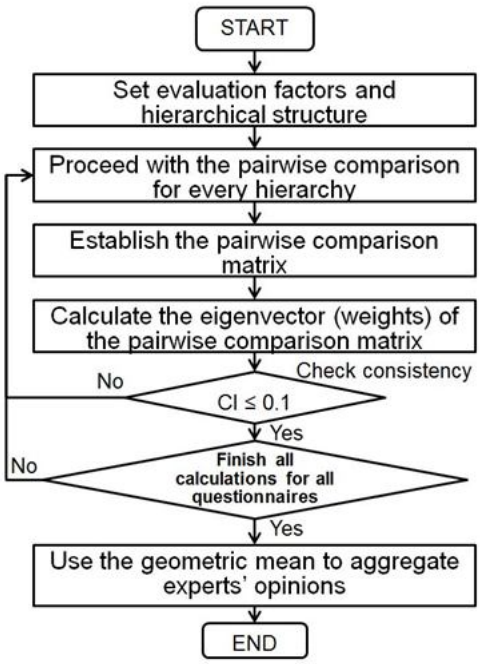

Figure 3.3 Analysis process of this study using AHP.

3.3 Results and discussion

3.3.1 Evacuation decision-making factors by local governments

(1) Level 1 survey results

According to the method described in the previous section, the results of the evacuation decision-making factors for local governments are shown in **Table 3.5**. The level 1 weights of the evacuation decision-making factors obtained from the county, township, and village levels in this survey were similar. W*arning information* and *current circumstances* were the most important evacuation decision-making factors; the sum of their total weights exceeded 50%. It is worth noting that more primary governments were more distrustful of the warning information, but more trustful of the current circumstances. The results are consistent with the findings by *Chen and Mars* [2008].

(2) Level 2 survey results

The level 2 evacuation decision-making factors of *warning information* indicated that *actual rainfall* and *on-site situation reports* were the main considerations; the sum of their total weights exceeded 50%. These results suggest that the local governments doubted the accuracy of the existing warning system; thus, evacuation decision-making emphasized the on-site situation. Even during a debris-flow alert for debris-flow potential areas, the more primary governing units were more distrustful of the alert.

For *current circumstances*, the total weights of *disasters occurring* and *partial traffic interruption* were ~56%; however, the weights of preventive considerations (e.g., *communications disrupted* and *disaster occurring at night*) were relatively low. This suggests that the disaster prevention strategies of local governments focus on the emergency response after a disaster has occurred; less consideration is given to taking action in the early stages to reduce the disaster risk. This should be included in the follow-up education improvements for disaster preparedness training.

For *past experience*, *historical disaster events* was the primary factor; its weight was ~59%. Another point worth noting is that the survey results showed that the *warning hit rate* was more significant than the *false alert rate*. Thus, enhancing the warning hit rate should be given more priority than reducing false alerts as an improvement goal for existing warning systems. Additionally, providing local historical disaster information during an alert can assist local governments in making

evacuation decisions.

For *hazards*, the survey results showed that the importance of *being located in a hazard area* and *vulnerable to interrupted traffic* had equal weighting. This was because in recent years, several large-scale disasters have caused a number of important roads and bridges to be damaged, resulting in difficulties evacuating and rescuing disaster victims.

For *community conditions*, the survey results showed that *the capability for disaster prevention* (e.g., whether a community has disaster prevention organizations and adequate supplies) to be the most important consideration for local governments when ordering mandatory evacuations. More primary governments paid more attention to this factor. Therefore, if local governments wish to reduce evacuation costs and inhabitants' complaints, strengthening the capacity for disaster prevention in the community should be considered.

Finally, for *administrative considerations*, *inhabitants' cooperation* occupied almost half of the weight; more primary governments (i.e., more directly in contact with the inhabitants and actually executing the evacuation action) put greater weights on this factor. In contrast, the weights of *costs of evacuation and shelters* were < 20%, which imply that the direct costs of evacuation were lower than the indirect costs. That is, how to enhance the proportion of the inhabitants who will voluntarily evacuate during typhoons or heavy rainfalls should be a priority in the disaster prevention education for inhabitants.

Because the Central Emergency Operation Center in Taiwan uses the results of hazard analyses to request county governments to evacuate inhabitants in warning zones, the weight of *superior's orders* was ~40% for county governments, and lower for township and village governments. This trend is contrary to *inhabitants' cooperation*, and reflects how the different levels of local governments focus on the pressures they face. This also highlights the difficulties in evacuation decision-making when a decision maker faces a conflict between a disaster potential analysis (i.e., theory) and an actual evacuation operation.

Table 3.5 Weights of factors in evacuation decisions by local governments.

Level 1 (elements/clusters)	Level 2 (elements/factors)	Average	County	Township	Village
Warning information		**0.236**	0.311	0.190	0.209
Current circumstance		**0.272**	0.238	0.244	0.329
Past experience		0.107	0.101	0.114	0.100
Hazard		0.146	0.110	0.221	0.120
Community condition		0.157	0.145	0.140	0.179
Administrative considerations		0.083	0.095	0.091	0.062
Warning information	Typhoon alert	0.053	0.056	0.068	0.038
	Forecast rainfall	0.091	0.067	0.103	0.102
	Actual rainfall	**0.269**	0.192	0.289	0.333
	Debris-flow alert	0.172	0.202	0.183	0.131
	Flood alert	0.095	0.104	0.084	0.094
	Traffic alert	0.086	0.124	0.075	0.065
	On-site situation report	**0.233**	0.256	0.198	0.236
Current circumstances	Start of intense rainfall	0.125	0.123	0.114	0.136
	Disaster occurring	**0.309**	0.353	0.289	0.283
	Partial traffic interruption	**0.251**	0.213	0.252	0.291
	Communications disrupted	0.155	0.152	0.158	0.155
	Disaster occurring at night	0.159	0.159	0.187	0.135
Past experience	False alert rate	0.111	0.144	0.114	0.082
	Warning hit rate	0.300	0.305	0.300	0.291
	Historical disaster events	**0.589**	0.551	0.586	0.627
Hazard	Being located in a hazard area	0.499	0.464	0.505	0.527
	Vulnerable to interrupted traffic	**0.501**	0.536	0.495	0.473
Community conditions	Population structure	0.227	0.276	0.228	0.178
	Capability for disaster prevention	**0.530**	0.413	0.554	0.620
	Location of shelters	0.243	0.311	0.217	0.202
Administrative considerations	Superior's orders	0.315	0.399	0.299	0.257
	Costs of evacuation and shelters	0.198	0.174	0.209	0.210
	Inhabitants' cooperation	**0.486**	0.427	0.492	0.533

Note: The results are presented in terms of the relative weights of each cluster. The primary factors (i.e., sum of the weights greater than or close to 50%) in each cluster are highlighted in bold type.

(3) Absolute weights of factor in evacuation decisions by local governments

While the study results in **Table 3.5** were presented using the relative weights for each cluster, the results are easy to transform into absolute weights for all factors by using Eq. (3.6).

$$W_{ij} = w_i \times \frac{N_i}{\sum_{i=1}^{n} N_i} \times w_j \quad \text{for } i = 1,2,\dots\dots,n \quad \text{for } j = 1,2,\dots\dots,m \tag{3.6}$$

$$\sum_{i=1}^{n}\sum_{j=1}^{m} W_{ij} = 1 \tag{3.7}$$

where W_{ij} is the absolute weights of factor j (level 2) in the cluster i (level 1), w_i is the relative weights of cluster i, N_i is the number of the factors in cluster i, w_j is the

relative weight of factor *j*, *n* is the number of clusters, *m* is the number of factors in each cluster. **Figure 3.4** to **Figure 3.7** are the charts of the absolute weights of factors in evacuation decision by different level of local governments.

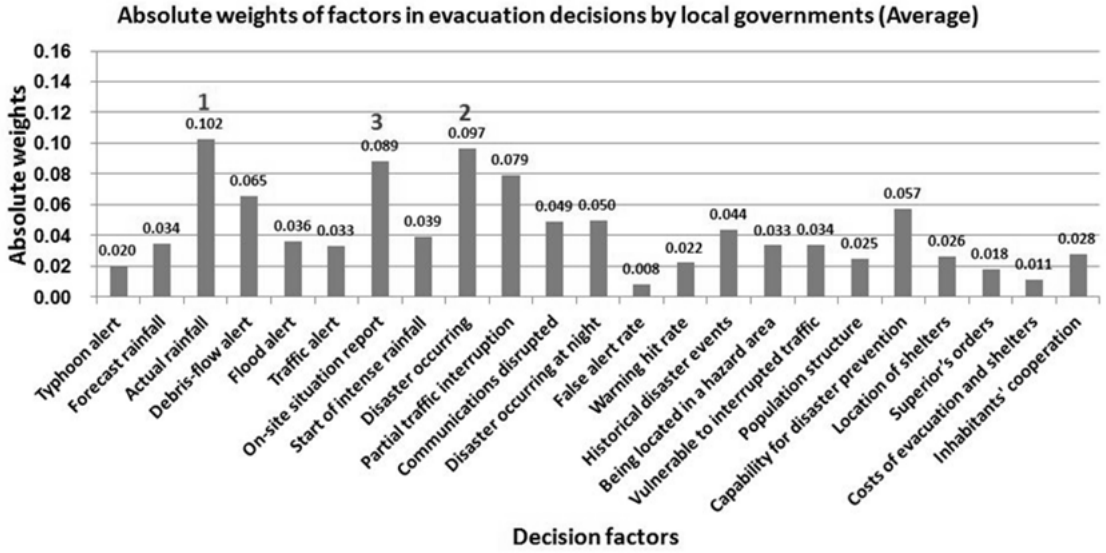

Figure 3.4 Absolute weights of factors in evacuation decisions by local governments (Average)

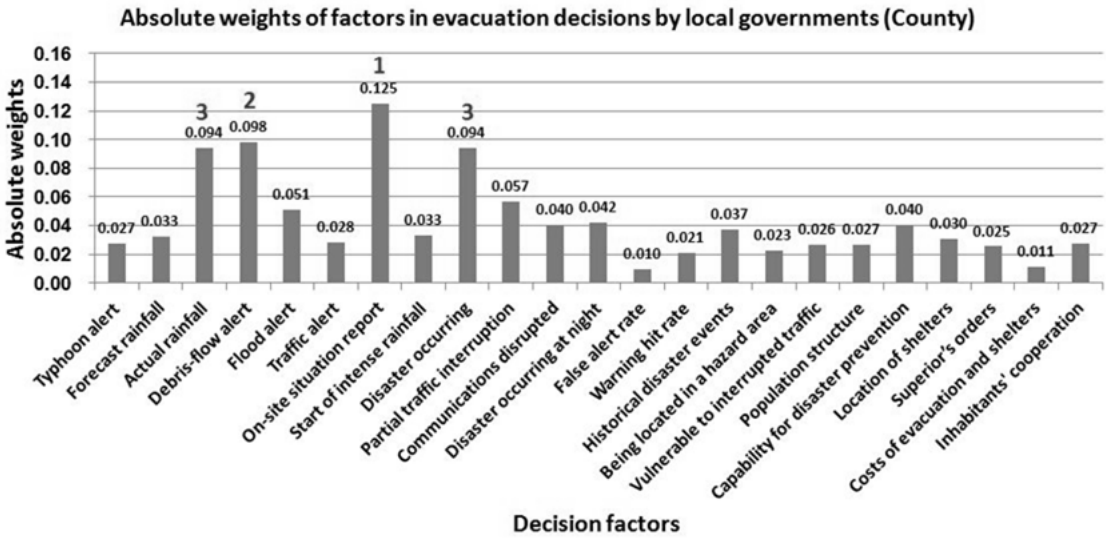

Figure 3.5 Absolute weights of factors in evacuation decisions by local governments (County)

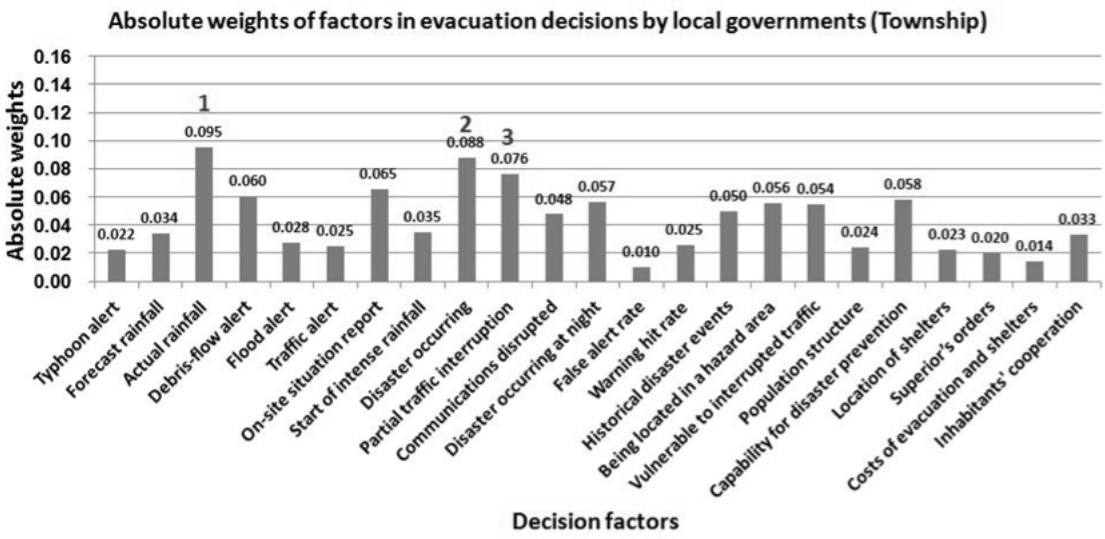

Figure 3.6 Absolute weights of factors in evacuation decisions by local governments (Township)

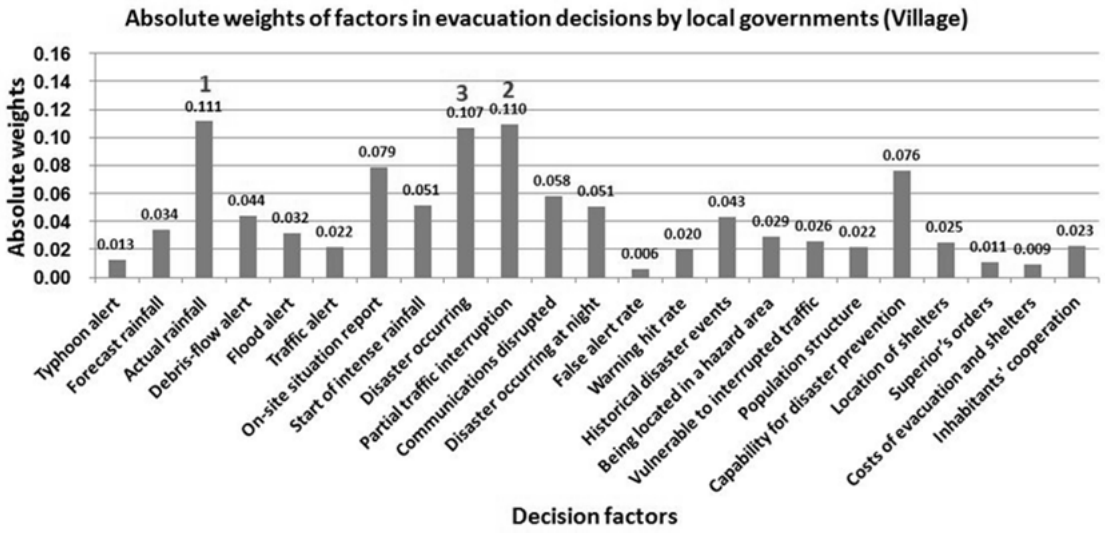

Figure 3.7 Absolute weights of factors in evacuation decisions by local governments (Village)

3.3.2 Evacuation decision-making factors by inhabitants

(1) Experienced inhabitants

A. Level 1 survey results

The results of the survey for the inhabitants are shown in **Table 3.6**. The survey results show that inhabitants experienced with evacuations deemed *shelter conditions* and *circumstances* to be the most important level 1 factors for evacuation decision-making; the sum of their weights was ~50%. However, the study also showed

the diversity of evacuation decision-making factors for different regions. For example, the inhabitants of the surrounding slopes of cities mostly respected *shelter conditions* and *family and income* (the sum of their total weights was ~65%), while the inhabitants of shallow mountainous areas paid more attention to *circumstances* and *shelter conditions*, and the inhabitants of mountainous areas attached great importance to *circumstances* and *past experience*. Moreover, the findings indicated the weights of *past experience* and *circumstances* to be higher if the respondents lived closer to the mountains; the weights of *shelter conditions* and *family and income* were higher if the respondents lived closer to cities. Thus, disaster prevention education should consider the differences in the terrain and area.

B. Level 2 survey results

The level 2 evacuation decision-making factors of *receive alerts* indicated that *evacuation orders* and *debris flow alerts* were the main considerations; the sum of their total weights was almost 59%. For *past experience*, *disaster experience* and *evacuation drill experience* were the important factors affecting inhabitants' evacuation decisions. The survey results showed that the weights of *disaster experience* were higher if the inhabitants lived in mountainous areas, while the weights of *evacuation drill experience* were opposite. This suggests that existing evacuation drills do not satisfy certain special needs of disaster prevention in mountainous areas, although, the drills have reached their goal of enhancing inhabitants' risk perception.

For *circumstances*, *disaster occurring* and *whether an evacuation takes place in the daytime or at night* were the primary factors. Additionally, the weights of *whether neighbors evacuated* were clearly higher in the surrounding slopes of cities. For *shelter conditions*, *security* was the most important factor. For *family and income*, the *disadvantaged members* (e.g., elders or children) in the family were the main considerations of evacuation. The survey results also showed that inhabitants living closer to cities paid more attention to *income affected* and *stolen or unattended livestock*.

Table 3.6 Weights of factors in evacuation decisions by inhabitants.

Level 1 (elements/ clusters)	Level 2 (elements/ factors)	Experienced				Inexperienced			
		Average	Surrounding slopes of cities	Shallow mountainous area	Mountainous area	Average	Surrounding slopes of cities	Shallow mountainous area	Mountainous area
Receive alerts		0.173	0.121	0.172	0.177	0.172	0.135	0.145	0.250
Past experience		0.223	0.164	0.212	0.250	0.220	0.142	0.227	0.231
Circumstances		**0.239**	0.061	0.261	0.273	**0.284**	0.149	0.305	0.308
Shelter conditions		**0.258**	0.393	0.243	0.233	**0.230**	0.249	0.251	0.148
Family and income		0.107	0.260	0.111	0.066	0.094	0.325	0.073	0.062
Receive alerts	Typhoon alerts	0.140	0.064	0.155	0.134	0.132	0.103	0.156	0.092
	Debris flow alerts	**0.256**	0.328	0.241	0.259	**0.273**	0.304	0.275	0.215
	Flood alerts	0.108	0.081	0.094	0.157	0.158	0.242	0.156	0.105
	Evacuation orders	**0.329**	0.360	0.314	0.339	**0.273**	0.267	0.206	0.458
	Community hazards	0.167	0.167	0.196	0.110	0.164	0.084	0.207	0.130
Past experience	Disaster experience	**0.315**	0.219	0.296	0.386	0.227	0.129	0.256	0.222
	False alert experience	0.102	0.109	0.087	0.135	0.081	0.089	0.089	0.055
	Potential for isolation	0.222	0.137	0.259	0.169	**0.255**	0.391	0.195	0.321
	Evacuation drill experience	**0.261**	0.432	0.261	0.207	**0.255**	0.284	0.230	0.268
	Comparison with historical typhoons	0.101	0.102	0.096	0.104	0.182	0.106	0.230	0.134
Circumstances	Start of intense rainfall	0.150	0.200	0.123	0.195	0.191	0.446	0.173	0.102
	Disaster occurring	**0.311**	0.308	0.278	0.370	**0.322**	0.227	0.418	0.166
	Neighbors evacuated	0.256	0.357	0.239	0.245	**0.328**	0.193	0.281	0.506
	Daytime or at night	**0.283**	0.135	0.360	0.189	0.160	0.135	0.128	0.226
Shelter conditions	Distance	0.234	0.200	0.189	0.359	0.256	0.388	0.269	0.159
	Accommodation conditions	0.132	0.200	0.097	0.206	0.157	0.224	0.146	0.134
	Security	**0.634**	0.600	0.714	0.435	**0.587**	0.388	0.585	0.708
Family and income	Disadvantaged members	**0.477**	0.143	0.489	0.588	**0.548**	0.536	0.648	0.316
	Income affected	0.229	0.429	0.231	0.161	0.210	0.271	0.150	0.325
	Stolen or unattended livestock	0.293	0.429	0.280	0.251	0.242	0.194	0.202	0.359

Note: The results are presented in terms of the relative weights of each cluster. The primary factors (i.e., sum of the weights greater than or close to 50%) in each cluster are highlighted in bold type.

(2) Inexperienced inhabitants

A. Level 1 survey results

The level 1 weights of evacuation decision-making factors for inexperienced and experienced inhabitants were similar. However, different survey results were obtained for inexperienced inhabitants living in different regions.

B. Level 2 survey results

The level 2 evacuation decision-making factors for *receive alerts* indicated that *evacuation orders* and *debris flow alerts* were the most important factors; the survey results were similar to the findings for experienced inhabitants. For *past experience*, *potential for isolation* and *evacuation drill experience* were the main considerations; these findings were inconsistent with the results for experienced inhabitants, and may reflect the lack of disaster experience of inexperienced inhabitants.

Another special finding is that the survey results showed that inexperienced inhabitants in the surrounding slopes of cities paid more attention to the *potential for isolation* than mountainous area inhabitants. This is perhaps related to their occupation or work pattern, which may lead to lower tolerance for traffic interruption.

For *circumstances*, inexperienced inhabitants emphasized *neighbors evacuated* and *disaster occurring*, and mountainous area inhabitants showed the most regard for *neighbors evacuated*. The weights of the *daytime or at night* factor were quite different compared with experienced inhabitants in shallow mountainous areas. This perhaps shows that inexperienced inhabitants did not fully understand the difficulty of evacuations at night; thus, follow-up community disaster prevention education should be enhanced to address this issue. For *shelter conditions* and *family and income*, the survey results were similar to the findings for experienced inhabitants.

Many studies have pointed out the "crying wolf" effect (i.e., a false alert when a sediment disaster alert is issued but no disaster occurs). However, this survey indicated that this had little effect on the local government decision-makers or inhabitants. For example, the weight of *false alert rate* under the level 2 cluster of *past experience* for local governments was only ~11%; more primary governments paid less attention to this (**Table 3.5)**. The weight for inhabitants was also ~10% (see **Table 3.6**). The survey indicated that the weight of the warning hit rate (WHR) was almost three times that of the false alert rate (FAR). Thus, FAR < 75% could be used as a standard to evaluate the warning effectiveness of existing warning systems.

(3) Absolute weights of factor in evacuation decisions by inhabitants

Table 3.6 were presented using the relative weights for each cluster in evacuation decision by experienced and inexperienced inhabitants, and the results are easy to transform into absolute weights for all factors by using Eq. (3.6). **Figure 3.8**

and **Figure 3.9** are the charts of the absolute weights of factors in evacuation decision by experienced and inexperienced inhabitants.

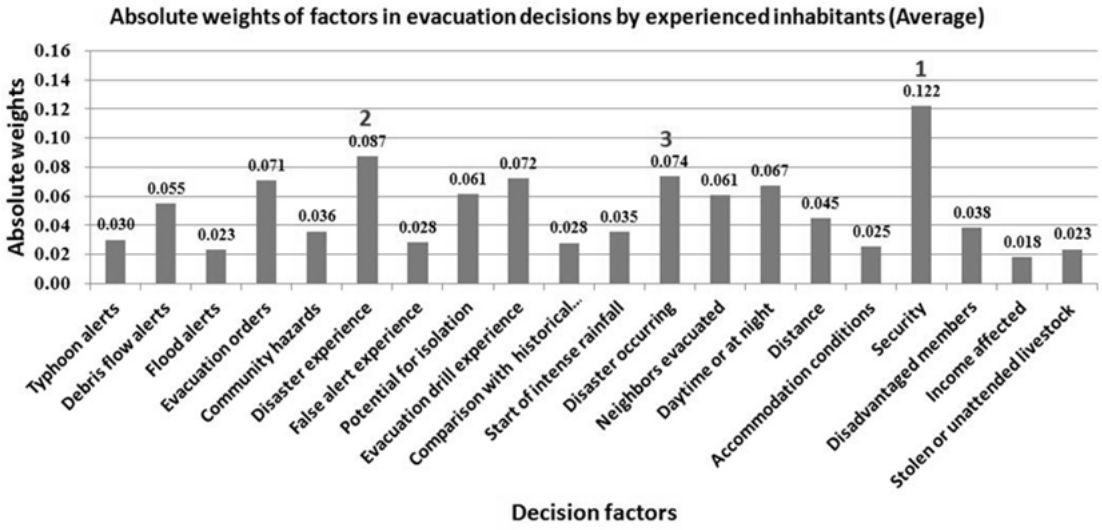

Figure 3.8 Absolute weights of factors in evacuation decisions by experienced inhabitants (Average)

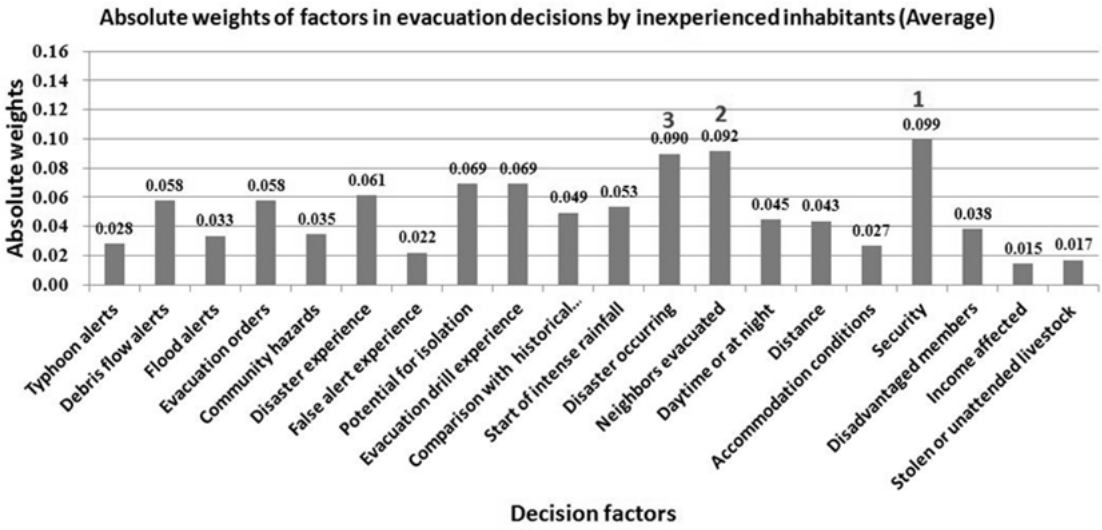

Figure 3.9 Absolute weights of factors in evacuation decisions by inexperienced inhabitants (Average)

3.3.3 Suggestions for improving the existing warning system

To explore the priorities in improving the existing warning system, the study also asked the respondents in local governments to prioritize the improvement items

according to their needs in the questionnaires, and the sequence method (i.e., the smaller cumulative sequence number is the more preferred) is then used to assess the priority. The contents of the questionnaire are described in **Table 3.7**, and the survey results are shown in **Table 3.8**.

Table 3.7 The Proposal to Improve the Existing Debris-flow Warning System

No.	Content	Description
1	Reducing the False Alert Rate (FAR)	■ False Alert Rate (FAR) = WTND/WT where WT is the number of towns which had issued sediment disaster warning; WTND is the number of towns which had issued sediment disaster warnings but with no disaster occurring. ■ FAR was around 87.8% in Japan in 2008; the average FAR for past five years is about 75.2% in Taiwan.
2	Raising the Warning Hit Rate (WHR)	■ WHR = DEAA/DE where DE is the number of sediment disaster events; DEAA is the number of sediment disaster events that are located within the warning areas and occurred after warning issued ■ WHR was about 53.2% in Japan in 2008; the average WHR for past five years is about 45.4%.
3	Narrowing the unit of warning area (i.e., Point out the definite place of the risk area)	■ The unit of warning area in Japan is township. In addition, the Sabo Department of the prefectures also offers detailed information which displays the various levels of risk by using 5 km grid meshes on the website. ■ The unit of warning area in Japan is village. In addition, the detailed warning information is also presented using Google Maps and Google Earth on SWCB's website
4	Adding the application of the debris-flow alert to other sediment disaster	■ Japan's sediment disaster alert is applied only to debris flow and slope failure but not landslide. ■ Taiwan's debris-flow alert is applied only to debris flow
5	Providing more detailed warning information	■ For example, in addition to providing alert level (yellow or red), the alert also offers the current rainfall, historical rainfall data, disaster cases, follow-up rainfall forecast, flood alert, and traffic interruption information.
6	Others	■ Please fill out the specific demand:_____

Table 3.8 The Recommended Priorities to Improve the Existing Debris-flow Warning System

Content	County	Township	Village
Reduce the False Alert Rate (FAR)	4	4	4
Raise the Warning Hit Rate (WHR)	1	2	2
Narrow the unit of warning area (i.e., Point out the definite place of the risk area)	2	1	4
Add the application of the debris-flow alert to other sediment disaster	5	5	3
Provide the more detailed warning information	3	3	1
Others	6	6	6

The findings indicate that, for the county and township governments, *raising the warning* hit *rate* and *narrowing the unit of warning area* are the most important

improvement direction for existing warning system. In other words, obtaining more accurate predictions of disaster occurring time and location are the greatest need in executing evacuation and related disaster prevention actions.

For the village heads, perhaps due to the difficulty to obtain more detailed warning information by themselves, *providing more detailed warning information* is the number-one priority in improvement recommended. The finding could be applied to improve the disaster prevention education of village heads and enhance their ability to collect warning information.

In addition, many studies have pointed out the *crying wolf* effect (false alert; i.e., the sediment disaster alert has been issued, but no disasters occur), but this survey seems to show little effect for local government decision-makers and inhabitants. For example, the weight of *false alert rate* under the cluster of *past experience* of level 2 for local governments is only about 10%, and the more primary the government is, the less it pays attention in **Table 3.5**. Moreover, the weight of *false alert experience* under the cluster of *past experience* of level 2 for inhabitants is also about 10 % (see **Table 3.6**). There is a similar result in **Table 3.8**; that is, the priority order of *reducing false alert rate* is only 4. The results seem to confirm that *raising warning hit rate* is the most important priority in improving the existing warning system.

3.4 Summary

This study establishes the evacuation decision-making models based on the pair-wise comparison and the hierarchy process (AHP) for local governments and inhabitants. The results and recommends are summarized as the follows.

(1) The findings show that the evacuation decisions made by different levels of local governments are quite diverse, and the decisions are also various depending on the spatial position of the local governments. The study also found that local governments and inhabitants all believe that raising the warning hit rate of the existing warning system is more important than reducing the false alert rate.

(2) The evacuation decision-making model established by this study not only showed the importance of each evacuation decision factor, but also identified the deficiencies in current disaster prevention actions. For example, the insufficiency of the existing warning system in small-scale areas created distrust of warning information from local governments; the diversity of evacuation decisions by

inhabitants in different regions can also become the direction of improvement for disaster prevention actions.

(3) Due to the weight assignment to factors affecting evacuation decisions, the AHP method was able to accurately reflect the most important decision-making factors under the present conditions. The weights of the decision-making factors will change as conditions change (e.g., the sediment disaster alert system accuracy increases dramatically). Therefore, the survey of relevant decision-making factors should be regularly updated, and the results should be evaluated to determine whether or not the adjusted disaster prevention strategies have achieved the desired goals.

(4) The findings also indicated that evacuation decision-making in mountainous areas not only considers the warning information, but also includes multiple and complex factors such as time, space, and socio-economic factors. Using only a single disaster warning system is not sufficient to assist local governments or the general public in making the correct evacuation decisions during typhoons or heavy rainfall.

(5) The increasingly complex types of disasters in mountainous areas (such as the multi-modal sediment disasters that occurred in Taiwan during Typhoon Morakot) emphasize the need to establish a decision support system for warning and evacuation against multi sediment hazards as one of the main priorities in future disaster prevention actions. While the study results in **Table 3.5** and **Table 3.6** were presented using the relative weights for each cluster, the results are easy to transform into absolute weights for all factors by Eq. (3.6) (see **Figure 3.4** to **Figure 3.9**), and they can also serve as basic information for the primary stages of developing a decision support system for warning and evacuation against multi sediment hazards.

(6) The findings indicate that *raising the warning hit rate*, *narrowing the unit of warning area*, and *providing more detailed warning information* are the most important improvement direction for existing warning system. Because most disasters in mountainous areas result from floods and the moving of sediment, this study uses landslides, floods from river channels, and riverbed deformation as disaster types of the multi-hazards to conduct the simulation and establish the new warning system. Integrating the study results of Chapter 2 and Chapter 3, the new warning system should meet the following requirements.

(i) It can accurately predict the occurring time, location, type, and scale of potential disaster. This study recommends using slope units as the target to predict landslides and using unit channel as the target to predict the water level and riverbed deformation.

(ii) It considers the geological, geomorphologic, and hydrological characteristics of slopes and channels as well as the scenario simulation capacity. Thus, this study recommends using basin scale simulation as overall consideration perspective.

(iii) It can provide more detailed warning information.

(iv) Raising the warning hit rate of the existing warning system is more important than reducing the false alert rate.

References

Amano, A. and Takayama, T. (2006): On the situation of early warning information for sediment-related disasters – Teachings of evacuation from the T0514 disaster, Journal of the Japan Landslide Society, Vol. 43, No. 6, pp. 370–375 (in Japanese).

Baker, E. J. (1991): Hurricane evacuation behavior, International Journal of Mass Emergencies and Disasters, Vol. 9, No. 2, pp. 287.

Chen, C.Y., and Fujita, M. (2013): An analysis of rainfall-based warning systems for sediment disasters in Japan and Taiwan, International Journal of Erosion Control Engineering, Vol. 6, No. 2, pp. 47-57.

Chen, L.C. and Mars, S.Y. (2008): A study of evacuation decisions of governments under large-scale disasters, National Science Council, Taiwan (in Chinese).

Chen, L.C., Wu, J.Y., Liu, Y.C., and Lee, I.H. (2007): A study of residential evacuation behavior and decision-making in a vulnerable debris flow area: The case of typhoon Talim, Journal of Chinese Soil and Water Conservation, Vol. 38, No. 4, pp. 325–340 (in Chinese).

Chen, S. C., Ferng, J. W., Wang, Y. T., Wu, T. Y., and Wang, J. J. (2008): Assessment of disaster resilience capacity of hillslope communities with high risk for geological hazards, Engineering Geology, Vol. 98, No. 3–4, pp. 86–101.

Council of Agriculture (COA) (2010): Directions governing the evacuation for debris flow disasters (in Chinese).

Department of Erosion and Sediment Control (DESC) (2007): Guidelines for warning systems and evacuations, Japan (in Japanese).

Dow, K. and Cutter, S. L. (1998): Crying wolf: Repeat responses to hurricane evacuation orders, Coastal Management, Vol. 26, No. 4, pp. 237–252.

Gladwin, H. and Peacock, W. G. (1997): Warning and evacuation: A night of hard choices. In: W. G. Peacock, B. H. Morrow, and H. Gladwin (eds) Hurricane Andrew: Gender, Ethnicity and the Sociology of Disasters Routledge, London, pp. 52–73.

Irasawa, M. and Endo Y. (2010): An opinion poll administered to Kamaishi City residents about sediment disaster generated by rainfall in July 2002, Journal of

Iwate University, Vol. 41, pp. 259–272 (in Japanese with English abstract).
Lin, C.Y. (2007): A study of evacuation of commercial populations under large-scale disasters, National Science Council, Taiwan (in Chinese).
Lindell, M. K., Lu, J.-C., and Prater, C. S. (2005): Household decision making and evacuation in response to hurricane Lili, Natural Hazards Review, Vol. 6, No. 4, pp. 171–179.
Lindell, M. and Prater, C. (2007): A hurricane evacuation management decision support system (EMDSS), Natural Hazards, Vol. 40, No. 3, pp. 627–634.
National Institute for Land and Infrastructure Management (NILIM) (2010): Studies of warning systems and evacuation for sediment disasters, 23th Sabo Research Report (in Japanese).
Okamoto, A., Tomita, Y., Mizuno, M., Hayashi, S., Nishimoto, H., Ishii, Y., and Chiba, S. (2012): Data analysis regarding warning and evacuation information against sediment-related disasters, National Institute for Land and Infrastructure Management (NILIM), Japan (in Japanese).
Pai, J.T. (2008): A study of the evacuation of disadvantaged groups under large-scale disasters, National Science Council (in Chinese).
Regnier, E. (2008): Public evacuation decisions and hurricane track uncertainty, Management Science, Vol. 54, No. 1, pp. 16–28.
Sataty, T. L. (1980): The Analytic Hierarchy Process, John Wiley, New York.
Soil and Water Conservation Bureau (SWCB) (2012): Debris flow disaster prevention website (http://246eng.swcb.gov.tw) (11/3/2012).
Ushiyama, M. (2012): The possibility of reducing sediment disaster victims based on information, Conference of Japan Society of Erosion Control Engineering 2012, pp. 138–139 (in Japanese).
Whitehead, J. C., Edwards, B., Van Willigen, M., Maiolo, J. R., Wilson, K., and Smith, K. T. (2000): Heading for higher ground: Factors affecting real and hypothetical hurricane evacuation behavior, Global Environmental Change Part B: Environmental Hazards, Vol. 2, No. 4, pp. 133–142.
Wolshon, B., Urbina, E., Levitan, M, and Wilmot, C. (2005): Review of policies and practices for hurricane evacuation. I: Transportation planning, preparedness, and response, Natural Hazards Review, Vol. 6, No.3, pp. 143–161.
Wu, J.Y. (2009): A comparative study of residential evacuation decisions and behavior for vulnerable debris flow areas, Journal of Slopeland Hazard Prevention, Vol. 8, No. 1, pp. 1–14 (in Chinese).
Zeigler, D. J. and Johnson, J. H. (1984): Evacuation behavior in response to nuclear power plant accidents, The Professional Geographer, Vol. 36, No. 2, pp. 207–215.

Chapter 4

Landslide Prediction on a Basin Scale Using Regression-Numerical Model

4.1 Introduction

According to the study results and recommendation of Chapter 2 and Chapter 3, this study adopts basin scale simulation as overall consideration perspective. In the past decades, using the distributed model to conduct a basin model has been extensively used [*Takasao and Shiiba*, 1988; *Ichikawa et al.*, 1999; *Lee et al.*, 2011; *Egahsira and Matsuki*, 2000; *Takahashi et al*., 2000].

This study uses the composition of unit channels and unit slopes to conduct the basin model proposed by *Egashira and Matsuki* [2000]. Water discharge and sediment runoff in a basin was calculated with the basin model. The basin model, which is based on a unit channel with two inflow points and one outflow point (see **Figure 4.1(a)**), can reproduce stream channels distributed in a drainage basin. Each unit channel has two unit slopes which represent the watershed of the unit channel (see **Figure 4.1(b)**). However, Unit slope was sometimes unsuitable to conduct the slope stability analysis because of the too-great size and the complex aspect and slope. Hence, this study divided each unit slope into several slope units according to the slope aspect and other parameters (see **Figure 4.1(c)**).

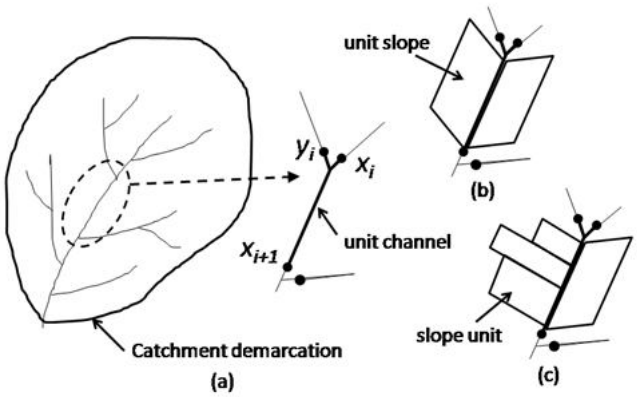

Figure 4.1 Basin model (a)a unit channel has two inflow points and one outflow point (b)each unit channel has two unit slopes (c)each unit slope can be divided into several slope units according to the slope aspect and other parameters

Generally, the methods of predicting landslides can be divided into two types - statistical model and physically-based model. The statistical model usually uses historical disaster inventories to extract the easy-to-collect indicator (e.g., rainfall) to identify the triggering value of landslides [*Caine*, 1980; *Wieczorek and Glade*, 2005; *Osanai et al*., 2010; *Chen and Fujita, 2013*]. The statistical model is easy to employ and can be used in wide-area monitoring, but it can't offer the exact occurring time, location and scale of landslide [*Chen and Fujita, 2013*]. On the contrary, the physically-based model can give not only the occurring time but also the occurring location and scale of landslide [*Xie et al*., 2006; *Tsutsumi et al*., 2007]. However, the physically-based model is usually only applied in a specific slope because of the time-consuming calculation. That is, it is difficult to apply a physically-based model to predict landslide in a real-time warning system on a basin scale. This study proposes a new warning indicator (Critical water content, W_{cr}) for predicting landslides [*Chen and Fujita*, 2014]. This indicator is derived from physically-based model and has a clear physical meaning, as well as it also has high-performance calculations to predict occurring time, location, and scale of landslides on a basin scale.

4.2 Materials and methodology

4.2.1 Slope unit and study area

Many studies used grid as a unit for slope stability analysis on basin scale [*Casadei et al*., 2003; *Chang and Chiang*, 2009; *Lee and Ho,* 2009], because the grid-based analysis units could be easily obtained and managed, as well as the algorithm was simpler. However, the grid cell didn't represent geological, geomorphologic or other environmental boundaries, so the results by the grid-based method were relatively unacceptable in physical terms [*Xie et al*., 2004].

This study used slope units as the slope stability analysis targets (see **Figure 4.1(c)**), because of using a physically-based model to simulate landslide. The slope units were also used to conduct the landslide hazard evaluation [*Carrara et al*., 1991; *Crosta et al*., 2006] and landslide prediction [*Xie et al*., 2004; *Xie et al*., 2006; *Wang et al*., 2006].

Due to a large number of slopes in a basin, it will be too time-consuming to

demarcate the slope units by the manual method. This study uses the approach proposed by *Xie et al.* [2004] to obtain slope units by overlaying the watershed polygon of the DEM and its reversed DEM (see **Figure 4.2**). Moreover, the detail adjustment of the slope units will be processed according to the slope aspect and the rationality of the centroid which will be employed to estimate the length of the slope. In addition, this study assumes that landslide will not occur at the slope which the slope of ground surface is less than 15^{o}. Accordingly, the part of slope near river channel and the slope of ground surface less than 15^{o} will be removed. **Figure 4.3** showed the result of demarcating slope units, and the different colors represented the different slope aspects as well as the length of the slope unit could be defined by the distance between the centroid and the unit channel.

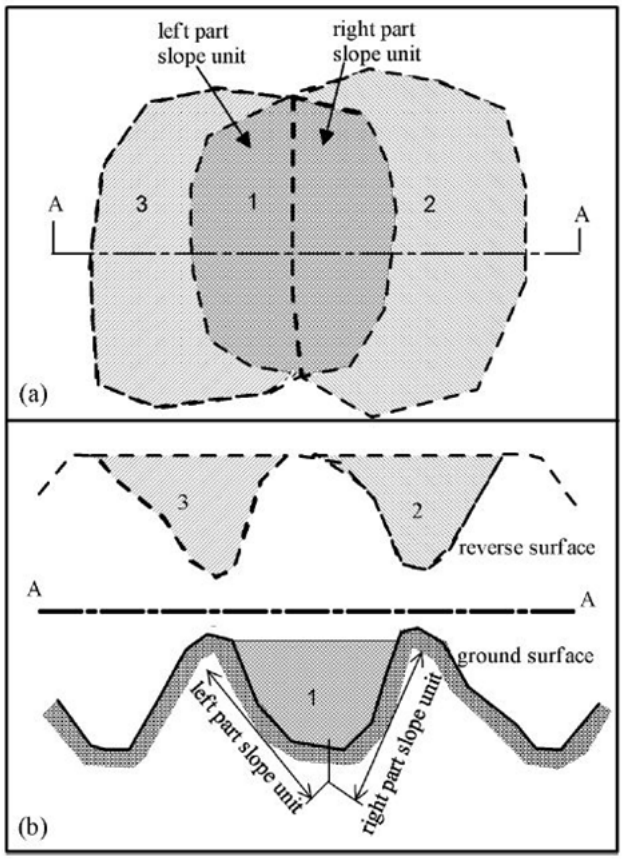

Figure 4.2 Slope unit derived using a GIS-based hydrological and modeling tool. No. 1 watershed is the result of using DEM for watershed analysis, No. 2 and No. 3 watersheds can also be obtained using reverse DEM (a). One watershed polygon can then be divided to two slope units (a) and (b) [*Xie et al*., 2004]

The study area is located in the Shizugawa basin, Uji, Kyoto Prefecture, and sandstone-shale interface is the most common lithology in the study area. The basin

area is about 10.8 km^2, and is divided into 127 unit channels and 435 slope units by using 15m resolution DEM. **Figure 4.4** shows the elevation and the distribution of the unit channels and slope units in the study area. To simplify the analysis, each slope unit was defined as a simple slope model which consisted of four parameters (see **Figure 4.5**), where α is the mean slope of the ground surface, β is the inclination of bedrock, L is the horizontal length of the slope, n is the soil thickness of the downstream of the slope. The value of α and L can be calculated by GIS software. According to the field survey after the disaster in August 2012, all slope failures were shallow landslides, and the mean depth was about 2m. Accordingly, the value of β was set the same as α, and n was set as 2m for all slope units.

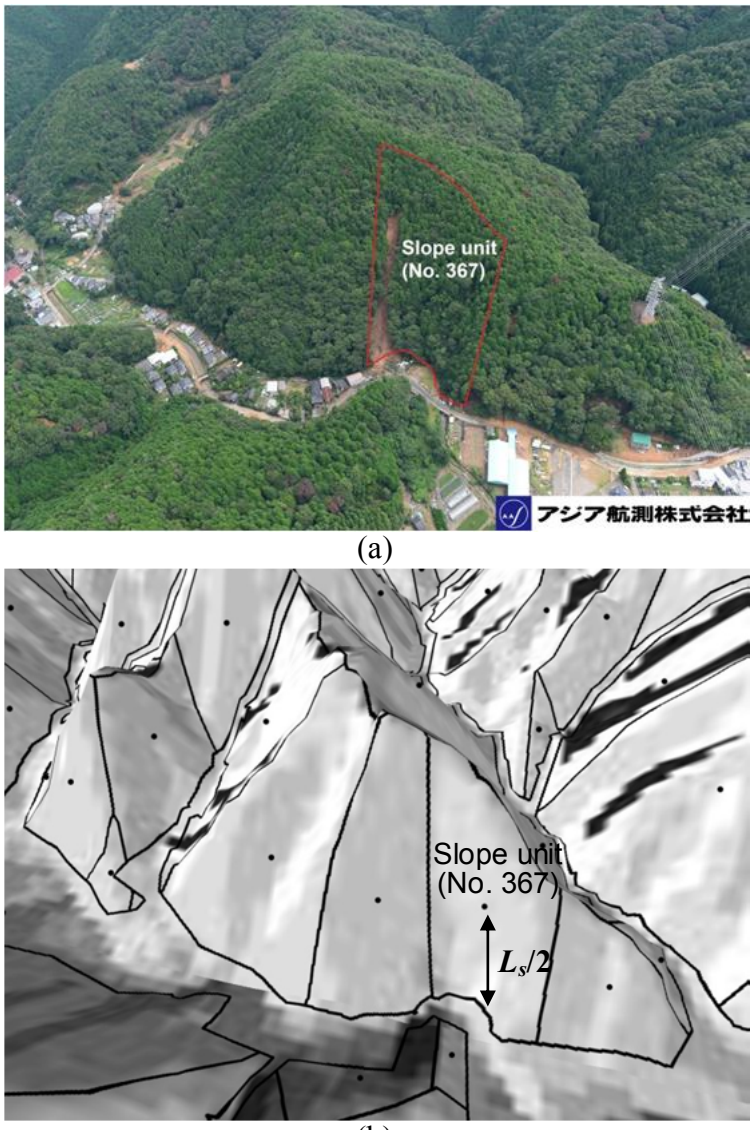

Figure 4.3 (a) The aerial photo of landslide on the slope unit (No.367) after heavy rainfall event on August 14, 2012 [Asia air survey co., LTD, 2012] (b) The paradigm of the slope units

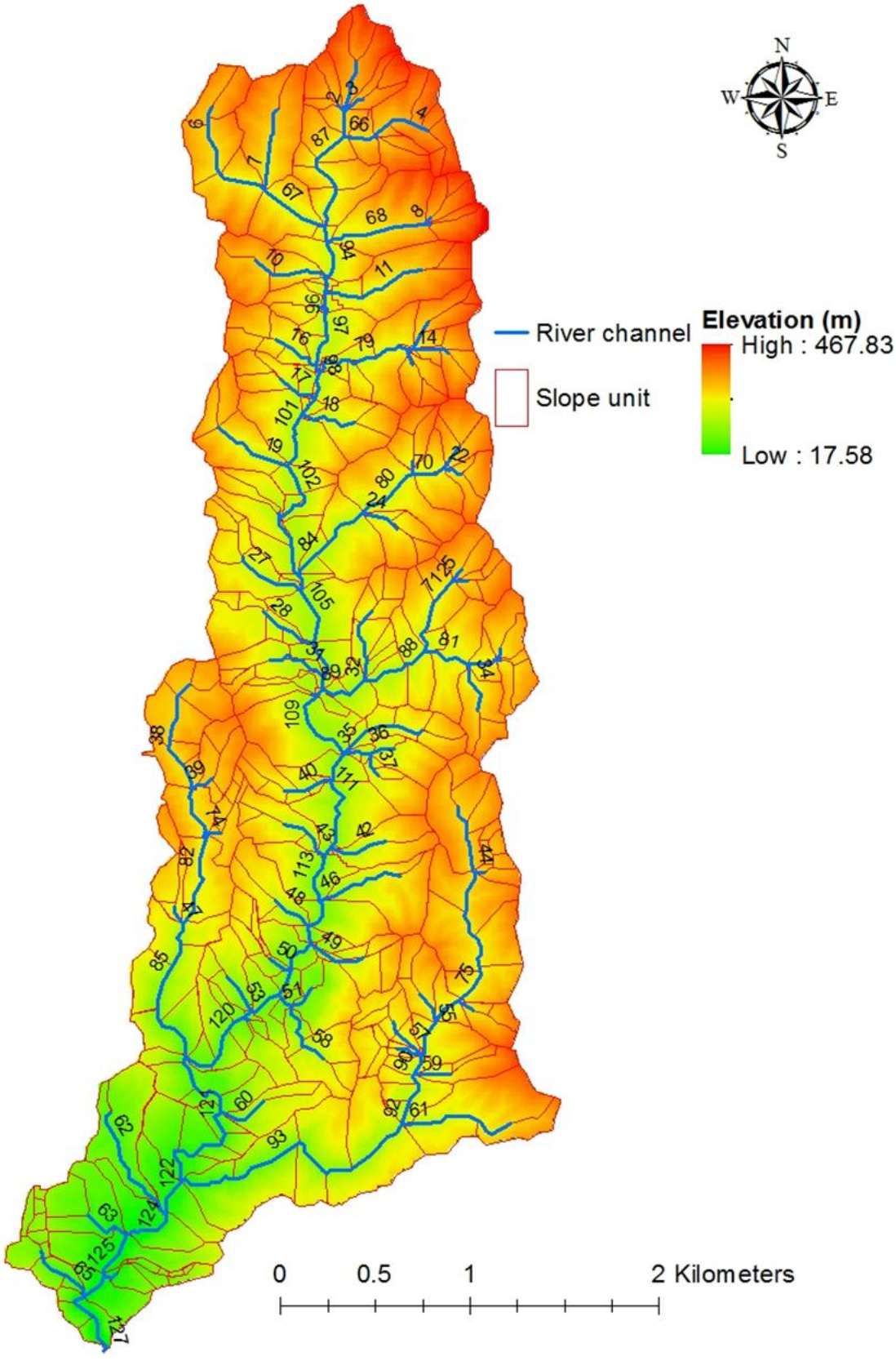

Figure 4.4 The elevation and the distribution of the unit channels and slope units in the study area (Black numbers are the number of unit channels)

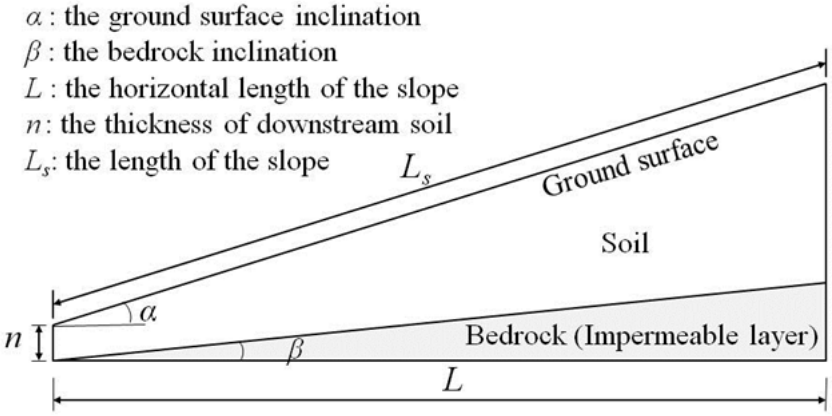

Figure 4.5 The simplified model of slope unit for the following stability analysis

This study selected the heavy rainfall disaster on August 13-14 in 2012 as the simulation case. This disaster was typical heavy rainfall with high intensity and short duration. Taking the data of rain gauge on Uji city as an example, the accumulated rainfall was 311mm, but the three-hours rainfall is up to 186mm. In fact, the three-hours rainfall was about 2 times of the maximum record since 1945 [*Kyoto Prefecture*, 2013]. Moreover, according to the analytic rainfall data of X-band radar, the rainfall on the Shizugawa basin was stronger than in Uji city. Such kind of heavy rainfall caused many shallow landslides and floods on the Shizugawa basin. **Figure 4.6** and **Figure 4.7** are the aerial photo of floods and landslide on the Shizugawa basin after the heavy rainfall event on August 13-14, 2012 [Asia air survey co., LTD, 2012; *Kyoto Prefecture*, 2013].

While the aerial photos can offer the high resolution discrimination to detect the landslides and floods, they only focus partial area of the Shizugawa basin and lack geometrically corrected (orthorectified). That is, they can't be applied to measure true distances and areas of landslides. Hence, this study adopted the satellite images to detect the overall basin. Using the orthorectified satellite images of RapidEye on September 24 in 2012, 38 slope units were identified as newly collapsed slopes after the rainfall event (See **Figure 4.8**). According to the aftermath disaster survey, the occurring time of landslides was identified between 04:30~06:00 on August 14. The simulation results of this study would be verified by using the above-mentioned information.

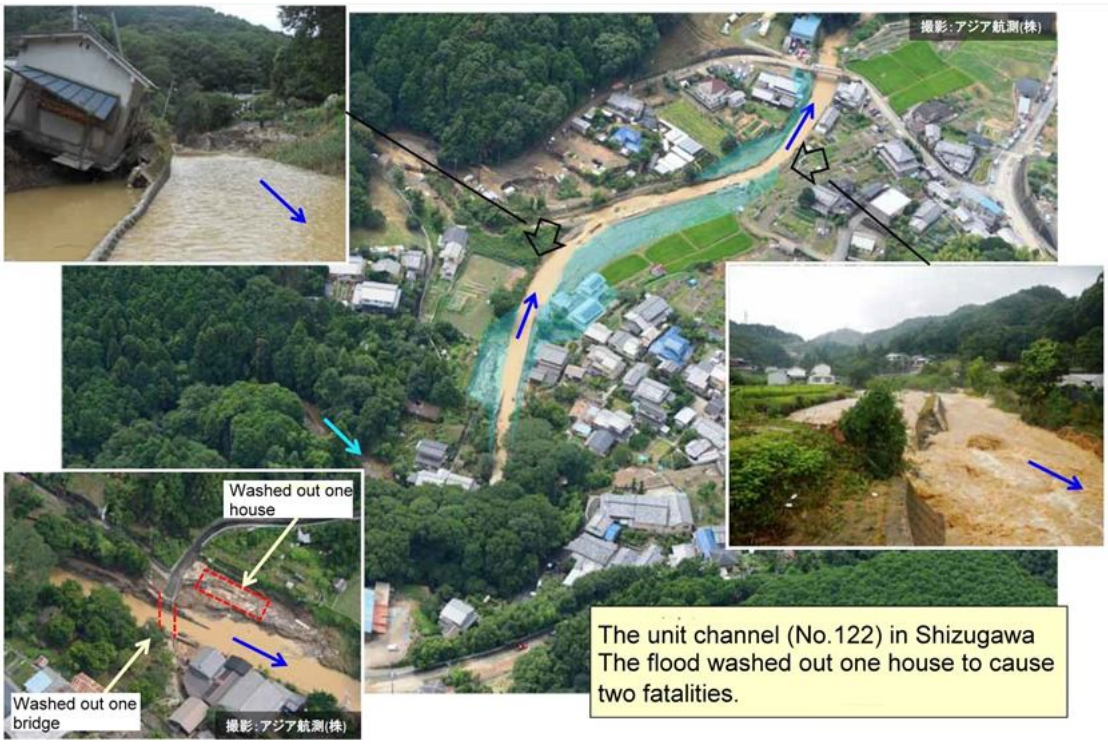

Figure 4.6 The aerial photo of flood on the Shizugawa basin, Uji, Kyoto Prefecture after heavy rainfall event on August 14, 2012 [Modified from the disaster report by *Kyoto Prefecture*, 2013]

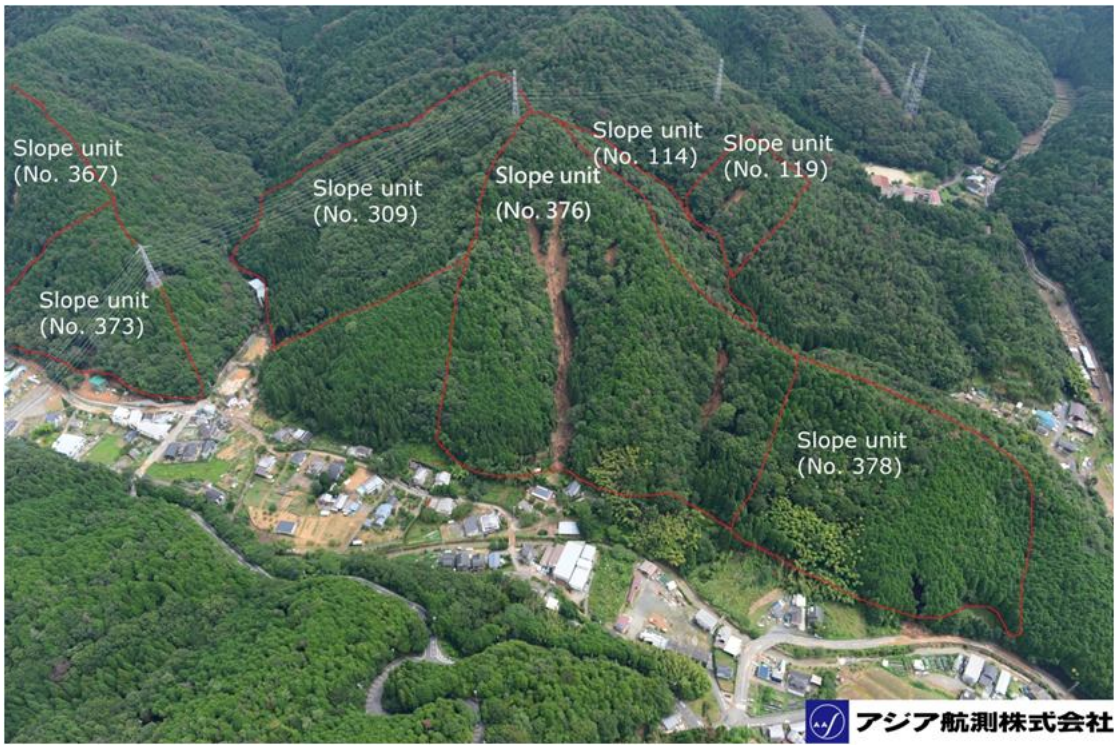

Figure 4.7 The aerial photo of landslide on the Shizugawa basin, Uji, Kyoto Prefecture after heavy rainfall event on August 14, 2012 [Modified from Asia air survey co., LTD, 2012]

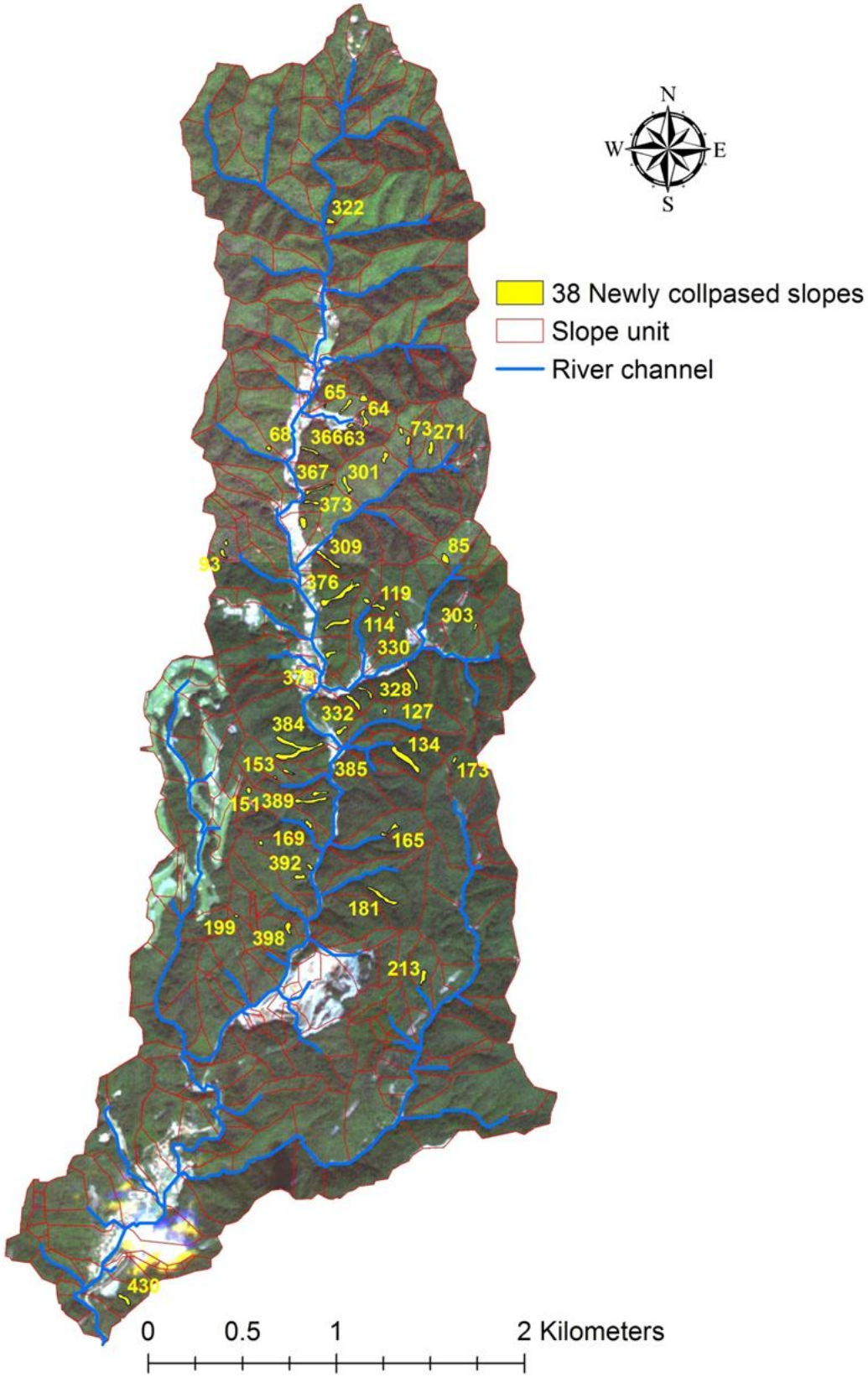

Figure 4.8 38 newly collapsed slope after heavy rainfall disaster on August 14, 2012 on the Shizugawa basin, Uji, Kyoto Prefecture (Yellow numbers on the graph are the number of slope units)

To better the simulation result, this study used the rainfall data of X-band radar with spatial resolution of 285m and time step of 1 minute. **Figure 4.9** showed the range of rainfall data of X-band radar on the Shizugawa basin in this study.

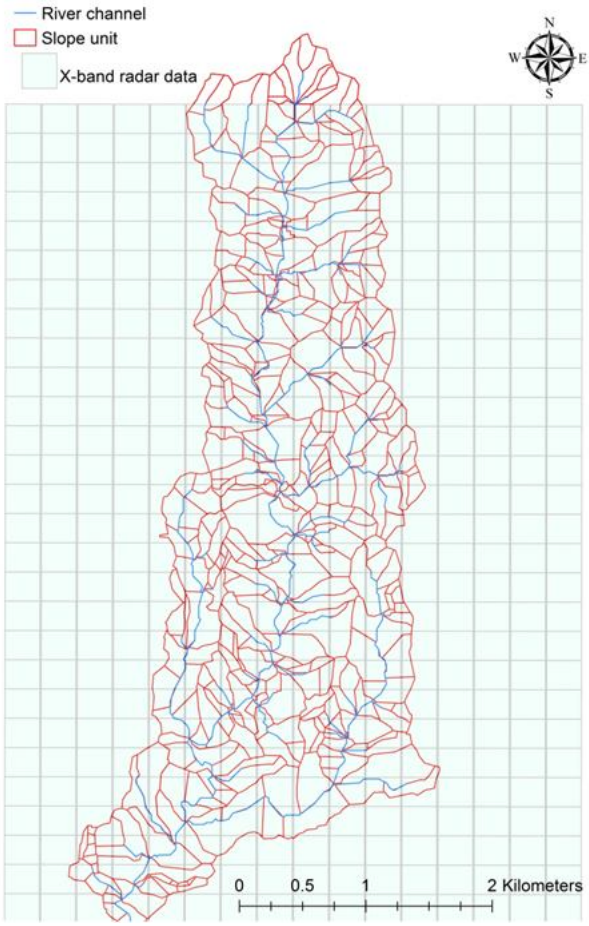

Figure 4.9 The range of rainfall data of X-band radar on Shizagawa basin

4.2.2 Slope stability analysis model

This study used the Integrated Rainfall Infiltration Slope stability (IRIS) model to conduct the slope stability analysis [*Tsutsumi et al.*, 2007; *Chen et al.*, 2013]. The IRIS model can be divided into several modules. The rainfall-infiltration module adopts the Richard's equation to simulate the infiltration and water flow in the soil. The result of infiltration analysis, which was calculated by the finite-element method, was then used to conduct a slope stability analysis simultaneously. A simplified Janbu method and dynamic programming (DP) method were used to determine the factor of safety and the critical slip surface. The following will elucidate the relative theory.

(1) Infiltration model

The IRIS model adopts the Richard's equation to simulate the infiltration and water flow in the soil.

$$C(\psi)\frac{\partial \psi}{\partial t} = \nabla \cdot \{K(\psi)[\nabla(\psi + z)]\} \tag{4.1}$$

where C(ψ) is the soil water capacity and $K(\psi)$ is the hydraulic conductivity. The lognormal model proposed by *Kosugi* [1996] can be used to represent $S_e(\psi)$, C(ψ) and $K(\psi)$ for unsaturated condition ($\psi < 0$):

$$S_e\left(\equiv \frac{\theta - \theta_r}{\theta_s - \theta_r}\right) = Q\left(\frac{\ln(\psi/\psi_m)}{\sigma}\right) \tag{4.2}$$

$$C(\psi) = \frac{d\theta}{d\psi} = \frac{\theta_s - \theta_r}{\sqrt{2\pi}\sigma(-\psi)}\exp\left\{-\frac{[\ln(\psi/\psi_m)]^2}{2\sigma^2}\right\} \tag{4.3}$$

$$K(\psi) = K_s\left[Q\left(\frac{\ln(\psi/\psi_m)}{\sigma}\right)\right]^{1/2}\left[Q\left(\frac{\ln(\psi/\psi_m)}{\sigma} + \sigma\right)\right]^2 \tag{4.4}$$

Where $S_e(\psi)$ is effective saturation, θ_s[m^3/m^3] is the saturated soil water content, θ_r[m^3/m^3] is the residual soil water content, ψ_m[m] is the pressure potential corresponding to the median soil pore radius, σ is a dimensionless parameter related to the width of the pore-size distribution, and K_s [m/s] is the saturated hydraulic conductivity. The function $Q(x)$ represents the residual normal distribution and can be expressed as

$$Q(x) = \int_x^\infty \frac{1}{\sqrt{2\pi}}\exp\left(-\frac{u^2}{2}\right)du \tag{4.5}$$

For saturated condition ($\psi \geq 0$), value are set at, $K(\psi) = K_s$ and C(ψ) = 0.

The IRIS model uses the 3D finite element method to solve Richard's equation [Istok 1989].

(2) Slope stability analysis model

The result of infiltration analysis which was calculated by the finite element method aforementioned will be used to conduct a slope stability analysis simultaneously. That is, the spatial distribution of pore water pressure, calculated through a rainwater infiltration analysis, was used as input data in the slope stability analysis. A simplified Janbu method was used to analyze slope stability because this

method can be applied to any shape of slip surface. In the simplified Janbu method, a soil layer is divided into vertical slices, and the balance of stresses and slip condition within each slice is assessed. This method is used to calculate the factor of safety F_s, which can be expressed as

$$F_s = \frac{\sum\left[\left\{c_i' l_i \cos a_i + (W_i - u_i l_i \cos a_i)\tan\phi_i'\right\}\right]/m_a}{\sum \tan a_i} = \frac{\sum A_i}{\sum B_i} \tag{4.6}$$

$$m_a = \cos^2 a_i\left(1 + \frac{\tan a_i \tan\phi_i'}{F_s}\right) \tag{4.7}$$

where subscript i indicates the number of vertical slices of soil layer, c_i' and ϕ_i' represent the cohesion and internal friction angle of the soil, W_i is the weight of slice, a_i and l_i represent the angle and length of the slip surface of the slice, and u_i is the water pressure affected on the slip surface.

(3) Determining critical slip surface

Based on previous studies by *Baker*[1980], *Kubota and Nakamura* [1991] and *Yamagami and Ueta* [1986;1988], the dynamic programming (DP) method was used to determine the slip surface that provides a minimum factor of safety. Because the dynamic programming is applicable only to 'additive functions', however, the forms of Eq. (4.6) don't meet the requirement. Therefore, *Baker*[1980] define the new auxiliary function G as

$$G = \sum_{i=1}^{n}\left(A_i - F_s \cdot B_i\right) \tag{4.8}$$

Baker[1980] also had proved that minimizing the function F_s in Eq. (4.6) is equivalent to minimizing the new function G in Eq. (4.8). That is, the value of F_s depends on the location of the slip surface. Thus, the critical slip surface will yield the minimum of not only the function F_s but also the function G. Because the A_i itself also contains F_s implicitly, it is necessary to assume a initial value of F_s.

To use the dynamic programming process on the slope-stability problem, the slope should be divided into $(n+1)$ stages, as the vertical lines in the **Figure 4.10(a)**. In addition, each stage could be divided into appropriate number of states, as the points in **Figure 4.10(a)**. Let points (i, j) and $(i+1, k)$ denote arbitrary states j and k at two arbitrary successive stages, respectively, as shown in **Figure 4.10(b)**. The

segment *jk* could be considered as a part of a possible trial slip surface. That is, the quadrilateral *abkj* could be considered as a slice, and it could be calculated the corresponding values of A_i and B_i from Eq. (4.6). Then, the change in G, $DG_i(j,k)$, on passing from the point (i, j) to the point $(i+1, k)$ is expressed as

$$DG_i(j,k) = A_i - F_s \cdot B_i \tag{4.9}$$

At this stage, the function $H_i(j)$, which is called the 'optimal value function', is defined as the minimum value of G between initial stage and the point (i, j). Then, the recurrence relation for the present situation can be written as

$$H_{i+1}(k) = \min_{j=1\sim S_{n+1}} \left[H_i(j) + DG_i(j,k) \right]_{k=1\sim S_i+1}^{i=1\sim n} \tag{4.10}$$

with the boundary conditions:

$$H_1(j) = 0, \quad j = 1 \sim S_1 \tag{4.11}$$

and

$$G_m = \min G = \min_{j=1\sim S_{n+1}} \left[H_{n+1}(j) \right] \tag{4.12}$$

where S_i= the number of states at the stage i.

According to the abovementioned means, the critical slip surface, which is corresponding with minimum F_s, could be determined. Finally, using the critical slip surface calculates the A_i and B_i, and then obtains the value of F_s.

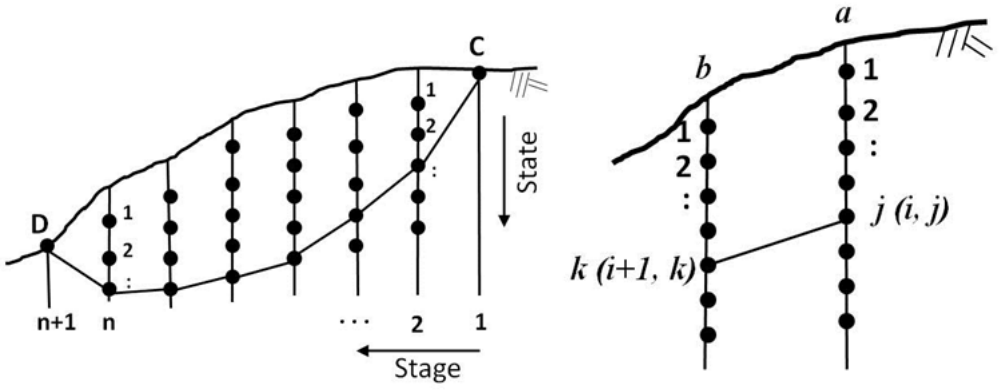

(a) (b)

Figure 4.10 (a)Schematic representation of stages and states for DP (b)Schematic definition of stages and states

4.2.3 Verification of the IRIS model

To confirm the applicability of this model, two different types of actual landslide cases were simulated as verification. One case was the deep-seated landslide which occurred in volcanic debris slope located in Senokuchi area, Taketa, Oita Prefecture, and the other was the shallow landslide which occurred in sandstone-shale interface slope located in Shizugawa basin, Uji, Kyoto Prefecture (i.e., the study area).

(1) Senokuchi area, Taketa City

In September 2005, a deep-seated landslide induced by typhoon 0514 occurred in Senokuchi area, Taketa, Oita Prefecture. The soil consists of loam and volcanic debris. Although the maximum rainfall intensity was only 32mm/h, the duration of the rainfall was more than 48 hours, and the accumulated rainfall was about 536mm. The simulation used the actual rainfall from August 1 to September 3 as antecedent rainfall data, and the prime simulation duration was from September 4 to September 6 with 10 minimums as the time-step of the simulation. **Table 4.1** lists the parameters used in the simulation and the simulation results are expressed in **Figure 4.11**.

Table 4.1 Hydraulic characteristics and soil strength of the soil of the slope in Senoguchi, Taketa city

Hydraulic parameters	*Ks*	*θs*	*θr*	*ψm*	*σ*
	cm/s	m^3/m^3	m^3/m^3	cm	-
Surface	2.42×10-2	0.646	0.477	-792	0.875
Middle	3.32×10-3	0.595	0.441	-595	1.36
Lower	5.69×10-4	0.682	0.577	-797	1.02
Soil strength	*γ*		*C*	*φ*	
	t/m^3		tf/m^2	degree	
	1.92		2.0	17	

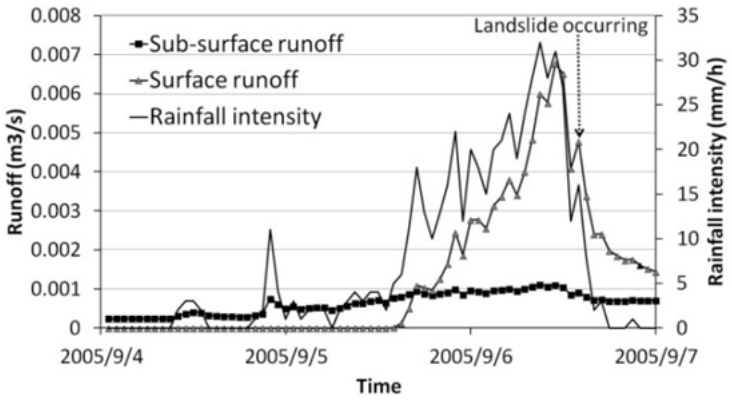

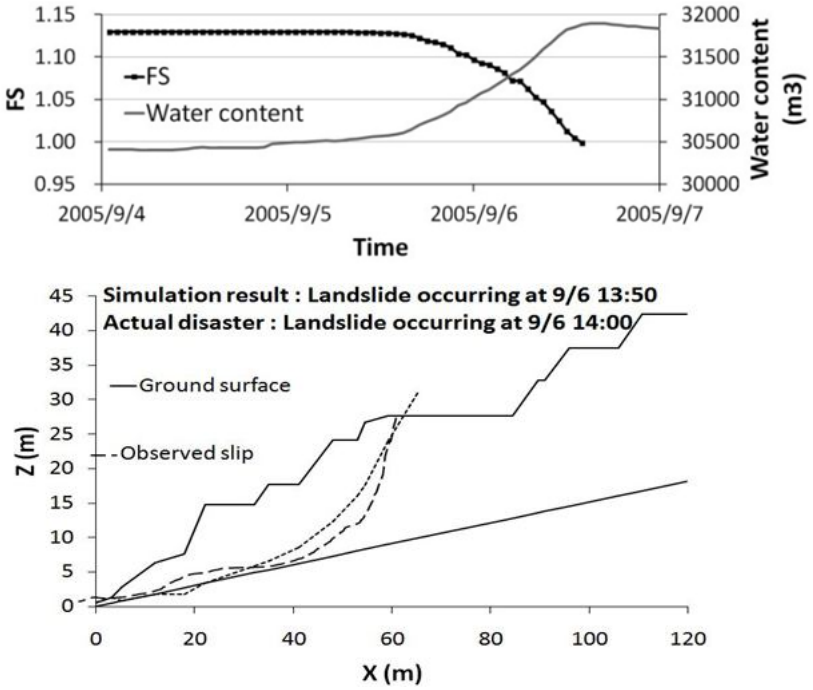

Figure 4.11 The simulation of the landslide due to typhoon 0514 in Taketa City

The results show the simulation can calculate not only the change of the safety factor and the scale of the landslide but also the relation of the runoff and the rainfall. In this case, the landslide scale and the occurring time of the simulation results are very similar with the actual landslide.

(2) Shizugawa basin, Uji City

Here, this study selected a representative slope unit (No.376, see **Figure 4.7**), which occurred a landslide at around 05:00 on August 14, 2012, for model verification. The simulation used the rainfall data of X-band radar from July 1 to August 12 as the antecedent rainfall, and prime simulation duration was from August 13 to August 14 with 1 minute interval. According to the field survey, this study assumed the thickness of soil as 2m. The parameters used in the simulation are listed in **Table 4.2**, and they were obtained by field survey and laboratory experiment. The simulation results are shown in **Figure 4.12**. The landslide occurring time from the simulation was very similar compared with the actual event. However, the actual collapse maybe developed in multi-stage, thus the landslide scale from the simulation was smaller.

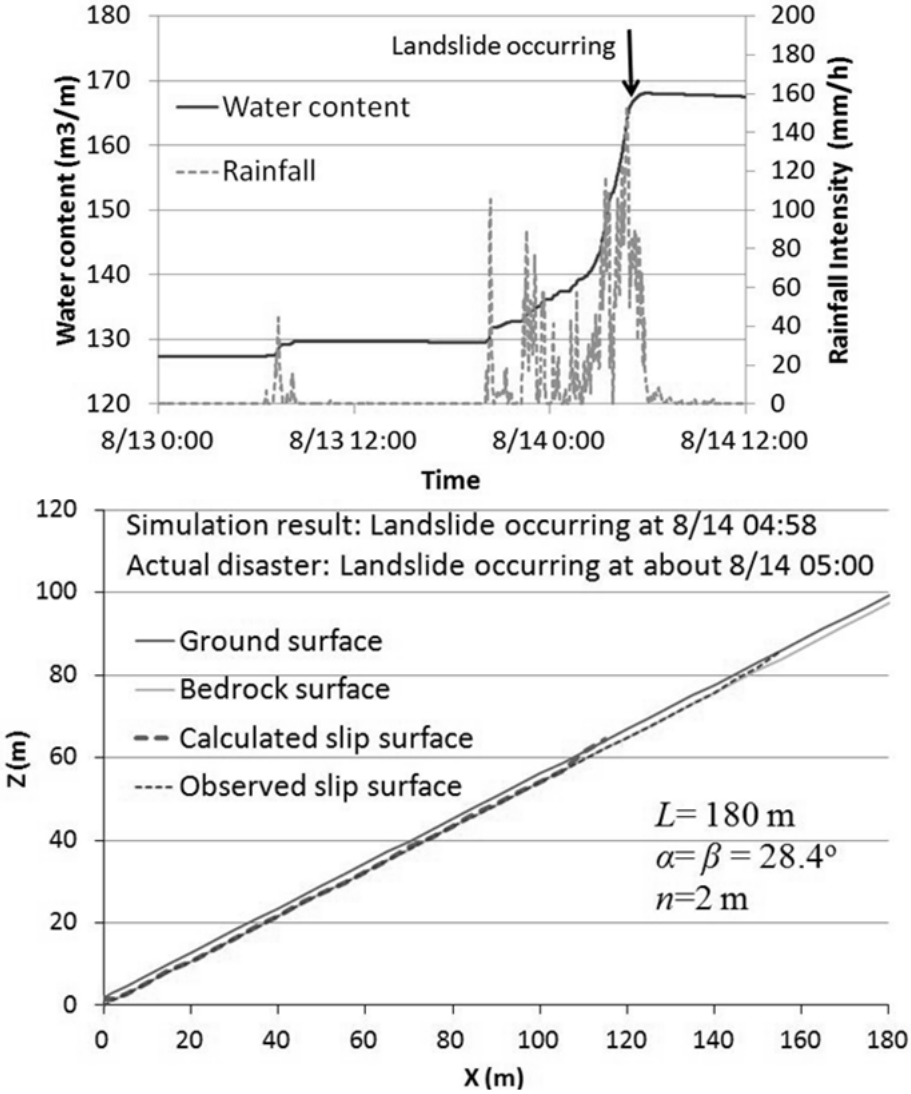

Figure 4.12 The simulation of the landslide due to heavy rainfall on August 14, 2012 in the Shizugawa basin, Uji, Kyoto (Slope unit, No. 376)

Table 4.2 Hydraulic characteristics and soil strength of the soil of the slope in the Shizugawa basin

Hydraulic parameters	Ks	θs	θr	ψm	σ
	cm/s	m^3/m^3	m^3/m^3	cm	-
Upper layer	0.0035	0.467	0.240	-31.2	1.40
Lower layer	0.0005	0.468	0.270	-23.7	1.17
Soil strength		γsat	C	ψ	
		t/m^3	tf/m^2	degree	
		1.64	0.7	31	

4.2.4 Water content index for landslide prediction

(1) Critical water content index

While the IRIS model can effectively simulate both shallow landslide and deep-seated landslide [*Chen et al*., 2013], the large computing time makes the IRIS

model difficult to employ on a basin scale.

In the process of the landslide simulation by using IRIS model, *Fujita et al*. [2010] found that the water content in the slope was very similar when the slope collapsed even if the different rainfall patterns were employed. Therefore, they suggested the water content could be used as a warning indicator for landslide prediction. To verify the feasibility of above suggestion, this study used two types of tentative slopes to conduct landslide simulation by using IRIS model under different rainfall scenarios. These two types of tentative slopes adopted the simplified model which consisted of four parameters (see **Figure 4.5**). One is non-parallel between bedrock and ground surface, and the other is parallel.

(i) Type I - Bedrock and ground surface is non-parallel

In this case, the tentative slope was set as L=110m, α=21.24^{o}, β=8.6^{o}, n=0.5m, and the width of slope was 1 m. The tentative slope was conducted the landslide simulation by using IRIS model under 14 different rainfall patterns (see **Figure 4.13**). The hydraulic characteristics and soil strength of the soil of the slope were same as the simulation case in Taketa City (see **Table 4.1)**. The simulation results were shown as **Table 4.3**. The results showed that although the landslide occurring time of the tentative slope varied greatly; the water content was within a similar range when the landslide occurred. In addition, the profile of the slip surface (i.e., the scale of landslide) seemed to imply that the scale of landslide was smaller when the rainfall intensity was higher.

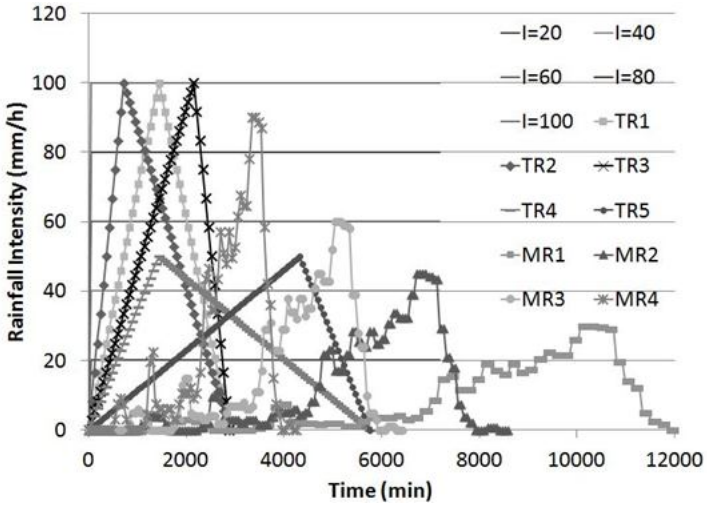

Figure 4.13 Fourteen different rainfall patterns for verifying the feasibility of using water content as the landslide warning indictor

Table 4.3 The water content of the type I slope when the landslide occurred during 14 different rainfall patterns

Rainfall (mm/h)	W_{cr} (m^3/m)	Landslide occurring time (min)	Profile of the slip surface (m^2)
I=20	1017.3	2950	882.89
I=40	1012.2	1740	835.66
I=60	1010.9	1120	834.35
I=80	1009.7	940	834.35
I=100	1009.6	860	834.35
TR-1	1011.4	1300	834.35
TR-2	1011.2	920	834.35
TR-3	1011.4	1550	834.35
TR-4	1012.3	1810	834.35
TR-5	1015.9	2820	882.53
MR-1	1017.0	8520	882.89
MR-2	1016.3	5670	882.53
MR-3	1015.4	4230	835.66
MR-4	1014.1	2930	834.35
mean	1013.2	2668.6	848.40
Standard deviation (SD)	2.7	2189.0	22.6
SD /mean (%)	0.27	82.03	2.66

(ii) Type II - Bedrock and ground surface is parallel

In this case, the tentative slope was set as L=154m, α=31°, β=31°, n=2m, and the width of slope was 1 m. The hydraulic characteristics and soil strength of the soil of the slope were same as the simulation case on Shizugawa basin (see **Table 4.2)**. In order to verify the findings that the scale of landslide was related to rainfall intensity, this case used 8 constant-intensity rainfall scenarios to conduct the landslide simulation by using IRIS model. The simulation results were shown as **Table 4.4**.

Table 4.4 The water content of the tentative slope unit when the landslide occurred during 8 different rainfall patterns

Rainfall (mm/h)	W_{cr} (m^3/m)	Landslide occurring time (min)	Profile of the slip surface (m^2)
I=10	140.84	1359	123.25
I=20	140.77	809	77.42
I=30	140.45	638	68.25
I=40	140.06	556	68.25
I=50	139.74	509	68.25
I=60	139.41	479	68.25
I=80	138.84	445	57.42
I=100	138.20	427	57.42
mean	139.79	652.75	73.56
Standard deviation (SD)	0.936	311.16	21.11
SD/mean (%)	0.670	47.67	28.69

The results also showed that although the landslide occurring time varied greatly under 8 different rainfall patterns; the water content was within a similar range when the landslide occurred. This finding indicated that using water content as the landslide warning indicator was feasible. Besides, the landslides will occur earlier and the scale of landslide will decrease when the rainfall intensity is higher.

(2) Procedures of conducting multiple regression formulas for the W_{cr} method

This study used water content as a landslide warning indicator. First, the critical water content (i.e., the water content when the slope collapsed, W_{cr}) for each slope had to be set. Then, the system had to calculate the change of water content (W_t) during the rainfall duration. Because the IRIS model is time-consuming, this study used multiple regression formulas, which was based on the IRIS model, to calculate W_{cr} and W_t. If W_t was greater than W_{cr}, the slope unit would be determined as collapsed.

The procedures of conducting the multiple regression formulas were summarized as follows:

(i) Divided the slope units into 8 groups based on the distribution of slope lengths, and a representative slope length were selected from each group (see **Table 4.5**). Because the number of slope units was fewer in the 7th and 8th group, this study selected two actual slope units as the representative slope length.

(ii) 42 virtual slope units were established by taking different representative slopes of ground surface α (at 1^o interval).

(iii) To eliminate the influence of different initial water content in slope stability analysis, the method of setting initial water content for all slope units in this study was described as follows: a) The uniform water pressure head (ψ= -0.01m) was given in all soil and drained off the water naturally for 900 days. b) To avoid the soil becoming excessively dry, all slope units were given a constant-intensity rainfall (0.1mm/h) during the drainage period. c) All slope units were given the actual antecedent rainfall (2012/7/1~8/12) to simulate the distribution of water in the soil by the IRIS model.

(iv) Conduct rainfall-infiltration-slope-stability simulation of the 42 virtual slope units with IRIS model and 8 constant-intensity rainfall scenarios (as shown in **Table**

4.4), using parameter listed in **Table 4.2**.

(v) Using the simulation results of the IRIS model to proceed multiple regression to generate the multiple regression formulas I, II, III, and IV, which were employed to predict the initial water content (W_{ini}), the critical water content (W_{cr}), the change of the water content during the simulation (W_t), and the volume of landslide sediment (V_s) for each slope unit.

Table 4.5 The representative slope lengths and slopes

	Distribution of slope length (m)	Number of slope units	representative slope length (m)	representative slope (degree)
1	15.0~54.8	96	42	30~35 (6 sets)
2	54.9~94.5	138	74	30~37 (8 sets)
3	94.6~ 134.3	102	114	29~37 (9 sets)
4	134.4~174.0	44	154	29~34 (6 sets)
5	174.1~213.8	29	194	29~33 (5 sets)
6	213.9~ 253.5	18	234	29~32 (4 sets)
7	253.6~ 293.2	5	258, 259	28.7, 31.9(2sets)
8	293.3~333.0	3	299, 311	27.9, 31.8(2sets)

* Total are 42 virtual slope units

The flowchart of predicting landslides by W_{cr} method is shown in **Figure 4.14**.

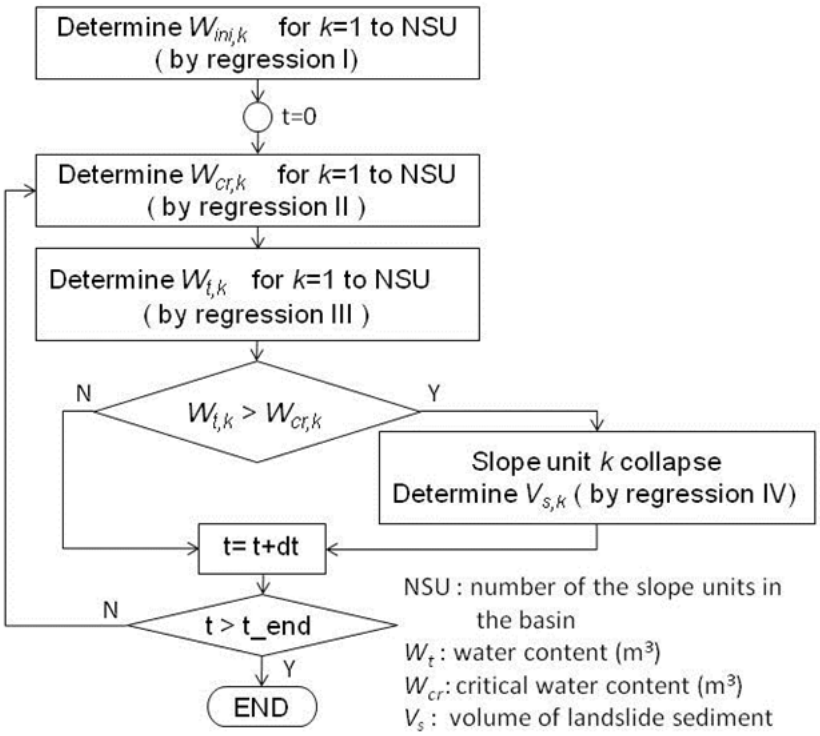

Figure 4.14 The flowchart of predicting landslides by W_{cr} method

(3) Multiple regression result and verification

(i) Initial water content (Regression I)

Based on the simulation results of initial water content setting for the 42 virtual slope units, the regression formula of W_{ini} can be expressed as follows (called regression formula I):

$$\theta_{ini} = c_1 + c_2 \cdot L + c_3 \cdot \alpha \tag{4.13}$$

$$W_{ini} = \theta_{ini} \cdot V \tag{4.14}$$

where c_1 to c_3 are regression coefficients (see **Table 4.6**), L is the horizontal length of the slope unit (m), α is the inclination of the ground surface (deg), θ_{ini} is the initial water content ratio (m^3/m^3), V is the soil volume of the slope unit in unit width (m^3/m). The regression coefficients are divided into four sets by the slope length. For example, the regression coefficients of $L \leqq 95$m were obtained by using the simulation results of the 14 virtual slopes (L=42m and L=74m) after initial water content setting by IRIS model. To verify the accuracy of the regression formula I, this study used 6 actual slope units to calculate W_{ini} by IRIS model and regression formula individually. The results are shown in **Table 4.7**.

Table 4.6 The regression coefficients of W_{ini}

	$L \leqq 95$ m	$95 < L \leqq 185$	$185 < L \leqq 255$	$L > 255$ m
c1	0.318859	0.332008	0.336314	0.342907
c2	0.00027	7.47E-05	9.19E-05	0.000124
c3	0.000209	0.000319	6.26E-05	-0.00041

Table 4.7 The verification result of predicting W_{ini} by regression

No. slope	L (m)	α (deg)	W_{ini} (m^3/m) (by IRIS)	W_{ini} (m^3/m) (by Regression)	error (%)
31	29	34.3	19.35	19.36	0.09
192	71	33.3	49.01	48.99	-0.04
71	137	31.4	96.54	96.52	-0.02
413	165	29.5	116.70	116.74	0.03
406	214	32.2	153.12	153.23	0.07
136	299	27.9	220.70	220.52	-0.08

(ii) Critical water content W_{cr} (Regression II)

Using the simulation results of the 42 virtual slope units under 8 different constant-intensity rainfalls (**Table 4.4**), the regressions formula of W_{cr} can be expressed as Eq. (4.15) and (4.16). The regression coefficients were shown in **Table 4.8**. The comparison of critical water content by the IRIS model and the multiple regression formula is shown in **Table 4.9**.

$$\theta_{cr} = c_1 + c_2 \cdot L + c_3 \cdot \alpha + c_4 \cdot I_{60} \tag{4.15}$$

$$W_{cr} = \theta_{cr} \cdot V \tag{4.16}$$

where c_1 to c_4 are regression coefficients, I_{60} is the rainfall intensity in 60 minutes (mm/h), θ_{cr} is the critical water content ratio (m^3/m^3).

Table 4.8 The regression coefficients of W_{cr}

	$L \leqq 95$ m	$95 < L \leqq 185$	$185 < L \leqq 255$	$L > 255$ m
c1	0.54789	0.522459	0.553529	0.776762
c2	-0.00029	-3.1E-05	-8.2E-05	-2.5E-05
c3	-0.00212	-0.0019	-0.0026	-0.01065
c4	-9.3E-05	-0.0001	-0.00033	-0.00029

Table 4.9 The verification result of predicting W_{cr} by regression

No. slope	L (m)	α (deg)	I (mm/h)	W_{cr} (m^3/m) (by IRIS)	W_{cr} (m^3/m) (by Regression)	error (%)
31	29	34.3	40	26.87	26.87	0.00
192	71	33.3	40	64.36	64.38	0.03
71	137	31.4	40	124.55	124.55	-0.00
413	165	29.5	40	150.42	150.90	0.32
406	214	32.2	40	188.97	188.68	-0.16
136	299	27.9	40	277.34	275.38	-0.70

(iii) Change of water content during rainfall (Regression III)

Because the changing of water content were not only related to slope unit size but also rainfall intensity and saturation of soil, the multiple regression formula III was expressed as Eq. (4.17) and (4.18). The simulation results of the 42 virtual slope units which were calculated by the IRIS model under the actual representative rainfall (60 hours) were used to generate the regression formula III.

$$d\theta_t = c_1 + c_2 \cdot L + c_3 \cdot \alpha + c_4 \cdot I_t + c_5 \cdot \theta_{t-1} \quad (4.17)$$

$$W_t = (\theta_{t-1} + d\theta_t) \cdot V \quad (4.18)$$

where c_1 to c_5 are regression coefficients (see **Table 4.10**), I_t is the rainfall intensity (mm/h) at time t, θ_t is the water content ratio of the soil (m^3/m^3), θ_{t-1} is the water content ratio at the previous time-step, $d\theta_t$ is the change of the water content ratio (m^3/m^3), W_t is the water content of the soil in unit width (m^3/m). **Figure 4.15** shows that the result of using the regression formulation is similar to the result of the IRIS model in calculating the water content.

Table 4.10 The regression coefficients of the water content

	$L \leqq 95$ m	$95 < L \leqq 185$	$185 < L \leqq 255$	$L > 255$ m
c1	7.87E-05	8.22E-05	8.23E-05	9.05E-05
c2	9.33E-09	-1.5E-10	-7.4E-09	-9E-09
c3	1.12E-08	-4.2E-09	1.62E-08	5.44E-08
c4	6.37E-06	5.61E-06	5.22E-06	4.74E-06
c5	-0.00023	-0.00022	-0.00022	-0.00023

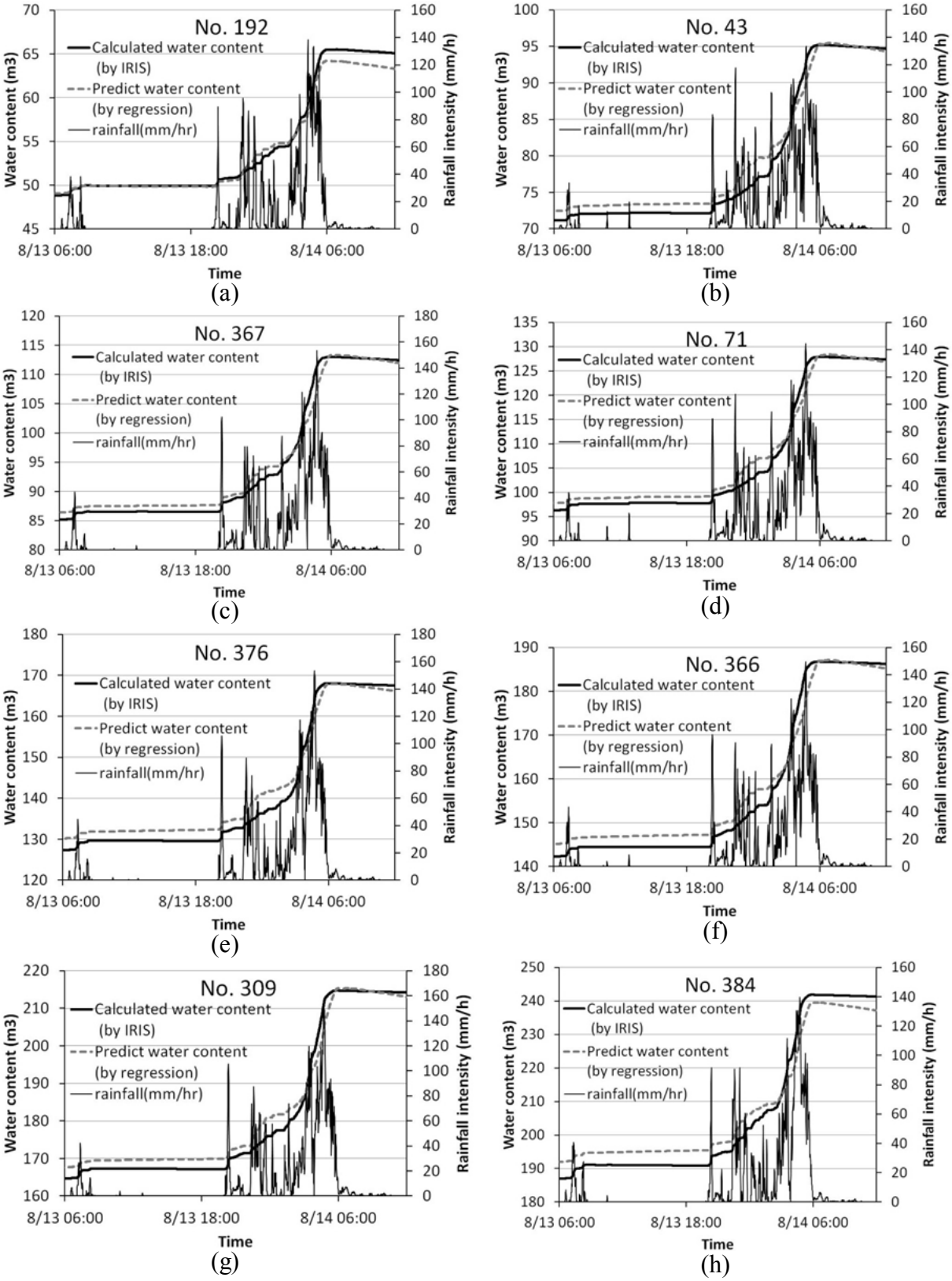

Figure 4.15 The change of water content using the IRIS model and the regression formula (a) No. 192 (L=71m, α=33.3^o) (b)No. 43 (L=102m, α=32.8^o) (c) No. 367 (L=121m, α=36.3^o) (d) No. 71 (L=137m, α=31.4^o) (e) No. 376 (L=180m, α=28.4^o) (f) No. 366 (L=200m, α=31.8^o) (g) No. 309 (L=230m, α=29.2^o) (h) No. 43 (L=259m, α=31.9^o)

(iv) Scale of landslide (Regression IV)

Because **Table 4.3** and **Table 4.4** implied that the scale of landslide was smaller when the rainfall intensity was higher, this study adopted Eq. (4.19) and (4.20) to predict the scale of landslide. The regression coefficients (see **Table 4.11**) were obtained from the regression results of the aforementioned 42 virtual slope units of calculating W_{cr} by the IRIS model under 8 different constant-intensity rainfall. The verification results are shown in **Table 4.12**.

$$R_s = c_1 + c_2 \cdot L + c_3 \cdot \alpha + c_4 \cdot I_{60} \tag{4.19}$$

$$V_s = R_s \cdot V \tag{4.20}$$

where R_s is the landslide volume ratio (m^3/m^3), V_s is the volume of the landslide debris in unit width (m^3/m).

Table 4.11 The regression coefficients of *Vs*

	$L \leqq 95$ m	$95 < L \leqq 185$	$185 < L \leqq 255$	$L > 255$ m
c1	2.580216	1.726502	0.646846	3.204391
c2	-0.00816	-0.00214	0.000756	0.00284
c3	-0.0467	-0.03181	-0.01912	-0.12285
c4	-0.00169	-0.00253	-0.00129	-0.00038

Table 4.12 The verification result of predicting *Vs* by regression

No. slope	*L* (m)	α (deg)	I (mm/h)	*Vs* (m^3/m) (by IRIS)	*Vs* (m^3/m) (by Regression)	error (%)
31	29	34.3	40	40.25	39.09	-2.9
192	71	33.3	40	54.17	53.65	-1.0
71	137	31.4	40	64.40	64.38	23.5
413	165	29.5	40	70.00	110.14	57.3
406	214	32.2	40	50.25	61.55	22.5
136	299	27.9	40	433.25	365.36	-15.7

4.3 Results and discussions

Using the rainfall data of X-band radar, this study employed the regression formula I to IV to predict landslides for all slope units in the Shizugawa basin from July 1 to August 14 in 2012.

4.3.1 Results of landslide prediction on the study area

The simulation result indicated 187 slope units had collapsed (see **Table 4.13**). Compared with the location of the 38 newly collapsed slopes identified from satellite image, 28 slopes were predicted as collapsed, and the others were not (see **Table 4.14**). The comparison of prediction and actual cases are shown in **Figure 4.16**. Moreover, the occurring time of predicting landslide concentrated between 04:34~05:39, which

is very similar to the disaster survey. In addition, the warning hit rate (*WHR*), the false alert rate (*FAR*), and the accuracy of landslide prediction (*ALP*) can be determined by Eq.(4.21) to (4.23).

$$WHR = PCAC/AC \times 100\% \tag{4.21}$$

$$FAR = PCAN/PC \times 100\% \tag{4.22}$$

$$ALP = (PCAC + PNAN)/NSU \times 100\% \tag{4.23}$$

where *PCAC* is the number of slope units which were predicted as collapsed and actually collapsed, *AC* is the number which actually collapsed, *PCAN* is the number of slope units which were predicted as collapsed and actually did not collapse, *PC* is the number of slope units which were predicted as collapsed; *PNAN* is the number of slope units which were predicted non-collapsed and actually did not collapse; *NSU* is the number of slope units. In this case, *WHR* is 73.7% , *FAR* is 85.0%, and *ALP* is 61.2%.

Table 4.13 The comparison of prediction and actual landslides in the Shizugawa basin

Number of slope units		Prediction	
		Collapsed	Non-Collapsed
Actual Event	Collapsed	28	10
	Non-Collapsed	159	238

Table 4.14 The prediction results of 38 newly collapsed slope unit

	No. slope	*L* (m)	*α* (deg)	No. channel	Predict collapse time		No. slope	*L* (m)	*α* (deg)	No. channel	Predict collapse time
1	384	259	31.9	109	03:34	20	389	156	28.7	111	05:17
2	322	190	32.5	87	03:59	21	153	134	28.3	40	05:24
3	134	228	30.8	36	04:34	22	332	120	26.7	89	05:24
4	309	230	29.2	84	04:38	23	127	82	25.9	35	05:25
5	366	200	31.8	101	04:40	24	165	124	29.2	42	05:26
6	301	258	28.7	80	04:43	25	151	86	26.4	40	05:28
7	367	121	36.3	102	04:43	26	373	96	26.7	103	05:30
8	392	223	31.8	113	04:43	27	378	124	25.2	106	05:34
9	68	86	32.5	19	04:49	28	173	113	25.9	44	05:39
10	328	209	27.5	88	04:53	29	199	58	29.3	50	-
11	181	211	29.4	46	04:55	30	330	126	20.4	88	-
12	64	118	32.3	18	05:01	31	93	118	21.1	27	-
13	73	108	32.0	21	05:01	32	119	77	23.7	32	-
14	376	180	28.4	105	05:03	33	385	63	25.5	109	-
15	63	140	29.2	18	05:10	34	303	278	25.5	81	-
16	271	161	28.4	70	05:10	35	213	150	26.2	55	-
17	85	126	28.8	25	05:11	36	169	78	27.4	43	-
18	65	128	29.2	18	05:13	37	398	152	28.8	116	-
19	114	80	27.3	32	05:17	38	430	225	18.3	126	-

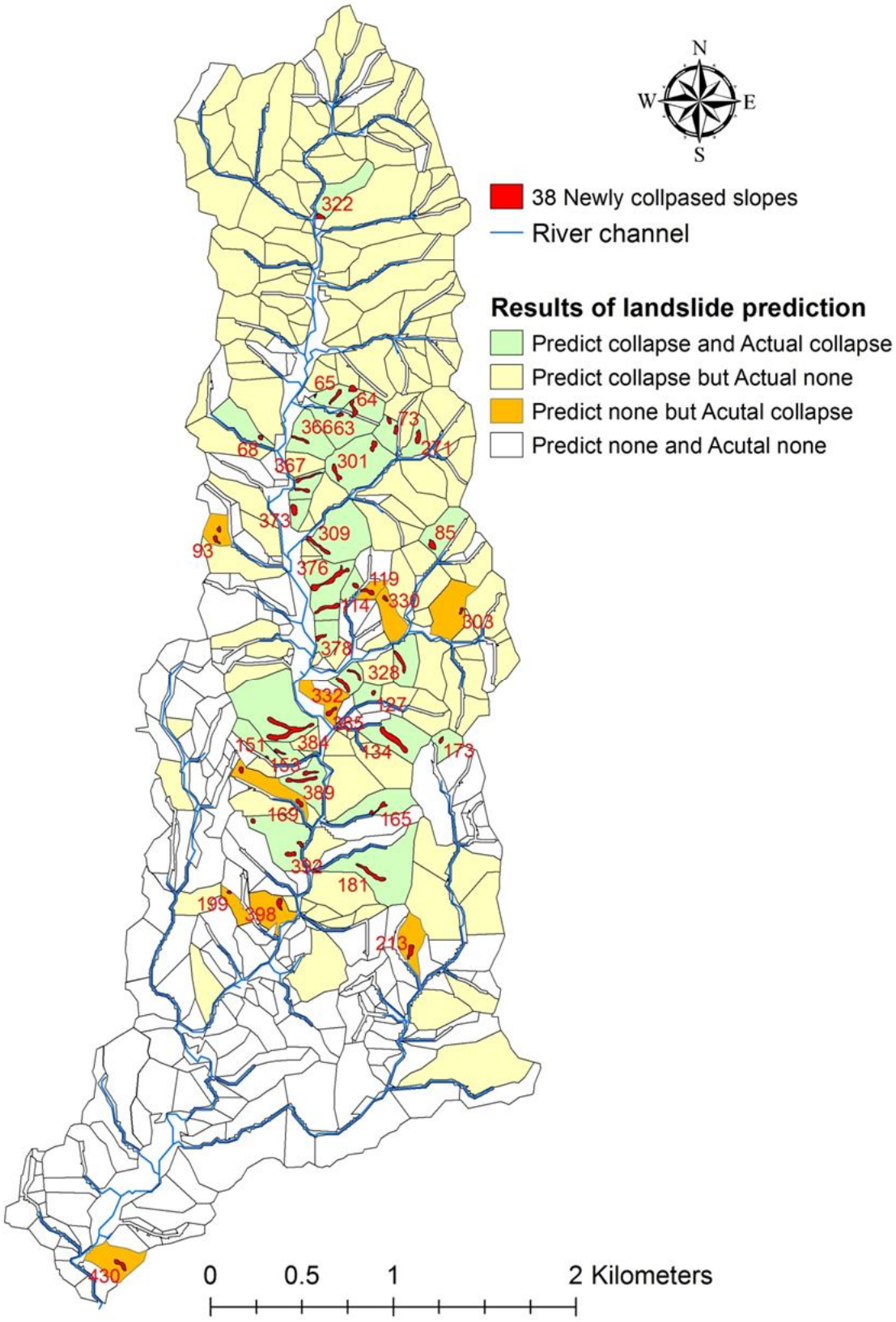

Figure 4.16 The result of comparing prediction with actuality for the landslides in the Shizugawa basin

To clarify the difference of predicting landslides by the IRIS model and the W_{cr} method, this study selected 8 actual slope units as the verification. Four of them were collapsed actually during the heavy rainfall event, and the others were non-collapsed.

Table 4.15 shows the comparison of the difference of predicting landslides by the IRIS model and the W_{cr} method. The results indicate that the prediction results of the both methods are almost same. That is, using the W_{cr} method to predict landslides instead of the IRIS model on a basin scale is feasible. It is worth noting that the scale of predicting landslides by the IRIS model is usually smaller than the actual situation because of multi-stage collapse (see **Figure 4.12**). The prediction results by the W_{cr} method might have the same situation.

Table 4.15 The comparison of landslide prediction by the IRIS model and the multiple regression formula

Case	No. Slope	L(m)	α (deg)	Actual collapse	Calculated by IRIS model		Predict by regression		Difference of occurring time (min)	Difference Slip surface area (%)
					Occurring time	Slip surface area (m^2/m)	Occurring time	Slip surface area (m^2/m)		
1	367	121	36.3	Y	8/14 4:31	23.5	8/14 4:43	31.8	12	35.0
2	366	200	31.8	Y	8/14 4:31	51.3	8/14 4:40	64.4	9	25.5
3	134	228	30.7	Y	8/14 4:42	74.8	8/14 4:34	73.8	-8	-1.4
4	309	230	29.2	Y	8/14 4:41	115.4	8/14 4:38	101.9	-3	-11.7
5	192	71	33.3	N	8/14 5:35	54.2	8/14 5:30	42.5	-5	-21.6
6	43	102	32.8	N	8/14 4:46	44.0	8/14 5:02	60.4	16	37.5
7	71	137	31.4	N	8/14 4:43	63.1	8/14 5:00	66.6	17	5.4
8	424	248	28.4	N	No collapse		No collapse		same	

4.3.2 Landslide risk

In addition, the risk of landslide of each slope unit for arbitrary times t can be defined by Eq.(4.24)

$$Risk = W_t / W_{cr} \tag{4.24}$$

where W_t is the water content of the slope unit at arbitrary times t; W_{cr} is the critical water content of the slope unit. The risk of each slope unit in the basin could be displayed on GIS platform, and help the local government officials to make the evacuation decision and verified disaster prevention plan. **Figure 4.17** showed the distribution of landslide risk in Shizugawa basin from 4:00 to 12:00 on August 14, 2012.

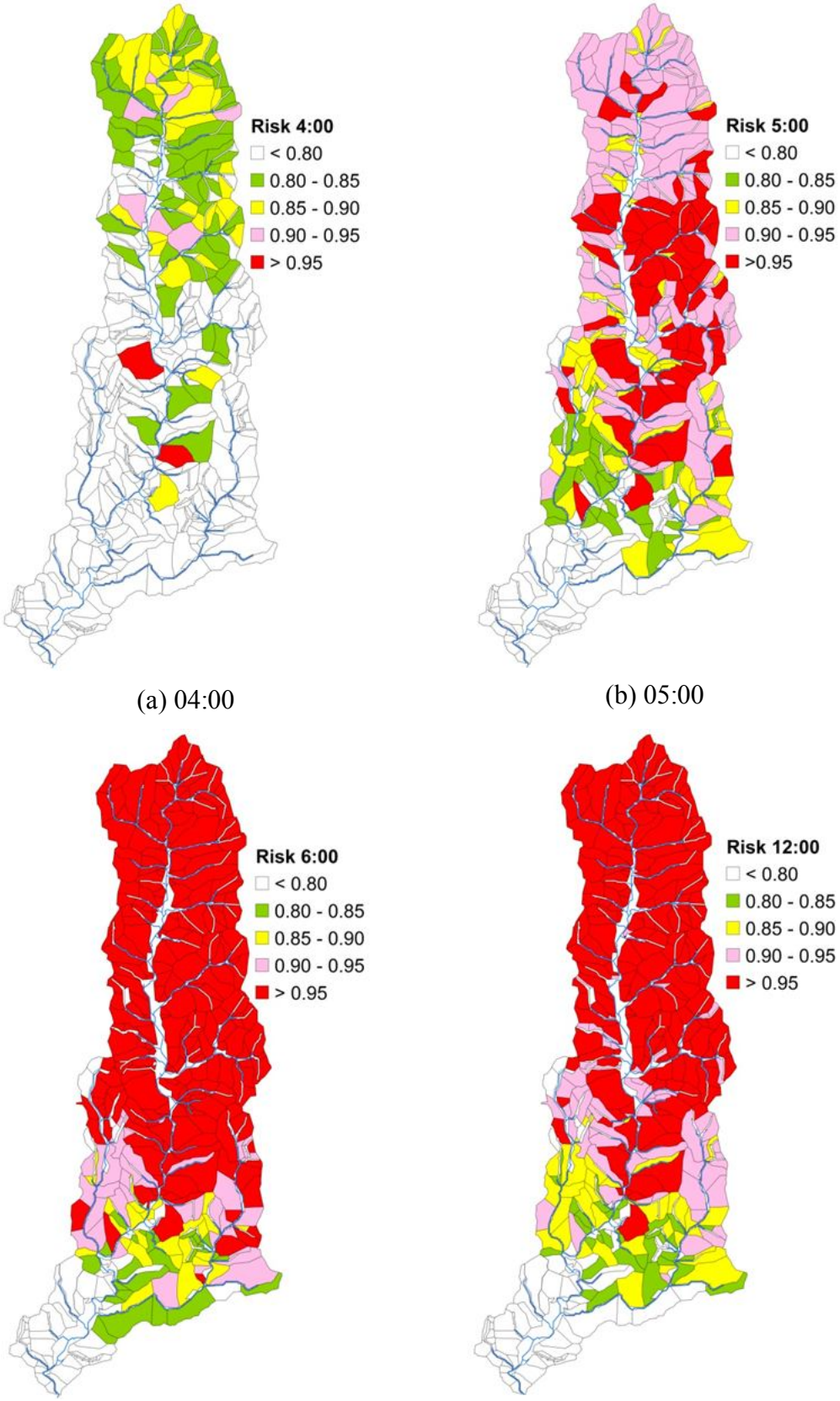

(a) 04:00 (b) 05:00

(c) 06:00 (d) 12:00

Figure 4.17 The distribution of landslide risk in Shizugawa basin from 4:00 to 12:00 on August 14, 2012

4.3.3 Discussions

Since the grid-based slope stability analysis usually uses the simplified infiltration formula and employs the infinite-slope stability analysis, these models can only apply to shallow landslide prediction. Relative to the limitation, the IRIS model can be used in both shallow landslide and deep-seated landslide prediction. Because the IRIS model requires more calculation time, it is inappropriate to be used on basin scale. Thus, this study proposed to use critical water content (W_{cr}) as the landslide warning indicator. The specific approach adopted the slope unit as the analysis target, and selected a number of the virtual slope units to conduct the rainfall-infiltration-landslide simulation by the IRIS model. Using the above results and multiple regressions, the regression formulas of W_{cr} and the change of water content were obtained. Then this study applied the regression formulas to predict the landslide.

The advantages of using W_{cr} as the landslide warning indicator can be described as follows:

(1) Since the W_{cr} method uses slope units, which has been demarcated before the simulation, as the slope stability analysis target, it can predict not only the occurring time and scale but also the location of landslides.

(2) Compared with the statistic method (e.g., rainfall warning indicator), the critical water content method still retains the characteristics of the physically-based model because it is derived from the IRIS model.

(3) Owing to using the regression formula directly, the critical water content method has high performance on calculation, and is very suitable to be applied to the landslide prediction on a basin scale.

(4) Because the water content is highly related to the slope stability, it is appropriate to express the risk of landslides on a basin scale. If the risk of each slope unit can be displayed on GIS platform, it is helpful to make the evacuation decision for the local government.

(5) The general sediment disaster warning systems (such as in Japan, Taiwan, etc.) usually use historical disaster records and rainfall data to demarcate the critical line of warning system by statistical methods [*Osanai et al.*, 2010]. In fact, not every area has enough historical disaster records to determine a critical line. In contrast, the critical water content method which based on the physically-based

model and multiple regressions only needs few historical disaster records to verify the related parameters for the IRIS model. Even if there is no disaster record in some areas, the parameter also can be obtained by experiments. Moreover, the IRIS model can generate a lot of results to enhance the accuracy of the regression formula to predict the landslide. Thus, the critical water content method can be easily applied to any area.

While the critical water content method has the potential to be developed as the sediment disaster warning system on a basin scale, however, some issues have to be solved:

(1) Despite *Xie et al.* [2004] had proposed the method of demarcating the slope units automatically, the manual method to divide some slope units, which had complex slope aspects or geology, was still necessary. How to reduce the manual procedure and remain the consistence should be further explored.
(2) While the causes of soil moisture distribution, which will affect the scale of landslides, are very complicated, this study only used I_{60} as the representative indicator. Compared with the occurring time and location of landslide prediction, the prediction result of landslide scale is poorer. It needs further studies.

For the effectiveness of warnings, the warning hit rate (WHR) in this study case was better than the average performance of the existing rainfall-based warning systems in Japan and Taiwan (see **Table 2.5**), and the false alert rate (FAR) was similar. However, it is worth noting that the method of evaluating warning effectiveness of the existing warning system used the township as an evaluation unit, thus it is easier to obtain a better result. According to the results of the questionnaire survey in Chapter 3, *raising the warning hit rate*, *narrowing the unit of warning area*, and *providing more detailed warning information* are the most important improvement direction for existing warning system. Moreover, compared to the requirements of expecting the new warning system, the study results showed that using W_{cr} method to predict landslide on a basin already reached the aforementioned goals.

In addition, this study generated the slope units by the simplified model which consisted of only four parameters (see **Figure 4.5**); that is, some detail characteristic of topography will be neglected. Moreover, because all landslides in the study case were shallow landslides, which mean depth was about 2m, this study assumed the

inclination of bedrock was same as the mean slope of ground surface as well as the soil thickness of 2 m. Based on above assumptions, the topographic factor for slope stability analysis will be simplified as two parameters- the mean slope of ground surface and the slope length. It should cause some prediction error.

In this study case, the W_{cr} method was unable to indicate 10 newly identified collapsed slopes (i.e., the 10 slope units were predicted as non-collapsed). Partial reasons might be the above-mentioned assumptions which were over-simplified for the topography of each slope unit, then caused prediction error. The other reasons might result from the lower resolution of the satellite images compared with the aerial photo. In fact, it is difficult to discriminate between landslides and slope erosion by using the RapidEye satellite images of 5m resolution. However, checking the topographic data of the 10 newly identified collapsed slopes, 8 slope units are gentle slope (average slope < 27.5^{o}), and 1 slope unit is small in length (L=58m). It implies that these 10 naked slopes might be the result of erosion, and this can be verified by detailed surveys or high-resolution aerial photos.

Besides, most of the over-predicting slope units, which were predicted as collapsed but did not collapse actually, concentrated in the north part of the study area (see **Figure 4.16**). **Figure 4.18** showed the elevation and mean slope of slope units in upstream, midstream, and downstream of Shizugawa basin, and the mean slope of slope units in the upstream is obvious larger. Because the soil characteristic specimens were only focused in the areas which occurred landslides (i.e., midstream), using same soil parameter for all slope units might cause prediction error. Moreover, the difference of land use and the thickness of soil also might affect the slope stability. If different soil parameters were used in different areas for predicting landslides, the FAR and accuracy (*ALP*) should be improved.

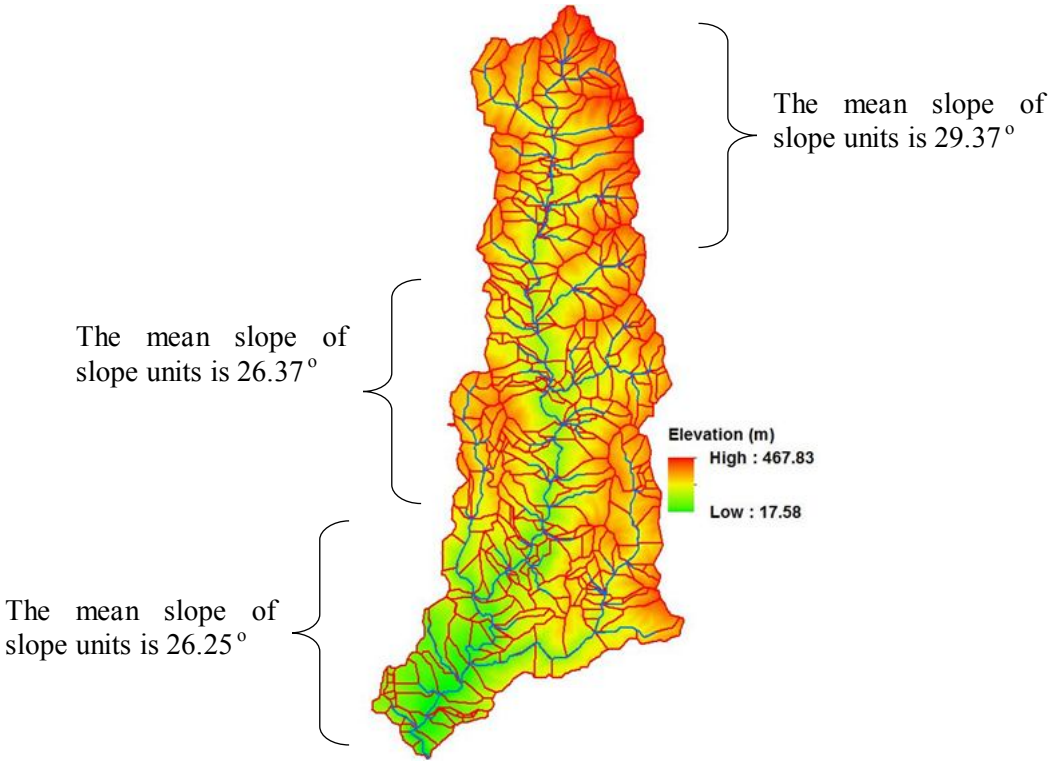

Figure 4.18 The elevation and mean slope of slope units in upstream, midstream, and downstream of Shizugawa basin

Because the critical water content method can simulate the change of the water content in each slope, that is, the method also can calculate runoff of each slope during the rainfall event. While the current rainfall-runoff simulation model on a basin scale almost uses the kinematic wave equation [*Takasao and Shiiba*, 1988; *Egahsira and Matsuki*, 2000], it is rough and lack of the physical meaning. The implementation of the critical water content method in the rainfall-runoff simulation on a basin will be introduced in Chapter 5.

4.4 Summary

Because the existing rainfall-based warning systems for sediment disasters in Japan and Taiwan can only provide the wide-area alerts, they cannot offer the detailed information about the occurring time, location, type, and scale of disasters. Accordingly, even if the local governments or inhabitants received the alerts, it is very difficult to perceive the imminent risk and make an appropriate evacuation decision. This study proposed a new approach (W_{cr}), which was based on physically-based model and the multiple regressions, to predict the occurring time, location, and scale

of landslides on a basin scale. This new method cannot only retain the characteristics of the physically-based model, but also has the advantage of high performance on calculation. It could provide the foundation of developing the simulation model for multi sediment hazards on a basin scale. The results and recommends are summarized as the follows.

(1) Using the slope units as analysis targets, the critical water content method can predict the occurring time, location, and scale of the landslide in each slope unit with high performance. That is, it can be employed on a basin scale.

(2) Compared with the prediction results using the physically-based model (the IRIS model), the prediction results of the occurring time and location of landslides using W_{cr} method were almost same as the IRIS model, only the prediction result of the scale of landslides sometime appeared large difference. Overall, using W_{cr} method instead of the IRIS mode to predict landslides on a basin scale is feasible.

(3) Since the landslide occurring during rainfall can be attributed to the water content, the W_{cr} method is appropriate to express the risk of landslides on a basin scale.

(4) The W_{cr} method only needs few historical disaster records to verify the related soil parameters to generate the multiple regression cases. Even if there are no disaster records in some areas, the parameter also can be obtained by experiments. That is, the W_{cr} method can be employed in any area.

(5) Generally, dividing the basin into several parts and using different soil parameters in different areas, the FAR and accuracy (*ALP*) will be improved.

(6) Because the critical water content method can simulate the change of the water content in each slope, in other words, it also can calculate runoff of each slope during the rainfall event.

References

Asia air survey co., LTD (2012): The aerial photos on the Shizugawa basin, Uji, Kyoto Prefecture after heavy rainfall event on August 14, 2012. (http://www.ajiko.co.jp/article/detail/ID4T3J5OYFD/)

Baker., R. (1980): Determination of the critical slip surface in slope stability computations, International journal for numerical and analytical methods in geomechanics, Vol.4, pp. 333-259.

Caine, N. (1980): The rainfall intensity: duration control of shallow landslides and debris flows, Geografiska Annaler. Series A. Physical Geography, 62A, pp. 23-27.

Carrara, A., Cardinali, M., Detti, R., Guzzetti, F., Pasqui, V., and Reichenbach, P.

(1991): GIS techniques and statistical models in evaluating landslide hazard, Earth Surface Processes and Landforms, Vol. 16, No. 5, pp. 427-445.
Casadei, M., Dietrich, W. E., and Miller, N. L. (2003): Testing a model for predicting the timing and location of shallow landslide initiation in soil-mantled landscapes, Earth Surface Processes and Landforms, Vol. 28, No. 9, pp. 925-950.
Chang, K.T., and Chiang, S.H. (2009): An integrated model for predicting rainfall-induced landslides, Geomorphology, Vol. 105, No. 3–4, pp. 366-373.
Chen, C.Y., and Fujita, M. (2013): An analysis of rainfall-based warning systems for sediment disasters in Japan and Taiwan, International Journal of Erosion Control Engineering, Vol. 6, No. 2, pp. 47-57.
Chen, C.Y., and Fujita, M. (2014): A method for predicting landslides on a basin scale using water content indicator, Journal of Japan Society of Civil Engineers, Ser. B1 (Hydraulic Engineering), Vol. 70, No.4, pp.I_13-I_18.
Chen, C. Y., Ikkanda, S., Fujita, M., and Tsutsumi, D. (2013): A study on mechanism of large-scale landslides and the prediction, 12th International Symposium on River Sedimentation, pp. 41.
Crosta, G. B., Chen, H., and Frattini, P. (2006): Forecasting hazard scenarios and implications for the evaluation of countermeasure efficiency for large debris avalanches, Engineering Geology, Vol. 83, No. 1–3, pp. 236-253.
Egahsira, S., and Matsuki, K. (2000): A method for predicting sediment runoff cased by erosion of stream channel bed, Annual Journal of Hydralic Engineering, JSCE, Vol. 44, pp. 735-740 (in Japanese with English abstract).
Fujita, M., Ohshio, S., Tsutsumi, D. (2010): Effect of climate change on slope failure risk degree in river basin, Annuals. Disaster Prevention Res. Inst., Kyoto Univ., Vol. 53, No. B, pp. 515-526 (in Japanese with English abstract).
Ichikawa, Y., Satoh, Y., Shiiba, M., Tachikawa, Y., and Tkaara, K. (1999): Development of a water and sediment flow model for a mountainous area, Annuals. Disaster Prevention Res. Inst., Kyoto Univ., Vol. 42, No. B-2, pp. 211-224 (in Japanese with English abstract).
Istok, J. (1989): Groundwater Modeling by the Finite Element Method, Washington DC, American Geophysical Union.
Kosugi, K. I. (1996):Lognormal distribution model for unsaturated soil hydraulic properties, Water Resource Research,Vol. 32, No. 9,pp. 2697-2703.
Kubota, T. and Nakamura, H. (1991): Landslide susceptibility estimation by critical slip surface analysis combined with reliable analysis, Journal of Japan Landslide Society, Vol.27, No. 4,pp. 18-25.
Kyoto Prefecture (2013): Disaster report for the heavy rainfall on August 13-14, 2012 (http://www.pref.kyoto.jp/shingikai/kasen-03/documents/1_nambugouu.pdf)
Lee, K. T., and Ho, J.-Y. (2009): Prediction of landslide occurrence based on slope-instability analysis and hydrological model simulation, Journal of Hydrology, Vol. 375, No. 3–4, pp. 489-497.
Lee, G., Kim, S., Jung, K., and Tachikawa, Y. (2011): Development of a large basin rainfall-runoff modeling system using the object-oriented hydrologic modeling system (OHyMoS), KSCE J Civ Eng, Vol. 15, No. 3, pp. 595-606.
Osanai, N., Shimizu, T., Kuramoto, K., Kojima, S., and Noro, T. (2010): Japanese early-warning for debris flows and slope failures using rainfall indices with Radial Basis Function Network, Landslides, Vol. 7, No. 3, pp. 325-338.
Takahashi, T., Inoue, M., Nakagawa, H., and Satofuka, Y. (2000): Prediction of sediment runoff from a mountain watershed, Annual Journal of Hydraulic

Engineering, JSCE, Vol. 44, pp. 717-722 (in Japanese with English abstract).
Takasao, T., and Shiiba, M. (1988): Incorporation of the effect of concentration of flow into the kinematic wave equations and its applications to runoff system lumping, Journal of Hydrology, Vol. 102, No. 1–4, pp. 301-322.
Tsutsumi, D., Fujita, M., Hayashi, Y. (2007): Numerical simulation on a landslide due to typhoon 0514 in taketa city, oita prefecture,Annual Journal of Hydralics Engineering, JSCE, Vol. 51, pp. 931-936 (in Japanese with English abstract).
Wang, C., Esaki, T., Xie, M., and Qiu, C. (2006): Landslide and debris-flow hazard analysis and prediction using GIS in Minamata–Hougawachi area, Japan, Environ Geol, Vol. 51, No. 1, pp. 91-102.
Wieczorek, G.F. and Glade, T. (2005): Climatic factors influencing occurrence of debris flows. In: Jakob, M. and Hunger, O. (eds), Debris-flow Hazards and Related Phenomena, Praxis, Springer Berlin, pp. 325–362.
Xie, M., Esaki, T., and Zhou, G. (2004): GIS-Based Probabilistic Mapping of Landslide Hazard Using a Three-Dimensional Deterministic Model, Natural Hazards, Vol. 33, No. 2, pp. 265-282.
Xie, M., Esaki, T., Qiu, C., and Wang, C. (2006): Geographical information system-based computational implementation and application of spatial three-dimensional slope stability analysis, Computers and Geotechnics, Vol. 33, No. 4–5, pp. 260-274.
Yamagami, T. and Ueta, Y. (1986): Noncircular Slip Surface Analysis of the Stability of Slopes- An Application of Dynamic Programming to the Janbu Method-, Journal of Japan Landslide Society, Vol. 22, No.4., pp.8-16.
Yamagami, T. and Ueta, Y. (1988):Search for critical slip lines in finite element stress fields by dynamic programming, Proc. 6th International Conference on Numerical Methods in Geomechanics, Innsbruck, Austria.

Chapter 5
Simulation Model of Multi Sediment Hazards on a Basin Scale

5.1 Introduction

During typhoon and heavy rainfall, rainfall infiltrates into the slope and causes the pore water pressure to rise, leading to the reduction of effective stress and resulting in landslides [*Iverson*, 2000; *Casadei et al.*, 2003; *Vieira and Fernandes*, 2004; *Tsutsumi et al.*, 2007]. Some of the sediment from the landslide would remain staying on the slopes; some might be the source of the debris flow, and some would enter the river channel and cause the riverbed to be raised. Such situation results in the reduction of the cross section area for drainage and makes flood risk higher, even forming the landslide dam and causing the potential secondary disaster [*Chen et al.*, 2011; *Kondo et al.*, 2012]. Thus, the rainfall-induced hazards usually occur as multi-modal types, i.e., a hazard could affect or trigger another one because of their complex spatial and temporal relationships [*Highland and Bobrowsky*, 2008; *Kappes et al*., 2012a; *Kappes et al*., 2012b]. Moreover, some actual disaster cases reveal that a hazard could affect the disaster prevention system and then resulted in the reduction of disaster prevention capability. If another hazard occurred simultaneously, the disaster prevention system might collapse, and the disaster happened. Hence, if the disaster prevention plan only considers single hazard individually, it cannot tackle the risk under the extreme climate situation. For instance, the disasters of Typhoon Morakot (2009) in Taiwan and the Typhoon Talas (2011) in Japan were the typical cases [*Chen and Fujita*, 2013a; *Chigira et al.*, 2013].

However, limited by the complexity of multi-hazards and the responsibility of disaster prevention for different government divisions, the existing warning systems only focus on a single type of hazard and lack the capability of overall consideration, especially on the evacuation decision-making. Thus, the existing warning systems only offer simplified alerts (e.g., the sediment disaster alert and the water level alert) to predict whether the disaster occurred in a wide area. They cannot accurately predict the location, scale, type, magnitude of potential disasters, and the probable change of the circumstance related to evacuation. Due to the inaccuracy of the existing warning

information, the inhabitants living in the potential hazard areas are not easily convinced of the imminent risk. Therefore, even if the local government issued the alerts, the inhabitants might refuse to evacuate [*Chen and Fujita*, 2013b].

In addition, because the existing warning systems are unable to foresee the routes which may be interrupted or damaged by the floods or landslides, the evacuation decision-making (including evacuation region, time, and routes) by local governments is very difficult. If the local governments given the inappropriate evacuation order, it would lead to more casualties and the failure of evacuation. Moreover, because the existing warning systems lack the capability of scenario simulation, they cannot demonstrate the severity of disasters even if the weather forecasting has predicted a rainfall of 1,000 or 2,000 mm. Hence, it is difficult for local governments to make the appropriate decision of how to allocate resources [*Chen and Fujita*, 2013a; *Chen and Fujita*, 2013b].

To improve the capability of the warning systems and prevention plans, the monitoring systems should target hazards on a basin-wide scale, and consider the multi-hazards, including the flood and sediment as well as their interaction. Thus, establishing a simulation model for the multi sediment hazards was the most important step to develop a basin-scale warning system and verify the feasibility of the disaster prevention plan.

To establish the basin model, some approaches have been explored. For example, *Takasao and Shiiba* [1988] used the distributed stream networks to simulate a basin; *Egashira and Matsuki* [2000] simulated the basin by using unit channels and unit slopes; *Lee et al.*[2011] conducted the basin model by using the composite of slope units. Kampf and Bugers [2007] had classified and compared for 19 representative distributed models (see **Figure 5.1)**. Moreover, the integrated model of rainfall-runoff and sediment-runoff also had been studied by some researches [*Ichikawa et al*., 1999; *Egahsira and Matsuki*, 2000; *Takahashi et al*., 2000]. However, the research which integrated the landslide prediction, landslide sediment transportation, rainfall-runoff, sediment-runoff, and road/bridge closure to simulate multi sediment hazards in mountainous areas was unexplored.

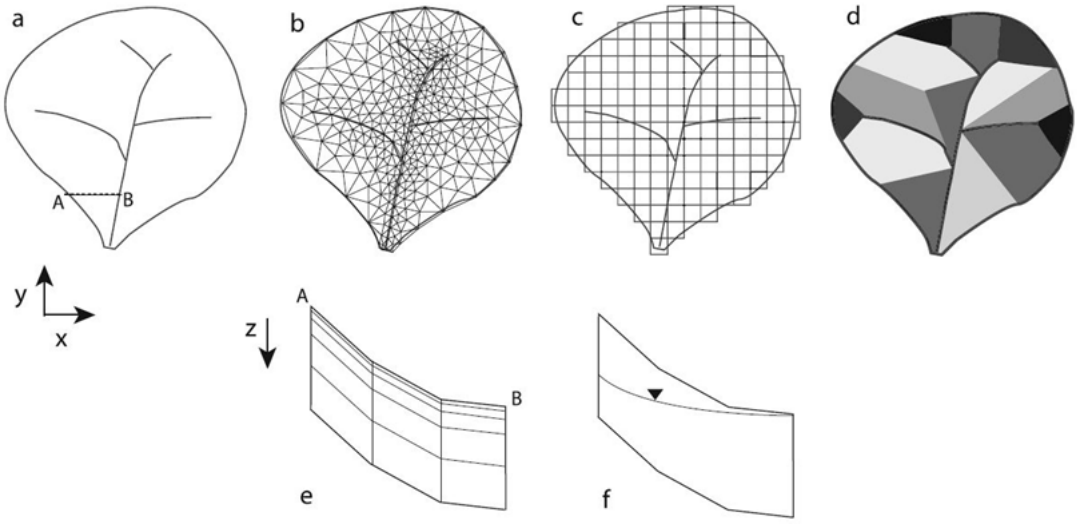

Figure 5.1 Examples of distributed model spatial configurations:(a)hypothetical catchment in plan (XY) view, (b) TIN discretization, (c) rectangular grid discretization, (d) planes and channel segments, (e) explicit discretization of depth (Z), and (f) separation of depth into unsaturated (above water table) and saturated (below water table) zones. [Kampf and Bugers, 2007]

In Chapter 4, this study had established the basin model by applying unit channels and slope units, and proposed a new method for landslide prediction on a basin scale. The new method, the critical water content (W_{cr}) method, was based on the IRIS (the Integrated Rainfall-Infiltration-Slope stability) model and multiple regression analyses to assess slope stability. It can swiftly predict which slope and when it would collapse on the basin scale. Because the W_{cr} method can estimate the change of the water content in the soil of slopes, this study employed the W_{cr} method to simulate the direct runoff (combining surface flow and interflow) of slopes, instead of the kinematic wave method. Although the kinematic wave method was used extensively [*Takasao and Shiiba*, 1988; *Egahsira and Matsuki*, 2000], it was too rough on evaluation and lacked of clear physical meaning.

In this chapter, the rainfall-infiltration, slope stability, water discharge, sediment runoff, and one dimension elevation-changing of the riverbed model were integrated to simulate the multi sediment hazards on a basin scale (see **Figure 5.2**). The results not only can help to verify the feasibility of the disaster prevention plan but also provide the foundation of developing the multi sediment hazards warning system.

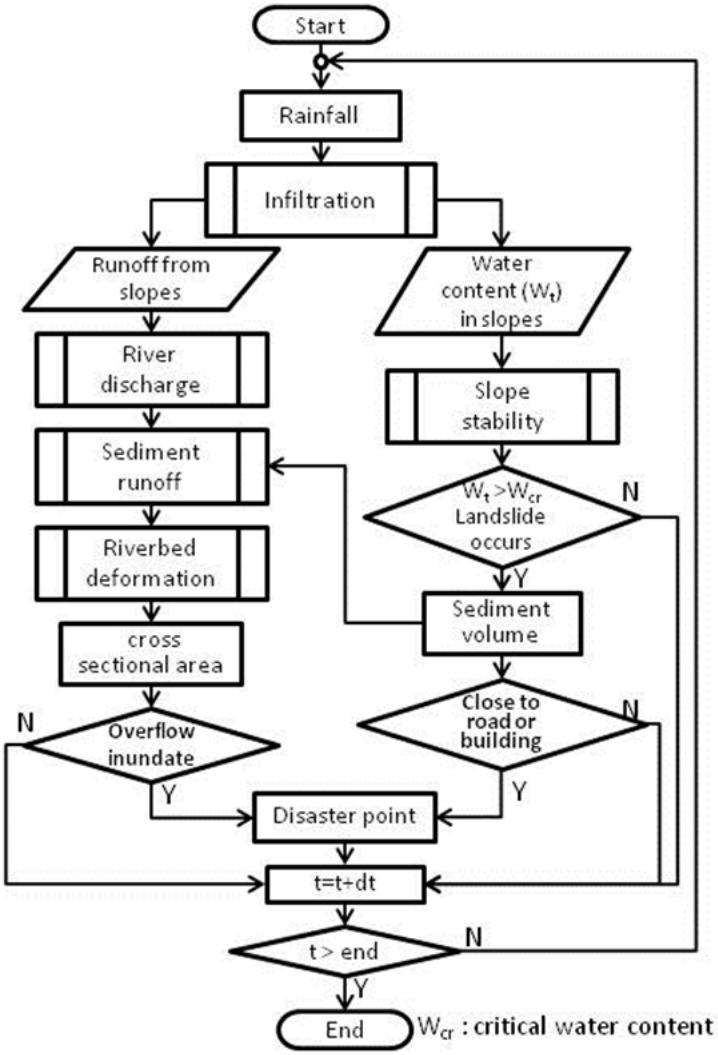

Figure 5.2 The simulation model for multi sediment hazards on a basin scale

5.2 Study area and the disaster in 2012

In this chapter, same study area as in Chapter 4 was used, i.e., the Shizugawa basin in Uji, Kyoto Prefecture. The simulation was conducted using the heavy rainfall event of August 13-14, 2012, and the rainfall data of X-band radar with the spatial resolution of 285m and the time step of 1 minute. According to the rainfall data observed at the Uji city hall, the maximum hourly rainfall was 78.5mm, three-hour rainfall was 186 mm, and the accumulated rainfall was 311 mm [*Uji City*, 2014; *Kyoto Prefecture*, 2013a]. The main precipitation was concentrated from 19:00, Aug. 13, to 7:00, Aug. 14. This was a typical rainfall event with high intensity (see **Figure 5.3**).

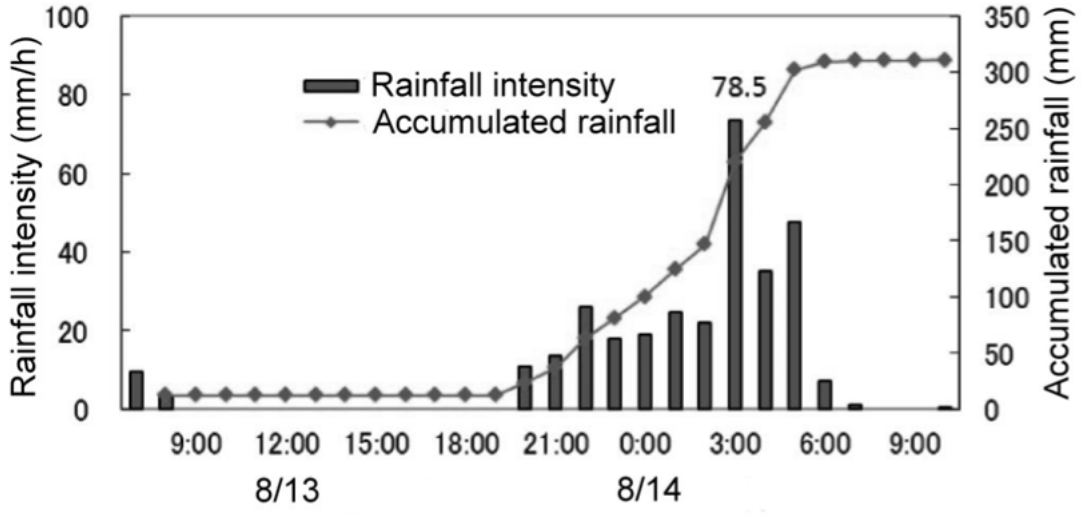

Figure 5.3 The rainfall at the Uji City hall during the heavy rainfall event on August 13-14, 2012 [*Uji City*, 2014]

To verify the simulation results of the multi-modal sediment disasters during the heavy rainfall event, field investigation was conducted and the disaster reports, aerial photos, as well as satellite images were collected to identify the occurring time, location, and scale of the disasters (including landslides and floods) [*DPRI*, 2012; *Asia air survey co., LTD*, 2012; *Kyoto Prefecture*, 2013a; *Uji City*, 2014]. Overall, the mainly affected areas of the Shizugawa basin during the heavy rainfall event were at two regions (see **Figure 5.4**). One was the Sumiyama area which is located in the upper basin, and landslides as well as floods were the main disaster types (**Figure 5.5** to **Figure 5.8**). In addition, some landslides caused inundation in this area. For example, some inhabitants indicated that the landslide on the slope unit of No.367 occurred at about 4:30~05:00, and the landslide sediment blocked the unit channel of No.102 to cause the inundation about 0.5~1.0 m at the nearby houses and the area of unit channel of No.101 (**Figure 5.6**). The other one was the Shizugawa area, which located in the downstream of Shizugawa river, and the flooding as well as sediment depositions were the main disaster types (**Figure 5.9** to **Figure 5.11**). Besides, because a lot of sediment deposited in some channels, the riverbeds were getting higher. Consequently, more severe floods occurred and caused the bridge and building to be washed out.

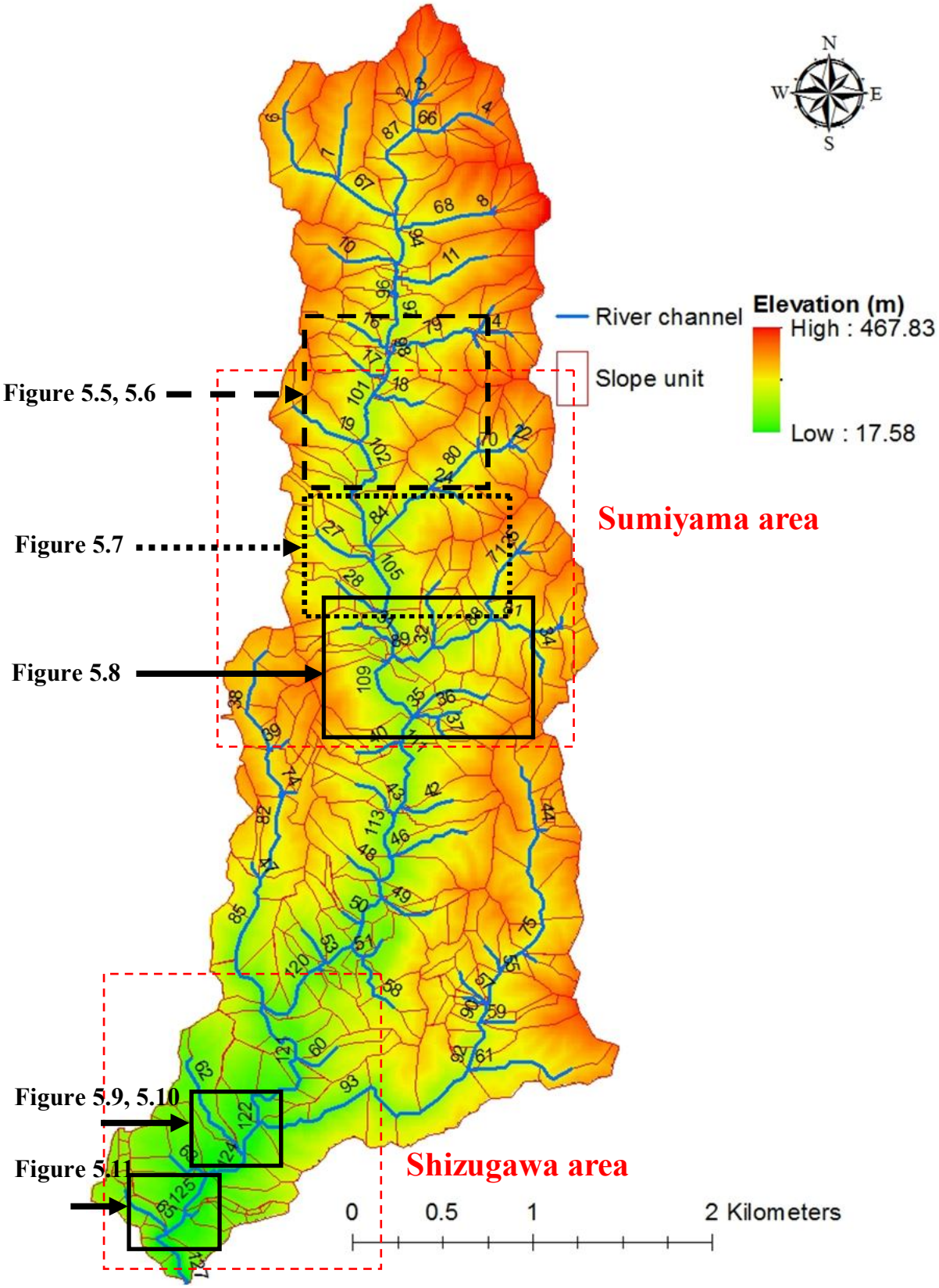

Figure 5.4 The disaster locations in Shizugawa basin during the heavy rainfall event on August 13-14, 2012 [*Uji City*, 2014]

Figure 5.5 The distribution of disaster locations in Sumiyama area (1/3) [modified from *Asia air survey co., LTD*, 2012]

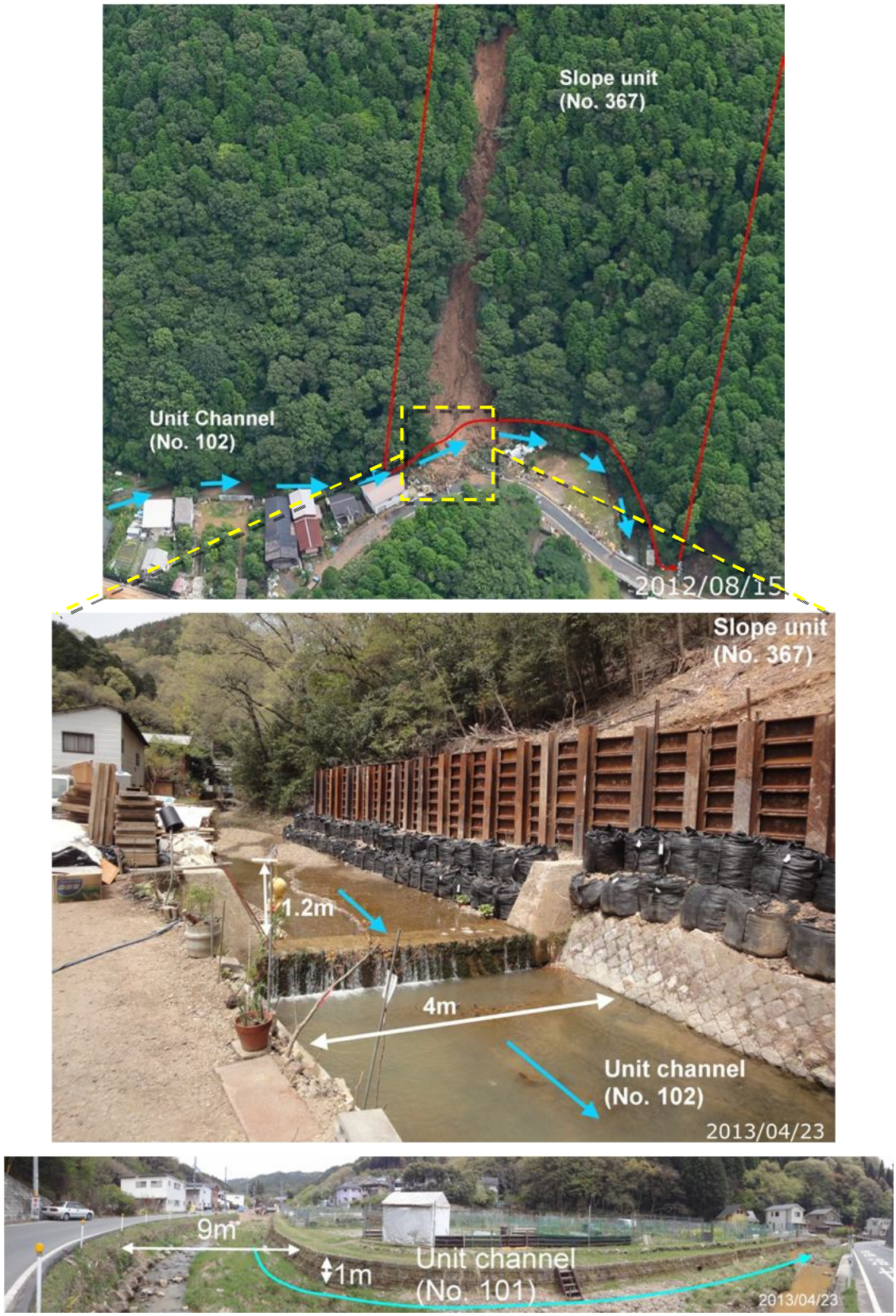

Figure 5.6 The landslide sediment blocked the unit channel of No.102, and induced flooding in the unit channel of No.101[upper aerial photo was modified from *Asia air survey co., LTD*, 2012]

Figure 5.7 The disaster locations in Sumiyama area (2/3), and flood occurred at the unit channel of No.105 [modified from *Asia air survey co., LTD*, 2012]

Figure 5.8 The disaster locations in Sumiyama area (3/3) [modified from *Asia air survey co., LTD*, 2012]

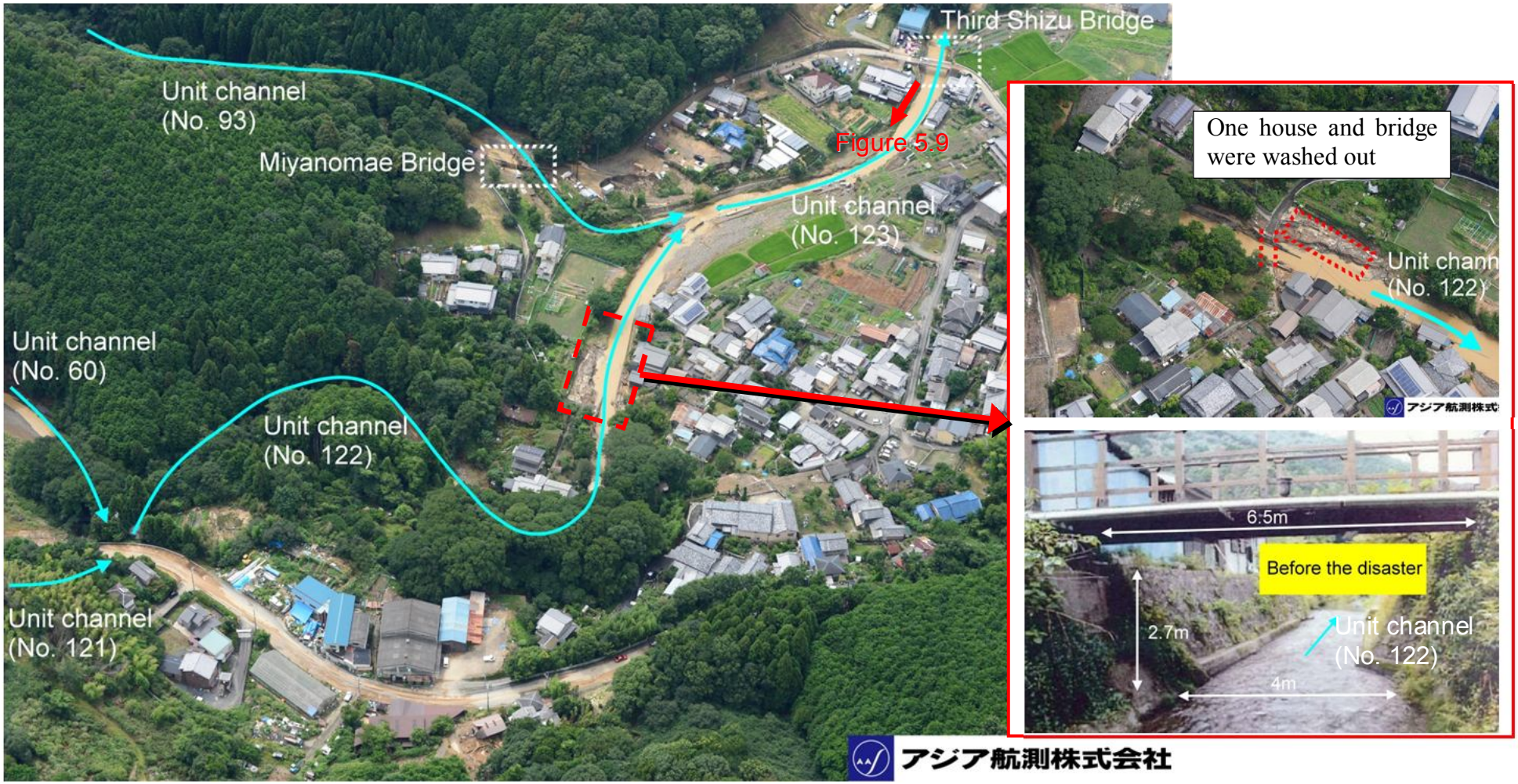

Figure 5.9 The disaster locations in Shizugawa area (1/2) [modified from *Asia air survey co., LTD*, 2012; *DPRI*, 2012]

Figure 5.10 The flood of unit channel No.123 (pictures from the third Shizu Bridge) [modified from *DPRI*, 2012; *Uji City*, 2014]

Figure 5.11 The distribution of disaster locations in Shizugawa area (2/2) [modified *DPRI*, 2012]

According to the abovementioned investigation and the related disaster reports, some significant disaster features and data were summarized as below, and these findings were applied to verify the simulation results.

(1) According to the study results in Chapter 4, 38 newly collapsed slopes were found by the satellite image of RapidEye and aerial photo [*Asia air survey co., LTD*, 2012] on the Shizugawa basin after the heavy rainfall event. Based on the interview with the inhabitants, the occurring time of landslides was between 04:30~06:00 on August 14.

(2) The landslide on the slope unit of No.367 occurred at about 4:30~5:00, and the landslide sediment blocked the unit channel of No.102, resulting in an overflow of the unit channel of No.101 and causing inundation with depth of 0.5~1.0 m at the nearby regions.

(3) The surrounding areas of the unit channel of No.104 and No.105 were inundated with depth of 0.3~0.5m during about 04:00~05:00.

(4) The bank erosion occurred at the upstream of the unit channel of No.93 and caused the road interrupted.

(5) The disaster survey reports from Kyoto Prefecture[2013a] and DPRI [2012] indicated that the flood overflowed the unit channel of No.122 during about 04:30~06:00, and the maximum water level raised about 3 m. The flood in the unit

channel of No.122 washed out one house causing two fatalities at about 5:30~06:00, and the maximum water discharge was about 80 CMS. Moreover, the maximum water discharge in the unit channel of No.127 was about 100 CMS.

(6) The flood overflowed the unit channels of No.123 to No.126 during about 04:30~06:00, and the maximum water level was raised about 3.5 m.

The composition of unit channels and slope units were used to conduct the basin model as in the Chapter 4. The study area was divided into 127 unit channels and 435 slope units as in **Figure 4.4**.

5.3 Simulation model

5.3.1 Landslide model

In this chapter, the critical water content (W_{cr}) method was used to predict the occurring time, location, and scale of landslides. According to the simulation results of Chapter 4, the landslide prediction result in the north part of the study area was relatively inaccurate if all slope units adopted the same soil parameters. Hence, using different soil parameters in the different area, as mentioned in Chapter 4, might improve the simulation results. The soil cohesion of 0.85 t/m^2 (C=0.85 t/m^2) was applied in the north part of the study area, and the other parameters in all areas were the same as **Table 4.2**.

Because both the IRIS model and the W_{cr} method were 2-D analysis, they can only predict the critical slip surface in unit width. According to the survey results after the disaster event, this study assumed the width of landslides as 20m for all slope units.

5.3.2 Rainfall and Sediment runoff model

(1) Rainfall runoff model

The basin model in this study consists of unit channels and slope units. The runoff of each slope unit entered the adjacent unit channel, and then drained to downstream (see **Figure 5.12**). Many studies used the kinematic wave method to estimate the runoff of the slope on a basin scale. While this method was easy to use, it was too rough on estimation and lacked of clear physical meaning.

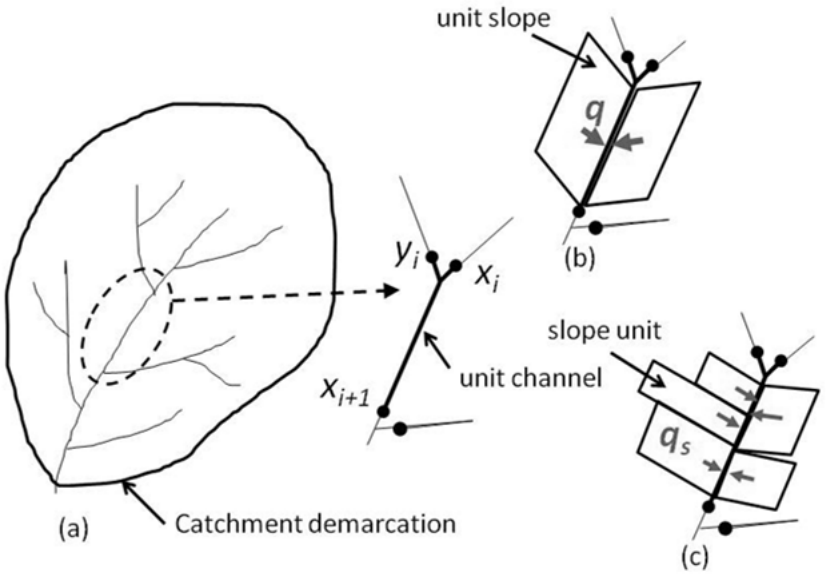

- q is the discharge from runoff of unit slopes into the unit channel
- q_s is the discharge from runoff of each slope unit into the unit channel

Figure 5.12 The diagram of rainfall runoff from the unit slope and slope unit

Because Eq. (4.17) and (4.18) can estimate the change of water content in the soil of the slope unit, the runoff of the slope unit (including surface runoff and undersurface runoff) during $\Delta\tau$ at time τ can be calculated by the difference between the rainfall and the change of water content. This study assumed the rainfall which did not infiltrate into soil of the slope unit would convert into the overland flow on each slope unit directly. Moreover, the overland flow was assumed to be distributed uniformly on the surface of the slope unit (see **Figure 5.13**, $O(\tau)$). Therefore, the volume of the overland flow on the slope unit during $\Delta\tau$ at time τ can be expressed as Eq. (5.1).

$$O(\tau) \cdot \mathrm{B_s} \cdot \Delta\tau = \mathrm{R}(\tau) \cdot \mathrm{B_s} \cdot \mathrm{L_s} \cdot \Delta\tau - \Delta W(\tau) \geq 0 \tag{5.1}$$

$$O(\tau) = R(\tau)\mathrm{L_s} - \frac{\Delta W(\tau)}{\mathrm{B_s}\Delta\tau} \tag{5.2}$$

where $O(\tau)$ is the discharge of overland flow (i.e., the non-infiltration precipitation) of the slope unit per unit width per second (m^3/m/sec) at time τ, B_s is the width of the slope unit (m), $R(\tau)$ is the rainfall intensity (m/sec) at time τ, L_s is the slope length (m), $\Delta W(\tau)$ is the change of the water content (m^3) at time τ.

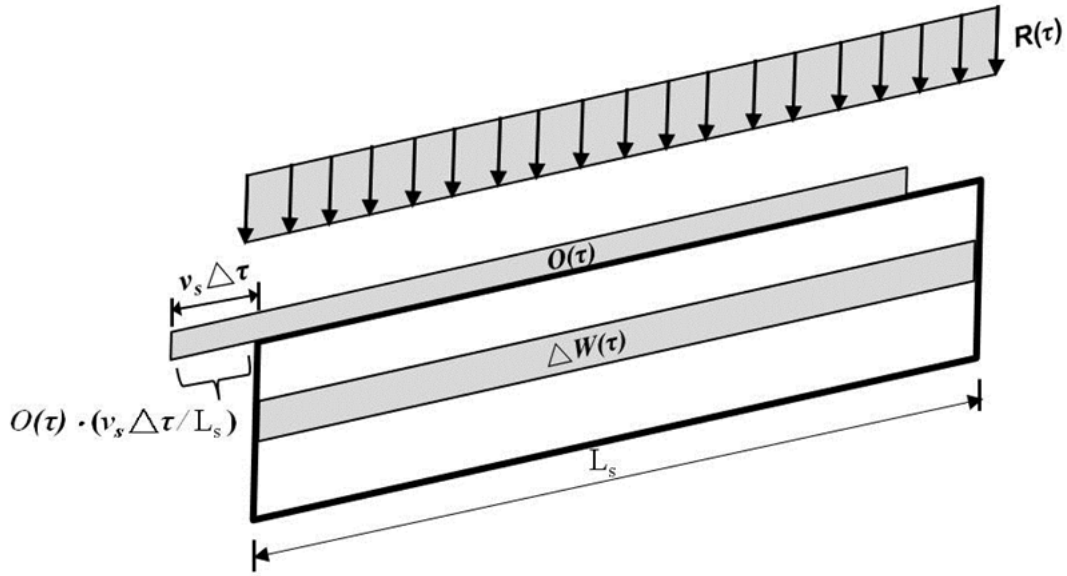

Figure 5.13 The diagram of estimating the discharge from the slope unit into the unit channel

Moreover, this study assumed that the overland flow of each slope unit drained into the adjacent unit channel with constant velocity. The velocity of overland flow can be estimated by Eq. (5.3) [*SCS*, 1986].

$$v_s = k \cdot S_o^{1/2} \tag{5.3}$$

where v_s is the velocity of overland flow (m/s), k is the coefficients of overland-flow velocity (k=0.21 (m/s), forest with heavy ground litter), S_o is the mean slope (m/m). Therefore, the time of concentration of overland flow on the slope unit (t_c) can be expressed as Eq. (5.4) (unit: sec).

$$t_c = \frac{\mathrm{L_s}}{v_s} \tag{5.4}$$

That is, $O(\tau)$ contributed the discharge, which is from the slope unit into the channel, from time τ to time (τ+ t_c). Therefore, the discharge from the slope unit into the unit channel at time t can be express as Eq. (5.5) (see **Figure 5.13**).

$$q_s(t) = \int_{t-t_c}^{t} O(\tau) \cdot \frac{v_s}{L_s} d\tau = \int_{t-t_c}^{t} \frac{O(\tau)}{t_c} d\tau \tag{5.5}$$

Substituting Eq. (5.2) into Eq. (5.5) leads to

$$q_s(t) = \frac{1}{t_c}\int_{t-t_c}^{t}\left[R(\tau)\mathrm{L_s} - \frac{dW(\tau)}{\mathrm{B_s}d\tau}\right]d\tau = \frac{1}{t_c}\left\{\int_{t-t_c}^{t} R(\tau)\mathrm{L_s}d\tau - \frac{1}{\mathrm{B_s}}\int_{t-t_c}^{t} dW(\tau)\right\}$$

$$= \frac{\mathrm{L_s}}{t_c}\int_{t-t_c}^{t} R(\tau)d\tau - \frac{1}{\mathrm{B_s}t_c}[W(t) - W(t-t_c)]$$

(5.6)

Because this study employed Eq. (4.17) and (4.18), which used one minute as the time-step on calculation, to calculate the change of water content for each slope unit, the calculation of discharge from the slope unit into the unit channel also adopted the same time-step of one minute. Thus, the time of concentration of each slope unit can be calculated by Eq. (5.7), and it was taken to integer of at least one minute.

$$t_c = \mathrm{L_s}/(60 \cdot k \cdot S_o^{1/2}) \quad \text{(unit: minute)} \tag{5.7}$$

Then using the segmental approach (see **Figure 5.14**) estimated the discharge q_s(t) from the slope unit into the unit channel at time t by Eq. (5.8).

$$q_s(t) = \sum_{t-t_c}^{t} \frac{O_t}{t_c} \qquad t = t_c + 1, t_c + 2, t_c + 3, \ldots\ldots \tag{5.8}$$

where O_t is the discharge of overland flow of the slope unit per unit width per minute (m^3/m/min).

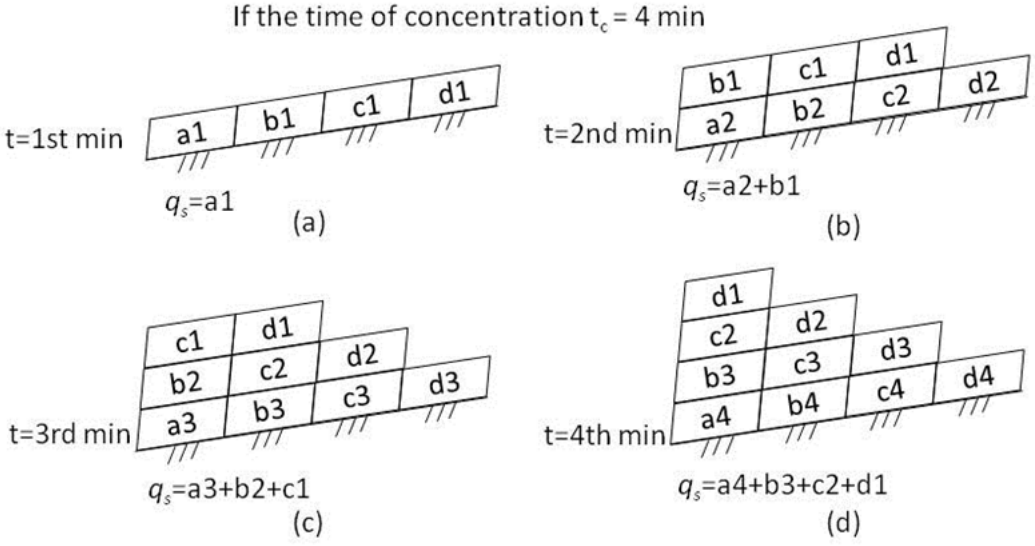

Figure 5.14 The diagram of calculating the discharge from the slope unit into the unit channel by segmental approach

Figure 5.14 illustrated the calculation process of the segmental approach. For example, a slope unit whose time of concentration of overland flow is four minutes has a uniformly-distributed overland flow on the slope at the first minute during rainfall. Because the time-step of calculation is one minute, the overland flow (i.e., O_t) can be divided into four parts- a1 to d1 (see **Figure 5.14 (a)**). Thus, the discharge at the toe of the slope is 1/4 overland flow (i.e., q_s=a1). At the second minute, the overland flow which was generated at the first minute will move 1/4 slope-length toward the toe of the slope, and the difference between precipitation and the increase of water content in the soil conducts another overland flow (see **Figure 5.14 (b)**). That is, the discharge at the toe of the slope is "a2+b1." Accordingly, the runoff of slope at any time can be calculated by using the same process.

Because the slope unit does not include the gentle slope area (slope of ground surface is less than 15°), the total runoff q into the adjacent unit channel can be calculated as in the **Figure 5.15** shown. This study assumes that all precipitation in the gentle slope area is converted into the surface flow (q_t), and directly enters the adjacent unit channel.

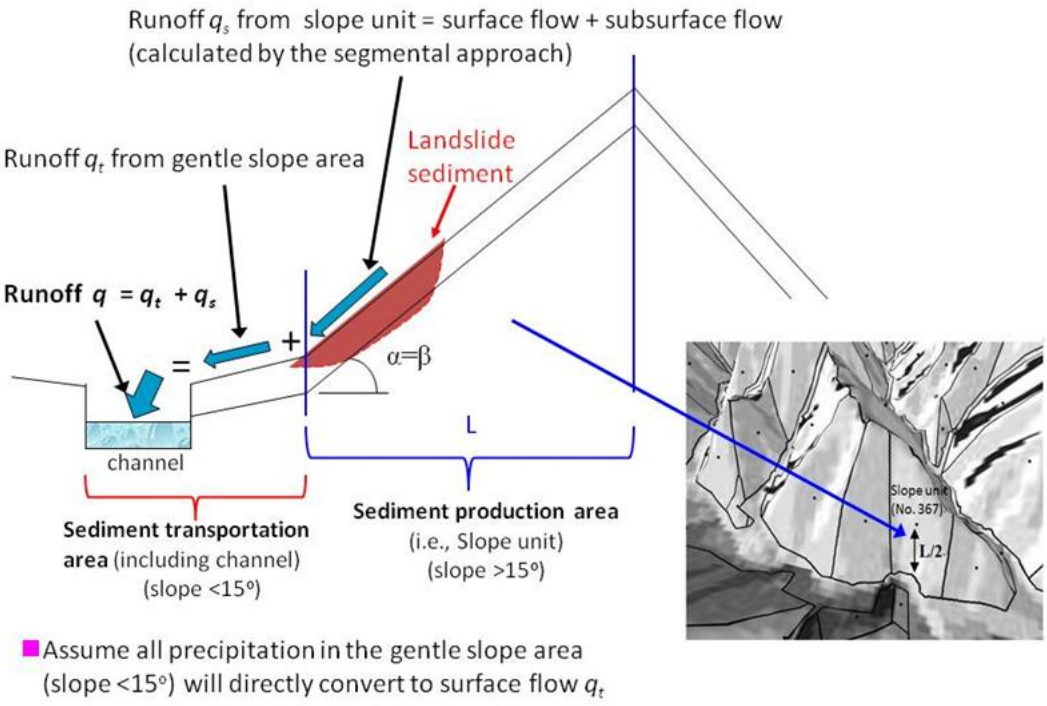

Figure 5.15 The diagram of calculating runoff from slope into the unit channel

This study assumes the cross-section of each river is rectangle shape, and the continuity equation can be expressed as follows:

$$\frac{\partial h}{\partial t} = \frac{1}{BL_c}\{Q(x_i) + Q(y_i) - Q(x_{i+1})\} + \frac{1}{B}q \tag{5.9}$$

$$Q(x_i) = \frac{1}{n_m} B\, I^{\frac{1}{2}} h^{\frac{5}{3}} \tag{5.10}$$

$$q = \sum(q_s + q_t) \tag{5.11}$$

where h is the mean depth of water, B is the width of the unit channel, L_c is the length of the unit channel, $Q(x_i)$ and $Q(y_i)$ are the water discharge from the upstream, $Q(x_{i+1})$ is the water discharge to the downstream, q is the runoff in per unit width from the catchment (including two unit slope, see **Figure 5.12(b)**), n_m is the Manning's roughness coefficient, and I is the slope of the unit channel.

(2)Sediment runoff model

According to the principle of mass conservation, the continuity equation of the sediment runoff is expressed as follows [*Egahsira and Matsuki*, 2000]:

$$(1-\lambda)\frac{\partial z}{\partial t} = \frac{1}{BL_c}\left(Q_b(x_i) + Q_b(y_i) - Q_b(x_{i+1}) + Q_l(x_i)\right) + D_s - E_s + D_w - E_w \tag{5.12}$$

where z is the elevation of riverbed, λ is the porosity of the sediment, $Q_b(x_i)$ and $Q_b(y_i)$ are the bed load discharge from the upstream, $Q_b(x_{i+1})$ is the bed load discharge to the downstream. $Q_l(x_i)$ is the volume of landslide sediment which enters into the channel x_i. D_s and E_s are the deposition rate and erosion rate of suspended load. D_w and E_w are the deposition rate and erosion rate of wash load. The detailed equations are described as follows.

(A) Bed load

The bed load discharge in the channel can be calculated by follows.

$$Q_b = B\sum_{k=1}^{n} q_{bk} \tag{5.13}$$

$$q_{bk} = 17\frac{\rho u_{*e}^3}{(\rho_s - \rho)g}\left[1 - \sqrt{K_c\frac{u_{*ck}}{u_*}}\right]\left[1 - K_c\frac{u_{*ck}^2}{u_*^2}\right]f_{bk} \tag{5.14}$$

where n is the number of grain-size order, ρ is density of water, ρ_s is density of sediment, u_{*e} is the effective friction rate and can be calculated as follows,

$$u_{*e}^2 = \frac{[Q/(Bh)]^2}{\left[6 + 2.5\ln\frac{h}{d_m(1+2\tau_{*m})}\right]^2} \tag{5.15}$$

where d_m is the mean diameter of sediment in the mixed layer on the riverbed. In addition, threshold friction velocity of the k_{th} order of grain-size can be calculated by follows.

$$u_{*ck}^2 = u_{*cm}^2\left[\frac{\log_{10}19}{\log_{10}(19d_k/d_m)}\right]^2\frac{d_k}{d_m} \qquad d_k/d_m \geq 0.4 \tag{5.16-1}$$

$$u_{*ck}^2 = 0.85u_{*cm}^2 \qquad d_k/d_m \leq 0.4 \tag{5.16-2}$$

The threshold friction velocity of the mean diameter of grain-size can be calculated by follows.

$$u_{*cm}^2 = 0.89d_m \qquad d_m \geq 0.303 \tag{5.17-1}$$

$$u_{*cm}^2 = 134.6d_m^{31/22} \qquad 0.118 \leq d_m < 0.303 \tag{5.17-2}$$

$$u_{*cm}^2 = 55.0d_m \qquad 0.0565 \leq d_m < 0.118 \tag{5.17-3}$$

$$u_{*cm}^2 = 8.41 d_m^{11/32} \qquad 0.0065 \le d_m < 0.0565 \qquad (5.17\text{-}4)$$

$$u_{*cm}^2 = 226 d_m \qquad d_m < 0.0065 \ (\text{Unit}: \text{cm}) \qquad (5.17\text{-}5)$$

K_c is modified function due to the influence of the slope of the riverbed, and it can be calculated by Eq(5.18).

$$K_c = 1 + \frac{1}{\mu_s}\left[\left(\frac{\rho}{\rho_s - \rho} + 1\right) tan\theta_x\right] \qquad (5.18)$$

where μ_s is static friction coefficient, θ_x is the slope of the riverbed in the unit channel.

$$tan\theta_x = I \qquad (5\text{-}19)$$

Besides, the deposition rate of suspended load D_s and the erosion rate of suspended load E_s can be calculated by follows.

$$D_s = \sum_{k=1}^{n} D_{sk} \qquad (5\text{-}20)$$

$$D_{sk} = c_{sbk} w_{fk} \qquad (5\text{-}21)$$

$$E_s = \sum_{k=1}^{n} E_{sk} \qquad (5\text{-}22)$$

$$E_{sk} = c_{sbek} w_{fk} \qquad (5\text{-}23)$$

(B) Suspended load

The transportation of suspended load concentration of grain-size order k is described as follows.

$$\frac{\partial c_{sk} h}{\partial t} = \frac{1}{BL}\left(c_{sk,x_i} Q(x_i) + c_{sk,y_i} Q(y_i) - c_{sk,x_{i+1}} Q(x_{i+1})\right) + E_{sk} - D_{sk} \qquad (5.24)$$

where c_{sk} is the mean concentration of suspended load in the unit channel, c_{sk,x_i} and c_{sk,y_i} are the concentration of suspended load from the upstream, $c_{sk,x_{i+1}}$ is the concentration of suspended load to the downstream. In addition, w_{fk} is settling velocity of sediment, it is determined by follows.

$$w_{fk} = \left[\sqrt{\frac{2}{3} + \frac{36v^2}{\left(\frac{\rho_s}{\rho} - 1\right) g d_k^3}} - \sqrt{\frac{36v^2}{\left(\frac{\rho_s}{\rho} - 1\right) g d_k^3}}\right] \sqrt{\left(\frac{\rho_s}{\rho} - 1\right) g d_k}$$

(5.25)

Equilibrium concentration of suspended sediment of grain-size order k (c_{sbek}) on the reference surface can be calculated by follows.

$$c_{sbek} = 5.55 \left[\frac{1}{2} \frac{u_*}{w_{fk}} exp\left(-\frac{w_{fk}}{u_*}\right)\right]^{1.61} f_{bk} \qquad \text{(unit: ppm)}$$

(5.26)

Here, the vertical distribution of concentration of suspended load is assumed in the exponential distribution, and the relationship of c_{sk} and c_{sbk} can be described as the follows. (c_{sk} is the mean concentration of suspended load of grain-size order k in mean depth of water, ; c_{sbk} is the concentration of suspended load of grain-size order k on the reference surface); f_{bk} is the proportion of bed load at the grain-size order k.

$$c_{sk} = \frac{c_{sbk}}{\beta_{sk}} \left(1 - e^{(-\beta_{sk})}\right) \tag{5.27}$$

$$\beta_{sk} = \frac{w_{fk} h}{D_h} \tag{5.28}$$

where D_h is the diffusion coefficient of suspended load in the water depth direction. To simplify the expression, ν is used to instead of D_h. D_w and E_w are the deposition rate and erosion rate of wash load, and they can be calculated by follows.

$$D_w = c_w w_f \tag{5.29}$$

$$E_w = -(1 - \lambda) f_w \frac{\partial z}{\partial t} \qquad \left(\frac{\partial z}{\partial t} \leq 0\right) \tag{5.30-1}$$

$$E_w = 0 \qquad \left(\frac{\partial z}{\partial t} \geq 0\right) \tag{5.30-2}$$

where f_w is the proportion of wash load, and f_w and f_{bk} satisfy the following relationship.

$$f_w + \sum_{k=1}^{n} f_{bk} = 1$$

(5.31)

(C) Wash load

The transportation equation of the concentration of wash load for grain-size order *k* is described as follows.

$$\frac{\partial c_w h}{\partial t} = \frac{1}{BL}\left(c_{w,x_i} Q(x_i) + c_{w,y_i} Q(y_i) - c_{w,x_{i+1}} Q(x_{i+1})\right) + E_w - D_w \tag{5.32}$$

where c_w is the mean concentration of wash load in the unit channel, c_{w,x_i} and c_{w,y_i} are the concentration of suspended load from the upstream, $c_{w,x_{i+1}}$ is the concentration of suspended load to the downstream.

(D) The continuity equation of the riverbed material

The distribution of grain-size of deposition sediment in the riverbed is calculated based on volume control condition in the mixed layer, and the water and sediment are assumed as the same in the same channel. According to the principle of mass conservation, the continuity equation of sediment in the mixed layer is expressed as follows.

$$(1-\lambda)E_b \frac{\partial f_{bk}}{\partial t} + (1-\lambda)F_{bk} \frac{\partial z}{\partial t} = \frac{1}{BL}\left(Q_{bk}(x_i) + Q_{bk}(y_i) - Q_{bk}(x_{i+1}) + Q_l(x_i)\right) + D_{sk} - E_{sk} + D_w - E_w$$

$$\begin{cases} F_{bk} = f_{dlk}\ , & \partial z/\partial t \le 0 \\ F_{bk} = f_{bk}\ , & \partial z/\partial t \ge 0 \end{cases} \tag{5.33}$$

were f_{dlk} is the proportion of grain-size distribution in the deposited layer; f_{bk} is the proportion of grain-size distribution of grain-size in the riverbed. In addition, this study assumed the increasing thickness was less than one deposited layer (0.4m) in each time-step (1sec).

5.3.3 Simulation model of sediment supply from landslides

Generally, the source of the increasing sediment in the riverbed might be from the landslide, debris flow, bank erosion, etc. This study only considered the source from the landslide sediment, excluding other sources. To estimate the volume of landslide sediment moving into channels, this study proposed the simplified model based on the following assumptions:

(A) The rate of landslide sediment entering the adjacent channel is related to the mean slope of the slope unit. That is, if the slope unit is steeper, the rate might be higher.

(B) The moving of landslide sediment is triggered by overland flow from the slope unit, and the overland flow can be calculated by the segmental approach (see **Figure 5.14**, Eq.(5.7) and (5.8)) as well as the width of sediment moving equals to the width of landslide (i.e., 20m)

(C) The volume of landslide sediment moving into channels can be calculated by the abovementioned sediment runoff model, and the amount of sediment runoff on the toe of the slope unit is considered as the amount of sediment entering the channel.

(D) The method of landslide sediment supply is uniformly distributed over the riverbed of the adjacent unit channel (see **Figure 5.16**).

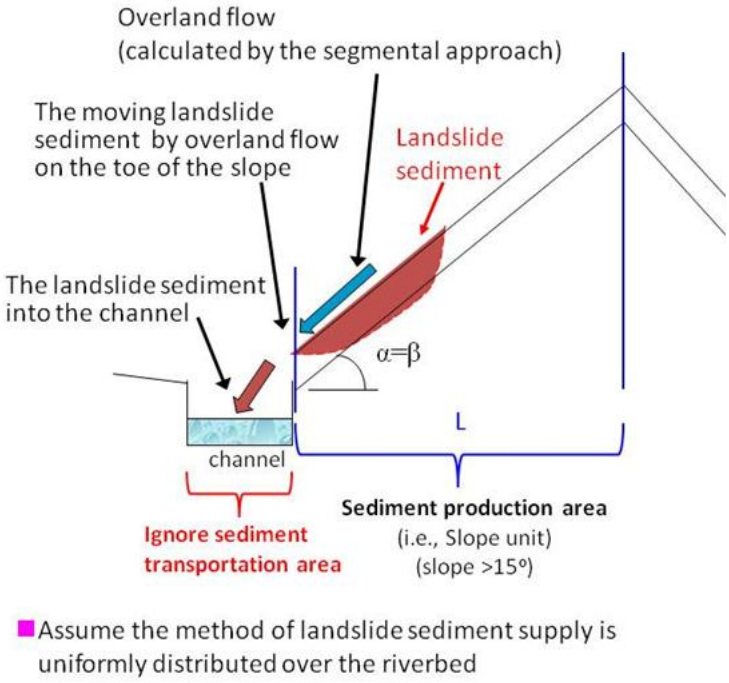

Figure 5.16 The diagram of calculating landslide sediment into the unit channel

5.3.4 Calculation condition

The Manning's roughness coefficient of all unit channels is set to 0.03 [m-s]. If the two sides of the river bank have concrete revetment, the width of the unit channel is set as the actual size. The others are estimated by $B = 3.5\sqrt{QA'/A}$, where B is the width of the unit channel, A is the area of the basin, A' is the accumulated area of upstream unit channel, and Q is set as 100 CMS. The grain size distribution is assumed to be the same in all unit channels, and the distribution is shown as in the **Figure 5.17**.

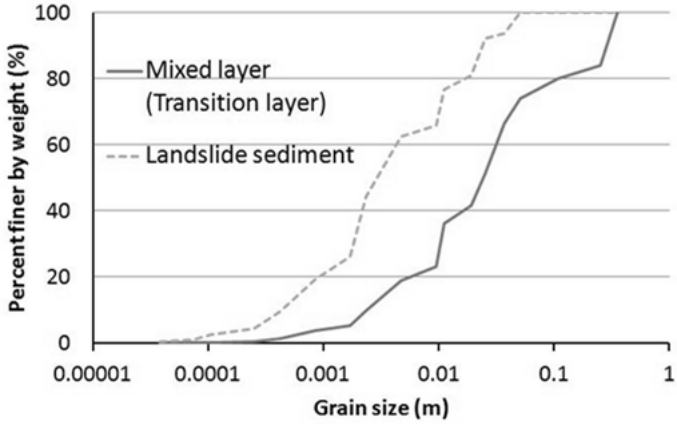

Figure 5.17 The grain size distribution of riverbed in the study area

5.4 Simulation results

5.4.1 Landslides

The simulation indicates 131 slope units collapsed (see **Table 5.1**), and the occurrence time of landslides was between 03:34~05:47, but 98.5% of the landslides occurred at 04:34~5:47. The simulation results were consistent with the field investigation. Of the 38 newly collapsed slopes which were identified from the satellite image, 28 slopes were simulated as collapsed, and the others were not (see **Table 5.1**). The simulation results of occurrence time and locations were the same as Chapter 4, so the warning hit rate (WHR) was also 73.7%. However, the false alert rate (FAR) decreased to 78.6%, and the accuracy of landslide prediction (ALP) increased to 74.0% because of the reduction of over-predicting slope units.

The comparison of simulation and actual cases is shown in **Figure 5.18**. The simulation results for the volume of landslide sediment in each unit channel watershed are shown as **Figure 5.19** and **Table 5.2**.

Table 5.1 The comparison of simulation and actual landslides in the Shizugawa basin

Number of slope units		Simulation results	
		Collapsed	Non-Collapsed
Actual Event	Collapsed	28	10
	Non-Collapsed	103	294

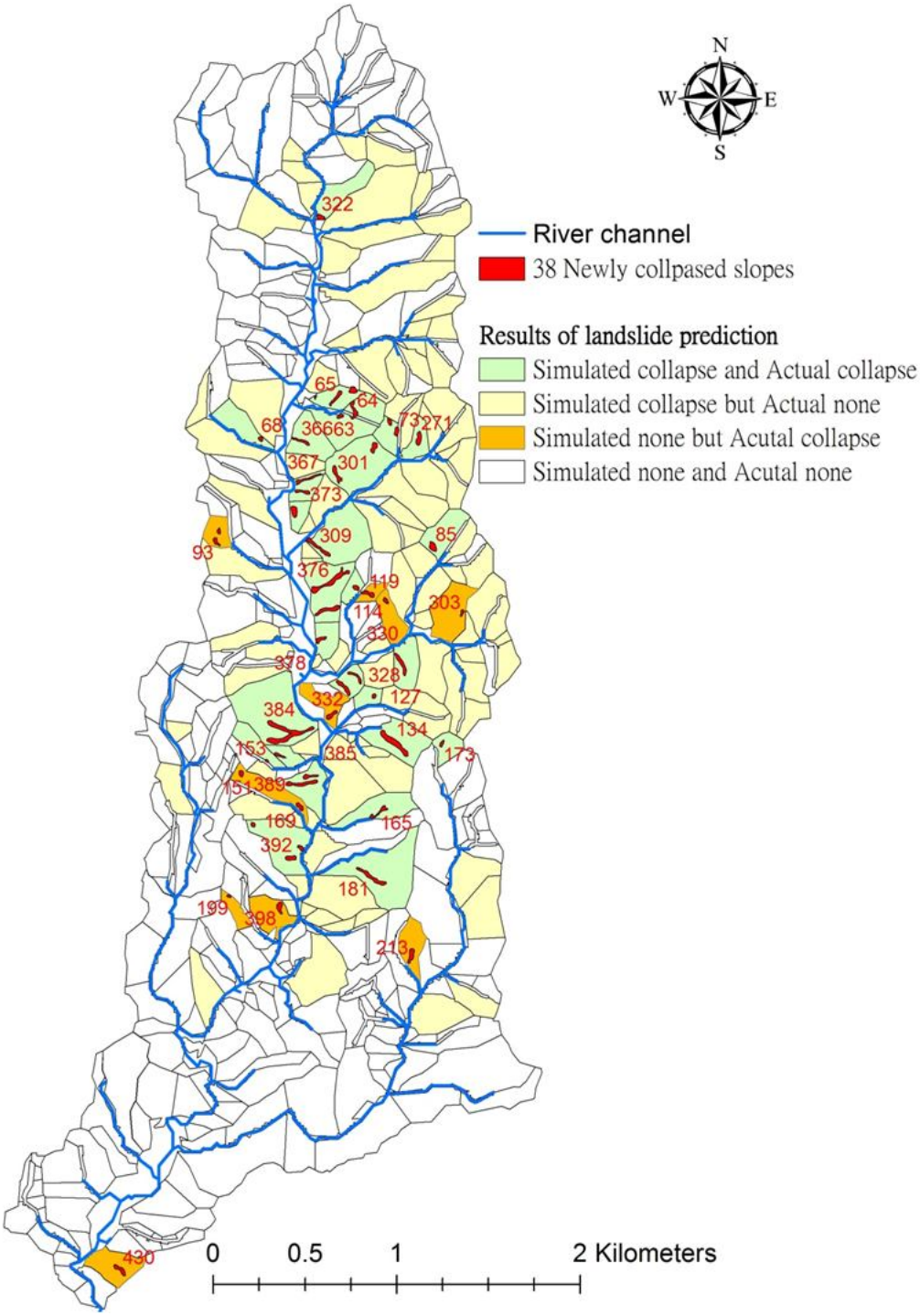

Figure 5.18 The comparison between the simulation and actual locations for the landslides in the Shizugawa basin (C=0.85 t/m^2 for the north part of the basin, the others C=0.7 t/m^2)

Table 5.2 The simulation results of the volume of landslide sediment in each unit channel watershed in the Shizugawa basin

Time	No. Unit channel	Volume of landslide sediment(m3)	Time	No. Unit channel	Volume of landslide sediment(m3)	Time	No. Unit channel	Volume of landslide sediment(m3)
03:34	109	37.9	05:09	84	1374.8	05:26	11	4625.4
03:38	114	2054.8	05:10	14	2157.8	05:26	42	1471.5
04:34	36	1475.2	05:10	18	1663.3	05:26	49	590.5
04:37	101	1545.8	05:10	22	1429.8	05:26	52	488.0
04:38	84	2038.0	05:10	70	3761.0	05:26	72	1768.0
04:40	101	1287.6	05:11	25	1635.1	05:26	73	692.0
04:43	80	3979.5	05:11	73	411.4	05:26	75	2773.6
04:43	102	635.6	05:11	75	2643.6	05:27	68	7744.3
04:43	113	1080.3	05:11	87	4026.4	05:27	87	2375.7
04:46	102	728.2	05:11	110	1259.5	05:28	26	1896.1
04:46	24	730.8	05:12	84	1295.0	05:28	40	1676.8
04:47	111	1717.5	05:12	120	927.1	05:28	110	1748.2
04:48	104	867.8	05:13	18	1687.6	05:29	34	1535.6
04:49	21	815.3	05:13	80	7611.0	05:29	99	3207.2
04:49	19	795.0	05:14	31	1459.2	05:30	49	855.3
04:50	14	933.2	05:14	35	1141.5	05:30	103	1746.5
04:51	71	1006.6	05:14	71	1609.5	05:31	94	4699.8
04:52	81	2975.4	05:14	88	1110.5	05:32	31	1918.9
04:52	37	7094.9	05:16	15	2353.9	05:32	79	2624.9
04:53	88	2527.6	05:16	34	1577.9	05:32	89	1969.0
04:53	22	1175.4	05:16	87	1887.1	05:33	40	568.4
04:55	46	1891.4	05:17	13	2250.7	05:33	68	3242.4
04:57	84	1069.8	05:17	32	1570.4	05:33	113	1346.8
04:57	19	1172.0	05:17	35	1582.3	05:34	5	2191.5
04:59	37	399.5	05:17	111	1395.8	05:34	11	3551.1
05:00	20	1331.1	05:17	114	965.3	05:34	106	2176.3
05:01	18	1247.3	05:18	40	1055.0	05:35	14	1848.2
05:01	21	1230.2	05:18	121	842.5	05:35	29	2128.6
05:03	20	1591.0	05:19	115	448.8	05:35	30	1942.9
05:03	35	1250.2	05:20	86	2233.5	05:35	43	1639.9
05:03	105	1394.8	05:22	26	1644.7	05:35	66	3664.7
05:04	9	1796.3	05:23	8	2381.3	05:36	13	3068.2
05:04	33	990.1	05:23	37	1436.7	05:36	27	2081.7
05:04	87	1668.1	05:23	49	575.9	05:36	29	1989.9
05:05	72	1120.1	05:23	115	433.9	05:36	71	2338.7
05:07	21	1017.3	05:24	15	2324.9	05:36	79	4166.8
05:07	67	2650.0	05:24	40	1576.9	05:37	5	3661.8
05:08	20	1277.0	05:24	71	2165.9	05:38	22	1839.5
05:08	24	3084.1	05:24	89	1811.6	05:38	25	1744.0
05:08	74	867.2	05:24	107	707.9			
05:08	88	1277.5	05:25	35	1770.9			
05:08	103	1718.1	05:25	38	1490.2			
05:09	34	1286.4	05:25	43	1059.4			

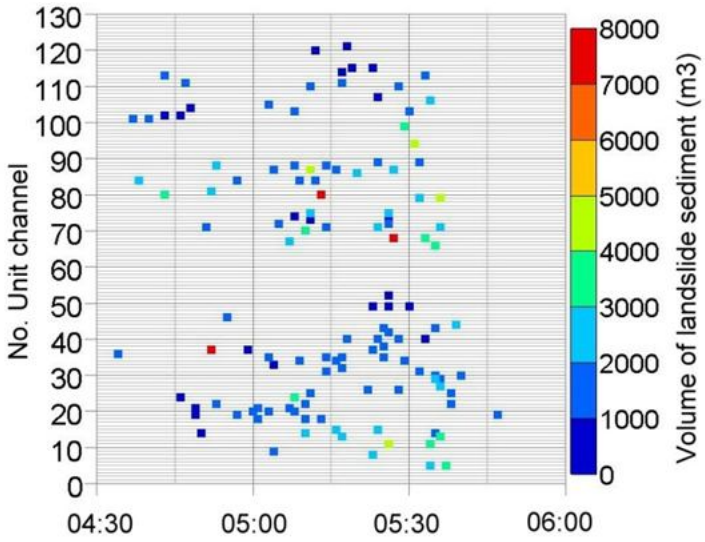

Figure 5.19 The simulation results for the volume of landslide sediment in each unit channel watershed in the Shizugawa basin

5.4.2 Landslides induced road-closure

The safety of the evacuation routes is the inevitable and indispensable issue for the disaster prevention strategy, and it will directly affect the evacuation result. The hazards which lead to road-closure usually can be divided into two types- landslides and floods. Landslides could bury the road and interrupt the traffic as well as causing casualties. Floods could erode the embankment to cause the road to collapse. Moreover, if the water level is higher than bridges, the bridges might be washed out.

In this study area, there are eleven main evacuation routes which connect the two main settlements and other areas. According to the simulation result, there are 42 slope units, which are close to the main evacuation routes in 10m, to occur landslides along seven main evacuation routes (see **Figure 5.20**). That is, the seven roads might be closure during the heavy rainfall event. **Table 5.3** shows the list of simulation results of road closure caused by landslides. The simulation result reveals the Sumiyama area became isolated because of road-closure during the heavy rainfall event, and the result is consistent with the related disaster reports [*Maki and Hayashi*, 2014; *Uji City*, 2014].

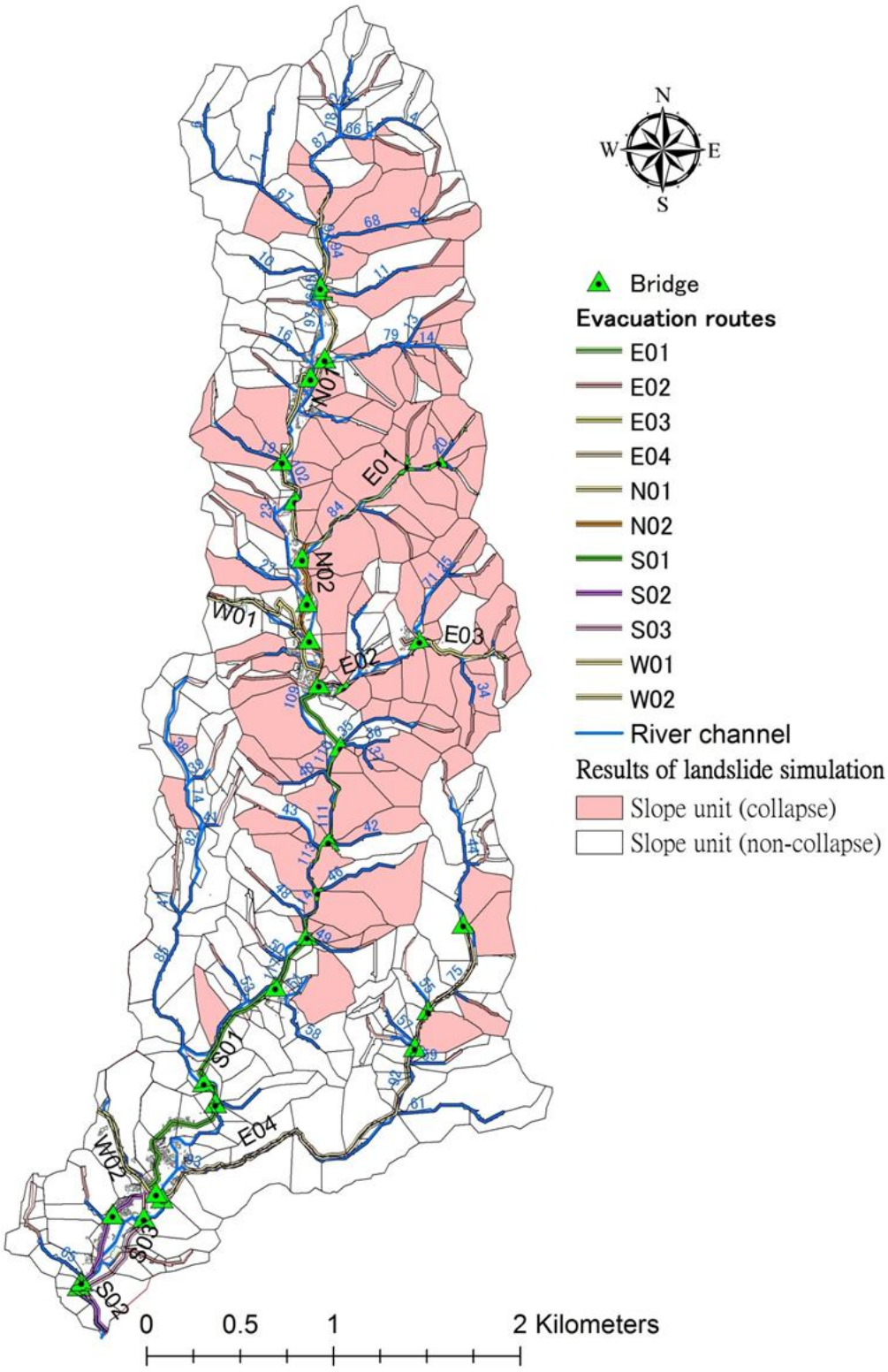

Figure 5.20 The simulation results for landslides along main evacuation routes in the Shizugawa basin

Table 5.3 The list of simulation result of road closure caused by landslides

	No. Road	No. slope unit	Landslide occurring time	volume of landslide sediment (m3)
1	E01	309	**2014/8/14 04:38**	2038.0
2		301	2014/8/14 04:43	3979.5
3		75	2014/8/14 04:49	815.3
4		76	2014/8/14 04:53	1175.4
5		311	2014/8/14 04:57	1069.8
6		71	2014/8/14 05:00	1331.1
7		73	2014/8/14 05:01	1230.2
8		70	2014/8/14 05:03	1591.0
9		72	2014/8/14 05:08	1277.0
10		78	2014/8/14 05:10	1429.8
11		270	2014/8/14 05:10	1953.6
12		271	2014/8/14 05:10	1807.4
13		77	2014/8/14 05:38	1839.5
14	E02	328	**2014/8/14 04:53**	2527.6
15		329	2014/8/14 05:08	1277.5
16		272	2014/8/14 05:24	2165.9
17		332	2014/8/14 05:24	1811.6
18		333	2014/8/14 05:32	1969.0
19	E03	276	**2014/8/14 05:05**	1120.1
20		277	2014/8/14 05:26	1768.0
21		104	2014/8/14 05:35	2128.6
22		107	2014/8/14 05:35	1942.9
23		105	2014/8/14 05:36	1989.9
24		275	2014/8/14 05:36	2338.7
25		106	2014/8/14 05:40	1876.6
26	E04	283	**2014/8/14 05:11**	2643.6
27		319	2014/8/14 05:20	2233.5
28		285	2014/8/14 05:26	2773.6
29	N01	365	**2014/8/14 04:37**	1545.8
30		367	2014/8/14 04:43	635.6
31		322	2014/8/14 05:11	4026.4
32		312	2014/8/14 05:12	1295.0
33		325	2014/8/14 05:27	2375.7
34		373	2014/8/14 05:30	1746.5
35	N02	381	**2014/8/14 05:24**	707.9
36		378	2014/8/14 05:34	2176.3
37	S01	394	**2014/8/14 03:38**	2054.8
38		388	2014/8/14 04:47	1717.5
39		280	2014/8/14 05:11	411.4
40		396	2014/8/14 05:19	448.8
41		386	2014/8/14 05:28	1748.2
42		393	2014/8/14 05:33	1346.8

Note: the earliest occurring time of predicting landslides on each road is highlighted in bold type

5.4.3 Sediment supply from landslides

Based on the previous assumption of the sediment supply from landslides in this study, landslide sediment into the channels is only triggered by overland flow from the slope unit. That is, the sediment supply approaches that sediment was moved by debris flow or the whole landslide sediment directly fell into the channel were not considered in this study. According to the order of mean slope of the slope unit, the simulation results of landslide sediment transportation into channels were shown as **Table 5.4**. The simulation results showed that the amount of landslide sediment into the channel trended to be more much on the steeper slope unit. In fact, because the moving of landslide sediment was triggered by overland flow; rainfall distribution and watershed area also might affect the simulation results.

Table 5.4 The simulation results of landslide sediment transportation into channels

	No. Slope unit	Volume of landslide sediment	Volume of landslide sediment into the channel	Proportion (%)	Length of the slope unit	Slope of the slope unit		No. Slope unit	Volume of landslide sediment	Volume of landslide sediment into the channel	Proportion (%)	Length of the slope unit	Slope of the slope unit
1	280	411.4	411.4	100.0	34	39.2	67	266	7744.3	95.6	1.2	231	30.3
2	138	399.5	399.5	100.0	52	38.6	68	276	1120.1	312.1	27.9	83	30.1
3	397	433.9	433.9	100.0	57	38	69	388	1717.5	134.7	7.8	210	30
4	396	448.8	448.8	100.0	65	36.9	70	329	1277.5	249.3	19.5	117	30
5	152	568.4	568.4	100.0	31	36.8	71	72	1277.0	317.6	24.9	79	30
6	367	635.6	465.3	73.2	121	36.3	72	387	1259.5	223.9	17.8	125	29.9
7	327	1668.1	481.5	28.9	110	35.6	73	128	1250.2	338.6	27.1	95	29.9
8	193	575.9	575.9	100.0	121	35.6	74	312	1295.0	290.6	22.4	73	29.7
9	201	148.0	148.0	100.0	221	35.5	75	70	1591.0	110.7	7.0	184	29.5
10	279	692.0	692.0	100.0	38	35.4	76	181	1891.4	131.9	7.0	211	29.4
11	30	1796.3	558.1	31.1	95	35.3	77	309	2038.0	87.8	4.3	230	29.2
12	49	933.2	487.5	52.2	108	35.2	78	65	1687.6	179.7	10.6	128	29.2
13	381	707.9	707.9	100.0	36	35	79	63	1663.3	161.2	9.7	140	29.2
14	46	2157.8	414.1	19.2	116	34.6	80	165	1471.5	239.7	16.3	124	29.2
15	194	590.5	590.5	100.0	78	34.5	81	166	1639.9	225.8	13.8	127	28.9
16	326	1887.1	504.5	26.7	81	34.3	82	137	1436.7	262.3	18.3	110	28.9
17	50	1848.2	676.3	36.6	63	34.3	83	83	1369.0	278.6	20.4	81	28.9
18	51	2353.9	425.3	18.1	110	34.2	84	85	1635.1	188.8	11.5	126	28.8
19	203	488.0	488.0	100.0	87	34.1	85	301	3979.5	69.9	1.8	258	28.7
20	264	2650.0	198.3	7.5	178	33.5	86	389	1395.8	149.0	10.7	156	28.7
21	18	2191.5	548.7	25.0	66	33.4	87	145	1490.2	256.8	17.2	105	28.6
22	42	2250.7	419.9	18.7	87	33.3	88	310	1374.8	235.9	17.2	81	28.6
23	192	855.3	681.9	79.7	71	33.3	89	124	1286.4	245.9	19.1	88	28.6
24	368	728.2	212.8	29.2	172	33.3	90	78	1429.8	242.7	17.0	84	28.5
25	390	842.5	651.0	77.3	67	33.2	91	319	2233.5	117.2	5.2	237	28.4
26	27	2381.3	421.6	17.7	84	33.1	92	271	1807.4	114.9	6.4	161	28.4
27	325	2375.7	432.2	18.2	81	33.1	93	376	1394.8	95.3	6.8	180	28.4
28	53	2324.9	382.4	16.4	93	33	94	153	1576.9	181.1	11.5	134	28.3
29	361	3207.2	315.8	9.8	123	32.9	95	274	1609.5	183.2	11.4	121	28.2
30	43	3068.2	397.1	12.9	102	32.8	96	129	1582.3	186.7	11.8	123	28.2
31	74	1017.3	525.7	51.7	69	32.7	97	81	1715.0	115.4	6.7	156	28
32	395	965.3	540.5	56.0	95	32.6	98	126	1535.6	302.6	19.7	71	28
33	322	4026.4	183.1	4.5	190	32.5	99	136	7094.9	49.3	0.7	299	27.9
34	68	795.0	403.2	50.7	86	32.5	100	87	1644.7	221.3	13.5	102	27.7
35	267	3242.4	385.0	11.9	98	32.4	101	109	1459.2	232.9	16.0	83	27.7
36	300	2624.9	352.7	13.4	90	32.4	102	328	2527.6	83.7	3.3	209	27.5
37	64	1247.3	313.1	25.1	118	32.2	103	371	1718.1	92.3	5.4	171	27.5
38	406	927.1	263.8	28.5	214	32.2	104	277	1768.0	175.7	9.9	117	27.4
39	311	1069.8	368.6	34.5	107	32.1	105	386	1748.2	160.8	9.2	128	27.4
40	82	730.8	358.4	49.0	93	32.1	106	114	1570.4	231.4	14.7	80	27.3
41	262	3664.7	311.1	8.5	110	32	107	67	1736.9	279.6	16.1	66	27.2
42	37	3551.1	345.0	9.7	104	32	108	283	2643.6	87.8	3.3	218	27.1
43	73	1230.2	348.0	28.3	108	32	109	125	1577.9	234.6	14.9	95	27.1
44	76	1175.4	219.7	18.7	149	31.9	110	285	2773.6	90.9	3.3	209	26.9
45	66	1172.0	295.4	25.2	122	31.9	111	270	1953.6	71.1	3.6	184	26.9
46	384	37.9	37.9	100.0	259	31.9	112	302	7611.0	37.3	0.5	281	26.8
47	394	2054.8	110.9	5.4	311	31.8	113	332	1811.6	145.5	8.0	120	26.7
48	366	1287.6	150.5	11.7	200	31.8	114	373	1746.5	160.4	9.2	96	26.7
49	392	1080.3	176.4	16.3	223	31.8	115	86	1744.0	250.1	14.3	69	26.7
50	273	1006.6	207.1	20.6	156	31.8	116	151	1676.8	194.4	11.6	86	26.4
51	75	815.3	326.4	40.0	93	31.8	117	304	2975.4	55.3	1.9	227	26.3
52	295	4166.8	219.2	5.3	142	31.7	118	106	1876.6	196.6	10.5	97	26.2
53	16	3661.8	342.4	9.3	101	31.7	119	77	1839.5	212.8	11.6	71	26
54	122	990.1	409.0	41.3	98	31.7	120	173	2058.2	154.0	7.5	113	25.9
55	167	1059.4	538.3	50.8	68	31.6	121	127	1770.9	182.0	10.3	82	25.9
56	71	1331.1	229.3	17.2	137	31.4	122	272	2165.9	74.7	3.4	159	25.6
57	36	4625.4	157.8	3.4	171	31.3	123	104	2128.6	125.1	5.9	119	25.5
58	331	1110.5	489.5	44.1	63	31.3	124	91	2081.7	139.2	6.7	110	25.4
59	351	4699.8	168.4	3.6	161	31.2	125	88	1896.1	156.2	8.2	83	25.4
60	374	867.8	251.4	29.0	92	31	126	378	2176.3	106.4	4.9	124	25.2
61	281	867.2	360.5	41.6	88	31	127	107	1942.9	152.8	7.9	83	25.2
62	365	1545.8	117.4	7.6	218	30.9	128	112	1918.9	157.9	8.2	82	25.2
63	157	1055.0	431.9	40.9	76	30.9	129	105	1989.9	146.3	7.4	84	24.9
64	134	1475.2	124.5	8.4	228	30.7	130	333	1969.0	148.6	7.5	81	24.9
65	393	1346.8	334.9	24.9	114	30.6	131	275	2338.7	69.8	3.0	92	22.5
66	131	1141.5	432.3	37.9	72	30.6							

5.4.4 Flood and sediment runoff

(1) Simulation of Maximum water discharge

For flood simulation, the discharge of the representative unit channels on the upstream (No.94), midstream (No.105) and downstream (No.122 and No.127) of the study area is shown in **Figure 5.21**. According to the disaster survey report [*Kyoto Prefecture*, 2013a] and the disaster rehabilitation plan [*Kyoto Prefecture*, 2013b], the maximum water discharge in the unit channel of No.122 was about 80 CMS, and the value in the unit channel of No.127 was about 100 CMS during the heavy rainfall event on August 13-14, 2012. In addition, the maximum water level in the unit channel of No.122 was about 3 m, and the overflow occurred during about 4:30~6:00.

Compared with the data of the disaster survey report, the simulation results (Q_{max}=82.3CMS, the maximum water level= 2.96m, and the duration of overflow was 03:37~03:48 and 04:31~05:32 on August 14) of the unit channel No.122 were consistent (see **Figure 5.21** and **5.22**). Besides, the simulation result of maximum water discharge of the unit channel No.127 (Q_{max}=105.3CMS) was also very close to the investigation result.

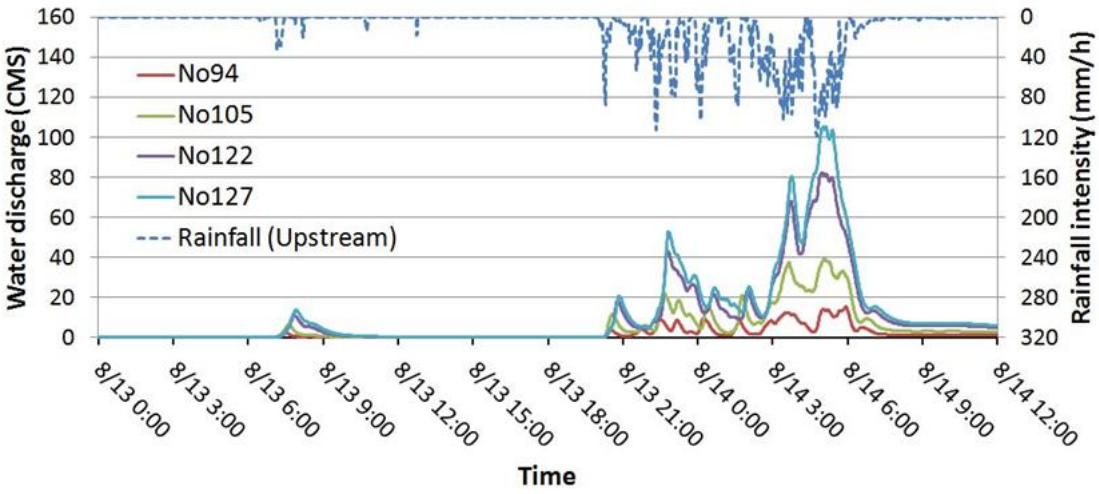

Figure 5.21 The simulation of the water discharge in the channels

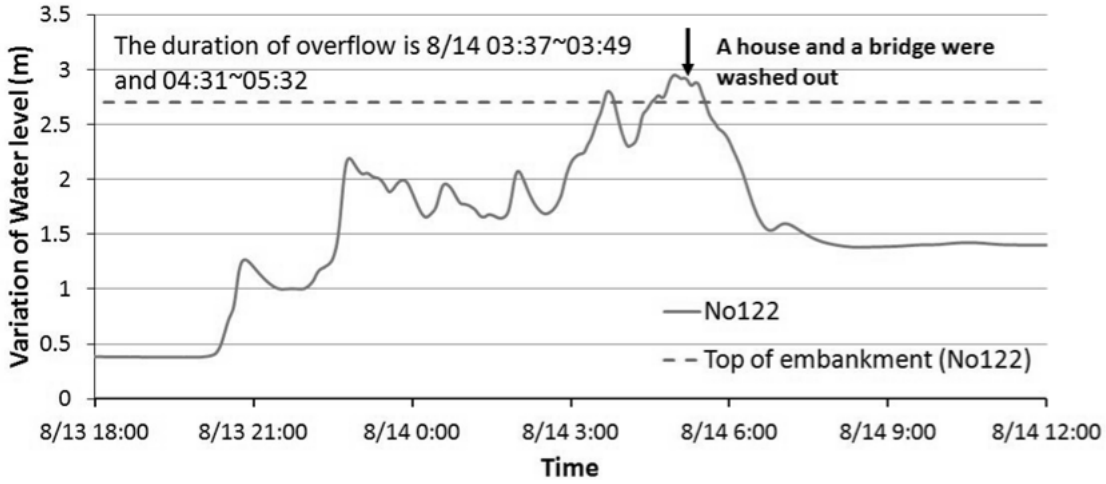

Figure 5.22 The simulation of water level in the channel (No.122)

(2) Overflow simulation on unit channels

Generally, overflows, which might cause road and bridge interrupted and inundation at the communities, are the most common flood disaster types in mountainous areas because the design drainage capacity of channels was usually lower, and the flash flood occurred frequently. The cross-section of each unit channel was assumed to be in a rectangle shape, and the embankment height was assigned based on the investigation results. Based on the comparison between the water level and embankment height, the simulation model identified that the overflows occurred at 9 unit channels during the heavy rainfall event. **Table 5.5** shows the comparison of overflow duration between the simulation and investigation results. **Figure 5.23** shows the prediction result of variation of water level in the unit channels listed in **Table 5.5** (excluded No.122, see **Figure 5.22**).

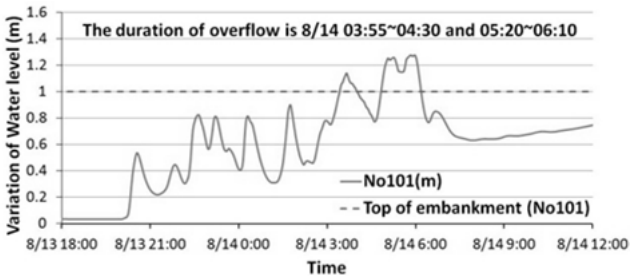

(a) No. 101

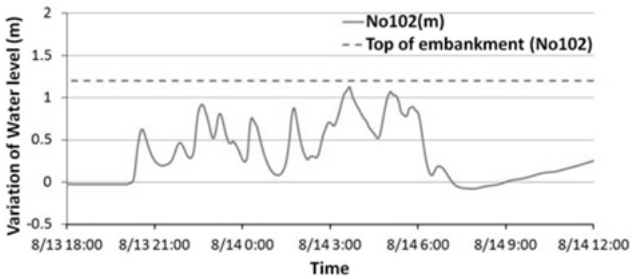

(b) No. 102

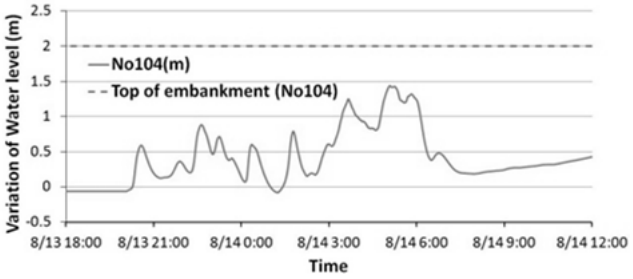

(c) No. 104

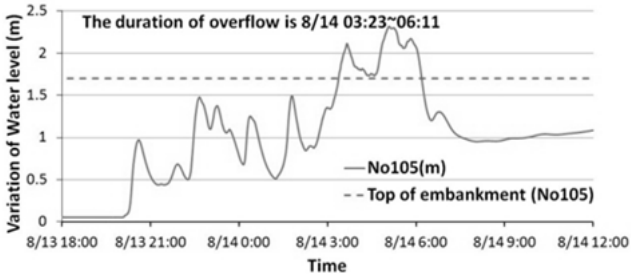

(d) No. 105

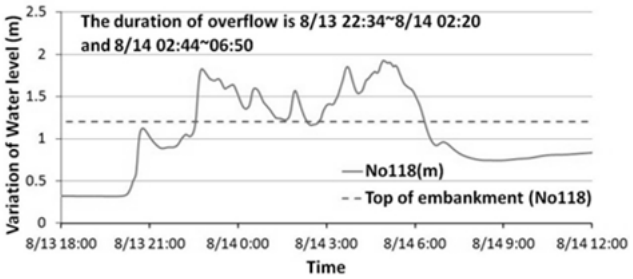

(e) No. 118

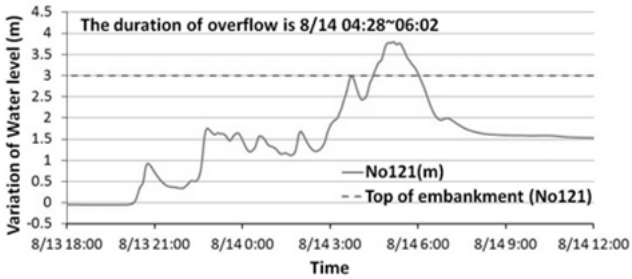

(f) No. 121

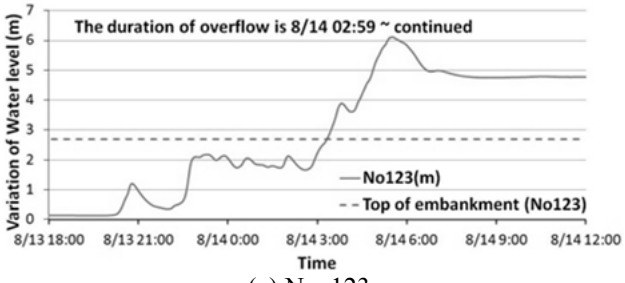

(g) No. 123

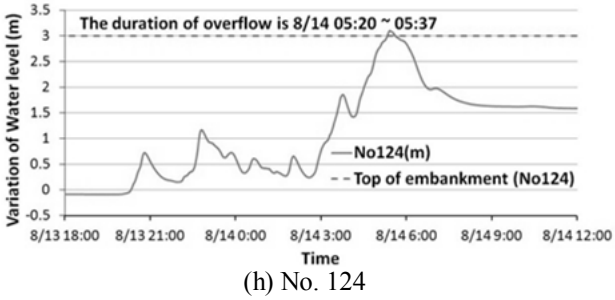

(h) No. 124

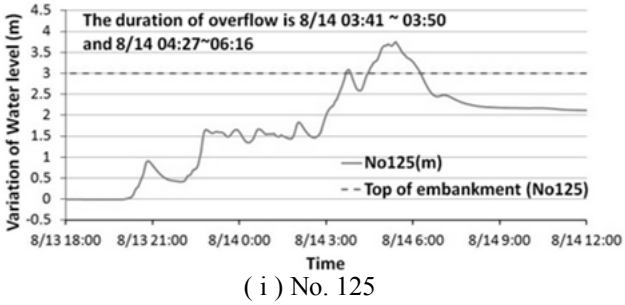

(i) No. 125

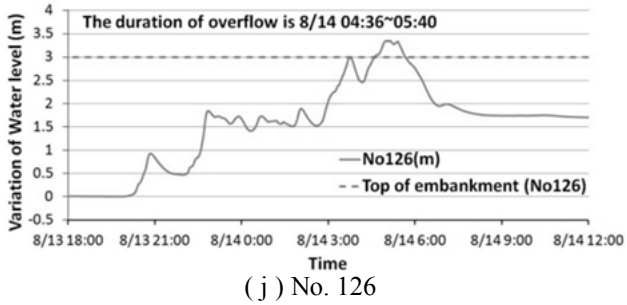

(j) No. 126

Figure 5.23 The simulation of water level in the unit channels which might overflow

* The zero in the figure was the riverbed position at the beginning of simulation (i.e., 8/12 0:00)

Table 5.5 The comparison of overflow duration between the simulation and investigation results

	Unit channel	Length of unit channel (m)	Slope of riverbed (%)	Revetment height (m)	Duration of overflow (Simulation results)	Duration of overflow (Investigation results)
1	No.101	314.4	1.29	1.0	8/14 03:55~04:30 8/14 05:20~06:10	8/14 about 4:30~06:00
2	No.102	396.5	1.75	1.2	Pass	8/14 about 4:30~06:00
3	No.104	96.2	2.33	2.0	Pass	8/14 about 04:00~6:00
4	No.105	321.4	1.15	1.7	8/14 03:23~06:11	8/14 about 04:00~6:00
5	No.118	183.5	1.01	1.2	8/13 22:34~8/14 02:20 8/14 02:44~06:50	Overflow (but occurring time is unknown)
6	No.121	432.9	2.36	3.0	8/14 04:28~06:02	Unknown
7	No.122	680.3	4.32	2.7	8/14 03:37~03:49 8/14 04:31~05:32	8/14 about 04:30~05:30 (A house and a bridge were washed out)
8	No.123	192.2	1.32	2.7	8/14 02:59~ continued	8/14 about 04:30~06:00
9	No.124	295.1	2.41	3.0	8/14 05:20~05:37	8/14 about 04:30~06:00
10	No.125	250.3	1.82	3.0	8/14 03:41~03:50 8/14 04:27~06:16	8/14 about 04:30~06:00
11	No.126	164.6	1.83	3.0	8/14 04:36~05:40	Overflow (but occurring time is unknown)

Overall, most simulation results are consistent with the investigation results. Some unit channels located in uninhabited areas (e.g., the unit channel of No.118, No.121, and No.126), so it is difficult to determine when the flood occurred. Nevertheless, by the field survey, it is certain that these areas did have floods. **Figure 5.24** shows the flood evidence in the unit channel of No.126.

Figure 5.24 The flood evidence in the unit channel of No. 126 [Uji City, 2014]

However, the simulation results of some unit channels (No.102, No.104, and No.123) were obvious different from the actual situations.

First, according to the survey, the unit channel of No.101 and No.102 overflowed after the landslide occurred at the slope unit of No.367 (at about 8/14 04:30~05:00). The simulation results indicated that the landslide occurred at two slope units (No.367 and No.368), which were adjacent to the unit channel of No.102, at 4:43 and 4:46, Aug. 14, and landslide sediment of 678.1 m^3 had entered the unit channel of No.102 (see **Table 5.4**). The simulation results seem to be consistent with the investigation results about the location, occurrence time, and scale of landslides. Nevertheless, because the study assumed that the method of landslide sediment supply was a uniform distribution over the riverbed, i.e., the riverbed rose to just about 0.34m (Length of unit channel of No.102 is 396.5m, and width is 5m), due to the landslide sediment supply. Such sediment deposition height was not enough to block the channel. Hence, the overflow only occurred at the unit channel of No.101, whose embankment height was lower. The same situation also happened in the unit channels of No.104 and No.105 (see **Figure 5.7**).

(3) Simulation of sediment runoff and riverbed deformation

Another unreasonable simulation result appeared at the unit channel of No.123. The simulation result implied that the riverbed was higher than the top of embankment after the flood (see **Figure 5.23(g)** and **Figure 5.25**).

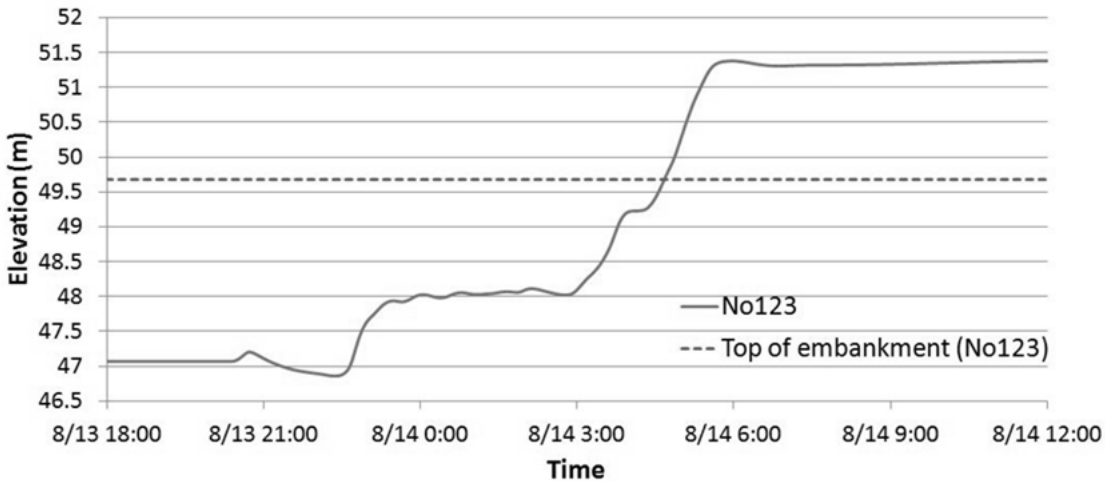

Figure 5.25 The variation of riverbed elevation in the unit channel of No.123

However, **Figure 5.10** showed that the situation didn't happen. In addition, because actual situation and the results of landslide simulation both indicated that no landslide occurred around the unit channel of No.123, the sediment source, which might cause the riverbed to rise, was only from the upstream channels. The upstream channels of unit channel of No.123 were No.93 and No.122 (see **Figure 5.9**). According to the survey, a lot of sediment from the unit channel No.93 was withheld at the Miyanomae Bridge (see **Figure 5.26**); however, the simulation model in this study didn't consider such a condition. Hence, the study assumed all sediment runoff from the unit channel No.93 would enter the unit channel of No.123. **Figure 5.27(a)** showed the process of sediment runoff in the unit channel No.93, 122, and 123. **Figure 5.27(b)** revealed the accumulated sediment deposition in the unit channel of No.123. From **Figure 5.27(a)**, the total discharge of the sediment runoff from the unit channel of No.93 was estimated as 8557m^3. That is, if the simulation considered the effect of sediment withheld by a dam or bridge, the simulation results might be close to the actual situation. **Figure 5.28** shows the prediction result of variation of riverbed elevation in the unit channels listed in **Table 5.5** (excluded No.123, see **Figure 5.25**).

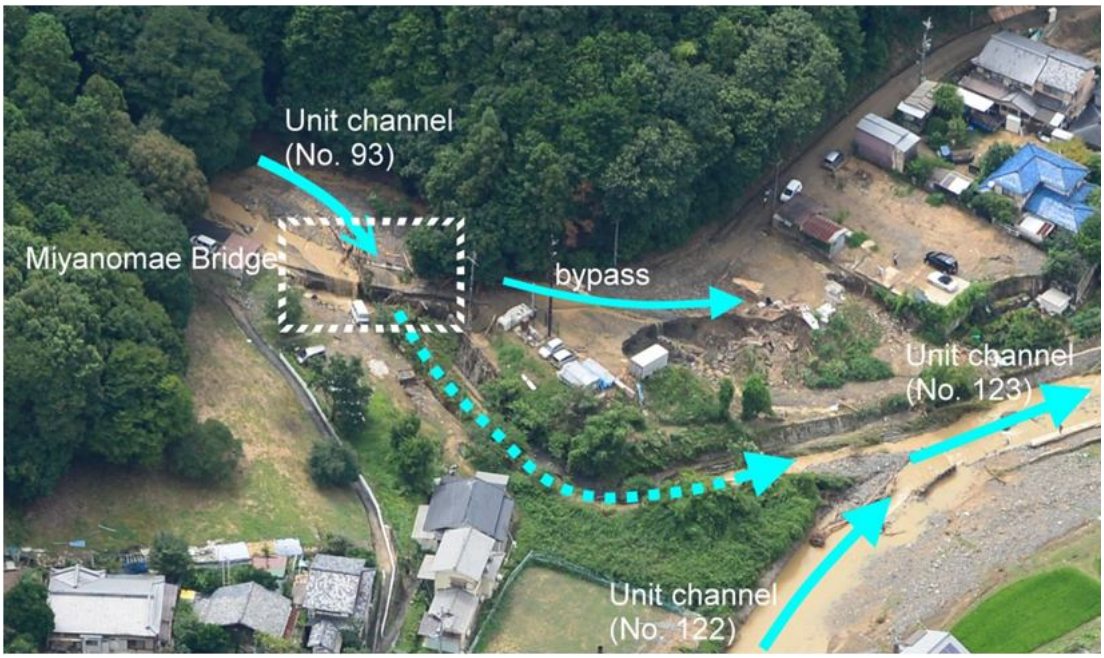

Figure 5.26 The sediment withheld at the Miyanomae Bridge had caused the flood bypassing and invading the residence area [modified from *Asia air survey co., LTD*, 2012]

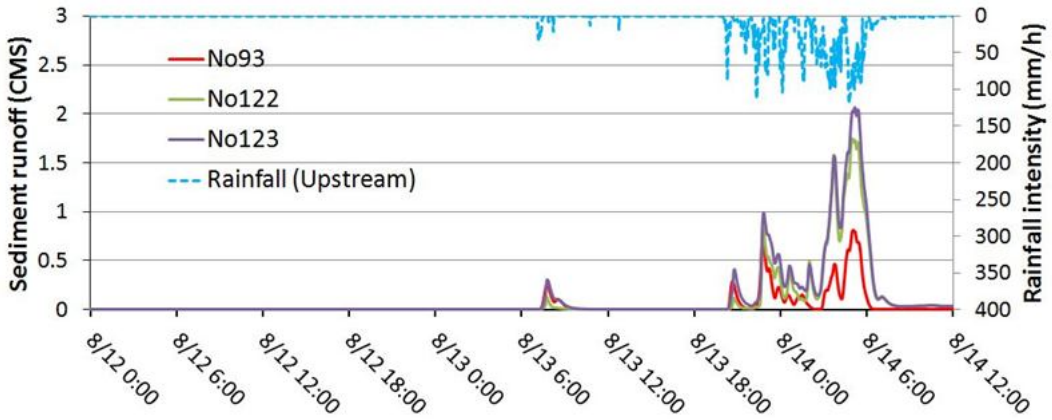

(a)

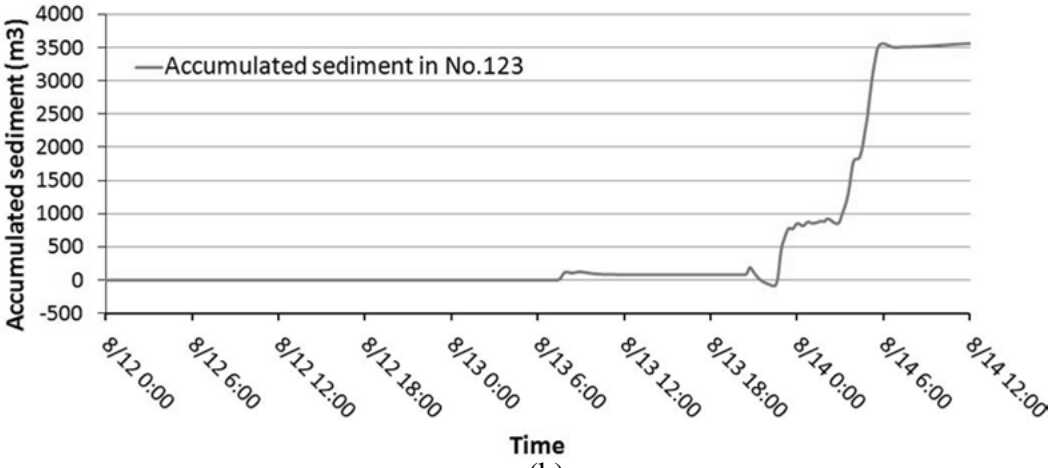

(b)

Figure 5.27 (a)The process of sediment runoff in the unit channel of No.93, 122, and 123 (b)The accumulated sediment deposition in the unit channel of No.123

While most flooding areas seemed to have sediment deposited in the river channel, leading to a higher riverbed, the simulation results and investigation results both indicated that the riverbed might degrade in some unit channel. **Figure 5.29** showed that the degradation of the riverbed had caused the embankment to collapse, resulting in the road interruption in the upstream of the unit channel of No.93 [*DPRI*, 2012]. **Figure 5.30** showed the simulation result of riverbed elevation variation in the unit channel of No.93. It was consistent with the investigation results.

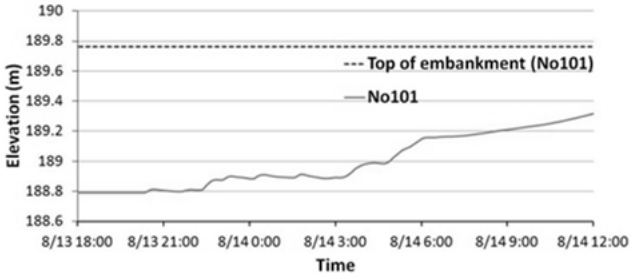

(a) No.101

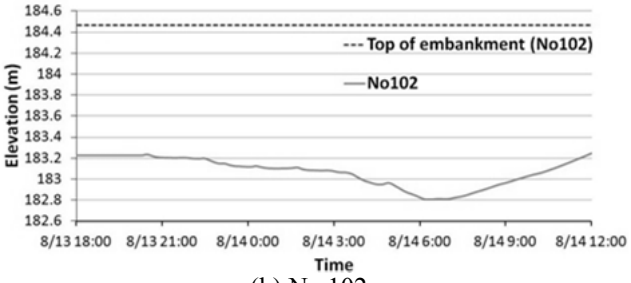

(b) No.102

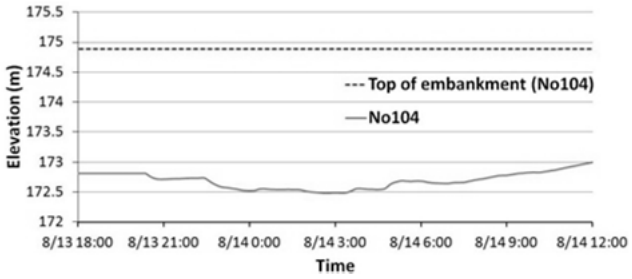

(c) No.104

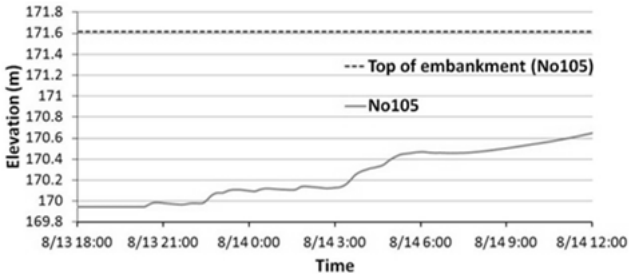

(d) No.105

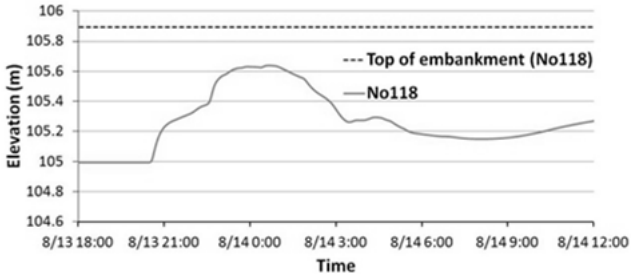

(e) No.118

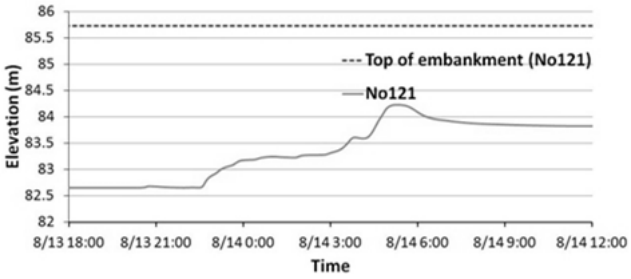

(f) No.121

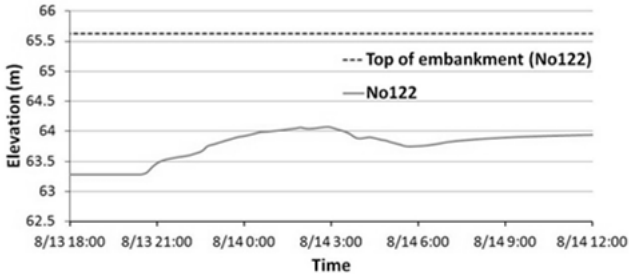

(g) No.122

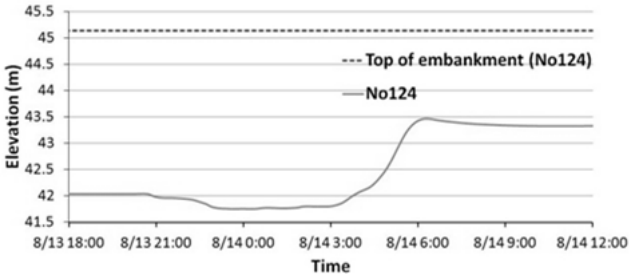

(h) No.124

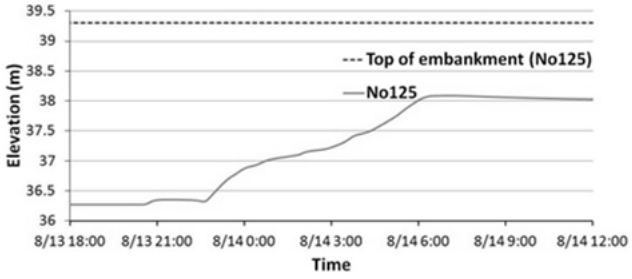

(i) No.125

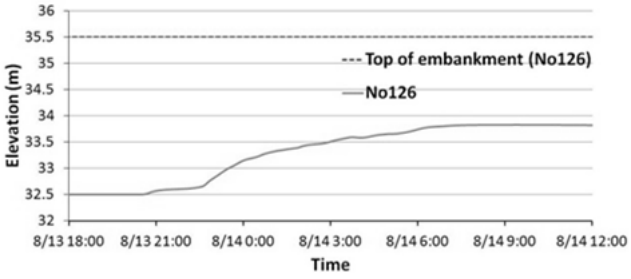

(j) No.126

Figure 5.28 The simulation of riverbed elevation in the unit channels which might overflow

Figure 5.29 The riverbed degradation had caused the embankment to collapse, resulting in the road interruption in the upstream of the unit channel of No. 93 [DPRI, 2012]

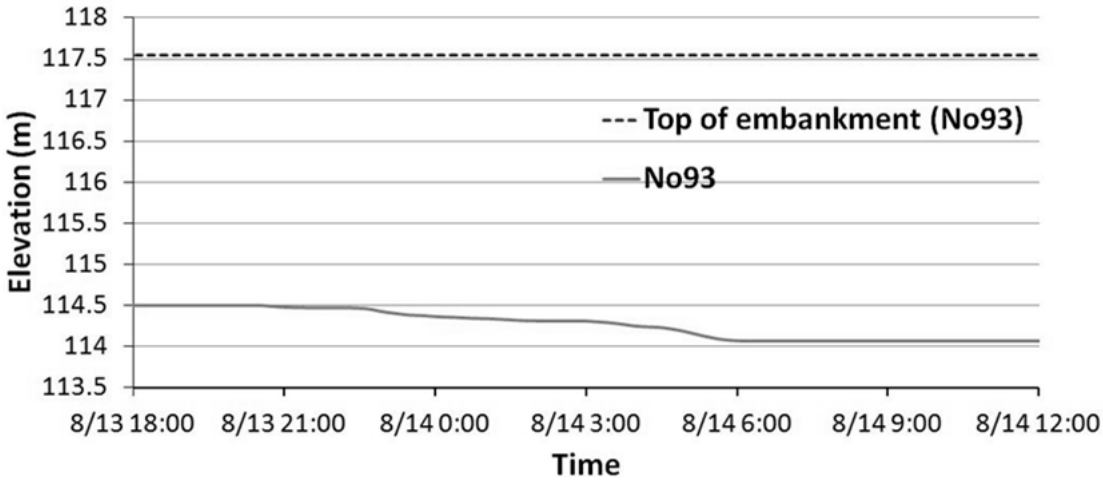

Figure 5.30 The simulation result of riverbed elevation variation in the unit channel of No.93

5.5 Simulation results under different rainfall patterns

To compare the difference of the landslide, water discharge, and sediment runoff in the basin under different rainfall patterns, as well as to verify the scenario simulation capacity of the simulation model of multi sediment hazards, this study used 4 rainfall patterns to conduct the simulation in the Shizugawa basin. To eliminate the effect of rainfall distribution diversity, this study assumed that the four rainfall patterns were uniformly distributed in the basin. **Figure 5.31** shows the four different rainfall patterns, and its time-step was 1 minute.

Case 1 is a rainfall pattern with normal intensity and duration, and the maximum rainfall intensity is 75 mm/h as well as accumulated rainfall is 167 mm. Case 2 is a rainfall pattern with high intensity and normal duration, and the maximum rainfall intensity is 150 mm/h as well as accumulated rainfall is 334 mm. Case 3 is a rainfall pattern with normal intensity and long duration, and the maximum rainfall intensity is 75 mm/h as well as accumulated rainfall is 334 mm. Case 4 is a rainfall pattern with high intensity and long duration, and the maximum rainfall intensity is 150 mm/h as well as accumulated rainfall is 668 mm.

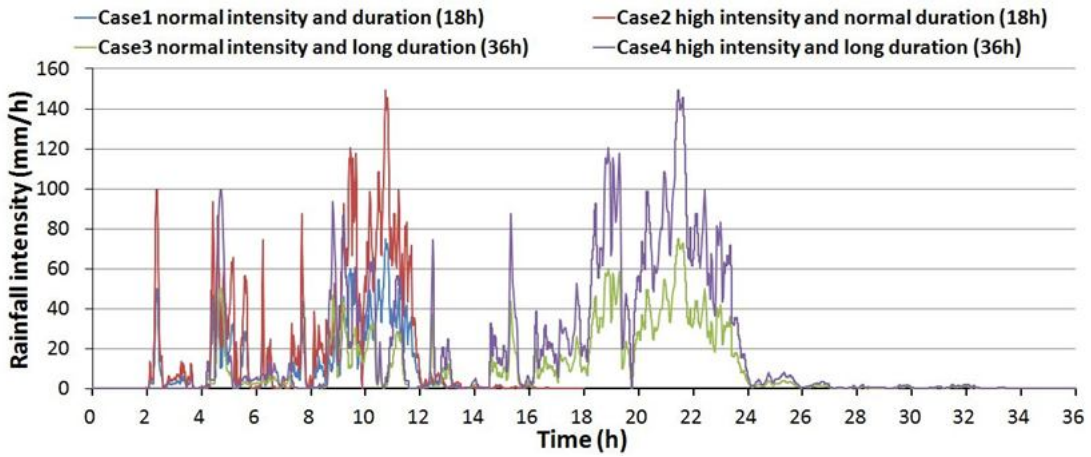

Figure 5.31 Four rainfall patterns for the simulation in the Shizugawa basin

5.5.1 Case 1: normal rainfall intensity and duration

In this case, the W_{cr} method predicted that no landslide would occur, but there were two channels overflows- No.118 and No.123 (see **Figure 5.32**). The maximum water discharge was 65.2 CMS in the downstream (see **Figure 5.33**). **Figure 5.34** showed the simulation of water level and riverbed of the two overflowed channels.

The results indicate that the sediment runoff, which led to riverbed raising and decreasing the drainage capacity, is the main cause of overflow. Therefore, the sediment arresting and storage seem to be one of the most important measures to decrease flood risk in these areas.

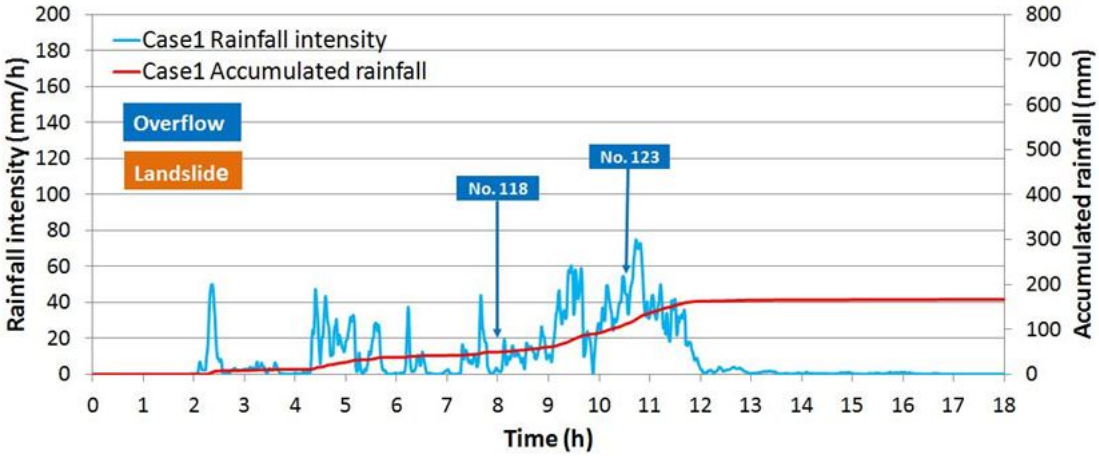

Figure 5.32 Rainfall and timeline of disaster events under normal rainfall intensity and duration

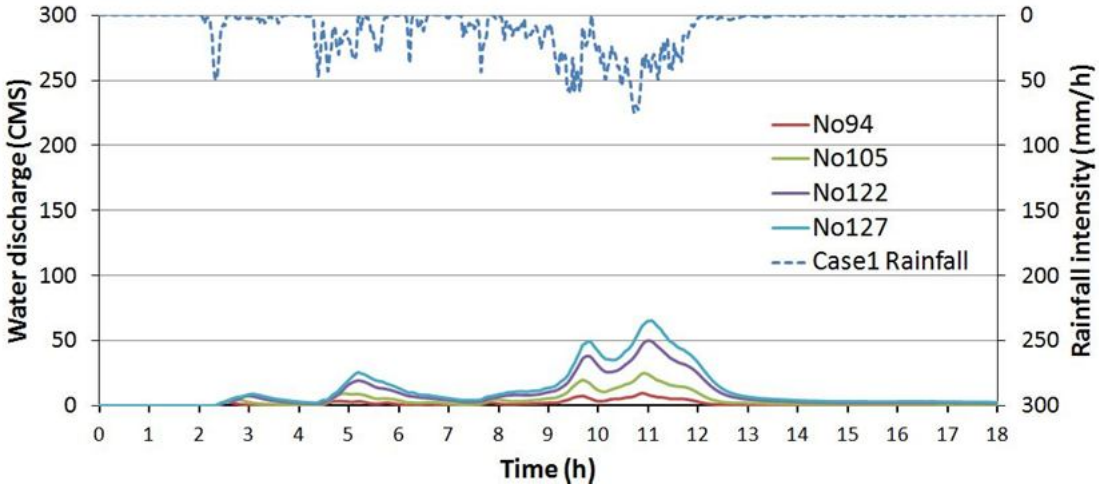

Figure 5.33 The simulation of the water discharge in the channels under normal rainfall intensity and duration

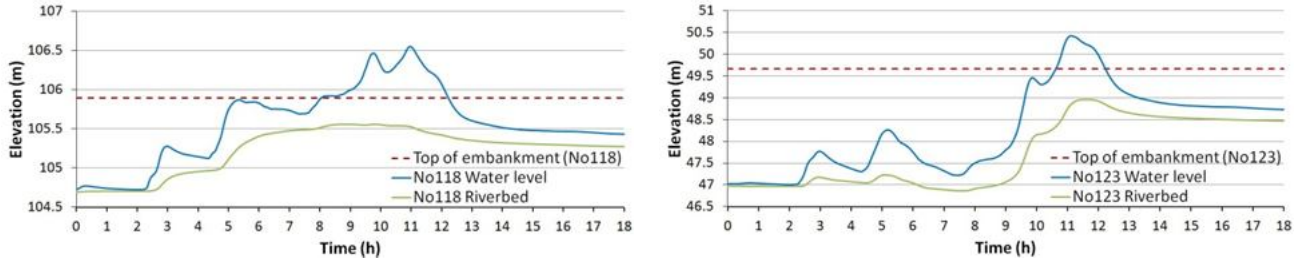

(a) No. 118 (b) No. 123

Figure 5.34 The simulation of the water level and riverbed elevation under the normal rainfall intensity and duration for the two overflowed channels

5.5.2 Case 2: high rainfall intensity and normal duration

In this case, the W_{cr} method predicted landslides to occur in 133 slope units which were distributed in 73 watersheds of the unit channels. The landslide locations were shown in the **Figure 5.35**. The volume of landside sediment and occurrence time in each unit channel were shown in the **Figure 5.36**, and the total volume was 184,376m^3. For the flood prediction, the simulation model of multi sediment hazards predicted overflows occurring at eleven channels (see **Table 5.6**). The maximum water discharge was 137.1 CMS in the downstream (see **Figure 5.37**). **Figure 5.38** showed the rainfall and timeline of disaster events under high rainfall intensity and normal duration.

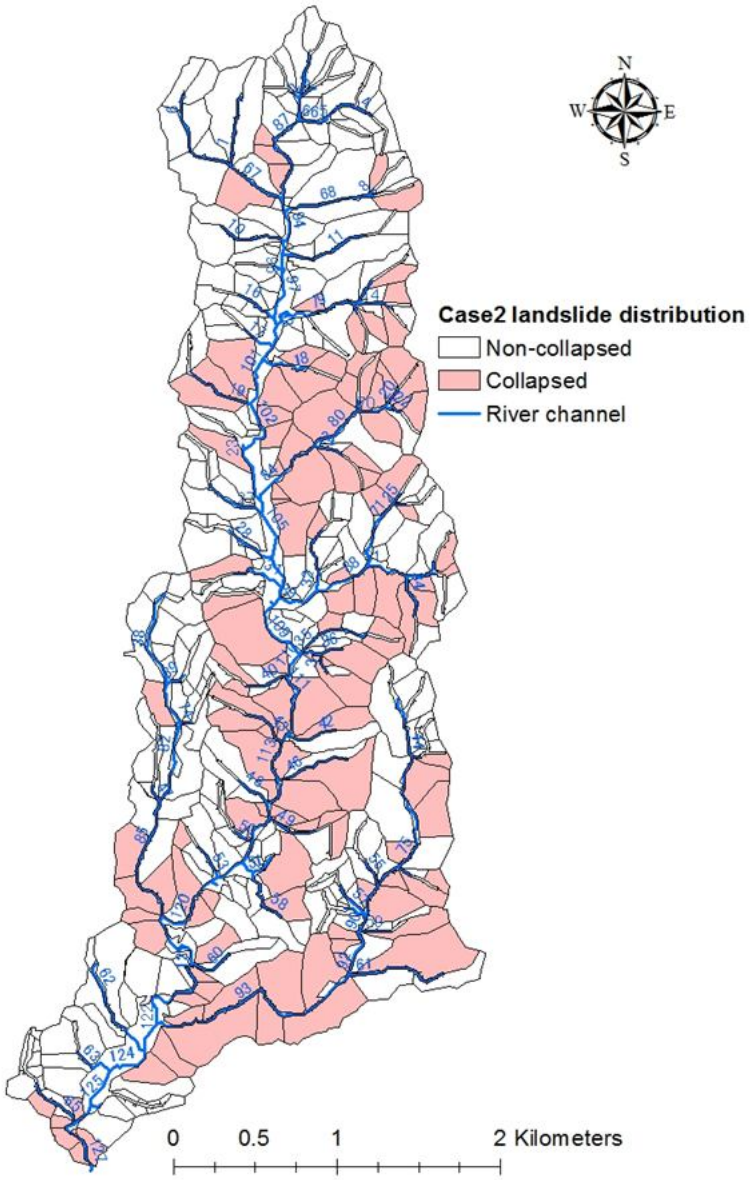

Figure 5.35 Landslide distribution under high rainfall intensity and normal duration

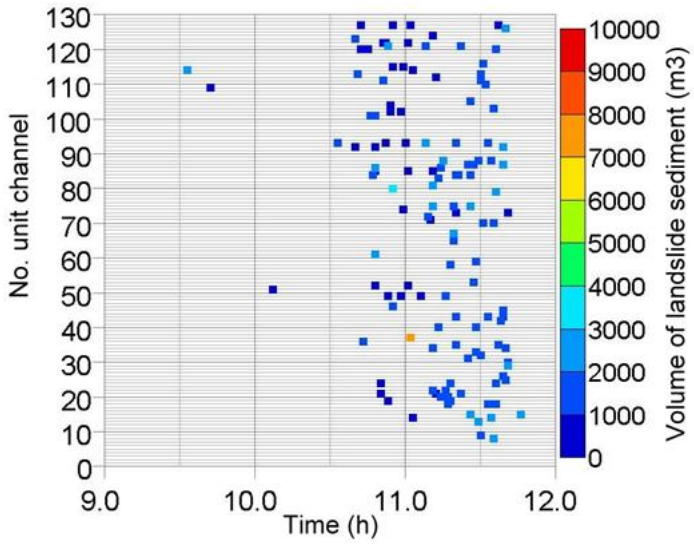

Figure 5.36 The volume of landslide sediment and occurrence time in each unit channel watershed under high rainfall intensity and normal duration

Table 5.6 List of unit channels at which the overflow was predicted to occur under high rainfall intensity and normal duration

	Unit channel	Length of unit channel (m)	Slope of riverbed (%)	Revetment height (m)	Duration of overflow
1	No.118	183.	1.01	1.2	■ the 4.7th~ 7.2th hour ■ the 7.6th~ 12.2th hour
2	No.123	192.2	1.32	2.7	■ the 9.3th~ continued
3	No.105	321.4	1.15	1.7	■ the 9.4th~ 10.0th hour ■ the 10.2th~ 12.0th hour
4	No.101	314.4	1.29	1.0	■ the 9.5th ~ 9.9th hour ■ the 10.2th ~ 12.1th hour
5	No.122	680.3	4.32	2.7	■ the 9.5th~ 9.9th hour ■ the 10.5th~ 11.4th hour
6	No.125	250.3	1.82	3.0	■ the 9.5th~ 10.0th hour ■ the 10.3th~ 12.3th hour
7	No.126	164.6	1.83	3.0	■ the 9.6th~ 9.9th hour ■ the 10.5th~ 11.8th hour
8	N. 102	396.5	1.75	1.2	■ the 9.6th ~ 9.7th hour ■ the 10.8th ~ 11.0th hour
9	No.121	432.9	2.36	3.0	■ the 9.6th~ 10.0th hour ■ the 10.4th~ 12.0th hour
10	No.124	295.1	2.41	3.0	■ the 10.8th~ 12.2th hour
11	No.106	205.3	1.37	2.0	■ the 10.87th~ 10.92th hour.

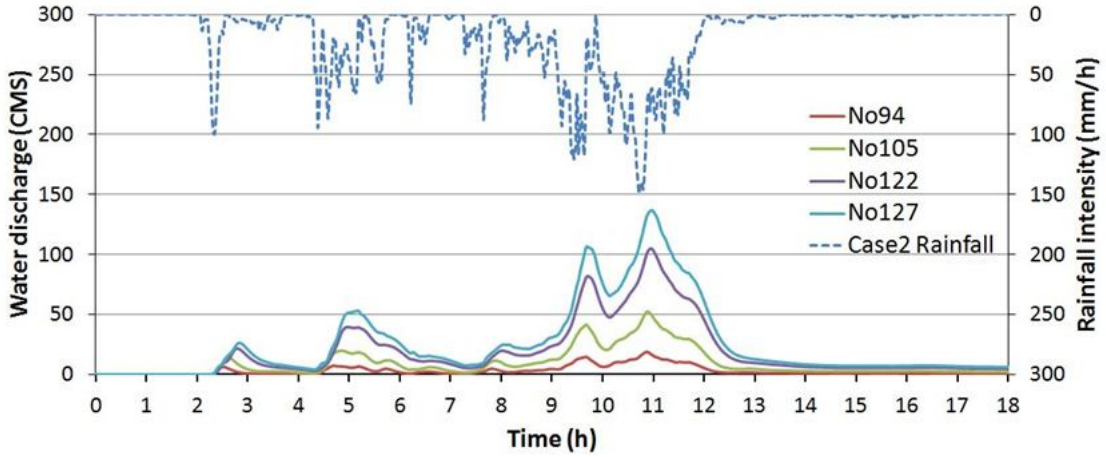

Figure 5.37 The simulation of the water discharge in the channels under high rainfall intensity and normal duration

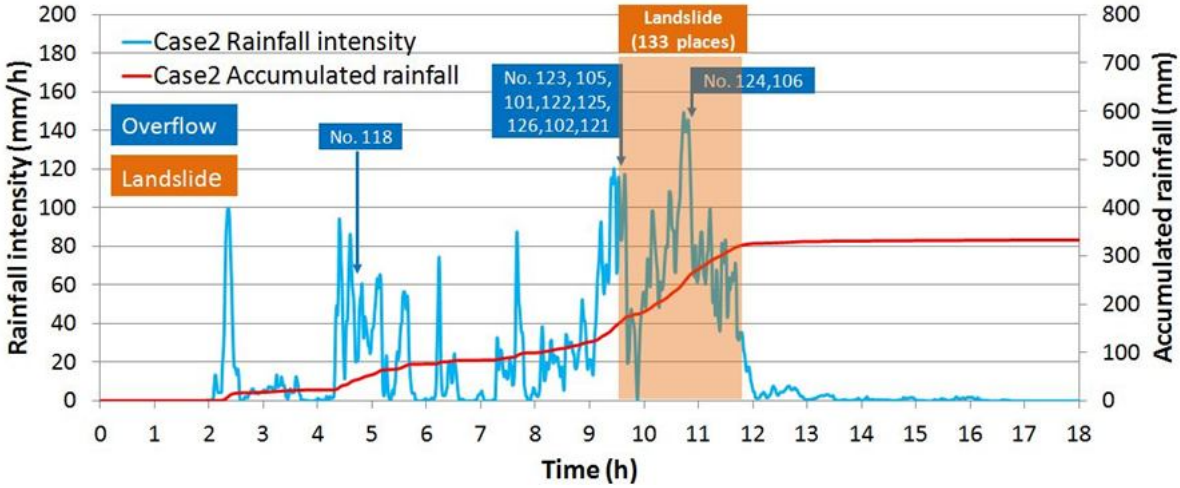

Figure 5.38 Rainfall and timeline of disaster events under high rainfall intensity and normal duration

5.5.3 Case 3: normal rainfall intensity and long duration

In this case, the W_{cr} method predicted landslides to occur in 66 slope units which were distributed in 42 watersheds of the unit channels. The landslide locations were shown in the **Figure 5.39**. The volume of landside sediment and occurring time in each unit channel were shown in the **Figure 5.40**, and total volume was 87,546m^3. For the flood prediction, the simulation model of multi sediment hazards predicted 5 channels occurring overflow (see **Table 5.7**). The maximum water discharge was 81.2 CMS in the downstream (see **Figure 5.41**). **Figure 5.42** showed the rainfall and timeline of disaster events under normal rainfall intensity and long duration.

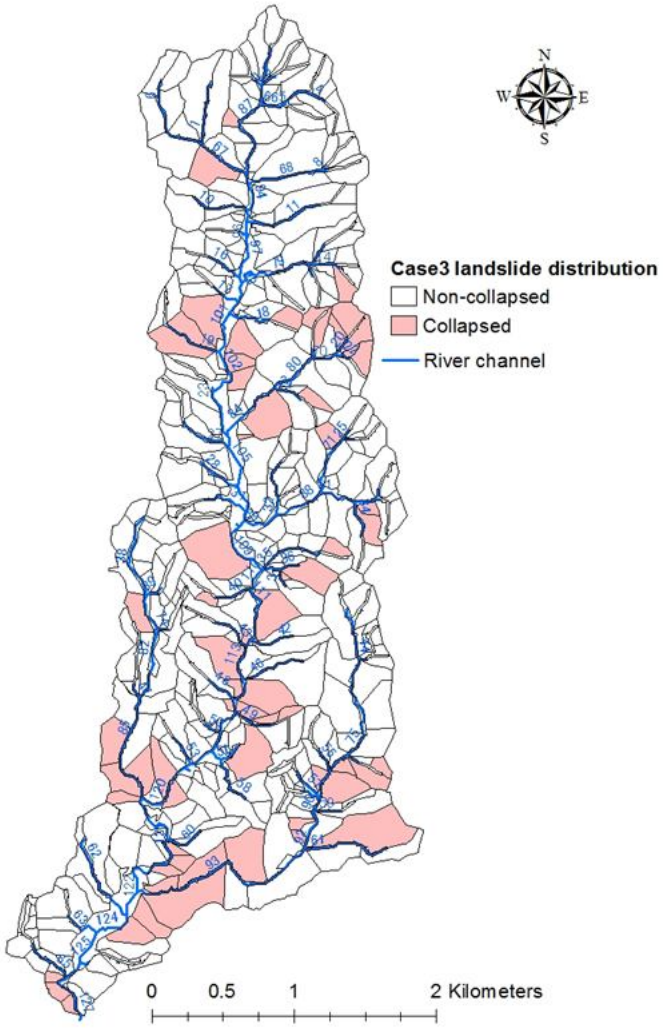

Figure 5.39 Landslide distribution under normal rainfall intensity and long duration

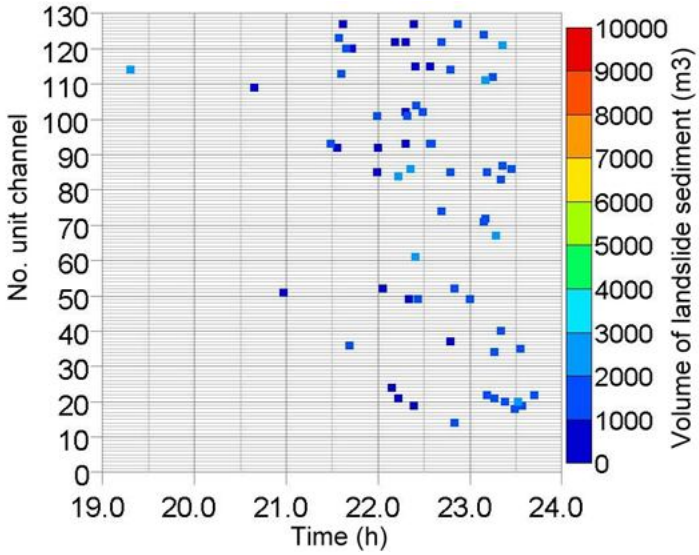

Figure 5.40 The volume of landslide sediment and occurrence time in each unit channel watershed under the normal rainfall intensity and long duration

Table 5.7 List of unit channels at which the overflows were predicted under normal rainfall intensity and long duration

	Unit channel	Length of unit channel (m)	Slope of riverbed (%)	Revetment height (m)	Duration of overflow
1	No.118	183.	1.01	1.2	■ the 9.3th~ 12.1th hour ■ the 13.1th~ 13.2th hour ■ the 15.6th~ 15.8th hour ■ the 18.9th~ 19.7th hour ■ the 20.4th~ 22.7th hour
2	No.123	192.2	1.32	2.7	■ the 19.1th~ 19.8th hour ■ the 20.5th~ continued
3	No.125	250.3	1.82	3.0	■ the 21.6th~ 22.1th hour
4	No.105	321.4	1.15	1.7	■ the 21.6th~ 21.8th hour
5	No.126	164.6	1.83	3.0	■ the 21.7th~ 21.9th hour

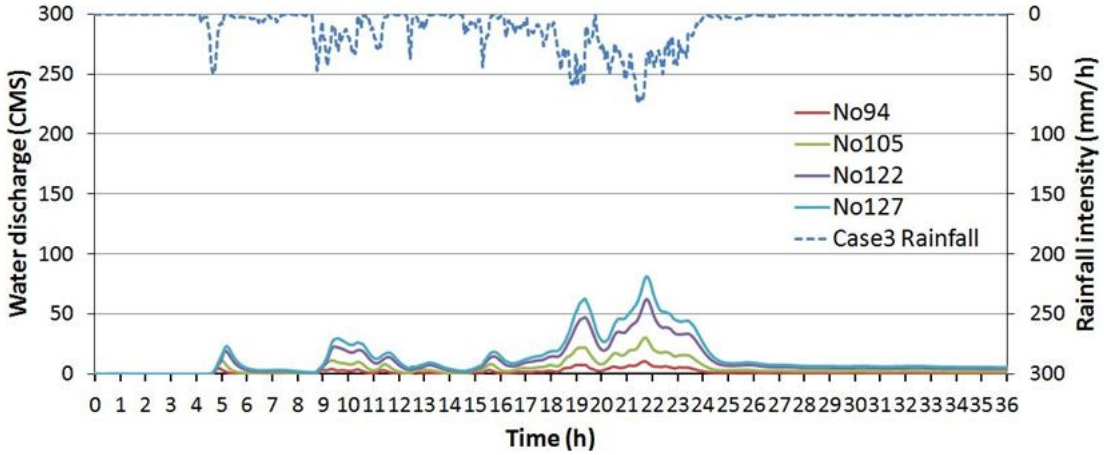

Figure 5.41 The simulation of the water discharge in the channels under normal rainfall intensity and long duration

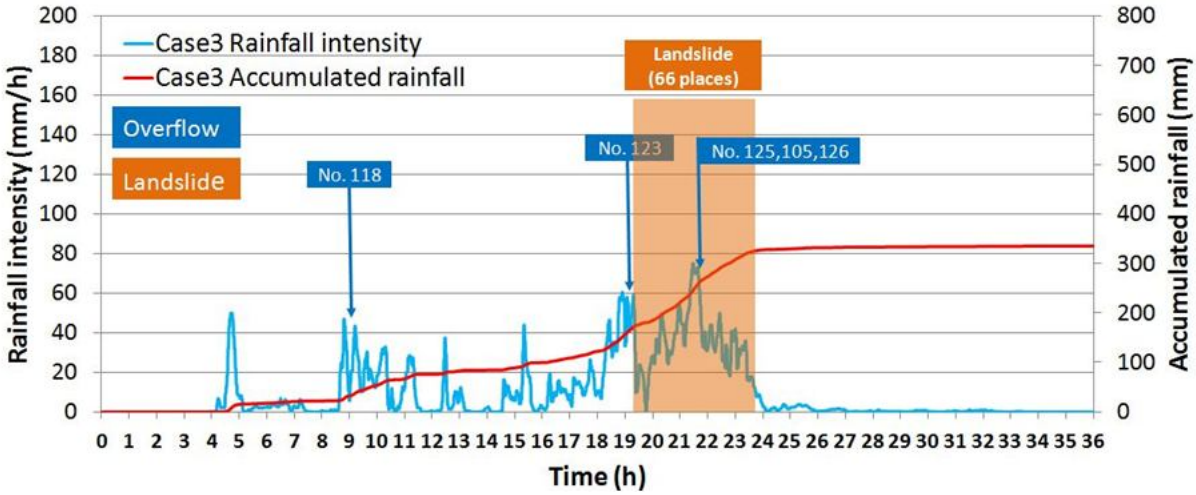

Figure 5.42 Rainfall and timeline of disaster events under normal rainfall intensity and long duration

5.5.4 Case 4: high rainfall intensity and long duration

In this case, the W_{cr} method predicted landslides to occur in 265 slope units which were distributed in 104 watersheds of the unit channels. The landslide locations were shown in the **Figure 5.43**. The volume of landside sediment and occurrence time in each unit channel were shown in the **Figure 5.44**, and total volume was 516,896m^3. For the flood prediction, the simulation model of multi sediment hazards predicted overflows at 23 channels (see **Table 5.8**). The maximum water discharge was 420.1 CMS in the downstream (see **Figure 5.45**). **Figure 5.46** showed the rainfall and timeline of disaster events under normal rainfall intensity and long duration.

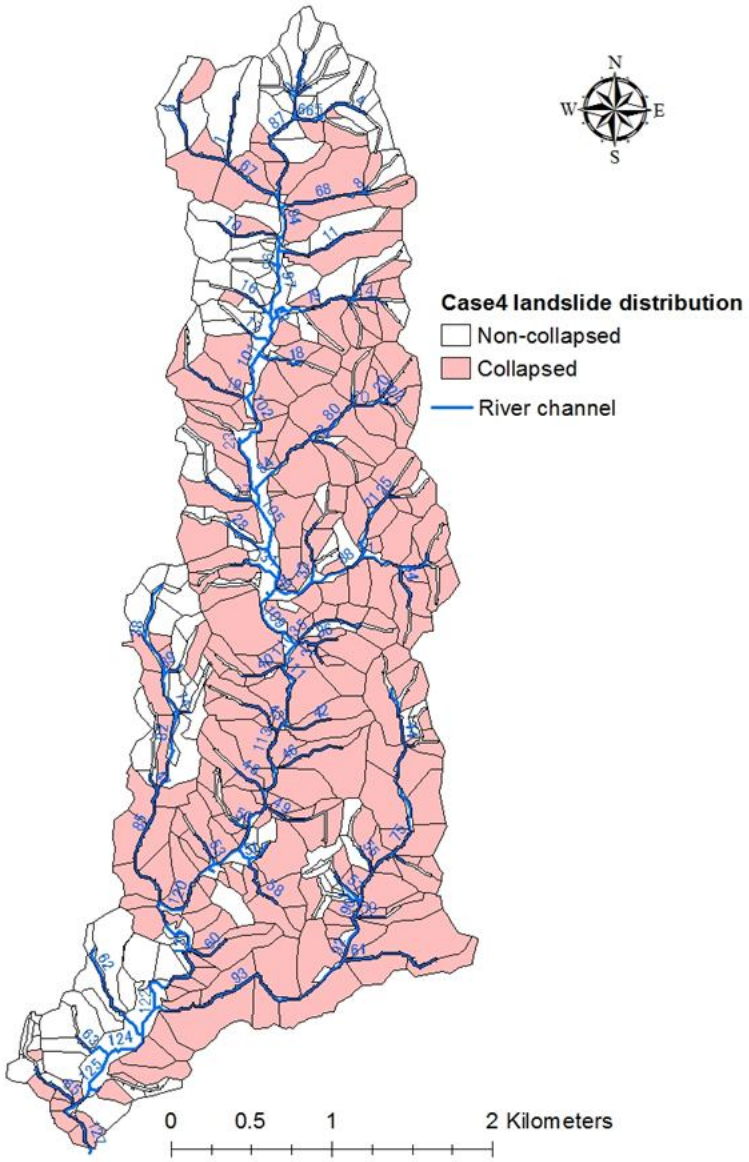

Figure 5.43 Landslide distribution under high rainfall intensity and long duration

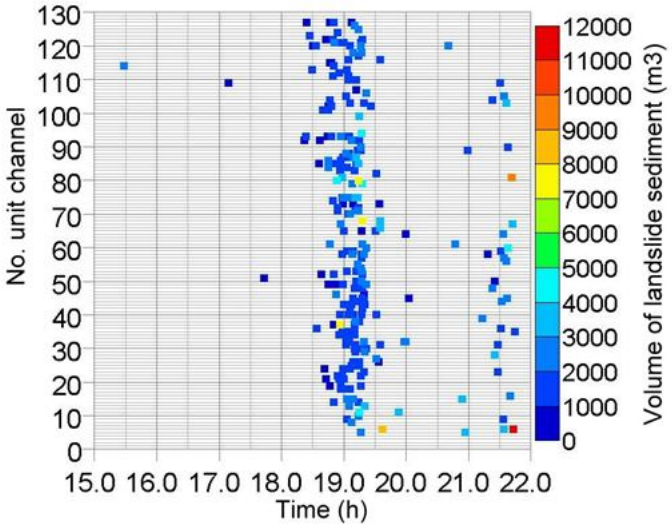

Figure 5.44 The volume of landslide sediment and occurrence time in each unit channel watershed under high rainfall intensity and long duration

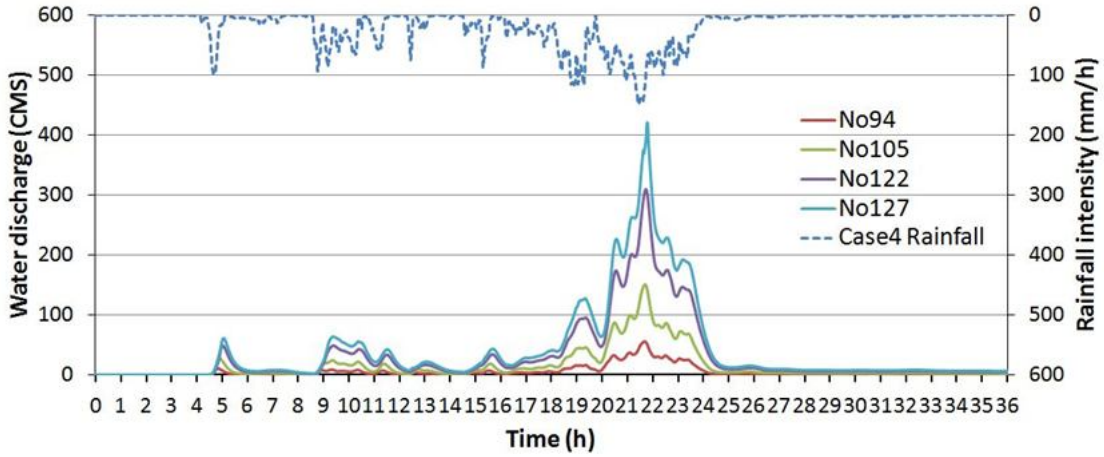

Figure 5.45 The simulation of the water discharge in the channels under high rainfall intensity and long duration

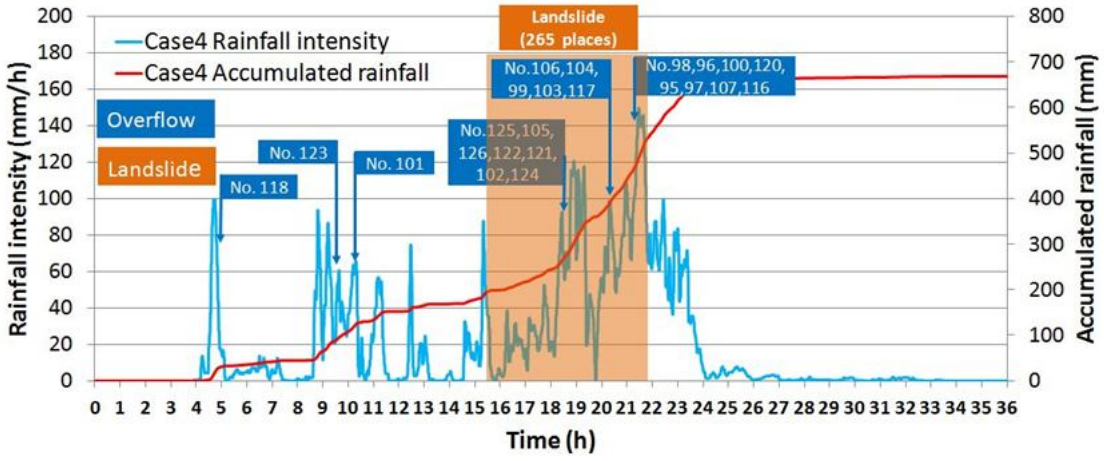

Figure 5.46 Rainfall and timeline of disaster events under high rainfall intensity and long duration

Table 5.8 List of unit channels at which the overflows were predicted under high rainfall intensity and long duration

	Unit channel	Length of unit channel (m)	Slope of riverbed (%)	Revetment height (m)	Duration of overflow
1	No.118	183.	1.01	1.2	■ the 4.9th~ 5.4th hour ■ the 8.9th~ 11.9th hour ■ the 18.7th~ 19.9th hour ■ the 20.0th~ continued
2	No.123	192.2	1.32	2.7	■ the 9.4th~12.0th hour ■ the 13.0th~13.2th hour ■ the 15.4th~16.1th hour ■ the 16.7th~ continued
3	No.101	314.4	1.29	1.0	■ the 10.3th~10.4th hour ■ the 18.6th~19.8th hour ■ the 20.0th~ continued
4	No.125	250.3	1.82	3.0	■ the 18.5th~ 21.7th hour
5	No.105	321.4	1.15	1.7	■ the 18.55th~ 19.9th hour ■ the 20.0th~ 24.5th hour ■ the 25.6th~25.9th hour ■ the 28.6th~ continued
6	No.126	164.6	1.83	3.0	■ the 18.6th~19.8th hour ■ the 20.1th~ 21.8th hour
7	No.122	680.3	4.32	2.7	■ the 18.7th~ 19.6th hour ■ the 20.2th~ 23.5th hour
8	No.121	432.9	2.36	3.0	■ the 18.9th~19.7th hour ■ the 20.1th~ 24.0th hour
9	No.102	396.5	1.75	1.2	■ the 19.0th~19.1th hour ■ the 20.2th~23.8th hour ■ the 31.9th~continued
10	No.124	295.1	2.41	3.0	■ the19.1th~ 19.7th hour ■ the 20.1th~ 21.8th hour ■ the 23.4th~ 23.5th hour
11	No.106	205.3	1.37	2.0	■ the 20.3~23.6th hour
12	No.104	96.2	2.33	2.0	■ the 20.3~ 23.8th hour ■ the 34.7~ continued
13	No.99	148.1	2.06	1.0	■ the 20.3th~ continued
14	No.103	334.2	1.73	2.0	■ the 20.4th~ 20.6th hour ■ the 21.0th~ 23.6th hour
15	No.117	149.3	3.37	1.2	■ the 20.5th~ 20.7th hour ■ the 20.9th~ 24.1th hour ■ the 30.9th~ continued
16	No.98	47.4	0.59	2.0	■ the 20.9th~ 24.2th hour ■ the 33.5th~ continued
17	No.96	129.8	2.63	2.0	■ the 21.0th~ 23.9th hour
18	No.100	96.0	3.28	1.0	■ the 21.0th~ 24.1th hour ■ the 34.8th~ continued
19	No.120	463.8	2.68	3.0	■ the 21.1th~ 22.8th hour ■ the 23.1th~ 23.5th hour
20	No.95	81.0	2.65	2.0	■ the 21.3th~ 23.6th hour
21	No.97	294.2	2.48	2.0	■ the 21.5th~ 24.2th hour
22	No.107	66.2	0.02	2.0	■ the 21.5th~ 21.9th hour
23	No.116	198.2	1.99	5.0	■ the 21.5th~ 22.0th hour

5.6 Discussions

Compared with the results of landslide simulation in Chapter 4, the simulation results, which used different soil strength parameters in the north part of the study area, are better on decreasing the false alert rate (FAR) and raising the accuracy of landslide prediction (ALP). However, more disaster cases or field investigations and samplings are bound to improve the prediction accuracy. In addition, using the rainfall data of the X-band radar instead of the rainfall data of rain gauges is advantageous to solve the problem of non-uniform rainfall distribution in a wide area. **Figure 5.47** shows the significant difference of rainfall distribution in the heavy rainfall event on August 13-14, 2102.

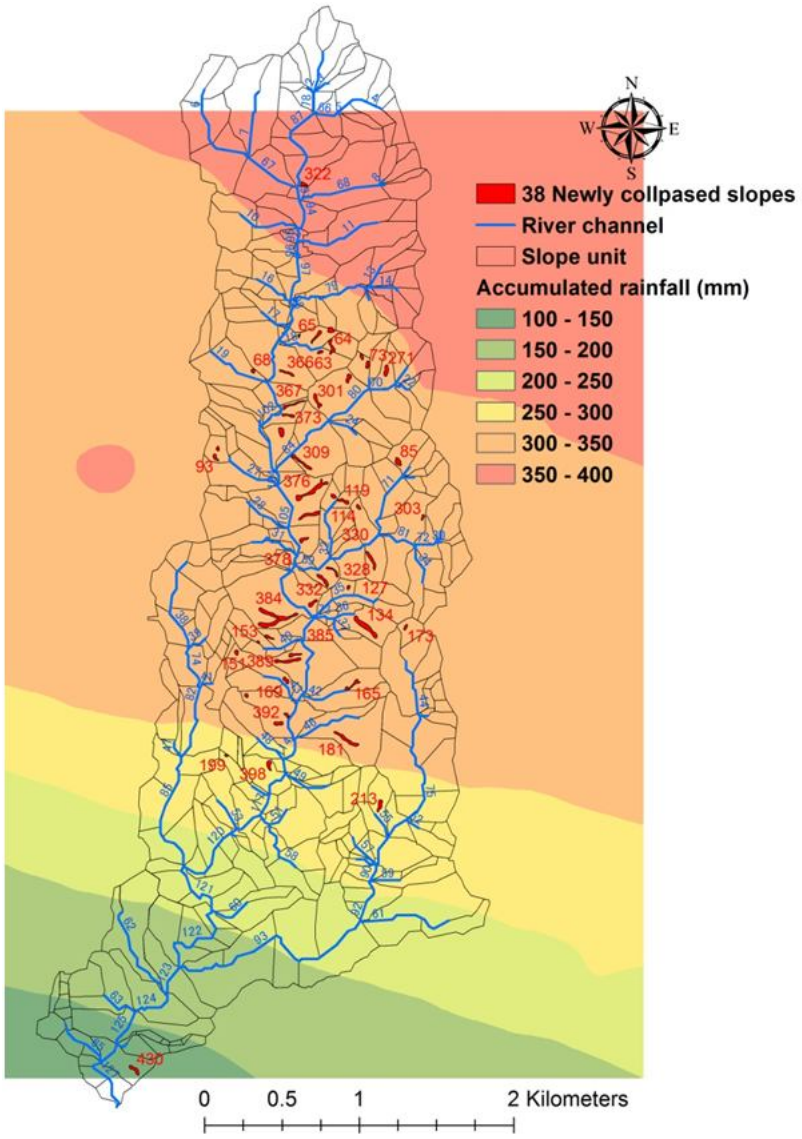

Figure 5.47 The difference of rainfall distribution in the heavy rainfall event on August 14, 2102.

For overflow, sediment runoff, and riverbed deformation simulation, most of the simulation results in the study case were consistent with the investigation results. In addition, based on some simplified assumptions, the study employed overland flow model and sediment runoff model in channels to simulate the process of landslide sediment moving into the channel during rainfall. However, the characteristic of the moving of landslide sediment on the slope is bound to be different from the sediment movement in the channel. Thus, although the simulation results seem to be reasonable, it should still need to further study. Moreover, the moving way of landslide sediment might be not only as overland flow but also as debris flow. Besides, it also might be that whole landslide sediment fell into the channel directly. This part should be explored further.

Limited to the one-dimension analysis of water discharge and riverbed deformation, this study assumed that the landslide sediment supply was uniform distribution on the riverbed and all sediment runoff would enter to the next channel. Therefore, the simulation results cannot properly explain the blocking effects of sediment in the channels and the abnormal simulation result of riverbed elevation in the unit channel of No.123. Besides, due to the change of the cross-section of drainage after overflow in the channel, the water level and water discharge should be lower [*Tanaka et al.*, 2014]. That is, some simulation results might overestimate the discharge. To solve abovementioned problem, using a two-dimension analysis seems to be necessary. However, partly because two-dimension analysis is time consuming on calculation, and partly because this study focuses on developing an early warning and evacuation system, adopting the one-dimension analysis for flood and riverbed deformation simulation should be appropriate at current stage in this study.

Due to the high-performance calculation of the regression formulas, the W_{cr} method can simulate the change of the water content for hundreds of slope units on a basin scale, and predict not only the landslides but also the runoff on the slope units. According to the abovementioned verification of simulation results, it was feasible to use the W_{cr} method to replace the IRIS model for landslide prediction. In addition, many studies employed kinematic wave method to simulate the rainfall-runoff because it could easily obtain the acceptable results by adjusting the parameters (e.g., the thickness, hydraulic characteristics, number of soil layers). However, the kinematic wave method lacked the explicit physical meanings. In the contrast, the W_{cr}

method estimated runoff from soil-water characteristic curve, and it can simulate the process of drainage from soil. It has the potential of replacing the kinematic wave method in the future.

Regarding the simulation of the river discharge and sediment runoff, some researchers proposed several approaches (see **Figure 5.1**) to establish the basin model. This study based on the *Egashira and Matsuki* [2000] method, which adopted the composite of unit channels and unit slopes to establish the basin model, and then proposed to divide a unit slope into several slope units according to the slope aspect and the rationality of the centroid (see **Figure 5.12(b)** and **(c)**) and obtained good results. It could be used as a reference for subsequent improvement direction of establishing a basin model.

To compare the difference of the landslides, water discharge, sediment runoff, and the change of the riverbed elevation under the different rainfall patterns, as well as to verify the scenario simulation capacity of the simulation model of multi sediment hazards, four diverse rainfall patterns were used to conduct the simulation. The results indicated that the location, occurrence time, and scale of disasters were obviously affected by the rainfall patterns, so the disaster prevention strategies and plans should consider the diversity of rainfall types to adopt appropriate emergency response and evacuation decision.

In addition, according to the order of occurring time, the top 15 of landslides under three different rainfall patterns were listed as **Table 5.9**. The results seemed to indicate that the order of landslide occurring was almost identical even if rainfall types were totally different. That is, the high-risk areas of landslide could be determined by using this method, and the feasibility of related disaster prevention plans could be reviewed and verified. Similarly, according to the **Table 5.6** to **5.8**, the high-risk channel of overflow also could be detected.

This study proposed a new simulation model of multi sediment hazards, which incorporated the topographical, geological and hydrological conditions as well as integrated several numerical models, to simulate the landslides, floods, and riverbed deformation on a basin scale. Combining the simulation results with the elevation of roads and the cross-sectional area of the bridges, the final results could be used to assess the critical points of the traffic and the potential flood hazard area. That is, if the spatial information of the public infrastructure (e.g., roads, bridges, lifelines, and

shelters) were added into the model, the model could be further developed into th multi sediment hazards warning system on a basin scale. It not only can provide the detailed warning information for local government and inhabitants to make decisions during the emergency, but also can be used as the platform to verify the disaster prevention plan during disaster preparation.

Table 5.9 The top 15 of landslides under three different rainfall patterns

	Case2 high intensity and normal duration				Case3 normal intensity and long duration				Case4 high intensity and long duration			
	Time (min)	Rainfall intensity (mm/h)	Accumu -lated rainfall (mm)	No. slope unit	Time (min)	Rainfall intensity (mm/h)	Accumu -lated rainfall (mm)	No. slope unit	Time (min)	Rainfall intensity (mm/h)	Accumu -lated rainfall (mm)	No. slope unit
1	573	110.5	161.8	394	1158	58.75	171.6	394	928	40.5	194.8	394
2	582	19.5	174.6	384	1239	28.75	207.1	384	1029	33.5	220.5	384
3	607	59.5	191.9	201	1258	54.25	220.0	201	1063	52.5	235.9	201
4	633	88.5	226.2	346	1289	72.25	246.8	346	1102	76.5	259.3	340
5	640	106.5	236.4	340	1293	70.25	251.5	340	1103	89.5	260.8	346
6	640	106.5	236.4	424	1294	70.25	252.6	424	1104	89.5	262.3	434
7	641	124.5	238.4	392	1296	71.25	255.0	392	1107	71.5	266.5	424
8	642	133.5	240.7	406	1297	72.75	256.2	434	1109	62.5	268.8	392
9	642	133.5	240.7	434	1299	68.25	258.6	406	1110	62.5	269.8	409
10	643	143.5	243.1	134	1301	61.25	260.7	134	1113	60.5	272.7	406
11	645	144.5	248.0	409	1303	53.75	262.6	409	1114	60.5	273.7	134
12	646	139.5	250.3	365	1319	32.25	272.3	314	1116	70.5	276.0	314
13	647	140.5	252.6	309	1319	32.25	272.3	365	1117	70.5	277.2	339
14	648	142.5	255.0	203	1320	32.25	272.8	339	1118	70.5	278.4	203
15	648	142.5	255.0	236	1323	40.75	274.7	203	1120	69.5	280.7	365

5.7 Summary

While the rainfall-induced hazards in mountain areas usually occur as multi-modal types, most of the existing warning system and disaster prevention plans consider only single hazard. Recently, several large-scale natural disasters implied that current strategies could not cope with such a situation of the climate change and the increasing human activities. In fact, estimating and predicting multi-hazards cannot just overlay several single hazards, but also has to consider the occurrence time and causal relationship. For example, the evacuation action in mountainous areas was often limited due to the road and bridge condition. That is, the evacuation of local residents was easily affected by the damaged roads or bridges. If the evacuation plan (including the evacuation time, route, shelter, transportation, etc.) considered only single hazard effect, it might lead to the improper evacuation decision, resulting in the failure of the disaster prevention plan.

This study suggested a basin model by combining slope units and unit channels, and integrated the rainfall-infiltration, landslide prediction, sediment runoff, riverbed deformation, and water discharge models to establish the simulation platform for multi sediment hazards. The results and recommendations are summarized as follows.

(1) The simulation model of multi sediment hazards can provide the warning information, such as the landslide prediction with slope unit as targets, the overflow prediction with unit channels as targets, the sediment runoff prediction, and the riverbed deformation prediction with unit channels as targets. The model performed good prediction based on the verification with the investigation results of the disaster event.

(2) This study proposed some simplified assumptions to conduct the simulation. For example, the study employed overland flow model and sediment runoff model in channels to simulate the process of landslide sediment moving into the channel during rainfall. However, the characteristic of the moving of landslide sediment on the slope is bound to be different from the sediment movement in the channel. Thus, although the simulation results seem to be reasonable, it should still need to further study. Moreover, the moving way of landslide sediment might be not only as overland flow but also as debris flow. Besides, it also might be that whole landslide sediment fell into the channel directly. This part should be explored further.

(3) Owing to the consideration of the calculation time and the feasibility of establishing the early-warning system, this study adopted the one-dimension model to conduct the simulation of overflow and riverbed deformation. In addition, this study assumed that sediment supply from landslides was distributed uniformly over the riverbed, and supposed that all sediment runoff would enter the next channel. Therefore, the simulation model in this study cannot simulate the blocking effect of sediment or sabo dam. It also cannot simulate the change of water level and water discharge after the occurrence of overflows which change the cross-section of drainage. For further study, the two-dimension analysis might be another direction for improvement.

(4) To verify the scenario simulation capacity of the simulation model of multi sediment hazards, this study adopted four different typical rainfall patterns to conduct simulations. The results indicated the occurrence time, location, and scale of disaster were significantly affected by the rainfall patterns. Therefore, the disaster prevention strategies and plans should consider the rainfall types to adopt appropriate emergency response and evacuation decision.

(5) Because of the high-performance calculation of the regression formulas, the W_{cr} method can simulate the change of the water content for hundreds of slope units on a basin scale, and the model can simulate not only the landslides but also the runoff on the slope units. According to the abovementioned verification of simulation results, it was feasible to use the W_{cr} method instead of the IRIS model and kinematic wave method for landslide prediction and runoff estimate on the slope unit.

(6) In the future, other types of disaster (debris flow, landslide dam, etc.) could be incorporated into the platform and the multi sediment hazards warning system can be developed. The warning system not only can provide the detailed warning information for local government and inhabitants to make decisions during emergencies, but also be used as the platform to verify the disaster prevention plan during disaster preparation.

References

Ashida, K., and Michiue, M. (1978): Study on hydraulic resistance and bed-load transport rate in alluvial streams, Proceedings of the Japan Society of Civil Engineers, Vol. 1972, No. 206, pp. 59-69 (in Japanese)

Caine, N. (1980): The rainfall intensity: duration control of shallow landslides and debris flows, Geografiska Annaler. Series A. Physical Geography, 62A, pp. 23-27.

Carrara, A., Cardinali, M., Detti, R., Guzzetti, F., Pasqui, V., and Reichenbach, P. (1991): GIS techniques and statistical models in evaluating landslide hazard, Earth Surface Processes and Landforms, Vol. 16, No. 5, pp. 427-445.

Casadei, M., Dietrich, W. E., and Miller, N. L. (2003): Testing a model for predicting the timing and location of shallow landslide initiation in soil-mantled landscapes, Earth Surface Processes and Landforms, Vol. 28, No. 9, pp. 925-950.

Chang, K.T., and Chiang, S.H. (2009): An integrated model for predicting rainfall-induced landslides, Geomorphology, Vol. 105, No. 3–4, pp. 366-373.

Chen, C.Y., and Fujita, M. (2013a): An analysis of rainfall-based warning systems for sediment disasters in Japan and Taiwan, International Journal of Erosion Control Engineering, Vol. 6, No. 2, pp. 47-57.

Chen, C.Y., and Fujita, M. (2013b): Evacuation Decision-Making Factors for Local Governments and Inhabitants in Debris-Flow Potential Areas in Taiwan, International Journal of Erosion Control Engineering, Vol. 6, No. 2, pp. 37-46.

Chen, C.Y., and Fujita, M. (2014): A method for predicting landslides on a basin scale using water content indicator, Journal of Japan Society of Civil Engineers, Ser. B1 (Hydraulic Engineering), Vol. 70, No.4, pp.I_13-I_18.

Chen, C. Y., Ikkanda, S., Fujita, M., and Tsutsumi, D. (2013): A study on mechanism of large-scale landslides and the prediction, 12th International Symposium on River Sedimentation, pp. 41.

Chigira, M., Tsou, C.Y., Matsushi, Y., Hiraishi, N., and Matsuzawa, M. (2013): Topographic precursors and geological structures of deep-seated catastrophic landslides caused by Typhoon Talas, Geomorphology, Vol. 201, pp. 479-493.

Crosta, G. B., Chen, H., and Frattini, P. (2006): Forecasting hazard scenarios and implications for the evaluation of countermeasure efficiency for large debris avalanches, Engineering Geology, Vol. 83, No. 1–3, pp. 236-253.

Disaster Prevention Res. Inst (DPRI)., Kyoto Univ. (2012): Investigation report for the heavy rainfall disaster on August 13-14, 2012 (in Japanese). (http://www.dpri.kyoto-u.ac.jp/web_j/saigai/disaster_report.html

Egahsira, S., and Matsuki, K. (2000): A method for predicting sediment runoff cased by erosion of stream channel bed, Annual Journal of Hydraulics Engineering, JSCE, Vol. 44, pp. 735-740 (in Japanese with English abstract).

Fujita, M., Ohshio, S., Tsutsumi, D. (2010): Effect of climate change on slope failure risk degree in river basin, Annuals. Disaster Prevention Res. Inst., Kyoto Univ., Vol. 53, No. B, pp. 515-526 (in Japanese with English abstract).

Highland, L. M., and Bobrowsky, P. (2008): The landslide handbook—A guide to understanding landslides, U.S. Geological Survey Circular 1325, Reston, Virginia.

Kampf, S. K., and Burges, S. J. (2007): A framework for classifying and comparing distributed hillslope and catchment hydrologic models, Water Resources Research, Vo. 43, No. 5, pp. W05423.

Kappes, M. S., Keiler, M., von Elverfeldt, K., and Glade, T. (2012a): Challenges of analyzing multi-hazard risk: a review, Natural Hazards, Vol. 64, pp. 1925-1958.

Kappes, M. S., Papathoma-Köhle, M., and Keiler, M. (2012b): Assessing physical vulnerability for multi-hazards using an indicator-based methodology, Applied Geography, Vol. 32, No. 2, pp. 577-590.

Kondo, S., Kataie, Y., Ota, K. (2012): Disaster Response of Municipal Government at Southern area of Wakayama Prefecture after Flood and Sediment Disaste by Typhoon Talas, SEISAN KENKYU, Vol. 64, No. 4, pp. 527-531. (in Japanese)

Kyoto Prefecture (2013a): Investigation report for the heavy rainfall disaster on August 13-14, 2012 (in Japanese).
(http://www.pref.kyoto.jp/shingikai/kasen-03/documents/1_nambugouu.pdf)

Kyoto Prefecture (2013b): Disaster rehabilitation plan for the heavy rainfall disaster on August 13-14, 2012 (in Japanese).
(http://www.pref.kyoto.jp/shingikai/kasen-03/documents/2_mokuhyou.pdf)

Kubota, T., and Nakamura, H. (1991): Landslide susceptibility estimation by critical slip surface analysis combined with reliable analysis, Journal of Japan Landslide Society, Vol. 27, No. 4, pp. pp.18-25.

Lee, G., Kim, S., Jung, K., and Tachikawa, Y. (2011): Development of a large basin rainfall-runoff modeling system using the object-oriented hydrologic modeling system (OHyMoS), KSCE J Civ Eng, Vol. 15, No. 3, pp. 595-606.

Lee, K. T., and Ho, J.-Y. (2009): Prediction of landslide occurrence based on slope-instability analysis and hydrological model simulation, Journal of Hydrology, Vol. 375, No. 3–4, pp. 489-497.

Maki, N. and Hayashi, H. (2014): The 2012 South Kyoto Flooding and Disaster Response of City of Uji; Essential Contents for a post-Tohoku Earthquake Disaster Response Plan, Journal of Social Safety Science, No.22.

Osanai, N., Shimizu, T., Kuramoto, K., Kojima, S., and Noro, T. (2010): Japanese early-warning for debris flows and slope failures using rainfall indices with Radial Basis Function Network, Landslides, Vol. 7, No. 3, pp. 325-338.

Soil Conservation Service. (1986): Urban Hydrology of Small Watersheds, Technical Release 55, Washington, D.C.

Tachikawa, Y., Nagatani, G., and Takara, K. (2004): Development of stage-discharge relationship equation incorporating saturated-unsaturated flow mechanism, Annual Journal of Hydraulics Engineering, JSCE, Vol. 48, No., pp. 7-12 (in Japanese with English abstract).

Takahashi, T., Inoue, M., Nakagawa, H., and Satofuka, Y. (2000): Prediction of sediment runoff from a mountain watershed, Annual Journal of Hydraulic Engineering, JSCE, Vol. 44, pp. 717-722 (in Japanese with English abstract).

Takasao, T., and Shiiba, M. (1988): Incorporation of the effect of concentration of flow into the kinematic wave equations and its applications to runoff system lumping, Journal of Hydrology, Vol. 102, No. 1–4, pp. 301-322.

Tanaka, T., Tachikawa, Y., and Yorozu, K. (2014): Development of a flood-inundation model nesting a distributed rainfall-runoff model, Journal of Japan Society of Civil Engineers, Ser. B1 (Hydraulic Engineering), Vol. 70, No.4, pp.I_1495-I_1500.

Tsutsumi, D., Fujita, M., Hayashi, Y. (2007): Numerical simulation on a landslide due to typhoon 0514 in taketa city, oita prefecture,Annual Journal of Hydralics Engineering, JSCE, Vol. 51, pp. 931-936 (in Japanese with English abstract).

Uji City. (2013): Uji regional disaster prevention plan (in Japanese). (http://www.city.uji.kyoto.jp/0000010399.html)

Uji City. (2014): The heavy rainfall disaster record collection in Kyoto southern region on August 13-14, 2012 (in Japanese).

(http://www.city.uji.kyoto.jp/0000012774.html)
Wang, C., Esaki, T., Xie, M., and Qiu, C. (2006): Landslide and debris-flow hazard analysis and prediction using GIS in Minamata–Hougawachi area, Japan, Environ Geol, Vol. 51, No. 1, pp. 91-102.
Xie, M., Esaki, T., Qiu, C., and Wang, C. (2006): Geographical information system-based computational implementation and application of spatial three-dimensional slope stability analysis, Computers and Geotechnics, Vol. 33, No. 4–5, pp. 260-274.
Xie, M., Esaki, T., and Zhou, G. (2004): GIS-Based Probabilistic Mapping of Landslide Hazard Using a Three-Dimensional Deterministic Model, Natural Hazards, Vol. 33, No. 2, pp. 265-282.

Chapter 6
Warning and Evacuation Decision Support System for Rainfall-Induced Multi Sediment Hazard

6.1 Introduction

Generally, the rainfall-related disasters in mountainous areas usually result from the moving of sediment and flooding as well as their interaction. That is, the sediment hazards should be considered as multi-modal types. In Chapter 5, this study defined the multi-hazards as "*a hazard could affect or trigger another one because of their complex spatial and temporal relationships.*" For example, rainfall might induce landslides, debris flow, and flood, and the landslide sediment then might become the source material of debris flow as well as the landside sediment and debris flow might form natural dam or block the river. Once the natural dam burst, then it might derive debris flow or flood to cause the secondary disaster. Moreover, if the abovementioned hazards affect the protected targets, they might cause disasters.

By their spatial characteristic, the protected targets could be classified as settlements and infrastructures. Generally speaking, the former is the most important protected target because it involves people lives and property. However, if the infrastructures (e.g., roads, bridge, lifeline, etc.) are damaged, they also will affect the evacuation action or result in the deterioration of the living environment, and then threaten the individuals. **Figure 6.1** illustrated the multi sediment hazards and their relationship as well as interaction.

On the other hand, using mobility to distinguish, the protected targets could be divided into two parts. One is the stationary objects such as infrastructure and buildings; the other is the movable objects such as inhabitants and moveable property. Facing the threat of sediment disasters, the former only could be protected or reduced loss by engineering method. For the latter, in addition to government's engineering efforts, establishment of early-warning systems and evacuation of inhabitants are recognized as the most important approaches for disaster risk reduction. However, it is worth noticing that an alarm only can motivate people to escape from potentially dangerous situations, but it does not stop the hazardous event itself [*Hübl*, 2000]. That

is, early-warning systems do not substantially decrease property damage [*National Research Council*, 2004].

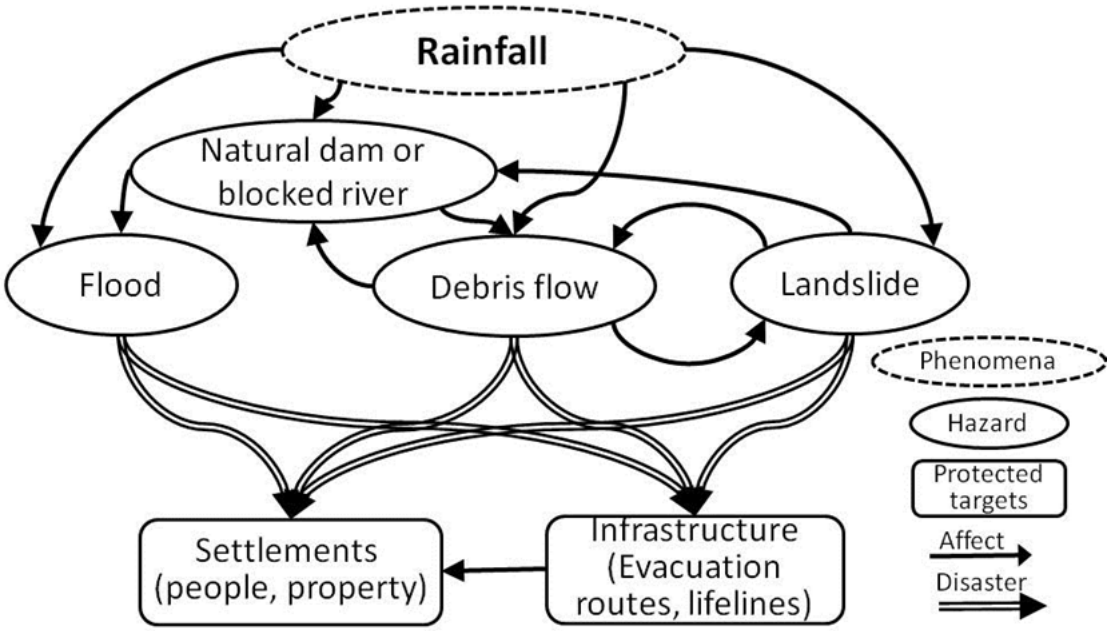

Figure 6.1 The multi sediment hazards and their relationship as well as interaction

According to the definition by *UNISDR* [2009], early-warning systems are described as "the set of capacities needed to generate and disseminate timely and meaningful warning information to enable individuals, communities and organizations threatened by a hazard to prepare and to act appropriately and in sufficient time to reduce the possibility of harm or loss." Therefore, good early-warning systems comprise identification and estimation of hazardous processes, communication of warnings and adapted reaction of local population [*Thiebes*, 2012].

In Chapter 2, this study described that a complete sediment disaster warning system should be comprised of two parts: a warning model and an alert issuing system. However, because most studies have only concentrated at the establishment of a warning model and have not considered alert issuing systems as well as the complex situation that may be encountered during practical operations, these models were difficult to be applied pragmatically. That is, all prediction results have to be transferred into an adequate warning message and distributed to the target population [*Thiebes*, 2012]. *Kunz-Plapp* [2008] indicated that warning messages should be believable, clearly formulated, adapted to the context of the target group, and should

contain clear instructions on appropriate protection action.

In addition, while in the past decades, many countries had established sediment disaster warning systems, most of them only coped with the single hazard, and were installed for single slopes or for entire regions. Moreover, most regional warning system can only issue warnings, such as a 70% probability of landslide occurrence for a wide area, and it cannot identify specifically which slopes might collapse [Wieczorek and Glade, 2005]. In Chapter 5, this study has established the simulation model of multi sediment hazards by integrating rainfall-infiltration, landslide prediction, sediment runoff, riverbed deformation, and water discharge models, as well as conducted a basin scale simulation platform by combining slope units and unit channels. Based on the recommends about the warning system and evacuation decision factors in Chapter 2 and Chapter 3, this study will establish the new advanced warning system (the Rainfall-Induced Multi Sediment Hazards warning system, RIMSH warning system) through integrating the research results in Chapter 4 and 5. The RIMSH warning system includes not only the warning mode but also the alert issuing system.

Using the heavy rainfall disaster event, which occurred in the Shizugawa basin in 2012, located in Uji City, Kyoto Prefecture, as a study case, this study employs the RIMSH warning system to predict the circumstances in every minute, and used the prediction results to assist the decision-making of evacuation and road closure as well as bridge closure. That is, using the simulation results, the local governments can evaluate where and when the risk is higher, and the information is useful to the evacuation decision and related emergency response. Additionally, the information also can help inhabitants to understand the imminent risk to increase the evacuation rate during the rainfall events. Therein, to verify the contribution of the RIMSH warning system to raise the will for the local government officials and inhabitants to evacuate, this study also made a series of questionnaires to explore the effect of more complete warning information. Finally, using various extreme rainfall scenarios, the warning model was employed to verify the existing evacuation plan in the Shizuagawa basin.

6.2 Materials and methodology

6.2.1 Warning model

In Chapter 4 and 5, using critical water content as the indicator, the multi-modal sediment disaster model can offer landslide prediction results, such as the occurring time, location, and scale of landslides. Moreover, based on the simulation of water discharge, sediment runoff, and riverbed deformation, it also can predict the location of overflow with unit channels as targets. That is, the RIMSH warning system in this study can predict the moving of sediment and flooding. Because the protected targets shown in **Figure 6.1** are settlements and infrastructure, this warning model will provide three kinds of alerts - the landslide alert, road closure alert, and flood alert to assist local government officials and inhabitants adopting appropriate protection action. Therein, the landslide alert is a regional alert which offered overall estimation of landslide risk in the basin; however, it pays more attention in the settlements to aid local government officials and inhabitants to make appropriate evacuation decisions. Based on the evaluation of landslide risk along the main evacuation routes, the road closure alert can provide the essential information about when the roads should be closed for safety. Due to high relationship between the water level and inundation as well as bridges damaged, the flood alert can offer the risk evaluation of overflow in the main channel, and it is useful not only for the decision of bridge closure but also for the protection action of flood. The integrated warning model is shown in **Figure 6.2**.

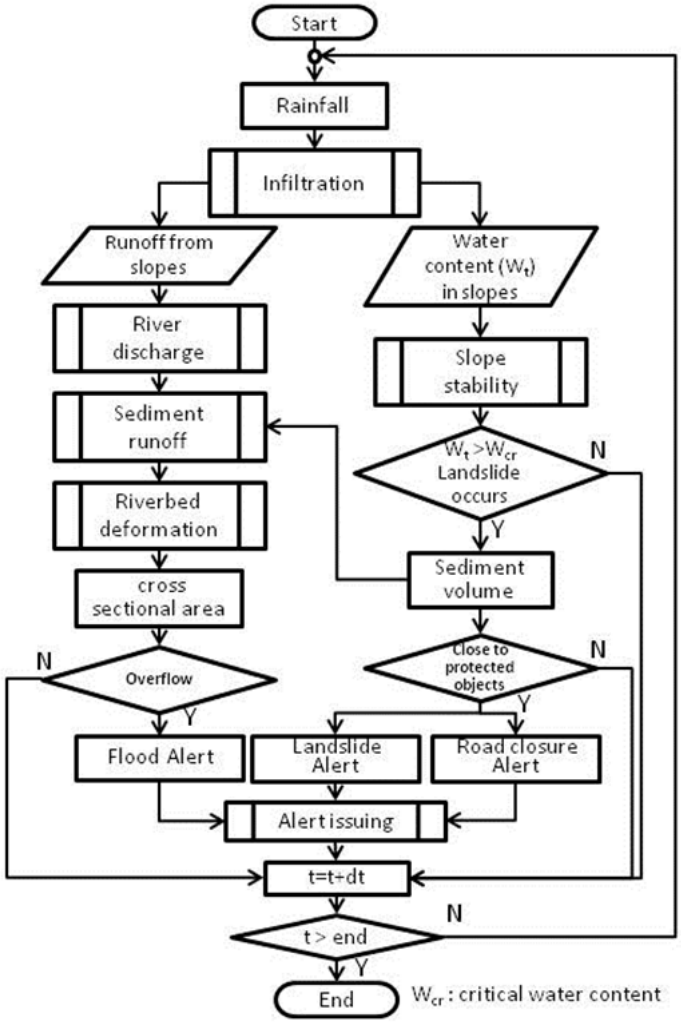

Figure 6.2 The integrated warning model for multi sediment hazards

In Chapter 1, **Table 1.4** shows the process from issuing early warning to evacuating inhabitants, and it means that some time is required for the alert dissemination and the evacuation. Moreover, in Chapter 2, this study defined RTE (remaining time for evacuation) as *the time from the alert being issued to the time the disaster occurs*. Accordingly, the shortest remaining time for evacuation (SRTE) should be different in different regions, because of the diversity of traffic conditions and population structure. In addition, most existing rainfall-based warning system established a warning threshold which is parallel to the triggering thresholds (curve A in **Figure 6.3**); however, it might cause the RTE insufficient in some rainfall scenarios (e.g., RAIN PATH0 in **Figure 6.3**). Thus, *Aleotti* (2004) adopted a curve to account for different rainfall paths (curve B in **Figure 6.3**) to keep the RTE as the same.

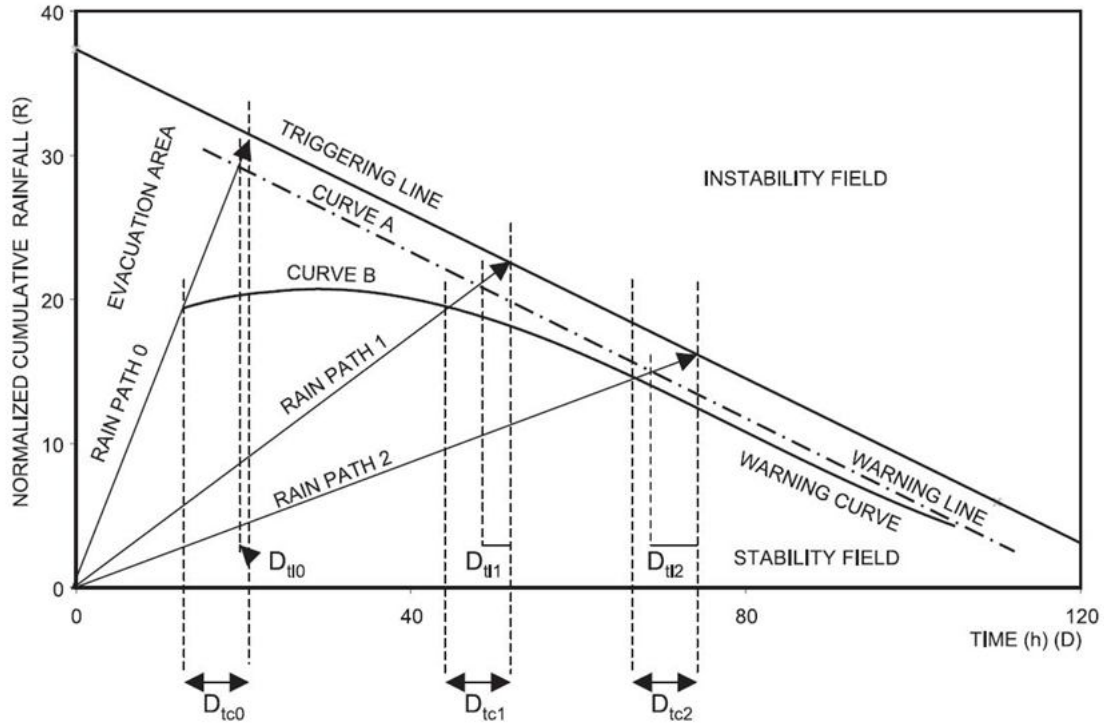

Figure 6.3 Comparison of warning curve and warning line thresholds and remaining evacuation time

While according to the statistic data in Taiwan, the study results in Chapter 2 recommend the SRTE as 3 hours. The SRTE in the study area can be shortened as 1 hour because the study area is very close to the Uji City hall (i.e., it is easy to communicate and disseminate the evacuation order). To ensure the sufficient RTE, this study used the predicting water content 60 minutes later (W_{t+60}) as the index of issuing landslide-related alerts (including landslide alerts and road closure alerts), and the landslide-related alert would be issued when the expected water content in the following one hour (W_{t+60}) would exceed the W_{cr} (see **Figure 6.4**). W_{t+60} can be calculated by Eq. (4.17) and (4.18) with time-step of 1 minute, but I_t should be replaced with constant-intensity of $I_{ta,60}$ in Eq. (4.17). $I_{ta,60}$ is the mean rainfall-intensity in 60 minutes at time t_a. **Figure 6.5** shows the comparison of actual water content (W_t) and prediction result (W_{t+60}), and the prediction result is very close to the actual value.

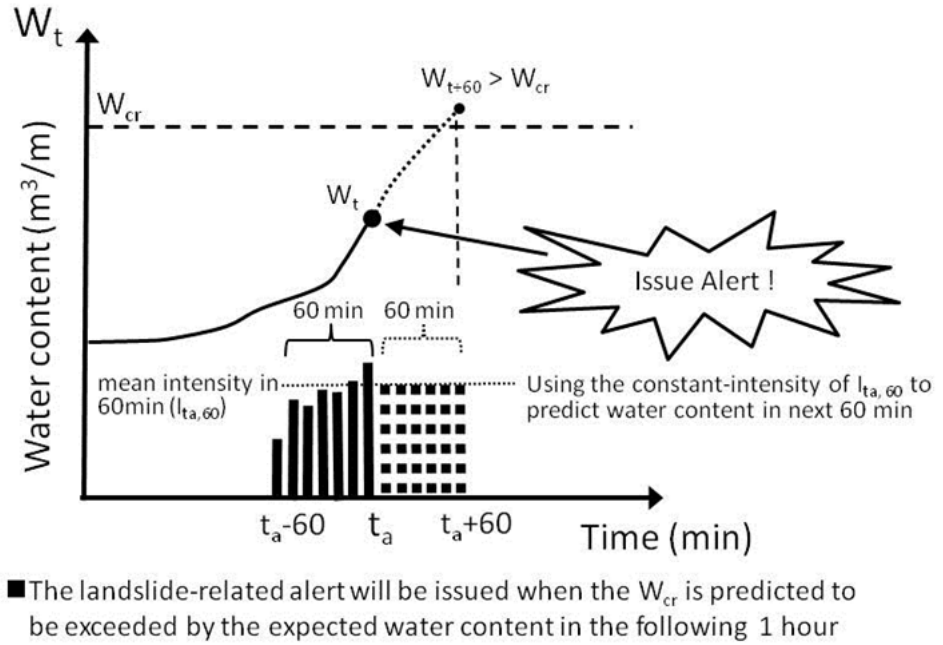

Figure 6.4 The diagram of issuing landslide-related alerts

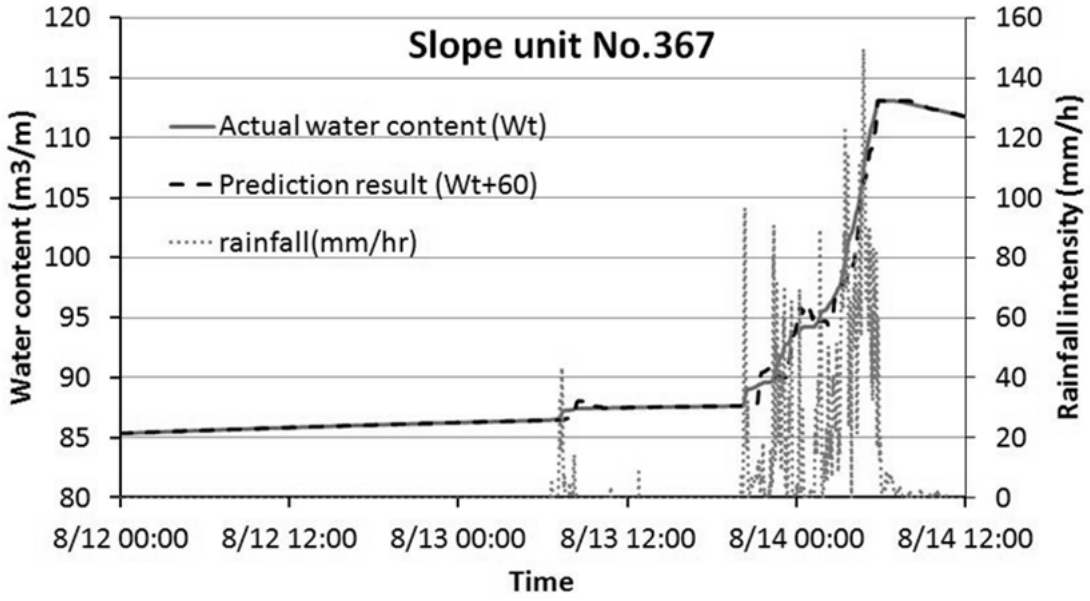

Figure 6.5 The comparison of actual water content (W_t) and prediction result (W_{t+60})

Compared with the landslide-related alerts which forewarn time is often shorter and lacks significant symptoms before occurrence, the flood alert can be fairly simple to issue because it has the manifest indications (e.g., the variation of water level). Hence, this study uses the relative water level as the index of issuing the flood alert.

6.2.2 Alert-issuing system

UNISDR [2006] indicated that four essential key parts for effective early warning can be defined as follows.

(1) Knowledge about the risks that threaten a community

(2) Monitoring and warning service for these risks

(3) Dissemination and communication of warning messages in a way that is understood by the local population

(4) Response capability of involved people, who need to know how to react appropriately in case of a warning.

To meet abovementioned essential elements, the same levels and representative color are used to establish the dissemination and communication of warning messages in all alerts in this study. That is, alerts are divided into two levels- yellow and red. The definitions, conditions for issuing, and protection actions for all alerts are shown in **Table 6.1**. **Table 6.2** shows the conditions for lowering the alert levels. The overall flowcharts for issuing alerts and lifting alerts in this study are shown in **Figure 6.6** and **6.7**.

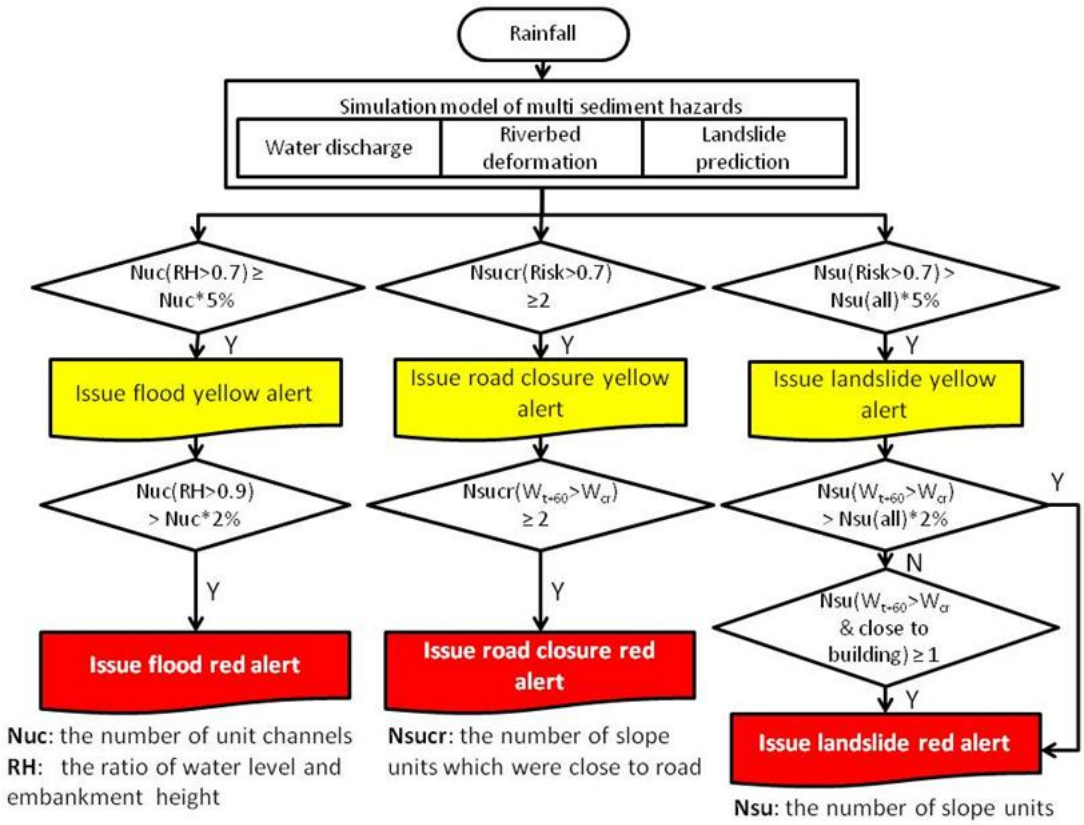

Figure 6.6 Process for issuing alerts in this study

Table 6.1 The definitions, conditions for issuing, and protection action for alerts

Type	level	Conditions for issuing alerts	Protection actions
Landslide	Yellow	The number of the high-risk slope units, which the landslide risk* was higher than 0.7, exceeded the 5% of total slope units.	■ Evacuation preparation ■ Precautionary evacuation
	Red	(1) Any one of the slope units, which were adjacent to buildings, was predicted that W_{t+60} will exceed W_{cr} at next one hour. or (2) The number of the slope units, which were predicted that W_{t+60} will exceed W_{cr} at next one hour, was more than 2% of total slope units.	■ Evacuate to the shelter
Road closure	Yellow	The number of the slope units, which were adjacent to main evacuation routes and their landslide risks* were higher than 0.7, exceeded two(included).	■ Preparation for road closure ■ Recheck the evacuation plan
	Red	The number of the slope units, which were adjacent to main evacuation routes and were predicted that W_{t+60} will exceed W_{cr} at next one hour, was more than two (included)	■ Road closure ■ Adjust the evacuation plan if necessary
Flood	Yellow	The number of the unit channels, which the water level was higher than 70% of the embankment height, was more than 5% of total unit channels.	■ Preparation for bridge closure ■ Preparation for protected action of flood
	Red	The number of the unit channels, which the water level was higher than 90% of the embankment height, was more than 2% of total unit channels.	■ Bridge closure ■ Protected action of flood ■ Vertical evacuation or evacuate to the shelter

* See Chapter 4 for the definition of landslide risk

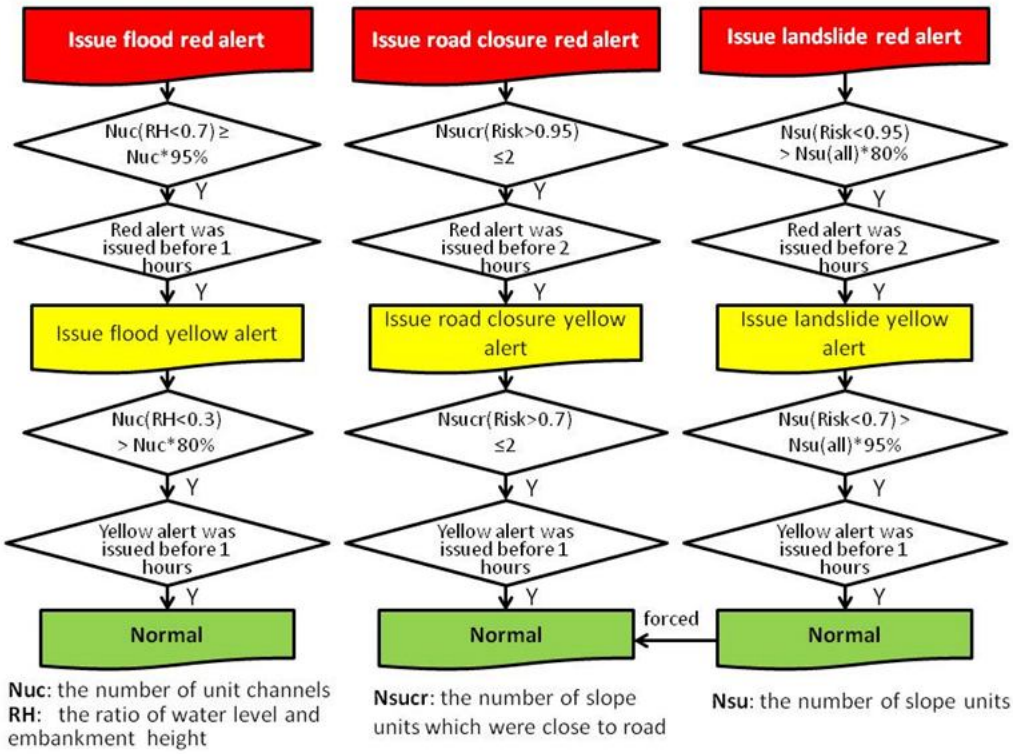

Figure 6.7 Process for lifting alerts in this study

Table 6.2 The conditions for lifting the alert levels

Type	level	Conditions for lowering/lifting the alert levels
Landslide	Red to Yellow	(1) The number of the slope units, which the landslide risk* was lower than 0.95, exceeded the 80% of total slope units. and (2) To avoid lifting too frequently, the action of lifting from red to yellow was prohibited in two hours after the issuing of landslide red alert.
	Yellow to normal	(1) The number of slope units, which the landslide risk* was lower than 0.7, exceeded the 95% of total slope units. and (2) To avoid lifting too frequently, the action of lifting from yellow to normal was prohibited in one hours after the issuing of landslide yellow alert.
Road closure	Red to Yellow	(1) The number of slope units, which were adjacent to main evacuation routes and their landslide risks* were higher than 0.95, was less than two. and (2) To avoid lifting too frequently, the action of lifting from the red to the yellow was prohibited in two hours after the issuing of road-closure red alert.
	Yellow to normal	(1) The number of slope units, which were adjacent to main evacuation routes and their landslide risks* were higher than 0.7, was less than two; or it would be forced to lifted to normal level when the landslide alert in the basin had been lifted to normal level and (2) To avoid lifting too frequently, the action of lifting from yellow to normal was prohibited in one hour after the issuing of road-closure yellow alert.
Flood	Red to Yellow	(1) The number of unit channels, which the water level was lower than 70% of the embankment height, was more than 95% of total unit channels. and (2) To avoid lifting too frequently, the action of lifting from red to yellow was prohibited in one hours after the issuing of flood red alert
	Yellow to normal	(1) The number of unit channels, which the water level was lower than 30% of the embankment height, was more than 80% of total unit channels. (2) To avoid lifting too frequently, the action of lifting from yellow to normal was prohibited in one hour after the issuing of flood yellow alert.

* See Chapter 4 for the definition of landslide risk

Because all alerts have been simplified as the clearly formulated content, and contained clear instructions on appropriate protection action, it would be easy to transfer the alerts into adequate warning messages (e.g., sirens, SMS, Fax, Email, and APP of smart phones) and distribute to the target population. In addition, the detail information and prediction results also can be displayed on the specific website on real-time.

6.2.3 Evacuation plan in the Shizugawa basin

The settlements in the Shizugawa basin are located at two regions - Sumiyama area and Shizugawa area (see **Figure 6.8**). According to the regional disaster prevention plan of Uji City, the shelters and main evacuation routes were marked in **Figure 6.8**. The evacuation plan for sediment disaster is divided into three stages, and the issuing-condition as well as the instruction of protected action is described in **Table 6.3** [*Uji City*, 2009; *Uji City*, 2013].

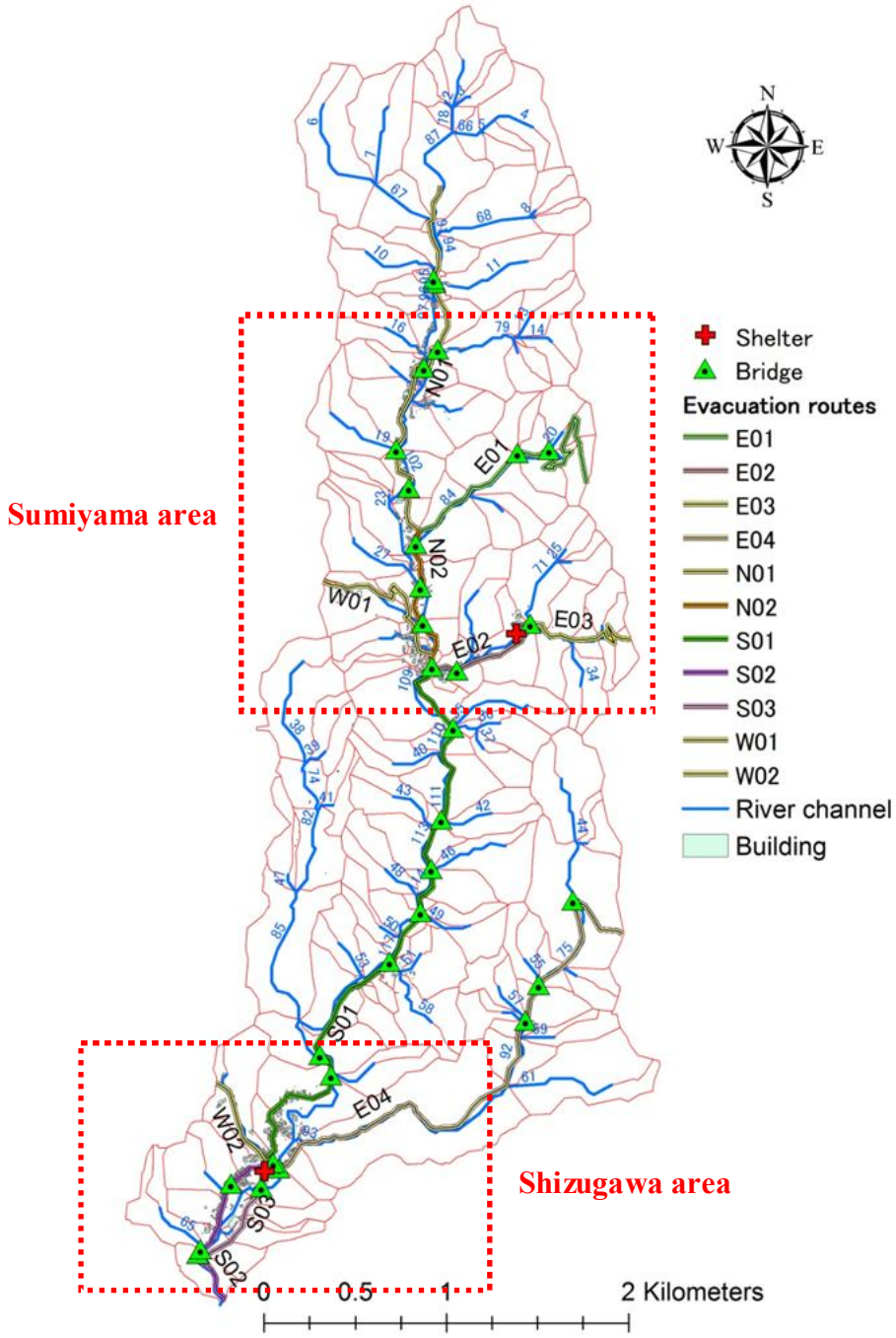

Figure 6.8 The shelters and evacuation routes in the Shizugawa basin

Table 6.3 The issuing-condition and instructions of protected action in different stages of the sediment disaster evacuation plan in Uji City

Stage	Issuing-condition	Protected action
Preparation evacuation	■ Heavy rainfall alert was issued ■ Sediment disaster alert was issued ■ Risk of sediment disaster in warning system of Kyoto Prefecture reached level 1 ■ Some omens appeared	■ Disadvantaged groups start evacuation ■ Others start preparation evacuation
Advice evacuation	■ Risk of sediment disaster in warning system of Kyoto Prefecture reached level 2 ■ Some omens occurred	■ Inhabitants start evacuation
Mandatory evacuation	■ Risk of sediment disaster in warning system of Kyoto Prefecture reached level 3 ■ Some disasters occurred	■ Enforce evacuation for all inhabitants living in the risk area

6.2.4 Questionnaire content and survey subjects

To understand whether the more detailed warning information might affect the evacuation decision for local government officials and inhabitants, this study designed two questionnaires for local government officials and inhabitants in the debris-flow potential area in Taiwan (with same areas in Chapter 3). The detailed warning information was provided by the abovementioned alert types (i.e., landslide yellow/red alerts, road closure yellow/red alerts, and flood yellow/red alerts), and the high-risk locations could be displayed on the website. The local government officials, including county, township, and village governments, were responsible for making evacuation decisions; therein, some of the respondents had abundant experience for evacuation decision while others did not. The survey subjects for inhabitants also can be divided into being experienced for evacuation and being inexperienced for evacuation. The statistics of valid questionnaires are shown in **Table 6.4**.

Because the factors affecting evacuation decision (e.g., the description in Chapter 3, including warning information, current circumstances, past experience, etc.) are too many and complex, the respondents were required to imagine that their living environment was as same as the description in the questionnaire. That is, the survey tried to evaluate the pure effects from the warning information based on the same environmental circumstances. The content of the questionnaires is summarized in **Table 6.5** and **6.6**.

Table 6.4 Statistics of valid questionnaires for the survey of the detailed warning information affecting evacuation decision

	Returned questionnaires	Local government officials								Inhabitants	
		Total		County		Township		Village			
		Evacuation decision-making experience		Evacuation decision-making experience		Evacuation decision-making experience		Evacuation decision-making experience		Evacuation experience	
		Y	N	Y	N	Y	N	Y	N	Y	N
Yilan County**	12	3	8	1		2	7		1	1	
Keelung City*	0	0	0								
Taipei City*	26	9	17	9	13		4				
New Taipei City*	26	11	10	1		9	8	1	2		5
Taoyuan County**	4	1	3		1	1	2				
Hsinchu County**	23	14	7			8	4	6	3	2	
Miaoli County**	7	0	0								7
Taichung City*	10	0	0							3	7
Changhua County*	16	1	5	1			5			3	7
Nantou County***	63	10	9	1	1	8	8	1		12	32
Yunlin County**	0	0	0								
Chiayi County***	6	0	3				3			2	1
Tainan City**	45	8	35			5	33	3	2	1	1
Kaohsiung City***	31	14	14	3	3	11	10		1	3	
Pingtung County***	23	4	15	1	3	2	10	1	2	1	3
Taitung County**	3	1	1	1	1					1	
Hualien County**	2	0	0							2	
Total	297	76	127	18	22	46	94	12	11	31	63

Note : According to transportation accessibility, the survey areas were divided into **surrounding slopes of cities*, ***shallow mountainous areas*, and ****mountainous areas*.

Table 6.5 The content of questionnaire for the local government officials

Environmental circumstances	
■ The north part of the village is located in the debris-flow potential area, and the critical accumulated rainfall of debris flow occurring is 250mm. The population structure comprises around 50 elders or disadvantaged members. ■ In the past five years, the debris-flow red alert was issued in the village at least once every year, but only small landslides occurred two times, and never caused any disaster. ■ The temporary (emergency) shelter was set at community center in the north part of the village. There were only simple facilities and food supply for one day in the community center, and there was no emergency communication equipment. ■ Most population lived in the south part of the village, where is relatively a safe location. The shelter, which has complete facilities and enough food, was set at this area. ■ It takes about 25 min for the people living in the north part of village to walk to the shelter (by car about 5min). However, the evacuation route would pass a temporary bridge, which has been washed out at least once every year. The evacuation route also passes a high landslide-potential slope, which often collapsed in the past years. (see **Figure 6.9**) ■ R=Accumulated rainfall (mm), I=Rainfall intensity (mm/h)	
Scenario 1	
■ The forecast accumulated rainfall is **500-800mm**, and debris-flow alerts could be offered.	
Stage 1 (11:00)	Debris-flow yellow alert has been issued (R =110mm, I=15 mm/h). What's your decision? (1)evacuate inhabitants to the shelter (2)evacuate inhabitants to the temporary shelter (3)inquire on-site situation (4)continued monitoring rainfall
Stage 2 (17:00)	Debris-flow red alert has been issued (R =220mm, I=18 mm/h). If you didn't select to evacuate on the former stage, now, What's your decision? (1)evacuate inhabitants to the shelter (2)evacuate inhabitants to the temporary shelter (3)inquire on-site situation (4)continued monitoring rainfall
Stage 3 (20:00)	Evacuation order from superior has been issued (R=280mm, I=20mm/h). If you didn't select to evacuate on the former stage, now, What's your decision? (1)evacuate inhabitants to the shelter (2)evacuate inhabitants to the temporary shelter (3)inquire on-site situation (4)continued monitoring rainfall
Stage 4 (23:00)	Village head reported that some roads have been inundated (R=350mm, I=30mm/h). If you didn't select to evacuate on the former stage, now, What's your decision? (1)evacuate inhabitants to the shelter (2)evacuate inhabitants to the temporary shelter (3)inquire on-site situation (4)continued monitoring rainfall
Scenario 2	
■ The forecast accumulated rainfall is **800-1200mm**, and debris-flow alerts could be offered.	
Stage 1 (11:00)	Same as Scenario 1.
Stage 2 (17:00)	Same as Scenario 1.
Stage 3 (20:00)	Same as Scenario 1.
Stage 4 (23:00)	Same as Scenario 1.
Scenario 3	
■ The forecast accumulated rainfall is **500-800mm**, and debris-flow alerts could be issued. ■ **The detailed warning information was provided** (landslide yellow/red alerts, road closure yellow/red alerts, and flood yellow/red alerts), and **the high-risk location in unit channels and slope units could be displayed on the website**.	

Stage 1 (11:00)	Debris-flow yellow alert and **landslide yellow alert** have been issued (R =110mm, I=15 mm/h). What's your decision? (1)evacuate inhabitants to the shelter (2)evacuate inhabitants to the temporary shelter (3)inquire on-site situation (4)continued monitoring rainfall
Stage 2 (17:00)	Debris-flow red alert, **landslide red alert, and flood yellow alert** have been issued (R =220mm, I=18 mm/h). If you didn't select to evacuate on the former stage, now, What's your decision? (1)evacuate inhabitants to the shelter (2)evacuate inhabitants to the temporary shelter (3)inquire on-site situation (4)continued monitoring rainfall
Stage 3 (20:00)	Evacuation order from superior has been issued (R=280mm, I=20mm/h). If you didn't select to evacuate on the former stage, now, What's your decision? (1)evacuate inhabitants to the shelter (2)evacuate inhabitants to the temporary shelter (3)inquire on-site situation (4)continued monitoring rainfall
Stage 4 (23:00)	Village head reported that some roads have been inundated (R=350mm, I=30mm/h). If you didn't select to evacuate on the former stage, now, What's your decision? (1)evacuate inhabitants to the shelter (2)evacuate inhabitants to the temporary shelter (3)inquire on-site situation (4)continued monitoring rainfall
Scenario 4	
■ The forecast accumulated rainfall is **800-1200mm**, , and debris-flow alerts could be offered. ■ **The detailed warning information was provided** (landslide yellow/red alerts, road closure yellow/red alerts, and flood yellow/red alerts), and **the high-risk location in unit channels and slope units could be displayed on the website**.	
Stage 1 (11:00)	Same as Scenario 3.
Stage 2 (17:00)	Same as Scenario 3.
Stage 3 (20:00)	Same as Scenario 3.
Stage 4 (23:00)	Same as Scenario 3.

Note : The different condition in each stage are highlight in bold type.

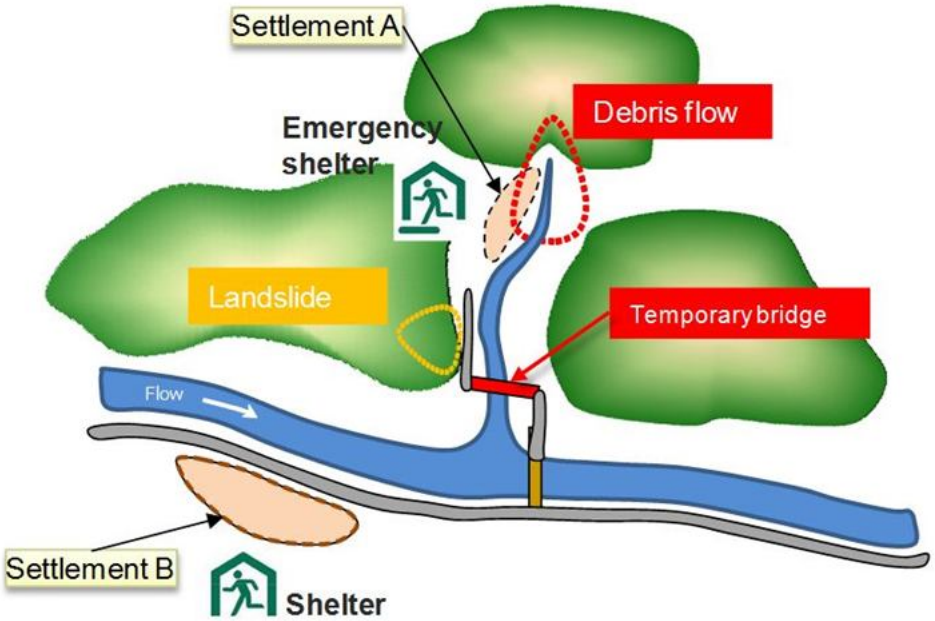

Figure 6.9 The environment diagram of the questionnaire for the local government officials

Table 6.6 The content of questionnaire for the inhabitants

Environmental circumstances	
■ Your house is a 30 years brick building and is located in the debris-flow potential area. ■ In the past five years, you had been advised to evacuate at least once every year, but disasters never happened. ■ It took about 25 min from your house to the shelter by walk (about 5 min by car). However, the evacuation route would pass a temporary bridge, which was washed out at least once every year. The evacuation route also would pass a high landslide-potential slope, which often collapsed in past years. (see **Figure 6.10**)	
Scenario A	
■ The forecast accumulated rainfall is 500-800mm, and debris-flow alerts could be issued.	
Stage 1 (11:30)	You received a message from the local government. It said the debris-flow yellow alert has been issued, and the light rain started from this morning. What's your decision? (1)evacuate to the shelter (2)prepare to evacuate (3)continued observing the on-site situation (4)do nothing
Stage 2 (17:30)	You received a message from the local government. It said the debris-flow red alert was issued, and the rainfall is continued. If you didn't select to evacuate on the former stage, now, What's your choice? (1)evacuate to the shelter (2)prepare to evacuate (3)continued observing the on-site situation (4)do nothing
Stage 3 (20:30)	You received a message from the local government. It said the evacuation order has been issued, and the rainfall continued. If you didn't select to evacuate on the former stage, now, What's your choice? (1)evacuate to the shelter (2)prepare to evacuate (3)continued observing the on-site situation (4)do nothing
Stage 4 (23:30)	The rainfall seems to get heavy, and some roads were inundated. If you didn't select to evacuate on the former stage, now, What's your choice? (1)evacuate to the shelter (2)prepare to evacuate (3)continued observing the on-site situation (4)do nothing
Scenario B	
■ The forecast accumulated rainfall is 500-800mm, and debris-flow alerts could be issued. ■ The local government developed a new warning system, and offered extra warning information as follows. [1] Landslide yellow/red alert (including the abovementioned high landslide-potential slope which located along the evacuation route. [2] Flood yellow/red alert (including the abovementioned temporary bridge which located along the evacuation route) [3] The accumulated rainfall data	
Stage 1 (11:30)	You received a message from the local government. It said the debris-flow yellow alert and **landslide yellow alert** has been issued, as well as **the accumulated rainfall was 110mm**. What's your choice? (1)evacuate to the shelter (2)prepare to evacuate (3) continued observing the on-site situation (4)do nothing
Stage 2 (17:30)	You received a message from the local government. It said the debris-flow red alert, **landslide red alert**, and **flood yellow alert** has been issued, as well as **the accumulated rainfall was 220mm**. If you didn't select to evacuate on the former stage, now, What's your choice? (1)evacuate to the shelter (2)prepare to evacuate (3)continued observing the on-site situation (4)do nothing

Stage 3 (20:30)	You received a message from the local government. It said the evacuation order has been issued, and **the accumulated rainfall was 280mm**. The rainfall is continued. If you didn't select to evacuate on the former stage, now, What's your choice? (1)evacuate to the shelter (2)prepare to evacuate (3)continued observing the on-site situation (4)do nothing
Stage 4 (23:30)	You received a message from the local government. It said **the accumulated rainfall was up to 350mm**. The rainfall seems to get heavy, and some roads were inundated. If you didn't select to evacuate on the former stage, now, What's your choice? (1)evacuate to the shelter (2)prepare to evacuate (3)continued observing the on-site situation (4)do nothing

Note : The different condition in each stage are highlight in bold type.

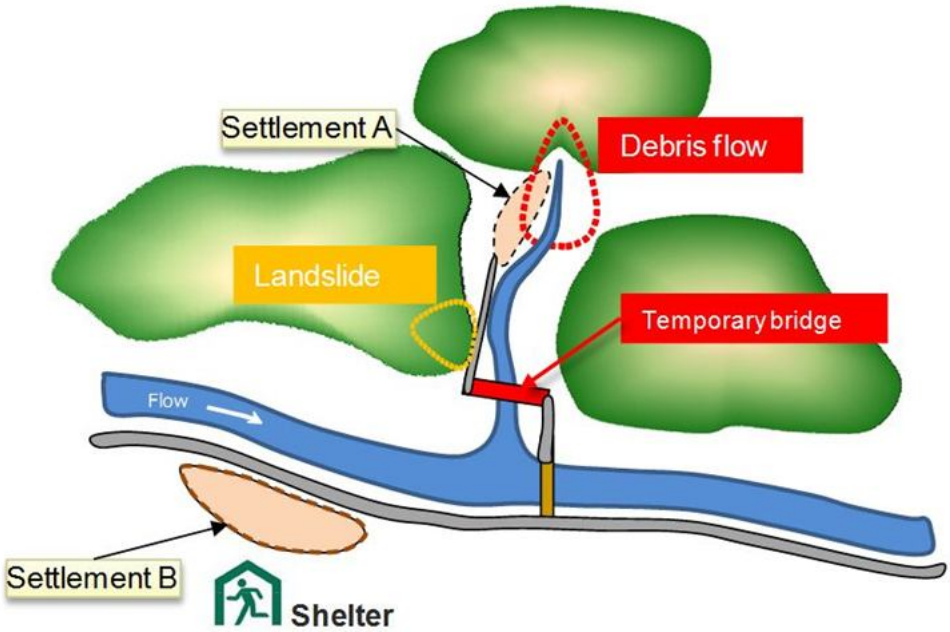

Figure 6.10 The environment diagram of the questionnaire for the inhabitants

6.3 Results and discussions

6.3.1 Issuing-alerts scenario simulation for the study case

Integrating the simulation results in Chapter 5 and the abovementioned warning model as well as the alert-issuing system, the issuing-warning scenario simulation results for the heavy rainfall event in the study area are shown in **Table 6.7, 6.8** and **Figure 6.11**.

Table 6.7 shows the process of issuing alerts including the landslide alerts, road closure alerts, and flood alerts. According to the investigation results, the occurring time of landslides were between 04:30~6:00 on August 14 (see Chapter 5). The RIMSH warning system issued the landslide yellow alert at 02:06 on August 14, and issued the landslide red alert at 03:21. That is, the RIMSH warning system provided at least 2.5 hours for evacuation preparation, and at least 1 hour for evacuating the inhabitants to shelters. It did accomplish the goal of early warning, and offered enough evacuation time. The RIMSH warning system also can provide the suggestions of road closure according to the risk of landslides. In fact, it is a very important task to close the high-risk road promptly during rainfall in the mountainous area to prevent cars from entering the hazardous area. In addition, the road-closure alert is the indispensable and irreplaceable key point for evacuation decision-making and to verify the evacuation plan. Besides, the RIMSH warning system also offered the recommends when the alerts could be lowered or lifted. Such the decision-making for the lifting alert-level sometime might trouble the official during practical operation, and most of the officials only depended on experience. The RIMSH warning system proposed an objective evaluation method to adjust the alert level, and it should be useful to assist the decision-maker in making appropriate decisions.

To verify the evacuation plan, the safety of bridges is another essential consideration. **Table 6.8** shows the list of the probably interrupted bridges in the evacuation routes because of overflow from the unit channels. Referring to the road closure alerts and flood alerts as well as the location of the shelters, the N02, E01, E02, E03, and S01 of evacuation routes might be interrupted during this rainfall event. That is, the situation was unfavorable in evacuation for the inhabitants living in Sumiyama area. In fact, according to the disaster reports, the Sumiyama area did become isolated during this rainfall event [*Maki and Hayashi*, 2014; *Uji City*, 2014].

The timeline of issuing-alerts and the disaster events during the heavy rainfall event are shown in **Figure 6.11**. The figure is very useful for examining the process of issuing alerts and emergency response. Combining with the spatial information and GIS platform, it also can be employed on the training and drill, especially for the novice among disaster prevention officials.

Table 6.7 The process of issuing alerts by using the RIMSH warning system during the heavy rainfall event in the Shizugawa basin on August 13-14, 2012

Alert types		Issue yellow alert	Issue red alert	Lower from red to yellow alert	Lift from yellow to normal
Landslide		8/14 02:06	8/14 03:21	8/14 15:33	8/17 15:08
Road closure	E01	8/14 02:01	8/14 04:00	8/14 15:33	8/17 15:08
	E02	8/14 03:13	8/14 04:41	8/14 14:51	8/17 07:03
	E03	8/14 03:22	8/14 04:43	8/14:14:00	8/17 00:01
	E04	8/14 02:52	8/14 05:00	8/14 07:01	8/17 06:33
	N01	8/14 01:34	-	-	8/17 15:08
	N02	8/14 03:27	-	-	8/16 23:44
	S01	8/14 02:47	-	-	8/17 15:08
	S02	-	-	-	-
	S03	-	-	-	-
	W01	8/14 03:47	-	-	8/16 06:37
	W02	-	-	-	-
Flood		8/13 22:30	8/14 03:17	8/14 06:34	8/14 07:35

Note: According to the investigation results, the occurring time of landslides was between 04:30~6:00 on August 14; the occurring time of floods was between 04:00~06:00 on August 14.

Table 6.8 The list of probable interrupted bridges along the evacuation routes due to overflow from the unit channels during the heavy rainfall event in the Shizugawa basin on August 13-14, 2012..

	Unit channel	Duration of overflow (Simulation result)	Duration of overflow (Investigation results)	No. Bridge	Evacuation Road
1	123	8/14 02:59~ continued	8/14 about 04:30~06:00	15	E04
2	105	8/14 03:23~06:11	8/14 about 04:00~06:00	7	N02
3	122	8/14 03:37~03:49 8/14 04:31~05:32	8/14 about 04:30~05:30 (A house and a bridge were washed out)	14	S01
4	121	8/14 04:28~06:02	Unknown	13	S01
5	124	8/14 05:20~05:37	8/14 about 04:30~06:00	14	S01

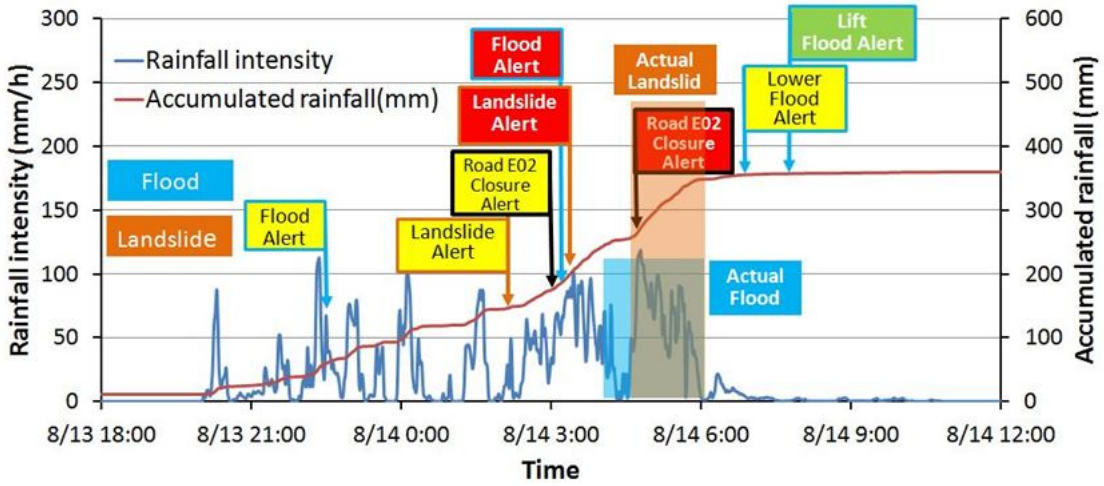

Figure 6.11 The rainfall and timeline of issuing-alerts and disaster events during the heavy rainfall event in the Shizugawa basin on August 13-14, 2012

6.3.2 Verification of the existing evacuation plan under extreme rainfall patterns

To examine the application of the RIMSH warning system under different extreme-rainfall patterns and the feasibility of the evacuation plan in the Shizugawa basin, this study uses four rainfall patterns, which were the same as in Chapter 5, to conduct the simulation of issuing alerts.

(1) Case 1: normal rainfall intensity and duration

In this case, although the simulation results indicated no landslide occurred (see **Figure 6.12**), the RIMSH warning system still issued the landslide red alert according to the warning model (see **Table 6.9**). It might be regarded as a false alert. But considering the safety reason, such the false alert should be tolerable. In addition, the flood yellow/red alerts were issued after the unit channels of No.118 and No.123 occurred overflow (**Figure 6.12**). It seemed to be insufficient to meet the conservative requirement. Nevertheless, according to the comparison between the simulation and investigation results in **Table 5.5**, the prediction results of overflow occurring-time in these two unit channels seemed to be earlier than the actual situation. Thus, in this case, it might have the same situation. However, the simulation results showed that all main evacuation routes were safe during the rainfall pattern. That is, the existing evacuation plan in this case is feasible.

Table 6.9 The process of issuing alerts by using the RIMSH warning system during the rainfall event with normal rainfall intensity and duration

Alert types		Issue yellow alert	Issue red alert	Degrade from red to yellow alert	Degrade from yellow to normal
Landslide		The 10.7th hour	The 11.2th hour	The 13.2th hour	The 33.9th hour
Road closure	E01	The 10.7th hour	-	-	The 18.1th hour
	E02	The 11.4th hour	-	-	The 15.4th hour
	E03	The 11.2th hour	-	-	The 18.4th hour
	E04	The 10.0th hour	-	-	The 33.9th hour
	N01	The 10.7th hour	-	-	The 38.2th hour
	N02	-	-	-	-
	S01	The 10.6th hour	-	-	The 33.9th hour
	S02	-	-	-	-
	S03	The 11.7th hour	-	-	The 16.9the hour
	W01	-	-	-	-
	W02	-	-	-	-
Flood		The 10.7th hour	The 10.9th hour	11.9th hour	12.9th hour

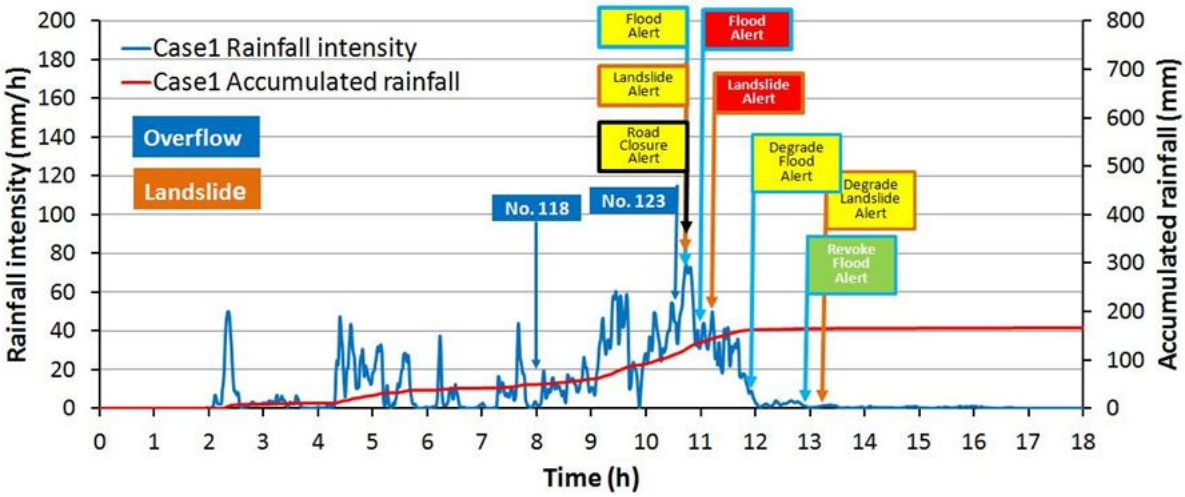

Figure 6.12 The rainfall and timeline of issuing-alerts and disaster events during the rainfall event with normal rainfall intensity and duration

(2) Case 2: high rainfall intensity and normal duration

In this case, the landslide yellow alert and landslide red alert were issued at the 9.1th and the 9.4th hour respectively (see **Table 6.10**). According to **Figure 5.35**, 98.5% of the landslides occurred after the 10.6th hour. It had reached the goal of early warning and offered at least one hour to evacuate. For the flood warning, the flood yellow alert and red alert were issued at the 9.2th and the 9.4th hour respectively (**Table 6.10**). While the simulation results of overflows (see **Table5.6**) indicated that most overflows occurred after the 9.5th hour, the actual occurring time of overflows might be later. **Figure 6.13** shows the timeline of issuing-alerts and disaster events during the rainfall event with high rainfall intensity and normal duration.

In addition, when considering road closure alerts and flood alerts jointly, some evacuation routes to the shelters might be interrupted. Therein, the N01 might be interrupted due to landslides and floods, and the N02, S01, and S03 might be interrupted due to floods. However, the occurring time of roads interrupted was after the landslide red alert. Thus, the evacuation plan seemed to be feasible in this rainfall pattern.

Table 6.10 The process of issuing alerts by using the RIMSH warning system during the rainfall event with high rainfall intensity and normal duration

Alert types		Issue yellow alert	Issue red alert	Degrade from red to yellow alert	Degrade from yellow to normal
Landslide		The 9.1th hour	The 9.4th hour	The 20.2th hour	The 94.8th hour
Road closure	E01	The 9.2th hour	The 10.7th hour	The 20.2th hour	The 94.8th hour
	E02	The 9.4th hour	-	-	The 79.3th hour
	E03	The 9.4th hour	The 10.8th hour	The 18.9th hour	The 72.4th hour
	E04	The 8.2th hour	The 10.5th hour	The 20.2th hour	The 94.8th hour
	N01	The 9.1th hour	The 10.8th hour	The 20.0th hour	The 94.8th hour
	N02	The 9.7th hour	-	-	The 71.4th hour
	S01	The 8.9th hour	The 10.7th hour	The 20.2th hour	The 94.8th hour
	S02	The 9.6th hour	-	-	The 62.4th hour
	S03	The 9.5th hour	-	-	The 83.5th hour
	W01	The 9.9th hour	-	-	The 58.2th hour
	W02	The 9.8th hour	-	-	The 59.1th hour
Flood		The 9.2th hour	The 9.4th hour	The 12.4th hour	The 13.4th hour

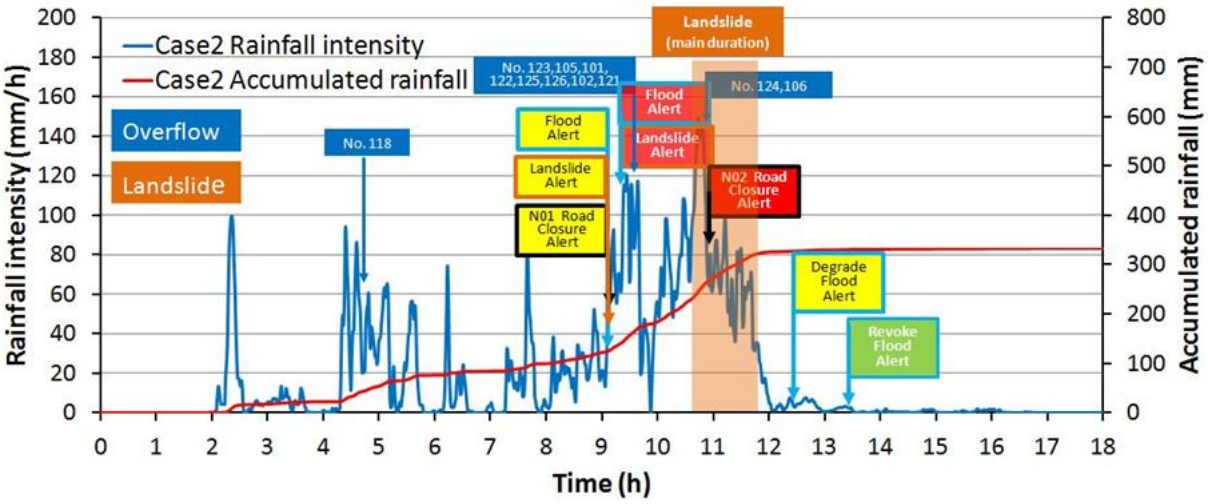

Figure 6.13 The rainfall and timeline of issuing-alerts and disaster events during the rainfall event with high rainfall intensity and normal duration

(3) Case 3: normal rainfall intensity and long duration

In this case, the landslide yellow alert and red alert were issued at the 18.4th and the 21.4th hour respectively (see **Table 6.11**). According to **Figure 5.39**, over 80% of the landslides occurred after the 22th hour. That is, the shortest remaining time for evacuation was only half hour. Compared with previous cases, it seemed to be insufficient. For the flood warning, the flood yellow alert and red alert were issued at the 19.1th and the 19.2th hour respectively (**Table 6.11**). Though the flood yellow alert and the flood red alert were too close, they still have provided at least two hours in advanced before the main flood occurred. In addition, only the evacuation route of N02 might be affected by flood in the unit channel of No.105. However, the duration of overflow in the unit channel of No.105 was only 12 minutes (**Figure 6.14**). It should not affect the evacuation plan. That is, the evacuation plan also seemed to be feasible in this rainfall scenario.

Figure 6.15 showed the timeline of issuing-alerts and disaster events during the rainfall event with high rainfall intensity and normal duration.

Table 6.11 The process of issuing alerts by using the RIMSH warning system during the rainfall event with normal rainfall intensity and long duration

Alert types		Issue yellow alert	Issue red alert	Degrade from red to yellow alert	Degrade from yellow to normal
Landslide		The 18.4th hour	The 21.4th hour	The 29.3th hour	The 105.3th hour
Road closure	E01	The 18.4th hour	The 21.7th hour	The 29.3th hour	The 105.3th hour
	E02	The 19.0th hour	-	-	The 89.4th hour
	E03	The 18.9th hour	-	-	The 82.5th hour
	E04	The 16.9th hour	The 21.7th hour	The 29.3th hour	The 105.3th hour
	N01	The 18.3th hour	-	-	The 105.3th hour
	N02	The 19.5th hour	-	-	The 81.6th hour
	S01	The 18.2th hour	-	-	The 105.3th hour
	S02	The 19.3th hour	-	-	The 71.3th hour
	S03	The 19.1th hour	-	-	The 93.7th hour
	W01	The 20.1th hour	-	-	The 67.35th hour
	W02	The 20.0th hour	-	-	The 68.2th hour
Flood		The 19.1th hour	The 19.2th hour	The 20.3th hour	The 24.4th hour

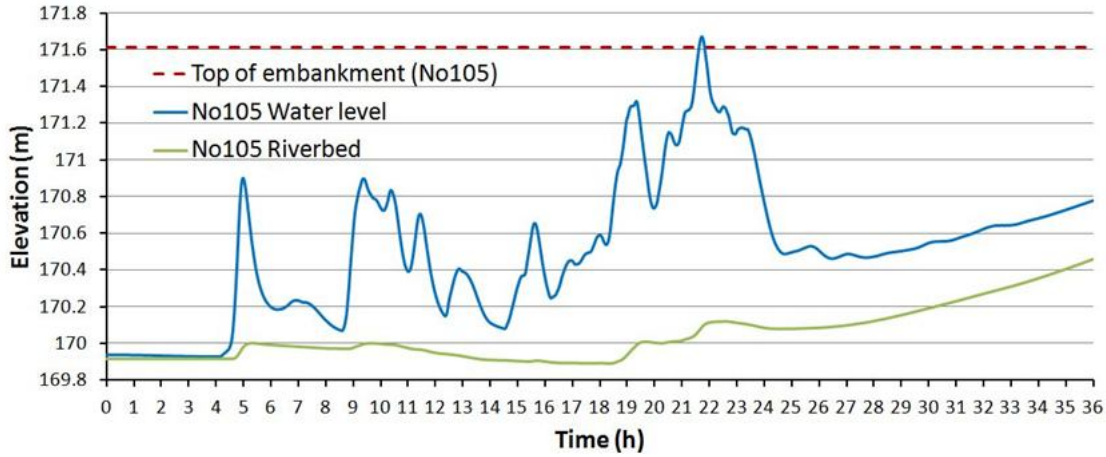

Figure 6.14 The simulation results of the water level and riverbed elevation in the unit channel of No. 105

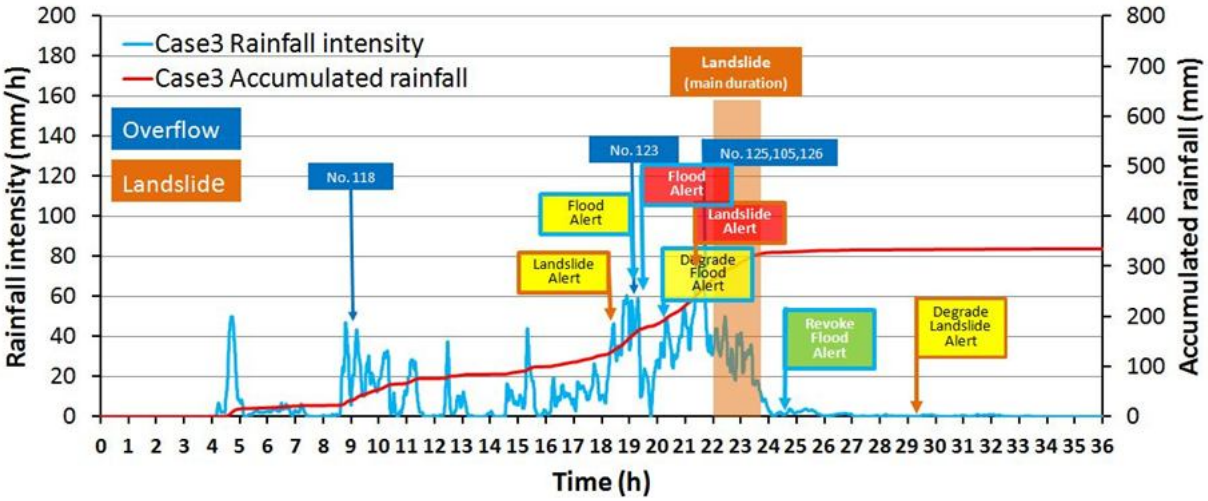

Figure 6.15 The rainfall and timeline of issuing-alerts and disaster events during the rainfall event with normal rainfall intensity and long duration

(4) Case 4: high rainfall intensity and long duration

In this case, the landslide yellow alert and red alert were issued at the 10.2th and the 15.4th hour respectively (see **Table 6.12**). According to **Figure 5.39**, over 99% of the landslides occurred after the 18.5th hour. That is, the RIMSH warning system has provided 3 hours in advanced to evacuate. For the flood warning, because the rainfall pattern was high intensity and long duration, the flood-alerts were issued and then lifted for four times. Unfortunately, most flood alerts cannot provide enough warning time, and the results seemed to indicate that using only the change of water level cannot cope with the rainfall pattern with high intensity and long duration. One of the improvement directions might incorporate the forecast rainfall into the warning model. In addition, due to a lot of landslides occurring in this rainfall pattern, a large amount

of landslide sediment deposited on riverbeds. Therefore, many riverbeds of unit channels raised significantly, and then caused the flood alert cannot be lifted.

For the safety of the evacuation routes to the shelters, the simulation results showed that the evacuation route of S01 would be closed because of landslide risk, and some evacuation routes might be affected because of overflow (e.g., N01, N02, S01, S03). According to the distribution of settlements in the Shizugawa basin (see **Figure 6.8**), the inhabitants living in the Sumiyama area might evacuate to the shelter, but it would become difficult to move to other areas because the roads have been interrupted. That is, although the evacuation plan was feasible in this area, the problem that Sumiyama area might be isolated should be considered carefully. **Figure 6.16** shows the timeline of issuing-alerts and disaster events during the rainfall event with high rainfall intensity and long duration.

Table 6.12 The process of issuing alerts by using the RIMSH warning system during the rainfall event with high rainfall intensity and long duration

Alert types		Issue yellow alert	Issue red alert	Degrade from red to yellow alert	Degrade from yellow to normal
Landslide		The 10.2th hour	The 15.4th hour	The 38.3th hour	The 115.8th hour
Road closure	E01	The 10.1th hour	The 18.6th hour	The 38.3th hour	The 115.8th hour
	E02	The 12.8th hour	-	-	The 100.3th hour
	E03	The 11.3th hour	The 18.7th hour	The 35.6th hour	The 93.8th hour
	E04	The 9.4th hour	The 18.4th hour	The 38.3th hour	The 115.8th hour
	N01	The 10.2th hour	-	-	The 115.8th hour
	N02	The 15.0th hour	-	-	The 93.1th hour
	S01	The 10.1th hour	The 18.8th hour	The 38.3th hour	The 115.8th hour
	S02	The 13.1th hour	-	-	The 79.2th hour
	S03	The 12.5th hour	-	-	The 104.9th hour
	W01	The 15.3th hour	-	-	The 75.7th hour
	W02	The 15.3th hour	-	-	The 75.8th hour
Flood		The 4.9th hour	The 4.9th hour	The 6.0th hour	The 7.0th hour
		The 9.2th hour	-	-	The 12.3th hour
		The 15.4th hour	-	-	The 16.4th hour
		The 18.5th hour	The 20.3th hour	-	-

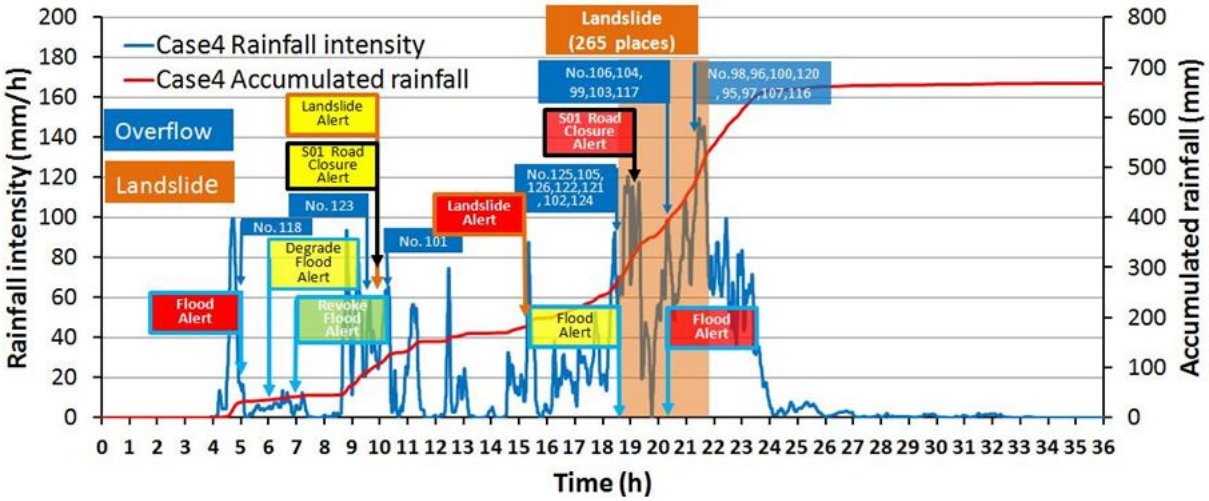

Figure 6.16 The rainfall and timeline of issuing-alerts and disaster events during the rainfall event with high rainfall intensity and long duration

6.3.3 Results of questionnaires

(1)The effects of providing more detailed warning information for the evacuation decision by local governments

The content of the questionnaire for local government officials can be divided into four parts- scenario 1 to scenario 4. The purpose of conducting scenario 1 and scenario 2 was to identify the effect of different forecast rainfalls in the evacuation decisions. Scenario 3 and scenario 4 were given the same forecast rainfalls as the scenario 1 and scenario 2, but extra detailed warning information was offered. The object was to explore the effect of extra detailed warning information in the evacuation decision-making. The survey results are shown in **Figure 6.17** to **Figure 6.20**.

Overall, the effects of the forecast rainfall and extra detailed warning information were obvious only in the first stage (11:00). That is, if the local governments can obtain more detailed warning information or perceived the higher risk (i.e., the forecast rainfall is higher), the willingness of executing precautionary evacuation will rise. In fact, precautionary evacuation is conducive to reduce the risk of casualty. On the contrary, it also increases the evacuation cost and the risk of losing authority credibility. In the other stages (17:00, 20:00, 23:00), almost all survey results showed the local governments will select to evacuate inhabitants in all scenarios.

For the effects of the forecast rainfall, the proportion of selecting to evacuate inhabitants for the experienced officials had been increased about 15.7% in the first

stage if the forecast rainfall was higher (i.e., compared between scenario 1 and scenario 2 to experienced officials). The source of the increase concentrated on county and township officials. Relatively speaking, the increasing proportion was lower (only about 7.1%) in the survey results of inexperienced officials. The source of the increase concentrated on township and village.

For the effect of extra detailed warning information, the proportion of selecting to evacuate inhabitants for the experienced officials as well as lower forecast rainfall condition had been increased about 14.4% in the first stage if the extra detailed warning information were provided (i.e., compared between scenario 1 and scenario 3 to experienced officials). The source of the increase also concentrated on county and township officials. On the other hand, the increasing proportion for the inexperienced officials was almost same as the survey results for experienced officials (about 14.3%). The source of the increase was from all levels. On the contrary, the proportion of selecting to evacuate inhabitants for the experienced officials as well as higher forecast rainfall condition had been increased only 5.3% in the first stage if the extra detailed warning information were provided (i.e., compared between scenario 2 and scenario 4 to experienced officials). The main reason is that the increase had been reflected on the higher forecast rainfall in scenario 2. However, the abovementioned reason didn't seem to affect the effect of extra detailed warning information for inexperienced official as well as higher forecast rainfall. Compared with the scenario 2 for inexperienced officials, the survey results of the scenario 4 still had been increased for 23.4% in the first stage.

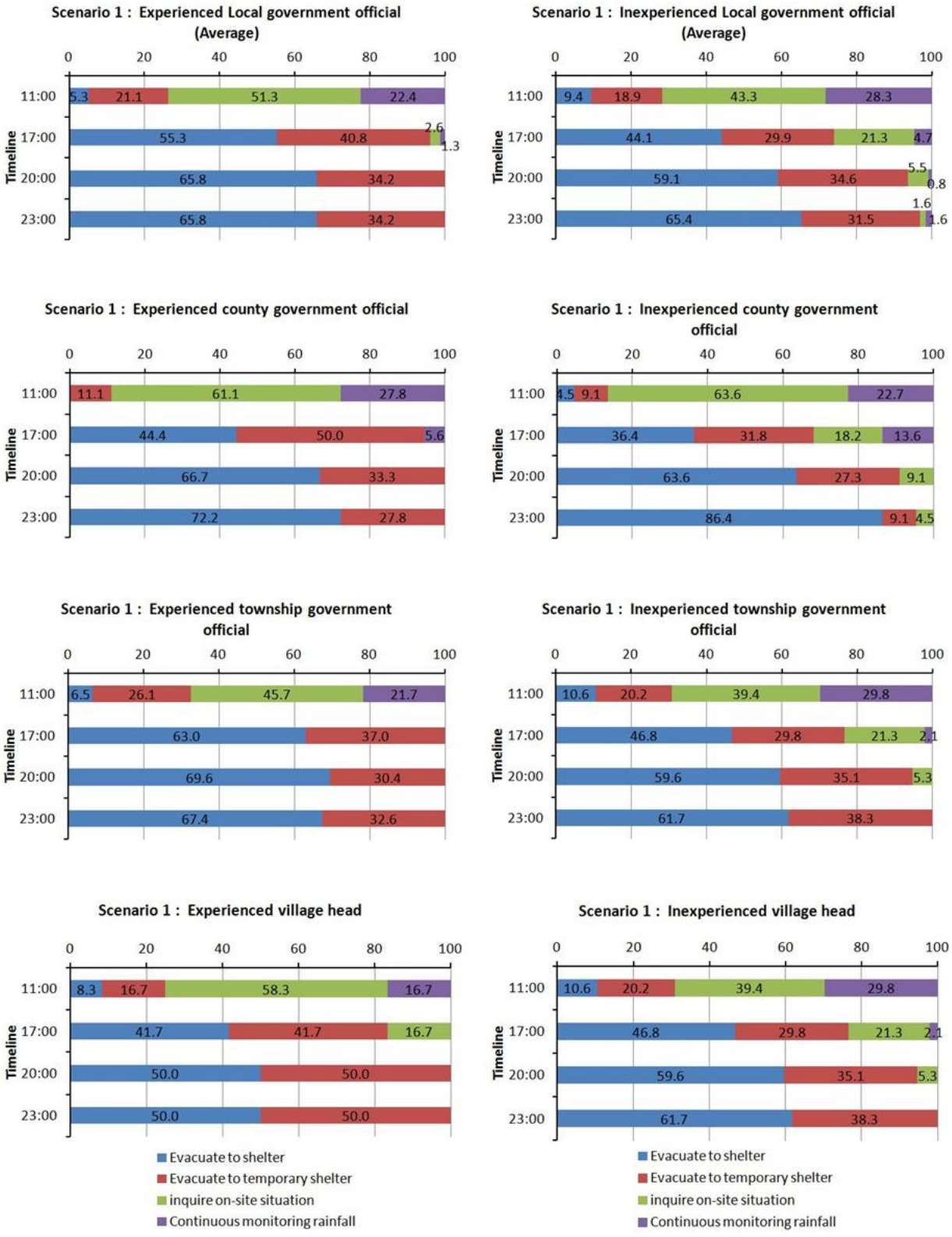

(a) Experienced local government officials (b) Inexperienced local government officials

Figure 6.17 The survey result of evacuation decision for the local government official (**Scenario 1** : the forecast accumulated is **500-800mm**, and provided only the existing simple warning information.)

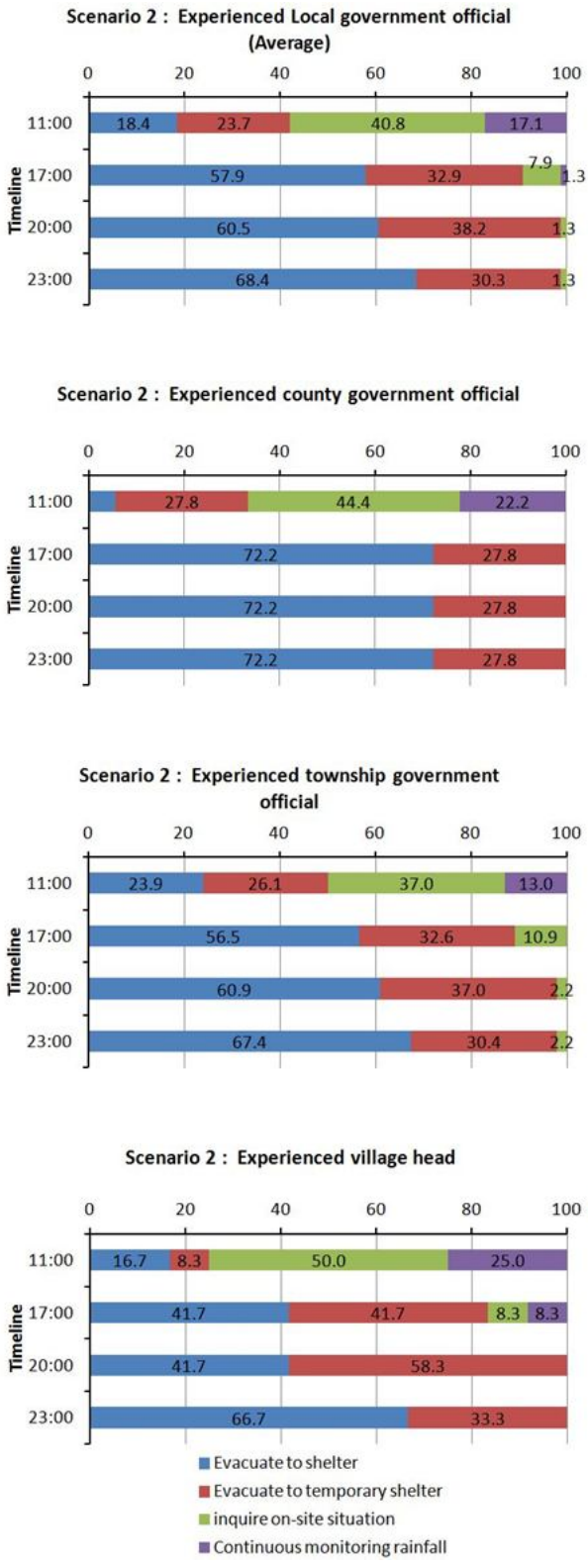

(a) Experienced local government officials

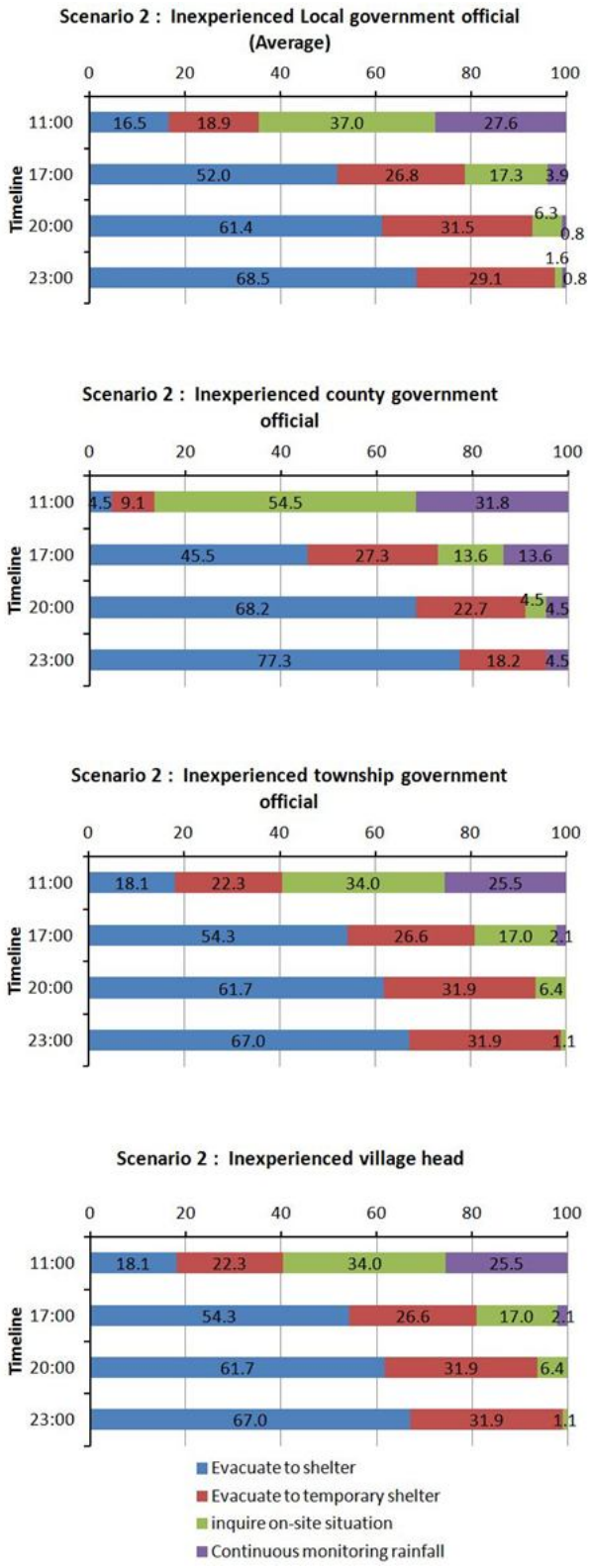

(b) Inexperienced local government officials

Figure 6.18 The survey result of evacuation decision for the local government official (**Scenario 2** : the forecast accumulated is **800-1100mm**, and provided only the existing simple warning information.)

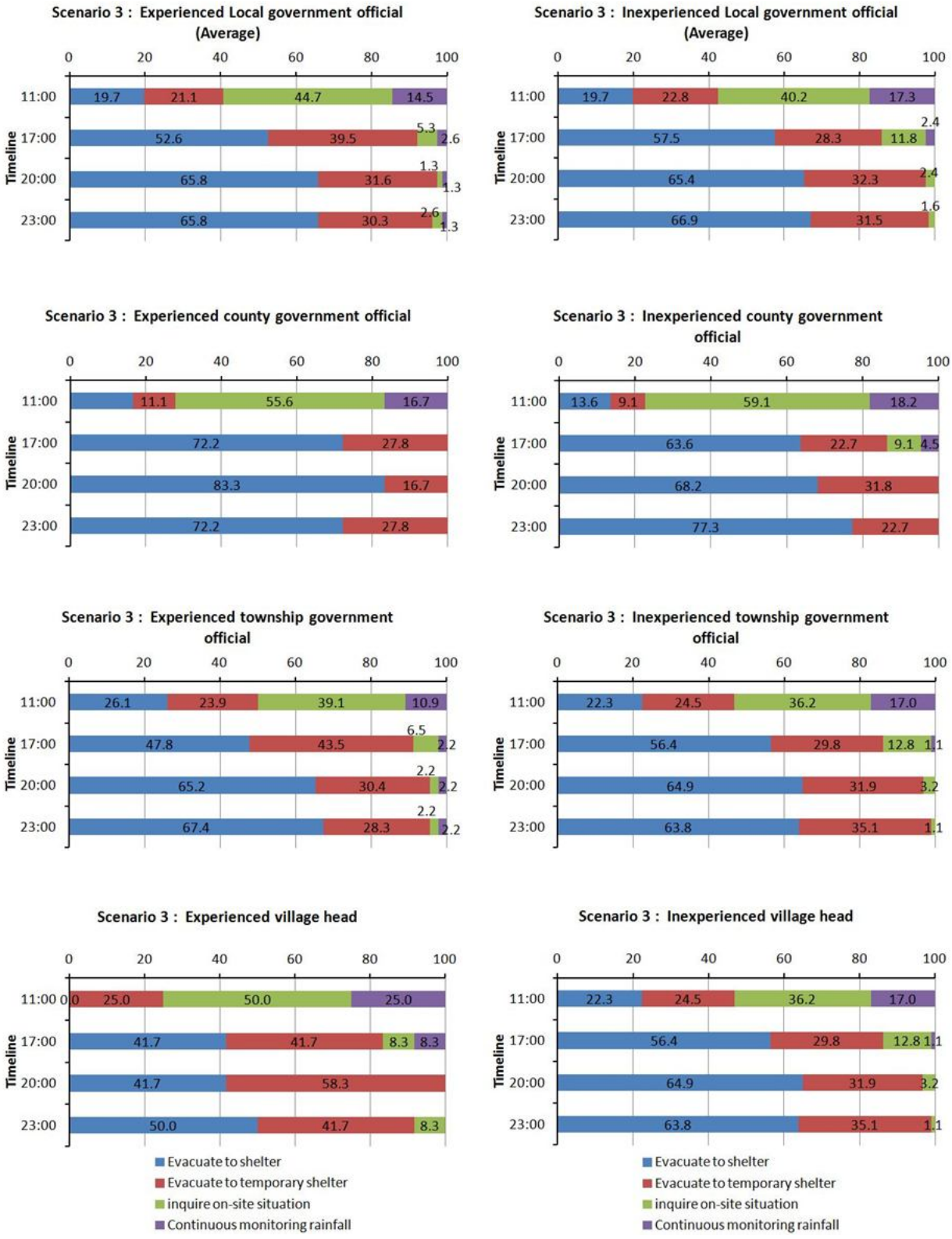

(a) Experienced local government officials (b) Inexperienced local government officials

Figure 6.19 The survey result of evacuation decision for the local government official (**Scenario 3** : the forecast accumulated is **500-800mm**, and provided more detailed warning information.)

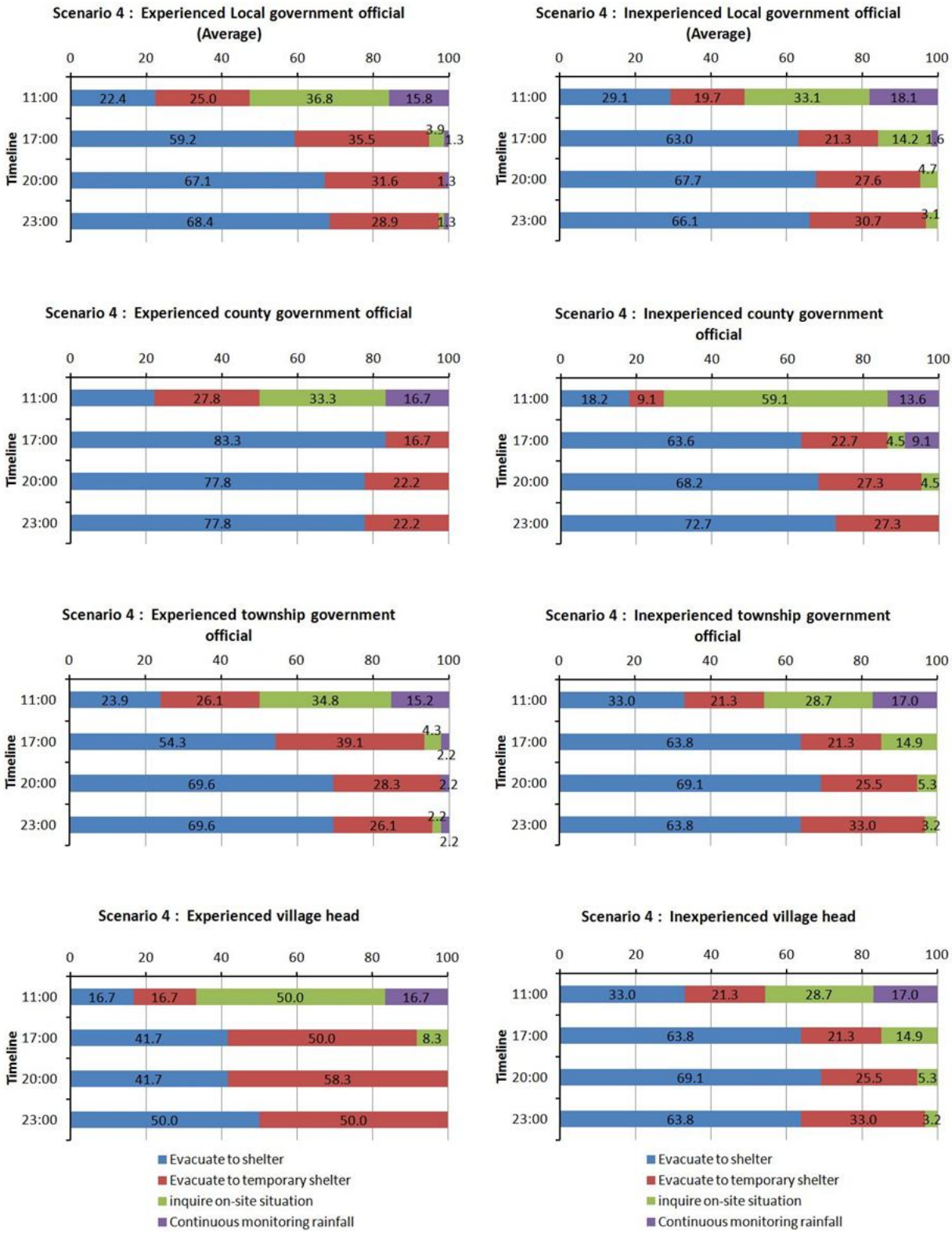

(a) Experienced local government officials (b) Inexperienced local government officials

Figure 6.20 The survey result of evacuation decision for the local government official (**Scenario 4** : the forecast accumulated is **800-1100mm**, and provided more detailed warning information.)

(2)The effects of providing more detailed warning information for the evacuation decision by inhabitants

The content of the questionnaire for inhabitants is divided into two parts-scenario A and scenario B. The purpose is to explore the change of the inhabitants' evacuation decisions if the extra detailed warning information is provided. The survey results are shown in **Figure 6.21** and **Figure 6.22**.

Overall, the effect of extra detailed warning information is very different in different stages. In the daytime (11:30), the proportion of selecting evacuation increased by 17.6% (for experienced inhabitants) and 10.7% (for inexperienced inhabitants) if inhabitants have obtained the extra detailed warning information. However, in the stage of before sunset (17:30), the proportion of selecting evacuation decreased by 29.4% (for experienced inhabitants) and 6.1% (for inexperienced inhabitants). The source of decrease concentrated in the shallow mountainous areas and mountainous areas. After that, in the nighttime (20:30, 23:30), more than half of the inhabitants chose to evacuate. The mean proportion of selecting evacuation increased by 8.8% (for experienced inhabitants) and 4.6% (for inexperienced inhabitants) compared with no extra detailed warning information. It seems to imply that some people trended to adopt the precautionary evacuation, but some people disliked. For the inhabitants who dislike precautionary evacuation, they seem to postpone the evacuation decision-making until nighttime or getting the evacuation order from the township government.

The survey results also indicated that the extra detailed warning information was conducive to increase the willingness of precautionary evacuation. This trend is as same as the survey results for the local government officials. In addition, compared with the survey results of experienced and inexperienced inhabitants, the extra detailed warning information seemed to have larger effect to the experienced inhabitants. That is, the extra detailed warning information might change their mind in the evacuation decision-making. According to another survey results in Chapter 3, the village heads considered that *providing more detailed warning information* was the number-one priority in improvement recommendation to the existing warning system (see **Table 3.8**). Therefore, developing a new warning system which can offer the detailed warning information is a momentous improvement direction.

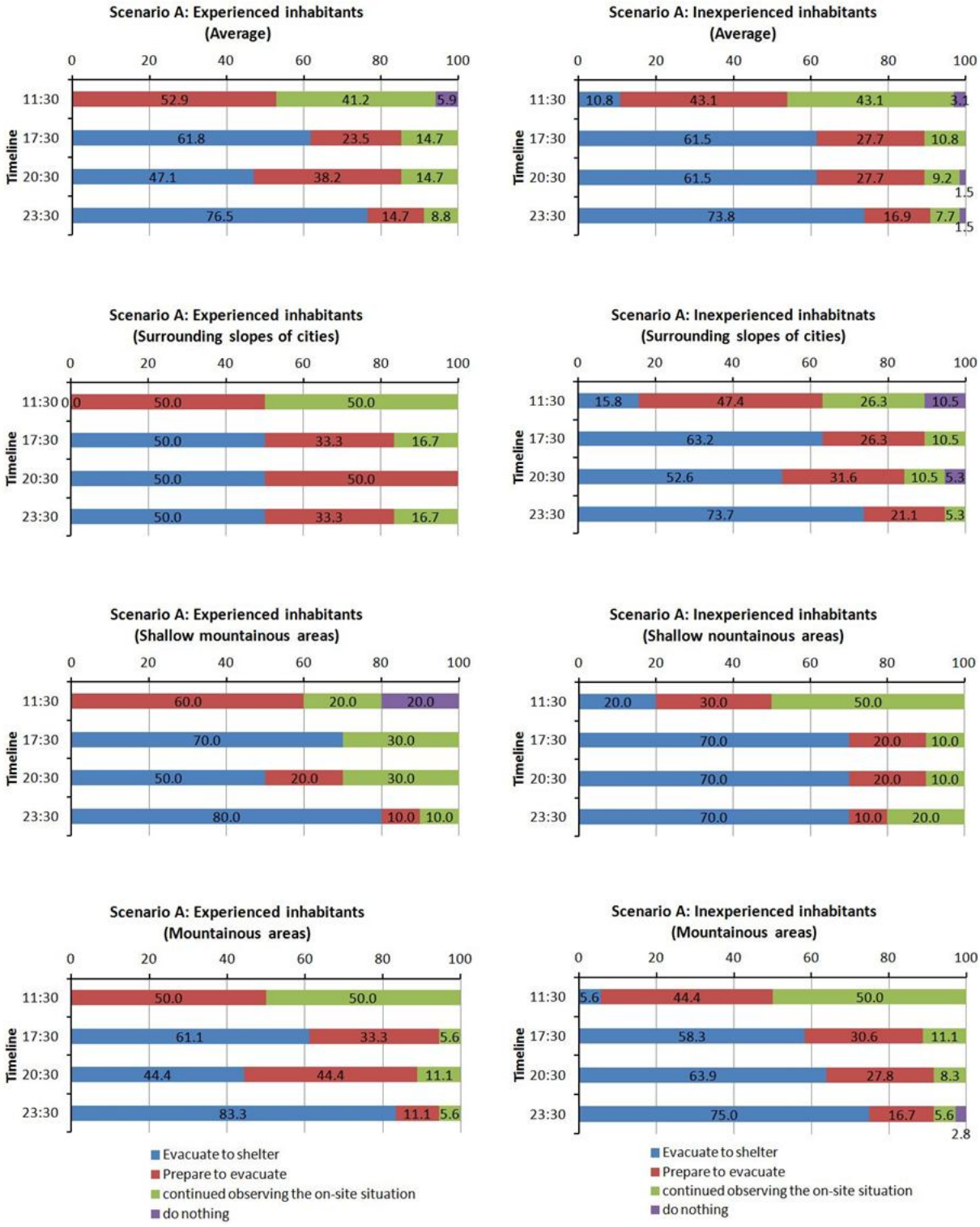

(a) Experienced habitants

(b) Inexperienced habitants

Figure 6.21 The survey result of evacuation decision for inhabitants (**Scenario A** : only offered the existing simple warning information.)

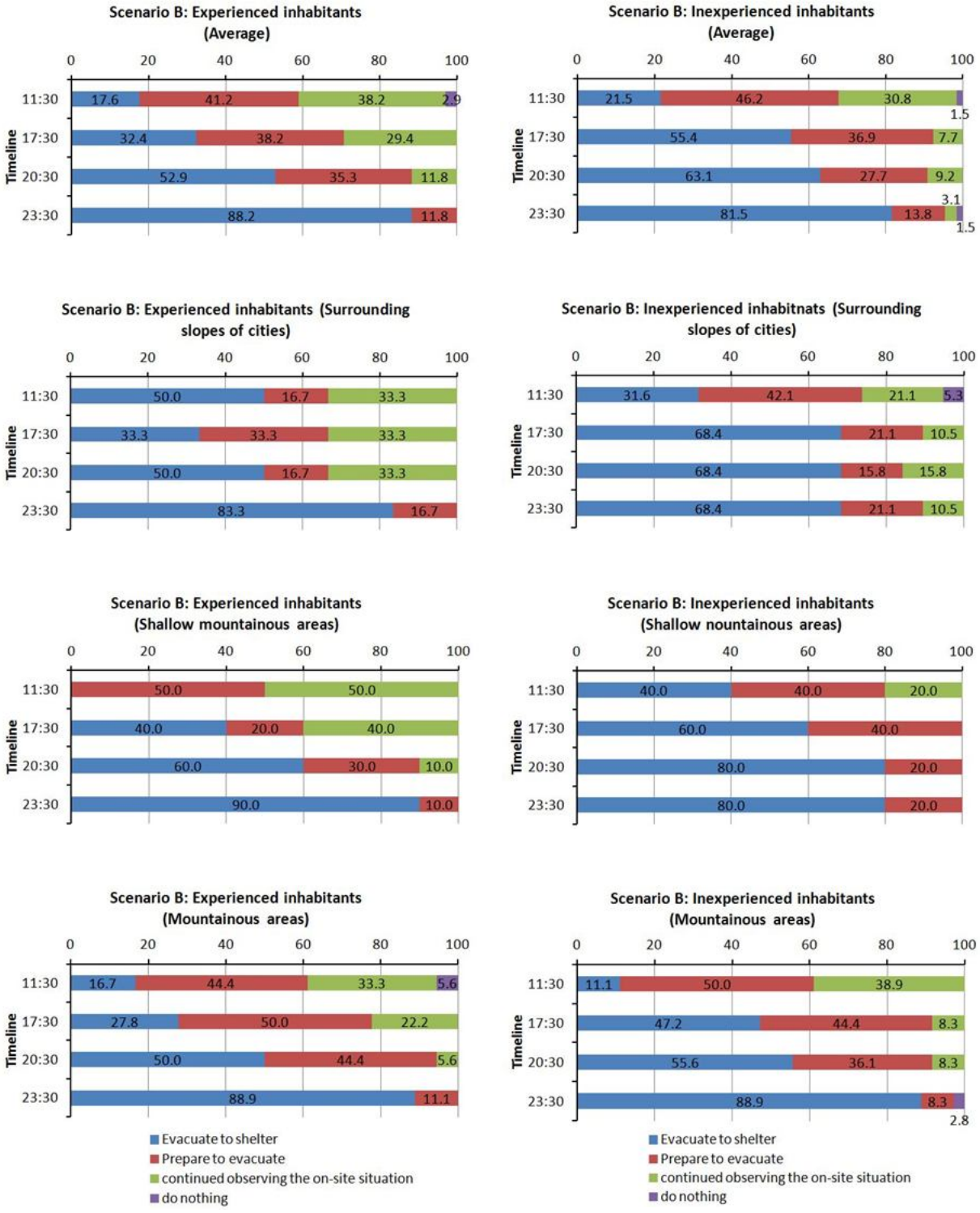

(a) Experienced habitants (b) Inexperienced habitants

Figure 6.22 The survey result of evacuation decision for inhabitants (**Scenario B** : offered more detailed warning information.)

6.3.4 Discussions

Due to lacking the forecast rainfall data, this study used $I_{ta,60}$ (the mean rainfall-intensity in 60 minutes at time t_a) to predict water content of 60 minutes later (W_{t+60}), and the landslide red alert would be issued if W_{t+60} was greater than W_{cr}. According to the simulation results under four diverse rainfall patterns, it seemed to show that this method could provide longer RTE (remaining time for evacuation) for the high rainfall-intensity case. However, if the rainfall pattern was long duration and normal intensity case, the RTE seemed to be insufficient. That's because $I_{ta,60}$ was smaller in the rainfall pattern with normal intensity and long duration, it caused the smaller W_{t+60} and then postponed the alert issued. To improve the model performance, incorporating the forecast rainfall data for the W_{t+60} calculation might be an appropriate solution. In addition, the recommendation in Chapter 2 mentioned that the new warning system should offer accurate long-time predictions (e.g., over the next 12 hours) and the scenario capacity to enhance the evacuation decision-making ability of local governments. If the next 12 hours forecast rainfall data can be obtained, the RIMSH warning system could reach these goals.

While the Uji City government had drawn up the evacuation plan, and the issuing-condition of evacuation orders in the three stages as well as the protected actions seemed to be defined well (see **Table 6.3**). In fact, Uji City government did not issue any evacuation order during the heavy rainfall event on August 13-14, 2012. The only evacuation order was issued at 14:10 on August 14 (i.e., the eighth hour after disaster) [*Maki and Hayashi*, 2014; *Uji City*, 2014]. This study proposed dividing all alert into two warning levels - yellow and red. Therein, the yellow alerts could be as the issuing-condition of preparation evacuation in the evacuation plan of Uji City, and the red alerts could be as the issuing-condition of advice evacuation. According to the simulation results in the study case, the RIMSH warning system could really assist the local government officials not only in the evacuation decision-making but also in the road/bridge closure decision-making.

Reviewing the process of issuing-alerts by the RIMSH warning system, the lifting time of landslide/road-closure yellow alerts seemed to be too late. That's because this study used the same standard to issue and lift the yellow alerts. In fact, if the forecast rainfall could be confirmed (e.g., no rainfall over next 12 hours), the yellow alerts could be lifted earlier. In addition, due to the serious deposition in the

simulation results of some unit channels, sometime the flood alert could not reach the standard of lifting. Therefore, it is still necessary to refer the on-site situation for adjusting the alert level.

Generally, flood warning could be fairly simple because it had obvious omens (e.g., water level) and everyone could perceive the risk directly. By contrast, the landslide warning is more difficult than the flood warning because the omens of landslides were not easy to find and forewarn time was often shorter. Accordingly, this study used the real-time water level to issue flood alerts, but employed the prediction results of the next one-hour to issue landslides alerts. That is, this study intended to obtain a longer remaining time for evacuation (RTE). However, it might induce the side effects of increasing the false alert rate (FAR).

Lindell et al.[2007] established the evacuation decision tree and evaluated evacuation decisions in terms of the number of lives lost, the economic costs incurred, and the credibility lost by local authorities (**Figure 6.23**). Therein, outcome A and D were correct decisions. On the contrary, outcome B is a decision error (a ‘‘false positive’’) because it becomes an unnecessary evacuation and incurs unnecessary economic costs as well as reduces credibility and decreases future warning compliance. Outcome C is the worst decision result (a ‘‘false negative’’). In fact, the costs of unnecessary evacuations due to false alerts are usually another major concern for decision-makers. False alerts are problems of early-warning systems as they can substantially compromise the credibility of early-warning systems [*Larsen*, 2008]. While precautionary evacuation is recognized as one of the best reduction risk method, it also implies that the possibility of outcome B might increase. Moreover, because precautionary evacuation also might cause increasing evacuation cost (e.g., the cost of shelter's operation) and reducing authority credibility as well as decreasing future warning compliance (if no disaster occurs), it often puts the local government officials in a dilemma. Therefore, developing a warning and evacuation decision support system to assist local government decision-making under standard criteria or rules is an important work to enhance disaster prevention capacity.

According to the results of the questionnaire survey, the detailed warning information could raise the proportion of precautionary evacuation for local governments and inhabitants. However, the survey results also showed that some inhabitants would postpone the evacuation decision. Therefore, if the new warning

system could offer more detail warning information to inhabitants, this situation should be considered. That is, this issue is worth to further study.

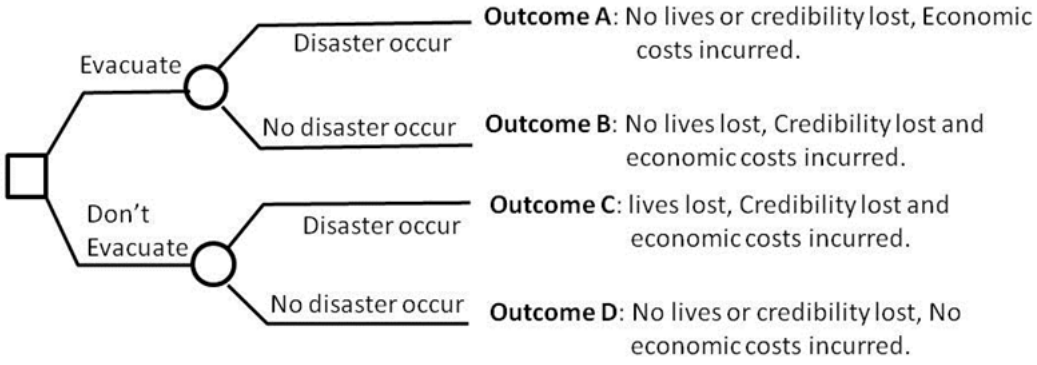

Figure 6.23 Evacuation decision tree [Modified from *Lindell et al*., 2007]

6.4 Summary

Establishment of early-warning systems and evacuation of inhabitants are recognized as the most important approaches for disaster risk reduction. However, a good early-warning system should comprise identification and estimation of hazardous processes, communication of warnings and adapted reaction of local population. Moreover, the warning messages should be credible, clearly formulated, adapted to the context of the target group, and should contain clear instructions on appropriate protection action. Therefore, a complete warning system should be comprised of two parts- warning model and issuing-alert system.

This study proposed the two-levels (yellow/red) alert for three kinds of disasters (landslide, road closure, and flood) to establish the alert-issuing system. Each alert was displayed as easy-to-understand content and had the definite issuing-condition as well as clear instructions on appropriate protection action. Integrating the simulation model of multi sediment hazards (see Chapter 5)and the issuing-alert system, this study developed the Rainfall-Induced Multi Sediment Hazards (RIMSH) warning system. The new warning system could offer not only the detailed early-warning information for inhabitants but also the evacuation and road-closure decision-making for local governments. The results and recommendations are summarized as follows.

(1) The RIMSH warning system can simulate the moving of sediment and flood in a basin, and according to the specific warning-issued criteria to issue the landslide alert for evacuating inhabitants, the road closure alert for

preventing vehicle from entering high-risk roads, the flood alert for bridge closure, and the related protection actions. Using the actual rainfall event and four extreme rainfall scenarios to verify, the RIMSH warning system could issue alerts promptly and assist the local government to make evacuation decisions by objective evaluation methods.

(2) This study proposed the alert-issuing system, which included three kinds of alerts and two levels for each alert, could be incorporated into the existing evacuation plan. Using color (yellow/red) as the metaphorical symbol, the meanings of the alerts were clearly formulated and easy to understand for local governments and inhabitants. In addition, all alerts also had specific definition of the issuing-condition, and had clear instructions on appropriate protection action.

(3) According to the questionnaires survey results, if the local government officials obtain the higher forecast rainfall or extra detailed warning information, the willingness of executing precautionary evacuation will raise. However, although the detailed warning information really could rise the proportion of precautionary evacuation for local governments and inhabitants, the survey results also showed that some inhabitants would postpone the evacuation decision. It is worth for further studies.

(4) Although precautionary evacuation is recognized as one of the best reduction risk method, it also implies that the possibility of issuing false alerts might increase. Moreover, because precautionary evacuation also might cause increasing evacuation cost (e.g., the cost of shelter's operation) and reducing authority credibility as well as decreasing future warning compliance (if no disaster occurs), it often puts the local government officials in a dilemma. Therefore, developing a warning and evacuation decision support system to assist local governments decision-making under standard criteria or rules is an important work to enhance disaster prevention capacity.

(5) The recommendation in Chapter 2 mentioned that an effective warning system could offer accurate long-time predictions (e.g., over the next 12 hours) and the scenario capacity to enhance the evacuation decision-making ability of local governments. If the next 12 hours forecast rainfall data can be obtained, the RIMSH warning system could reach these goals. Besides,

incorporating the forecast rainfall data into the RIMSH warning system also could solve the problem that the remaining time for evacuation might be insufficient when the rainfall pattern was long duration and normal intensity.

References

Aleotti, P. (2004): A warning system for rainfall-induced shallow failures, Engineering Geology, Vol. 73, pp. 247-265.

Larsen, M.C. (2008): Rainfall-triggered landslides, anthropogenic hazards, and mitigation strategies. Adv Geosci 14, pp.147–153

Lindell, M. and Prater, C. (2007): A hurricane evacuation management decision support system (EMDSS), Natural Hazards, Vol. 40, No. 3, pp. 627–634.

Kunz-Plapp, T. (2008): Vorwarnung, Vorhersage und Frühwarnung. In: Naturrisiken und Sozialkatastrophen. Grundlagen und Herausforderungen der Gefahren- und Risikoforschung. Felgentreff, C., T. Glade (eds.), Elsevier, Heidelberg, pp. 213-233.

Hübl, H (2000): Frühwarnsysteme als passive Schutzmaßnahmen in Wildbacheinzugsgebieten. In:Wildbach und awinenverbauung (ed) Jahresbericht 2000 des Bundesministeriums für Landwirtschaft, Forst, Wasser und Umwelt, pp. 46.

Maki, N. and Hayashi, H. (2014): The 2012 South Kyoto Flooding and Disaster Response of City of Uji; Essential Contents for a post-Tohoku Earthquake Disaster Response Plan, Journal of Social Safety Science, No.22.

National Research Council (2004): Partnerships for reducing landslide risk: assessment of the national landslide hazards mitigation strategy. The National Academies Press, Washington.

UNISDR (2006): Global survey of early warning system. UN/ISDR. (http://www.unisdr.org/2006/ppew/info-resources/ewc3/Global-Survey-of-Early-Warning-Systems.pdf)

UNISDR (2009): Terminology on Disaster Risk Reduction. UN/ISDR. (http://www.unisdr.org/files/7817_UNISDRTerminologyEnglish.pdf).

Thiebes, B. (2012): Landslide Analysis and Early Warning Systems: Local and Regional Case Study in the Swabian Alb, Germany. Springer Berlin Heidelberg.

Uji City (2009): The regional disaster prevention plan of Uji City, pp.3-44 - 3-45.

Uji City (2013): The regional disaster prevention plan of Uji City, pp.3-53 - pp.3-54. (http://www.city.uji.kyoto.jp/0000010399.html)

Uji City. (2014): The heavy rainfall disaster record collection in Kyoto southern region on August 13-14, 2012 (in Japanese). (http://www.city.uji.kyoto.jp/0000012774.html)

Wieczorek, G.F. and Glade, T. (2005): Climatic factors influencing occurrence of debris flows. In: Jakob, M. and Hunger, O. (eds), Debris-flow Hazards and Related Phenomena, Praxis, Springer Berlin, pp. 325–362.

Chapter 7
Conclusions and Recommendations

7.1 Conclusions

Facing the threat of natural disaster, establishment of early-warning systems and evacuation of inhabitants are recognized as the most important approaches for disaster risk reduction. However, although the existing rainfall-based warning systems in Japan and Taiwan provided a simple and easy-to-apply criterion method to issue alerts, they cannot predict which slope might collapse specifically. Therefore, even if the local government received the alerts, it was still difficult to make an appropriate evacuation decision. According to the statistics in Japan and Taiwan, the proportion of local governments and inhabitants actually executing the evacuation order and evacuation action after the sediment alert was issued was very low. It seemed to show that the existing rainfall-based warning system was not fully trusted. In addition, while the rainfall-induced disasters in mountainous areas usually occur as multi-modal types, limited by the complexity of multi-hazard analysis and lacked of the capability of overall consideration, the existing warning systems also cannot cope with risk of multi-hazards. However, recently several large-scale disasters implied that if the evacuation plan considered only single hazard effect, it might result in the evacuation failure. This study explored the insufficiencies of the existing warning systems and investigated the evacuation decision-making factors. Based on these research results, this study identified the needs of the new warning system. Moreover, this study proposed a novel method of predicting landslide and developed a simulation model of multi sediment hazards on a basin scale as well as established a complete warning and evacuation decision support system.

In Chapter 2, this study analyzed the characteristics of the existing warning system in Japan and Taiwan, and proposed the evaluation indexes of warning effectiveness as well as recommended for the future warning system. This study suggested developing a basin-scale warning system, which considers the geological, geomorphologic, and hydrological characteristics of slopes and channels. The new warning system should offer accurate long-time predictions and the scenario simulation capacity.

In Chapter 3, this study establishes the evacuation decision-making models based on the pair-wise comparison and the hierarchy process (AHP) for local governments and inhabitants. The results not only showed the importance of each evacuation decision factor, but also identified the deficiencies in current disaster prevention actions. In addition, the research results indicated that *raising the warning hit rate*, *narrowing the unit of warning area*, and *providing more detailed warning information* are the most important improvement direction for existing warning system. Based on the recommends of Chapter 2 and 3, the new warning system should offer the detailed warning information (e.g., the occurring time, location, type, and scale of potential disaster.), and used slope units as the target to predict landslides as well as employed unit channel as the target to predict the water level and riverbed deformation.

In Chapter 4, this study proposed a new approach (critical water content method, W_{cr}), which was based on physically-based model and the multiple regressions as well as used the slope units as analysis targets, to predict the occurring time, location, and scale of landslides on a basin scale. This W_{cr} method cannot only offer the similar accuracy to the physically-based model, but also has the high performance on calculation. Moreover, because the occurrence of rainfall-induced landslides was attributed to the water content, the W_{cr} method is appropriate to express the risk of landslide on a basin scale. In addition, it also can calculate runoff of each slope during the rainfall event. Therefore, the W_{cr} method could be as the foundation of developing the simulation model of multi sediment hazards on a basin scale.

Because the rainfall-induced disasters in mountainous areas usually related to flooding and sediment transportation, most of them occurred as multi-modal types. That is, a hazard could affect or trigger another one because of their complex spatial and temporal relationships. In Chapter 5, this study suggested a basin model by combining slope units and unit channels, and integrated the rainfall-infiltration, landslide prediction, sediment runoff, riverbed deformation, and water discharge models to establish the simulation model of multi sediment hazards on a basin scale. Simultaneously, using the heavy rainfall disaster event, which occurred in the Shizugawa basin in 2012, located in Uji City, Kyoto Prefecture, as a study case, the simulation model of multi sediment hazards had been verified the feasibility to simulate the process of rainfall, infiltration, landslide, water discharge, sediment runoff, and riverbed deformation. Besides, the simulation model of multi sediment

hazards was also confirmed the scenario simulation capacity through using four different rainfall patterns to conduct the simulation.

Finally, in Chapter 6, this study proposed the two-levels (yellow/red) alert for three kinds of disasters (landslide, road closure, and flood) to establish the alert-issuing system. Each alert was displayed as easy-to-understand content and had the definite issuing-condition as well as clear instructions on appropriate protection action. Integrating the simulation model of multi sediment hazards and the issuing-alert system, this study developed the Rainfall-Induced Multi Sediment Hazards (RIMSH) warning system. The warning system can offer not only the early-warning for inhabitants but also the decision support of evacuation and road-closure for local governments. Using the abovementioned heavy rainfall event as the verification, the RIMSH warning system provided at least 2.5 hours for evacuation preparation, and at least 1 hour to evacuate inhabitants to the shelters. It really reached the goal of early warning, and offered enough evacuation time. Moreover, the RIMSH warning system proposed an objective evaluation method to adjust the alert level, and it should be useful to assist the decision-maker of local governments in making appropriate decisions. In addition, to verify the contribution of the RIMSH warning system on raising the evacuation willing for the local government officials and inhabitants, this study made a series of questionnaires to explore the effect of more detailed warning information. The survey results indicated that if the local government officials obtain the higher forecast rainfall or extra detailed warning information, they will raise the willingness of executing precautionary evacuation. However, although the detailed warning information really could raise the proportion of precautionary evacuation for local governments and inhabitants, the survey results also showed that some inhabitants would postpone the evacuation decision.

7.2 Recommendations

To further study and enhance the current achievements, the following recommendations could be considered.

(1) Despite the method of demarcating the slope units automatically had been proposed, the manual method to divide some slope units, which had complex slope aspects or geology, is still necessary. How to reduce the manual procedure and remain the consistence should be further explored.

(2) While the causes of soil moisture distribution, which will affect the scale of landslides, are very complicated, this study only used I_{60} as the representative indicator. Compared with the occurring time and location of landslide prediction, the prediction result of landslide scale is poorer. It needs further studies.

(3) Based on some simplified assumptions, the study employed overland flow model and sediment runoff model in channels to simulate the process of landslide sediment moving into the channel during rainfall. However, the characteristic of the moving of landslide sediment on the slope is bound to be different from the sediment movement in the channel. Thus, although the simulation results seem to be reasonable, it should still need to further study. Moreover, the moving way of landslide sediment might be not only as overland flow but also as debris flow. Besides, it also might be that whole landslide sediment fell into the channel directly. This part should be explored further.

(4) Limited to the one-dimension analysis of water discharge and riverbed deformation, this study assumed that the landslide sediment supply was uniform distribution on the riverbed and all sediment runoff would enter to the next channel. Therefore, the simulation results cannot properly explain the blocking effects of sediment in the channels, and the abnormal elevation of riverbed in the unit channel No.123. Besides, due to the change of the cross-section of drainage after overflow in the channel, the water level and water discharge should be lower. That is, some simulation results might overestimate the discharge. To solve abovementioned problem, using a two-dimension analysis seemed to be necessary.

(5) The recommendation in Chapter 2 mentioned that the new warning system should offer accurate long-time predictions (e.g., over the next 12 hours) and the scenario capacity to enhance the evacuation decision-making ability of local governments. If the next 12 hours forecast rainfall data can be obtained, the RIMSH warning

system could reach these goals. Besides, incorporating the forecast rainfall data into the RIMSH warning system also could improve the problem that the remaining time for evacuation might be insufficient when the rainfall pattern was long duration and normal intensity.

(6) According to the results of the questionnaire survey, the detailed warning information really could raise the proportion of precautionary evacuation for local governments and inhabitants. However, the survey results also showed that some inhabitants would postpone the evacuation decision. Therefore, if the new warning system could offer more detail warning information to inhabitants, this situation should be considered. That is, this issue is worth to further study.

List of Figures

List of Tables

Curriculum Vitae

Name	Chen-Yu Chen
Citizenship	Taiwan
Birth/Place	June 10, 1970, Taichung, Taiwan

Ph.D. Student (2011-2014)
Department of Civil and Earth Resources Engineering,
Graduate School of Engineering, Kyoto University, Japan

M. Eng. in Civil Engineering (1993-1995)
Graduate School of Engineering, National Chiao Tung University, Taiwan

B.E. in Civil Engineering (1988-1993)
Department of Civil Engineering, Feng Chia University, Taiwan

Papers based on the Thesis

Chen, C.Y., and Fujita, M. (2014): A Warning and Evacuation System by means of a Multi Sediment Hazards Simulation Model on a Basin Scale, Proceeding of International Debris-Flow Workshop 2014. (Accepted)

Chen, C.Y., and Fujita, M. (2014): A Multi-modal Sediment Disaster Simulation on a Basin Scale, Proceeding of INTERPRAEVENT International Symposium 2014. (Accepted).

Chen, C.Y., and Fujita, M. (2014): A prediction model of landslide occurrence and its scale using numerical-regression equations, Proceeding Annual Meeting of Japan Society of Erosion Control Engineering, JSECE Publication, No.72, pp. B-308-309.

Chen, C.Y., and Fujita, M. (2014): A method for predicting landslides on a basin scale using water content indicator, Journal of Japan Society of Civil Engineers, Ser. B1 (Hydraulic Engineering), Vol. 70, No.4, pp.I_13-I_18.

Chen, C.Y., and Fujita, M. (2013): An analysis of rainfall-based warning systems for sediment disasters in Japan and Taiwan, International Journal of Erosion Control Engineering, Vol. 6, No. 2, pp. 47-57.

Chen, C.Y., and Fujita, M. (2013): Evacuation Decision-Making Factors for Local Governments and Inhabitants in Debris-Flow Potential Areas in Taiwan, International Journal of Erosion Control Engineering, Vol. 6, No. 2, pp. 37-46.

Chen, C.Y., and Fujita, M. (2013): Simulation of Sediment Disasters Due to Slope Failures and the Following Sediment Runoff, International symposium on sediment disasters under the influence of climate change and tectonic activity (3rd) (International Journal of Erosion Control Engineering, Vol. 7, No. 1, accepted)

Chen, C. Y., Ikkanda, S., Fujita, M., and Tsutsumi, D. (2013): A study on mechanism of large-scale landslides and the prediction, Proceeding of 12th International Symposium on River Sedimentation, pp. 41.

Chen, C.Y., and Fujita, M. (2013): Simulation of Landslides and the Following Sediment Runoff in a Basin Scale, Proceeding Annual Meeting of Japan Society of Erosion Control Engineering, JSECE Publication, No. 69, pp. A-232-233.

Chen, C.Y., and Fujita, M. (2012): The Evacuation Decision-Making Factors for Local Government and Inhabitants in Debris-Flow Potential Areas in Taiwan, Proceeding of the 3rd International Workshop on Multimodal Sediment Disasters, pp. D.3.1-D.3.11.

Chen, C.Y. (2012): Evaluation of rainfall-based warning systems for debris flows and slope failures in Japan and Taiwan, Proceeding Annual Meeting of Japan Society of Erosion Control Engineering, JSECE Publication, No. 66, pp. 286-287.